2012

Generation and characterization of high CO_2 requiring mutants in Chlamydomonas reinhardtii

Yunbing Ma
Louisiana State University and Agricultural and Mechanical College, yma3@tigers.lsu.edu

GENERATION AND CHARACTERIZATION OF HIGH CO_2 REQUIRING MUTANTS IN *CHLAMYDOMONAS REINHARDTII*

A Dissertation
Submitted to the Graduate Faculty of the
Louisiana State University and
Agriculture and Mechanical College
in partial fulfillment of the
requirements for the degree of
Doctor of Philosophy

in

The Department of Biological Sciences

by
Yunbing Ma
B.E., Shanghai University, 2005
August 2012

ACKNOWLEDGMENTS

First of all, I would like to express my deepest gratitude to my advisor Dr. James V. Moroney. With his patience, motivation, enthusiasm, and immense knowledge, he helped and supported me throughout my Ph.D. study and research. His understanding and guidance helped me in all the time of research and writing of this thesis.

Besides my advisor, I would like to thank the rest of my committee members: Dr. John Larkin, Dr. Sue Bartlett, Dr. David Longstreth and Dr. Graca Vicente for their encouragement, warm help, and insightful suggestions. My sincere thanks also goes to Dr. Zhiyuan Chen, for encouraging me all the time whenever I got depressed from experiments failures.

I thank my fellow lab-mates. I owe thanks to Bratati Mukherjee for her warmest friendship and emotional support over the long six years in LSU. I also want to thank Dr. Nadine Jungnick for her invaluable support especially during the end my Ph.D. study. I also want to thank Robert Dimario for his humor, for always creating a relaxing environment in the lab. And thanks to Kristen Bice for her efficient assistance whenever you need it; to Wes, Julie, Michael, Emily, and D.J., for their consistent help throughout the six years.

Last but not the least, I would like to thank my family: my parents Jiaqu Ma and Jianxiu Chen, for giving birth to me at the first place and supporting me spiritually throughout my life. I also want to give my special thanks to my husband, Xi Yang for his support for my Ph.D. studies. He also helped me pick hundreds of *Chlamydomonas* transformants without any complains!

TABLE OF CONTENTS

LIST OF FIGURES

LIST OF ABBREVIATIONS

AIR	350 ppm (v/v) CO_2 in air
CA	carbonic anhydrase
CBLP	G protein β subunit
CCM	CO_2 concentrating mechanism
CCP	chloroplast carrier protein
cDNA	complimentary DNA
DIC	dissolved inorganic carbon
DTT	Dithiothreitol
GAPDH	glyceraldehyde phosphate dehydrogenase
High CO_2	5% CO_2 in air (v/v)
IPTG	Isopropyl β-D-1-thiogalactopyranoside
LCI	low CO_2 inducible
LIP	low CO_2 inducible protein
LHC	light harvesting complex
Low CO_2	100 ppm CO_2 in air (v/v)
ORF	open reading frame
3-PGA	3-phosphoglycerate
PAGE	polyacrylamide gel electrophoresis
PS	photosystem
RbcS	Rubisco small subunit
RbcL	Rubisco large subunit
Rubisco	ribulose-1,5-bisphosphate carboxylase/oxygenase
SLC	sick on low CO_2
WT	wild- type

ABSTRACT

Chlamydomonas reinhardtii (referred to as *C. reinhardtii* hereinafter) possesses a CO_2 concentrating mechanism (CCM) that allows the alga to grow at low CO_2 concentrations (100 ppm CO_2 in air). This dissertation represents the results from the characterization of three CCM mutants, as well as generation of eleven more potential mutants deficient in the CCM.

One common feature seen in photosynthetic organisms possessing a CCM is the tight packaging of Rubisco within the cell. In many eukaryotic algae, Rubisco is localized to the pyrenoid, an electron dense structure within the chloroplast. The first mutant characterized has a highly disorganized pyrenoid. The results indicated that the gene disrupted in this mutant, *CIA6*, is required for the formation of the pyrenoid. Furthermore this showed that the loss of the pyrenoid correlated with the loss of the CCM. These results supported the hypothesis that the pyrenoid is required for a functional CCM. A second mutant investigated was a revertant of a mutant in the gene *PGP1*. Initially, the *pgp1* strain could not grow under low CO_2. But over time, it regained the ability to grow under low CO_2 conditions. Data is presented that shows the change in growth phenotype is a result of a second site reversion. The results from this study suggested that another phosphoglycolate phosphatase (PGP2) might play a role in the phenotype reversion. Thirdly, a cell wall deficient strain CC-503 was found to be missing a periplasmic carbonic anhydrase (CAH1). The possible reason for the loss of CAH1, and the resulting consequences of losing CAH1 were investigated in this strain.

Lastly, a PCR-based reverse genetics mutagenesis screen was performed to identify more genes involved in the CCM in *C. reinhardtii*. Eleven potential mutants

were isolated, and it was shown that this method could be used on a larger scale in the future to generate mutants missing key CCM genes.

CHAPTER 1
INTRODUCTION

Photosynthesis converts solar energy into chemical energy and provides the raw materials for the food we eat and the fuel we use. This physico-chemical process (Govindjee, 2000) uses carbon dioxide (CO_2) and water (H_2O) and produces carbohydrates and oxygen (O_2) in the chloroplasts. The acquisition of the chloroplast made green algae and plants separate from animals and fungi, and represents an important step in evolution. The unicellular eukaryotic green algae, *Chlamydomonas reinhardtii* (referred to as *C. reinhardtii* hereinafter) has been a model organism for more than half a century (Harris et al., 2009). *C. reinhardtii* is widely regarded as an excellent system for photosynthesis studies due to: 1) the published sequences of all three genomes in the nucleus, chloroplast and mitochondria (Gray and Boer, 1988; Michaelis et al., 1990; Merchant et al., 2007) and the possibility of transforming all three genomes (Harris et al., 2009); 2) its full life cycle for controlled sexual or asexual reproduction and rapid doubling time; 3) its ability to grow heterotrophically using acetate as the sole carbon source facilitating the identification and characterization of photosynthesis mutants.

When photosynthetic organisms first appeared around 3.5 billion years ago, the early atmosphere was dominated by CO_2 and free O_2 was not present. However, by the time land plants appeared some hundreds of millions of years ago, the CO_2 level had fallen substantially and O_2 had risen to 20% (v/v). The catalytic imperfections of Rubisco (Ribulose-1,5-bisphosphate carboxylase oxygenase), the primary enzyme responsible for fixing inorganic CO_2 into organic carbohydrates, began to result in problem in CO_2 fixation. First of all, as the enzyme name suggests, Rubisco not only

catalyzes the carboxylation of RuBP using CO_2, but also produces phosphoglycolate by its oxygenase activity. Phosphoglycolate needs to be recycled through an energy dependent photorespiratory pathway or otherwise the phosphoglycolate would accumulate to a toxic level. Additionally, Rubisco has an extremely low turn-over rate. As a result, to improve the function of Rubisco, two major strategies evolved. The first is the emergence of several forms of Rubisco with varying catalytic efficiencies. For example, the Rubisco from higher plants and green algae can much better distinguish CO_2 from O_2 compared to the Rubisco from photosynthetic bacteria (Jordan and Ogren, 1981). However, the increased specificity came at the expense of decreased carboxylase activity as the photosynthetic bacteria have higher carboxylation rates than those in higher plants (Jordan and Ogren, 1981; Bainbridge et al., 1995). In a second adaptation, the local CO_2 concentration around Rubisco is elevated by placing Rubisco into various types of micro-compartments. This strategy alleviates the unwanted oxygenase activity, thus enhancing photosynthetic efficiency. The later approach is commonly referred to as a CO_2 Concentrating Mechanism (CCM).

For land plants, a successful example of a CCM is the C4 pathway, which is thought to have evolved from its C3 ancestors by adding a special "Kranz Anatomy" structure and biochemical components to concentrate CO_2 around Rubisco. For aquatic photosynthetic organisms, an additional challenge is the fact that the diffusion of CO_2 in an aqueous solution is 10,000 times slower than the diffusion of CO_2 in air. Prokaryotic cyanobacteria possess a micro-compartment called the carboxysome which packs a carbonic anhydrase and most of the Rubisco inside, allowing carbon dioxide to be produced where most needed. The whole CCM assembly is further completed by the

addition of a number of bicarbonate transporters on the cell membrane which accumulate bicarbonate in the cytosol. The importance of the carboxysome in the cyanobacterial CCM is illustrated by the fact that the ectopic expression of an active carbonic anhydrase in the cyanobacteria cytosol short-circuits the CCM (Price and Badger, 1989). In eukaryotic algae, especially *C. reinhardtii* whose CCM is under extensive study, the whole assembly is composed of three major components (Mukherjee and Moroney, 2011; Moroney and Ynalvez, 2007). First of all, multiple carbonic anhydrases in nearly each sub-cellular location, for example, α-CAs are found in the periplasmic space (CAH1, CAH2), while the two β-CAs (CAH4, CAH5) are associated within mitochondria. Secondly, a group of postulated inorganic carbon (C_i) transporters across membranes acticvely accumulate C_i. Candidate transporters include CCP1, CCP2, LCI1 and NAR1.2. Finally, active CO_2 fixation takes place in a differentiated region of the chloroplast called pyrenoid. The pyrenoid is an electron dense, proteinaceous structure found in most green algae and in the primitive moss *Anthoceros*, but not in higher plants.

The general aim of the research described in this dissertation was the elucidation of the biological function and roles of some of the components involved in the CO_2 Concentrating Mechanism in *C. reinhardtii*. First of all, a reverse genetic approach was used to identify potential CCM components (Colombo et al., 2002). Insertional mutants that show sick-on-low CO_2 (slc) phenotypes were investigated. Once the disrupted gene was identified, the mutant was further characterized. Secondly, a PCR-based forward genetics approach was used to obtain potential CCM mutants. Random insertional mutagenesis was first carried out. Subsequent PCR was performed on all the transformants to identify those with disrupted potential CCM genes. Additionally, a *C.*

reinhardtii mutant involved in photorespiration pathway, and one carbonic anhydrase (CAH1) spontaneous mutant was investigated.

The specific aims of this dissertation research include: 1) the identification and characterization of a mutant (*cia6*) with a disorganized pyrenoid (Chapter 4); 2) presentation of a transcriptional analysis of the three phosphoglycolate phosphatase genes (Chapter 5); 3) an initial characterization of a natural CAH1 mutant strain, CC-503 (Chapter 6) and 4) a pilot mutagenesis screen for future larger scale mutagenesis (Chapter 7).

CHAPTER 2
REVIEW OF LITERATURE

RUBISCO (Ribulose-1,5-bisphosphate carboxylase oxygenase)

The enzyme Rubisco (EC 4.1.1.39) is the most abundant protein on Earth (Ellis, 1979). In C3 plant leaves, Rubisco may account for nearly 50% of the entire soluble proteins (Portis and Parry, 2001; Makino, 2003). In C4 plant leaves, Rubisco may also account for around 30% of the total soluble proteins. Rubisco is also arguably the most important protein for its role in the first step of CO_2 assimilation, in which the inorganic CO_2 molecule is attached to a five-carbon sugar, ribulose-1,5-bisphosphate (RuBP), to generate organic compounds.

In the process of carboxylation, the primary CO_2 fixation step, a Rubisco-enediol complex formed by Rubisco and RuBP captures CO_2 and produces a C-6 intermediate product which immediately dissociates into 2 molecules of 3-phosphoglycerate (3-PGA). PGA then goes into the Calvin Cycle leading to the final production of glyceraldehyde 3-phosphate (G3P) which undergoes further metabolization. When compared to a carbonic anhydrase, whose typical catalytic rate ranges between 10^4 and 10^6 reactions per second (Lindskog, 1997), Rubisco is extremely slow, catalyzing only 2-3 carboxylation reactions per second per active site (Schneider et al., 1992). This slow action makes Rubisco the rate limiting enzyme for the Calvin Cycle. Additionally, Rubisco also catalyzes a competing oxygenation reaction by converting the RuBP into 3-PGA and 2-phosphoglycolate (2-PG). This competing reaction slows the already low carboxylation rate. In addition, the oxygenase product 2-PG will need to be recycled through the energy dependent photorespiration pathway. Without the pathway, the carbon in the 2-PG would

be lost, and the accumulation of 2-PG strongly inhibits the regeneration of RuBP in the Calvin cycle.

Structurally, Rubisco usually consists of large subunits (RbcL) and small subunits (RbcS). There are four main forms of Rubisco found in plants, algae, and other autotrophs, form I, II, III and IV (Tabita, 1999; Tabita et al., 2008). In *C. reinhardtii*, the enzyme adopts a hexadecameric complex containing eight RbcL and eight RbcS (L_8S_8, form I). The RbcL is encoded by a single chloroplast gene and is synthesized inside the chloroplast. The small subunits are encoded by two head-to-tail adjacent nuclear genes (*RBCS1/2*) on chromosome 2. The nucleotide sequences of the two *RBCS* genes are highly similar and the peptides encoded by these two genes differ in only four amino acid residues. The *RBCS* promoters are strong and primarily constitutive. The *HSP70A-RBCS2* dual promoter (Schroda et al., 1999) has been used in various transgenic applications in *C. reinhardtii*. The small subunits are synthesized inside the cytoplasm and are imported into the chloroplast after cleavage of the transit peptide, and assembled into the Rubisco holoenzyme. The *C. reinhardtii* Rubisco crystal structure was solved by two groups almost simultaneously (Taylor et al., 2001; Mizohata et al., 2002).

In addition to its complex structure, Rubisco also undergoes extensive post-translational modifications on the large and small subunits (Houtz et al., 2008). In *C. reinhardtii*, posttranslational modifications on Rubisco include N^{α}-Methyl-Met^{S}-1 on the small subunit and the hydroxylation on Proline-104, -151 (4-Hydroxy-Pro^{L}-104 and -151) and the methylation of the two Cysteines residues (S^{γ}-Methyl-Cys^{L}-256 and -369) on the large subunit. The biological functions of those posttranslational modifications are largely unknown, but they might be involved in protection from degradation after import

into chloroplast (for example, N^{α}-Methyl-Met^{S}-1) or Rubisco holoprotein assembly. The Rubisco large subunit methyltransferase was identified in pea (*Pisum sativum*) as a SET-domain containing protein (Klein and Houtz, 1995; Ying et al., 1999; Raunser et al., 2009). In the *C. reinhardtii* nuclear genome, RMT1 (protein id: 516263) and RMT2 (protein id: 513361) were annotated as Rubisco large and small subunit methyltransferase respectively, based on sequence similarity to pea Rubisco methyltransferases. However, experimental data supporting this assignment is not yet available.

Pyrenoid

The name pyrenoid (from the Greek. pyrén - stone fruit, grain and eidos - form, shape; See Chapter 4, Figure 4.4, Figure 4.7), was first introduced by Schmitz in 1882 to describe a "dense, highly refractive, spherical body" inside the chloroplast in diatoms (Drum and Pankratz, 1964). Most eukaryotic photosynthetic algae have pyrenoids (Griffiths, 1970; Bold and Wynne, 1985). In land plants, pyrenoids are almost absent with a few exceptions in Anthocerotophyta (Griffiths, 1970). The number and the shape of the pyrenoid inside the chloroplast was used as one of the many features to classify species within the *Chlamydomonas* genus before the usage of a more modern classification system based on the 18S rRNA sequences (Harris et al., 2009). *C. reinhardtii* has a single, prominent, basally located pyrenoid, which can be distinguished by light microscopy. A combination of protein crosslinking reagents and staining reagents, such as $HgCl_2$-bromonophenol blue (Kuchitsu et al., 1988), is often used to make the observation of the pyrenoid easier.

In electron micrographs of a *C. reinhardtii* cell, the pyrenoid appears as an electron-dense microcompartment enclosed inside the chloroplast stroma. The pyrenoid

protein has been isolated, revealing that the dense matrix of the pyrenoid consists mainly of Rubisco (Kuchitsu et al., 1988; Ramazanov et al., 1994; Rawat et al., 1996; Morita et al., 1997; Borkhsenious et al., 1998). In cyanobacteria, Rubisco is located in the carboxysomes while in higher plants it is located throughout the chloroplast stroma. In *C. reinhardtii*, Rubisco activase has also been shown to be present in the pyrenoid (McKay et al., 1991).

For the majority of the algal species that have been investigated, the pyrenoid appears to not be surrounded by membranes derived from the chloroplast (Griffiths, 1970). The only exception of membrane bound pyrenoid was observed in certain diatoms (Drum and Pankratz, 1964; Holdsworth, 1968) where a membrane ridge was observed surrounding the pyrenoid. In *C. reinhardtii*, the matrix of the pyrenoid is surrounded by a network of modified thylakoid tubules (Griffiths, 1970). Under photoautotrophic conditions especially, the accumulation of the starch plates surrounding the pyrenoid is often observed, which helps define the pyrenoid boundary (Ramazanov et al., 1994; Henk et al., 1995). The biological role of the pyrenoid will be discussed in more detail in the following sections.

CO_2 Concentrating Mechanism (CCM)

As discussed earlier, Rubisco plays a significant role in the evolution of the on the planet in fixing inorganic carbon to generate organic compounds. When the enzyme first evolved, the CO_2 concentration in the atmosphere was abundant while there was no oxygen present. In this environment, the carboxylase activity of Rubisco was not competed by the oxygenase activity. However, in the present day atmosphere, where O_2 accounts for more than 20% while CO_2 only accounts for less than 0.04% of the

atmosphere. Thus, photosynthetic efficiency is greatly decreased by competition from the oxygenation reaction and the energy cost of recycling the product of this reaction – phosphoglycolate.

In order to overcome the problems with Rubisco, photosynthetic organisms developed CO_2 Concentrating Mechanisms (CCM) to increase the CO_2 concentration at the active site of Rubisco, to increase photosynthesis efficiency. Generally, the CCM could be divided into three parts: 1) A central compartment within which CO_2 can be enriched around Rubisco; 2) A biochemical pathway that can actively deliver inorganic carbon into the cells, and prevent it from diffusing back, and 3) A centrally located enzyme responsible for converting any accumulated carbon back to CO_2 for Rubisco fixation. Examples of a plant that successfully employs a CCM is the C4 plant. In a C4 plant, the central compartment containing Rubisco is the bundle sheath cell (Figure 2.1A). In algal CCMs, the central compartment is the carboxysome in cyanobacteria, and is thought to be the pyrenoid in *C. reinhardtii* (Figure 2.1B).

In C4 plants possessing Kranz Anatomy, the CO_2 molecules that diffuse through the stomata and enter the mesophyll cells are converted to HCO_3^- by a carbonic anhydrase located in the cytosol. The HCO_3^- is further combined with a C3 acid to form a C4 acid, which is then translocated into the bundle sheath cell. In the bundle sheath cell, the C4 acid is converted back to C3 acid, and the CO_2 released is immediately fixed by Rubisco. The C3 acid is then transported back to the mesophyll cells and the process starts again. About only 3% of all land plants are C4 plants, however, C4 plants contribute 20%-25%

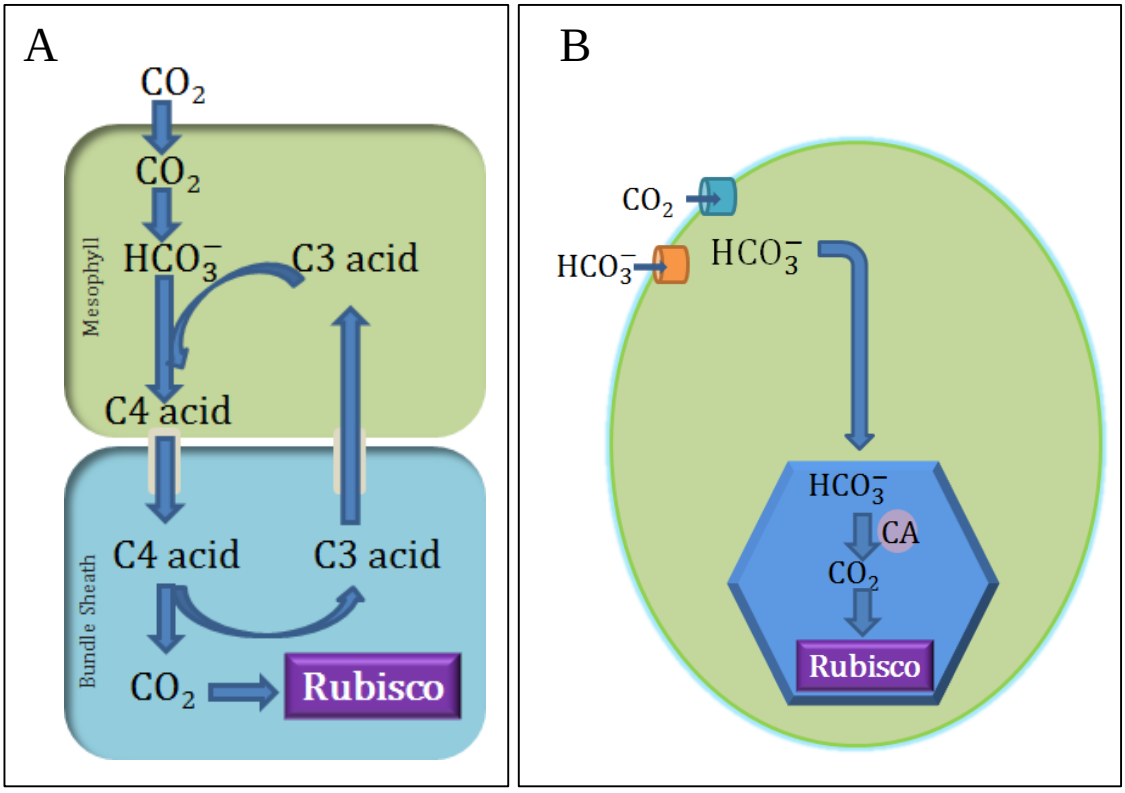

Figure 2.1. The CCM has evolved in C4 plants and in algae.

(A). In terrestrial plants, C4 plant is an example that possesses an active CCM. In the C4 pathway, a special Kranze Anatomy partitions Rubisco into the bundle sheath cell while CO_2 is trapped in the form of a C4 acid in the mesophyll cell. (B) While in the algal type CCM, CO_2 is trapped in the form of HCO_3^- by the cooperation of multiple carbonic anhydrases and Ci transporters. The accumulated HCO_3^- is converted back to CO_2 in the vicinity of Rubisco, by a centrally located carbonic anhydrase. The microcompartment where most of the Rubisco accumulate is the carboxysome in the cyanobacteria, or the pyrenoid in the *C.reinhardtii*.

of the global primary productivity (Sage, 2002) largely due to their increased radiation efficiency, reduced water loss and increased nitrogen use efficiency, especially when grown in arid areas (Hibberd et al., 2008).

CO_2 Concentrating Mechanism (CCM) in *C. reinhardtii*

In the algal type CCM, instead of fixing CO_2 into a C4 acid seen in the C4 pathway, CO_2 is accumulated as HCO_3^-, the charged C_i species (Figure 2.1B). This is somewhat analogous to the phosphorylation of glucose by hexokinase when glucose enters the cell. The charged phosphate group prevents the glucose from diffusing out of the cell. In the algae cell, the HCO_3^- is accumulated and then is converted back to CO_2 at the site of Rubisco by a co-localized carbonic anhydrase. It is generally thought that most algae, and all cyanobacteria express a CCM (Kaplan and Reinhold, 1999; Badger and Spalding, 2004; Giordano et al., 2005), although relatively few of the ~1500 described species of cyanobacteria, or ~53,000 described species of eukaryotic algae, have been examined for the existence of a CCM (Giordano et al., 2005; Bartlett et al., 2006). Studies using ^{13}C labeling have been done in many algae species and these ^{13}C documentations are consistent with the assumption that most of the aquatic photosynthetic organisms have a CCM. Among these, *Chlamydomonas reinhardtii* has been used as a model organism to study the details of CCM.

The study by Berry *et al*. (1978) for the first time demonstrated that a pre-incubation of *C. reinhardtii* cells in a low external CO_2 environment (330ppm) could increase the C_i affinity of the culture (Badger et al., 1980), and the photosynthetic kinetics of the low CO_2 acclimated cells resembled that of C4 terrestrial plants. In contrast, if the culture were incubated at high CO_2 conditions, a decreased C_i affinity was

observed and the photosynthetic kinetics of these cells closely resembled the C3 plant photosynthetic kinetics (Spalding, 2009). Later on, these findings were widely supported by a variety of other studies showing that the C_i uptake in *Chlamydomoans* is more active when cells are under low CO_2 stress (Badger et al., 1980; Spalding et al., 1983b; Moroney and Tolbert, 1985; Badger and Price, 1992). The hypothesis that the algal CCM is quite different than the CCM of the terrestrial C4 or CAM plants is well accepted. In addition, studies showed that the CCM in *C. reinhardtii* is inducible under limiting CO_2 conditions.

As mentioned previously, the model of a CCM can be divided into three parts, including a central location for Rubisco, a centrally located CA at the site of Rubisco, plus an active C_i delivery system (Figure 2.1). In the current *C. reinhardtii* CCM model (Figure 2.1B and Figure 2.2), the central location for Rubisco is hypothesized to be the pyrenoid. The centrally located CA is the CAH3 in the thylakoid lumen in the pyrenoid region (See *C. reinhardtii* CA section for details). This CA converts accumulated HCO_3^- to CO_2 at the site of Rubisco. The putative active delivery system incorporates inorganic carbon (CO_2, HCO_3^-, CO_3^{2-}) from the external environment to the inside of the cell, and traps the inorganic carbon as the charged species HCO_3^-.The delivery system can be further broken down into C_i transporters or channels, and carbonic anhydrases at each sub-cellular location (Figure 2.2). For simplicity, the following sections would be discussed in the order of pyrenoid, the C_i transporters, and the CAs.

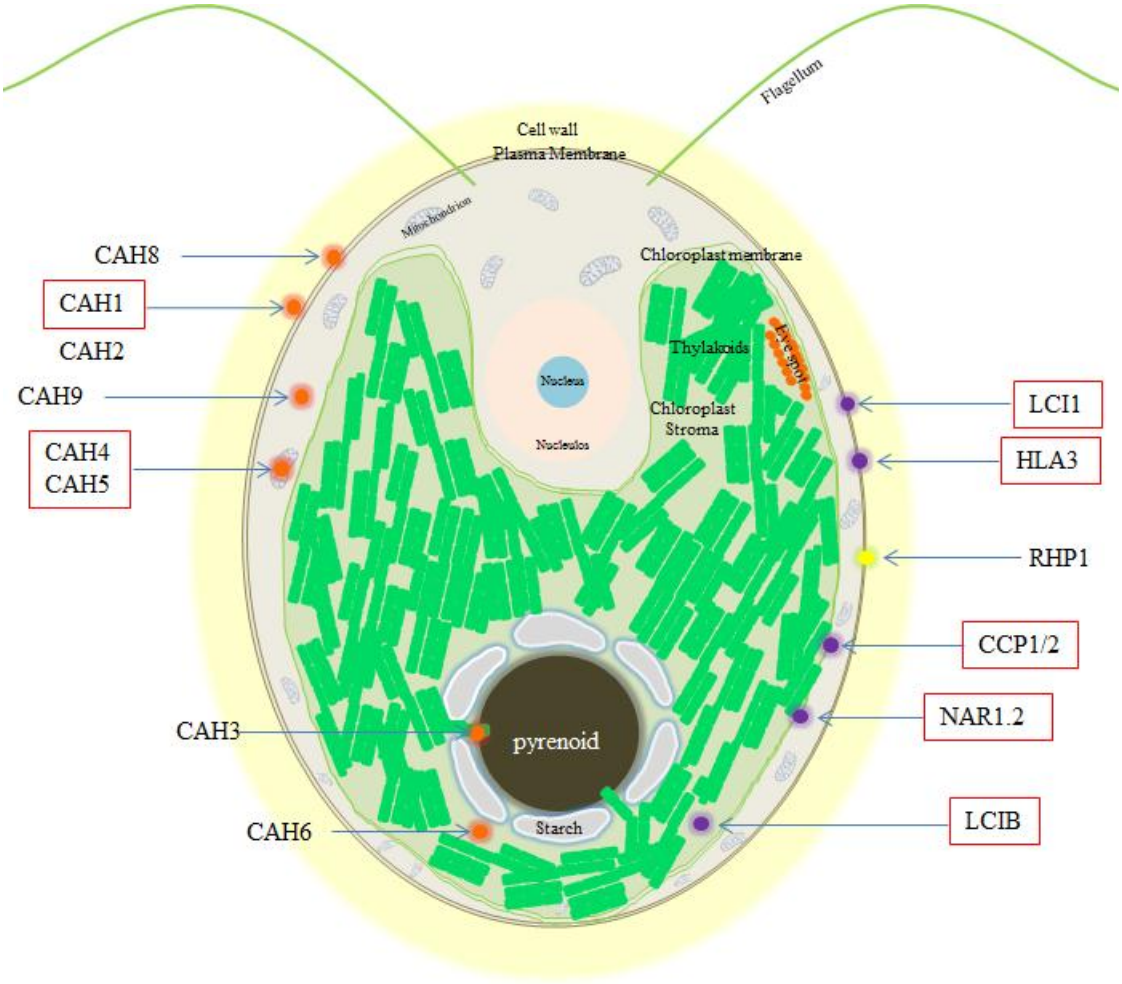

Figure 2.2. The CCM in *C.reinhardtii*.

The CCM in *C.reinhardtii* represents the cooperation between multiple enzymes and different subcellular locations in the cell. In *C.reinhardtii*, the pyrenoid houses most of the Rubisco in the cell. In the vicinity of Rubisco, a chloroplast thylakoid lumen located carbonic anhydrase (CAH3) assumes the role to convert any accumulated HCO_3^- to CO_2 for Rubisco fixation. A set of carbonic anhydrases at different locations help in converting CO_2 into HCO_3^-. A suite of C_i transporters that delivers HCO_3^- or CO_2 into the cells. This system is also inducible under limiting CO_2 condition. For the CCM components shown in here, the expression of most of the C_i transporters and a few CAs are depressed under high CO_2 conditions, while upregulated under low CO_2 conditions (highlighted with red squares).

1) Pyrenoid

The specific localization of Rubisco to the pyrenoid in *C. reinhardtii* is considered to be a key element in the optimal functioning of its CCM (Moroney and Ynalvez, 2007; Spalding, 2008; Yamano et al., 2010). Analogous to the packaging of Rubisco in cyanobacterial carboxysomes (Badger et al., 1998), the pyrenoid in *C. reinhardtii* could likewise be the location of the high CO_2 concentration generated by the CCM. Since this high CO_2 concentration is in the vicinity of Rubisco, the carboxylation reaction will be enhanced at the expense of the oxygenation reaction, hence reducing photorespiration. In the pyrenoid-containing hornworts, there is also good correlation between the operation of a CCM and the presence of a pyrenoid (Vaughn et al., 1990; Hemsley and Poole, 2004). Besides the role of compartmentalizing Rubisco away from the rest of chloroplast stroma, the dynamic nature of the pyrenoid in response to environmental changes adds extra complexity to the CCM. One notable observation made using immunolocalization was that in response to a switch from high CO_2 to low CO_2 environment, Rubisco in the wild-type chloroplast started to redistribute and accumulate in the pyrenoid after 2 hours in low CO_2 (Borkhsenious et al., 1998). The percentage of the pyrenoid-Rubisco labeling over the total labeling rose from 40% in high CO_2 grown cells to 90% within 4 hours on low CO_2. This process is tightly correlated with the time required for the appearance of a starch plate surrounding the pyrenoid (Henk et al., 1995), for the induction of most of the CCM genes (Miura et al., 2004) and for the maximal increase in Ci affinity (Borkhsenious et al., 1998). The rapid biochemical and morphological rearrangement indicates that the pyrenoid is a dynamic structure and is actively involved in the cell's acclimation to low CO_2 conditions.

One prediction based on the present CCM models is that, if the pyrenoid structure is disrupted, the CCM should also be adversely affected. However, among the few mutants with disrupted pyrenoid, either Rubisco was not present (Rawat et al., 1996), or chloroplast ribosomes were mutated leading to the absence of Rubisco (Goodenough, 1970), or the entire chloroplast structure was highly disrupted (Inwood et al., 2008). One piece of evidence supporting the role of the pyrenoid in an active CCM comes from a recent study by Genkov and his colleagues (Genkov et al., 2010). In their work, the *C. reinhardtii* Rubisco holoenzyme was engineered so that the *C. reinhardtii* native RbcL assembled with higher plants RbcS. Although the hybrid Rubisco had similar *in vitro* kinetic properties and was present in amounts equivalent to wild-type Rubisco, the resultant *C. reinhardtii* cells were found to lack the chloroplast pyrenoid, and failed to grow on low CO_2. This is strong evidence that the pyrenoid is playing an important role in the CCM. However, evidence that directly link the CCM and the pyrenoid was lacking since all the previous mutants characterized so far were deficient in Rubisco, which makes it impossible to measure the cell's CO_2 fixation kinetics.

2) Putative inorganic carbon (C_i) transporters

One difference between the habitats of land plants and aquatic algae is the inorganic carbon supply. For land plants, the only way that plants can fix inorganic carbon is to use CO_2 that passes through stomata or aquaporins (Hanba et al., 2004). For algae, on the other hand, the inorganic carbon in solution is constituted of CO_2, HCO_3^- and CO_3^{2-}, which are under dynamic equilibrium depending on the pH of the habitat (Equation 2.1). In environments where photosynthetic organisms are abundant, the pH is normally above the first pKa (pK_{a1}=6.3), resulting in CO_2 and HCO_3^- as the two dominant

species. Therefore, for most algae, CO_2 and HCO_3^- are considered to be the most relevant inorganic carbon species.

Equation 2.1 $$\mathbf{CO_2 + H_2O \overset{pK_{a1}=6.3}{\Longleftrightarrow} HCO_3^- + H^+ \overset{pK_{a2}=10.3}{\Longleftrightarrow} CO_3^{2-} + 2H^+}$$

In *C. reinhardtii,* both CO_2 and HCO_3^- need to cross the plasma membrane, chloroplast membrane, and the thylakoid membrane in order for the CCM to operate. This route dictates that transporters need to be present across multiple membranes. Although most of the C_i transporters in cyanobacteria have been characterized, there are only a few C_i transporters identified in *C. reinhardtii* that are directly linked to the CCM (Duanmu et al., 2009a; Ohnishi et al., 2010). Most of the C_i transporter candidates in *C. reinhardtii* were first recognized by their gene upregulation pattern under low CO_2 conditions (Burow et al., 1996; Chen et al., 1997; Im and Grossman, 2002; Miura et al., 2004). In the following section, the candidate proteins are listed in the order of subcellular locations based on either experimental data or *in silico* predictions.

a) HLA3, LCI1 and RHP1 on the plasma membrane

HLA3 is an ABC-type transporter of the multidrug-resistance-related protein family (MRP). It is predicted that HLA3 is targeted to the secretory pathway, and is presumably located on the plasma membrane. The decreased expression level of HLA3 by RNAi knockdown, combined with either LCIB mutants or with the simultaneous knockdown of *LCIA* (*NAR1.2*) mRNA, led to a severe growth defects and impaired C_i uptake (Duanmu et al., 2009b). LCI1 on the other hand, does not have identifiable domains except for the presence of four transmembrane domains. Homologues could only be found in *Chlorella*, *Coccomyxa*, and *Volvox*. The overexpression of LCI1 in the

lcr1 mutant background showed an increase in photosynthesis under limiting CO_2 conditions from high CO_2 acclimated cells, when the CCM is not usually induced naturally. It was also shown that LCI was mainly located on the plasma membrane (Ohnishi et al., 2010). The third plasma membrane protein, RHP1, is one of two homologs found in *C. reinhardtii* (RHP1, RHP2). The RHP proteins have 12 transmembrane domains and are similar to the Rhesus (Rh) proteins in the human red blood cell membrane. In *C. reinhardtii*, RHP proteins are predicted to be localized in chloroplast envelope although GFP-RHP1 fusion experiments indicated plasma membrane localization. The expression of *RHP1* appeared to be upregulated in high CO_2 conditions and the *RHP2* expression level was not detectable. The RNAi knockdown of *RHP1* resulted in growth defect in high CO_2 while no effects were seen in low CO_2 grown cells. Unlike the other components potentially involved in HCO_3^- transport, the RHP1 protein is thought to act as a CO_2 channel (Soupene et al., 2002; Soupene et al., 2004; Kustu and Inwood, 2006).

b) CCP1, CCP2, LCIA (NAR1.2), YCF10 on the chloroplast envelope

First identified as low CO_2 inducible proteins (Geraghty et al., 1990; Chen et al., 1997), the protein sequences of CCP1 and CCP2 are nearly identical (96%) and they belong to the mitochondria carrier (MTC) family (Chen et al., 1997). Both of them have six transmembrane domains, and were shown to be localized in the chloroplast envelope (Moroney and Mason, 1991; Ramazanov et al., 1993). The CCP1/2 RNAi strains were shown to have the typical CCM-deficient phenotype but no obvious decrease in Ci fixation was observed (Pollock et al., 2004). LCIA (NAR1.2) belongs to the formate/nitrite transporter family. Electrophysiology studies using *Xenopus laevis*

oocytes overexpressing *LCIA* mRNA were consistent with bicarbonate uptake (Mariscal et al., 2006). Unlike the other putative C_i transporters, YCF10 is encoded by a chloroplast gene *ycf10*. YCF10 has two to three transmembrane domains, and has been localized in the chloroplast envelope (Sasaki et al., 1993). A mutant with an insertion in the *ycf10* gene showed decreased C_i uptake (Rolland et al., 1997).

c) LCIB protein family in the chloroplast stroma

The LCIB family includes the proteins LCIB, LCIC, LCID, and LCIE in *C. reinhardtii*. These small proteins to date have no identifiable domains or transmembrane domains. They seem to be green algae specific since the homologies can only be found in *Ostreococcus taurii*, *O. Lucimarinus* and *Volvox cateri* (Wang and Spalding, 2006; Grossman et al., 2007). Evidence that indicated the LCIB is involved in C_i transport comes from the LCIB mutant studies (*pmp1* and *ad1*) that showed an interesting "air-dier" phenotype, and a low C_i uptake. However, the lack of transmembrane domains suggests that the LCIB might interact with some other membrane proteins to function in C_i delivery.

3) Carbonic anhydrase

Carbonic anhydrases (CAs, carbonate dehydratase; EC 4.2.1.1) are important components of CCM. CAs are zinc-metalloenzymes that catalyze the reversible interconversion of CO_2 and HCO_3^- in two steps (Lindskog, 1997). Many have turnover numbers in excess of 10^6 s^{-1} (Khalifah, 1973). The overall reaction catalyzed by a CA is shown below (Equation 2.2):

Equation 2.2 $$CO_2 + H_2O \leftrightarrow H_2CO_3 \leftrightarrow HCO_3^- + H^+$$

a) CA families

There are currently at least six CA families (α, β, γ, δ, ε, ζ). All CA families require zinc at the active site. However, there is no significant sequence homology between families and they appear to be examples of convergent evolution of catalytic function. A brief description of each family is given below.

α-Carbonic Anhydrases - The α-CAs are widely distributed and are found in vertebrates (Meldrum and Roughton, 1933), algae (Fujiwara et al., 1990; Fukuzawa et al., 1990a), higher plants (The Arabidopsis Genome Intiative, 2000; Moroney et al., 2001; Tuskan et al., 2006) and eubacteria (Soltes-Rak et al., 1997; Chirica et al., 2001; Elleby et al., 2001). Most α-CAs are active as monomers of about 30 kDa with three histidines coordinating the zinc atom (Moroney et al., 2001).

β-Carbonic Anhydrases - The β-CAs were first identified as carbonic anhydrases in higher plants (Burnell et al., 1990; Fawcett et al., 1990). Subsequently, β-CAs have been found in micro-algae (Eriksson et al., 1996), eubacteria (Hewett-Emmett and Tashian, 1996), archaebacteria (Smith and Ferry, 1999) and fungi (Götz et al., 1999). This CA family does not appear to be represented in any vertebrate genome. β-CAs have a histidine and two cysteine residues that act as zinc ligands (Bracey et al., 1994; Rowlett et al., 1994), and are usually active as dimers or multimers. In the *Pisum sativum* CA, dimers form tetramers which are held together by their C-termini to form octamers (Kimber and Pai, 2000). An active site is formed at the interface of two subunits.

γ-Carbonic Anhydrases - A γ-CA was first discovered in the archaebacterium *Methanosarcina thermophila* (Alber and Ferry, 1994). Since that time, genes encoding putative γ-CA proteins have been found in eubacteria and plants (Newman, 1994). The γ-

CA functions as a trimer containing three zinc atoms, one at each subunit interface. Recent work has indicated that γ- or γ-like CAs are part of Complex I of the mitochondrial electron transport chain in plants and algae (Sunderhaus et al., 2006; Klodmann et al., 2010).

δ-Carbonic Anhydrases - To date, δ-CAs have only been described in some diatoms (Roberts et al., 1997). Like the first three CA families, the δ-CA families appears to be a case of convergent evolution with almost no sequence similarity with the α-, β- or γ- CA types (Roberts et al., 1997).

ε-Carbonic Anhydrases - This CA family is limited to bacteria containing β-type carboxysomes (So et al., 2004; So and Espie, 2005). The active site of ε-CAs resembles the β-CAs with a histidine and two cysteine residues acting as zinc ligands (So et al., 2004). However, this type of CA is part of the carboxysome shell and has additional domains that serve this function (Tanaka et al., 2008). This class of CA has not been found in eukaryotes.

ζ-Carbonic Anhydrases - This CA gene family, also limited to marine protists, somewhat resembles the β-CA family (Lane and Morel, 2000; Lane et al., 2005; Park et al., 2007). What separates this CA family from the β-CA family is that other metals such as Cd or Co can substitute for Zn family (Lane and Morel, 2000; Lane et al., 2005; Park et al., 2007).

b) CAs in *C. reinhardtii*

In *C. reinhardtii* there are at least 12 genes that encode CA isoforms, including three alpha (*CAH1*, *CAH2*, *CAH3*), six beta (*CAH4*, *CAH5*, *CAH6*, *CAH7*, *CAH8*, *CAH9*)

and three gamma or gamma-like CAs (*CAG1*, *CAG2*, *CAG3*). Within these CA genes, a few cases of apparent gene duplication can be seen. The α-CAs, CAH1 and CAH2, are extremely closely related, showing only a few amino acid differences (Fujiwara et al., 1990; Fukuzawa et al., 1990a). In addition, these two genes are adjacent to each other on chromosome 4, forming a tandem repeat (http://genome.jgi-psf.org/Chlre4/Chlre4.home.html). It appears that *CAH2* might be the result of a gene duplication event. The expression of the CAH2 is also at a minimal level under any tested growth condition. The other α-CA, CAH3 (Funke et al., 1997; Karlsson et al., 1998) is quite different from CAH1 and CAH2.

The most complex CA gene family in *C. reinhardtii* is the β-CA family with six members (Mitra et al., 2005; Ynalvez et al., 2008). Two sets of these genes are quite closely related. First of all, *CAH4* and *CAH5* are 95% identical at the nucleotide level (Eriksson et al., 1996) and form an inverted repeat on chromosome 5 (http://genome.jgi-psf.org/Chlre4/Chlre4.home.html). Both genes are transcribed outwards from the center of the repeat, and like *CAH1* and *CAH2*, the two genes are likely the result of a gene duplication event. In addition, *CAH7* and *CAH8* are closely related (Ynalvez et al., 2008). These two genes, located on different chromosomes, code unusual CAs in that CAH7 and CAH8 have long C-terminal extensions (Ynalvez et al., 2008). With different N-terminal sequences, the proteins encoded by CAH7 and CAH8 may be directed to different subcellular localizations. The other two β-CA genes, *CAH6* and *CAH9*, are quite different from each other. The sequence of CAH9 is notable. The CAH9 sequence significantly diverges from the other β-CAs in *C. reinhardtii*.

The γ-CA genes, *CAG1*, *CAG2* and *CAG3*, align well with each other and also align well with γ-CAs from higher plants. The three γ-CA genes in *C. reinhardtii* are all on different chromosomes.

With so many CA isoforms, *C. reinhardtii* has CAs in many different subcellular compartments. The α–CA, CAH3, was found to be localized in the thylakoid lumen (Karlsson et al., 1995; Karlsson et al., 1998), serving the essential role to convert HCO_3^- to CO_2 at the site of Rubisco. One of the first CCM mutants obtained was *ca1* (Spalding et al., 1983a) which lacks the protein CAH3 (Funke et al., 1997). Other alleles of CAH3 were obtained (Moroney et al., 1986) and in all cases mutants lacking CAH3 have a very notable growth phenotype: the ability to grow photoautotrophically on elevated levels of CO_2 but exhibit poor growth under low CO_2 conditions (Spalding et al., 1983a; Spalding et al., 1983b; Moroney et al., 1986; Karlsson et al., 1998). This phenotype can be complemented by putting a wild type copy of *CAH3* genomic DNA back into the cell (Funke et al., 1997; Karlsson et al., 1998). In our current model (Figure 2.2), CAH3 is responsible for the increased concentration of CO_2 in the chloroplast by converting HCO_3^- to CO_2 in the relatively acidic environment of the thylakoid lumen (Raven, 1997; Karlsson et al., 1998; Rojdestvenski et al., 2000). In this model, HCO_3^- is brought into the thylakoid lumen in the light and the HCO_3^- is converted to CO_2 by CAH3. The CO_2 generated by CAH3 would leak from the lumen of the thylakoid to the pyrenoid region, where it is fixed by Rubisco.

The location of CAH1 and CAH2 has been known to be in the periplasmic region for almost two decades (Fujiwara et al., 1990; Fukuzawa et al., 1990b). In the current

CCM model in *C. reinhardtii*, this pair of CAs is mainly involved in facilitating the diffusion of C_i to the plasma membrane.

The first β-CAs CAH4 and CAH5 were found to be associated with mitochondria (Eriksson et al. 1995 and 1996). Recently using immonolocalization, the CAH4 and CAH5 were confirmed to be localized inside the mitochondria (Moroney et al., 2011). Like CAH3, CAH6 is localized to the chloroplast (Mitra et al., 2004). However, CAH6 is present in the chloroplast stroma instead of the thylakoid lumen. Immunogold labeling experiments show that CAH6 is within the chloroplast stroma (Mitra et al., 2004). However, we do not know whether CAH6 is freely soluble within the chloroplast stroma or is associated with some other protein complex or the thylakoid membrane. In addition, the immunogold labeling also appears stronger around the perimeter of the pyrenoid in some micrographs but it is not clear whether this increase in immunogold particles near the pyrenoid is significant. In light of the recent localization studies on LCIB, this question has increased in significance (Wang and Spalding, 2007; Yamano and Fukuzawa, 2009). There have also been unpublished reports that CAH6 might be bound to the thylakoid in some manner. If this were the case, the association with the thylakoid membrane would likely be through some protein-protein interaction, as CAH6 does not have a hydrophobic transmembrane helix. In summary, while the localization of CAH6 to the chloroplast is well-documented, further studies need to be done to determine whether CAH6 is associated with the pyrenoid or bound to the thylakoid membrane.

CAH7 and CAH8 are β-CAs with unusual C-terminal extensions (Ynalvez et al., 2008). So far, no solid data for the localization of CAH7 have been reported. CAH8 appears to be associated with the plasma membrane by immunolocalization studies

(Ynalvez et al., 2008). The last CA gene to be discovered was *CAH9* and the protein encoded by *CAH9* is the least characterized CA isoform. CAH9 is a small protein, leaving no room for a leader sequence without compromising the active site of the protein. An antibody against CAH9 has not been reported, so localization studies have no yet been done.

The γ-CAs, CAG1, CAG2 and CAG3 belong to the final group of CA isoforms. By analogy to work done with higher plants, these proteins are expected to be associated with Complex I of the mitochondrial electron transport chain, found in the inner mitochondrial membrane (Sunderhaus et al., 2006; Braun and Zabaleta, 2007; Klodmann et al., 2010). Proteomic studies done with *C. reinhardtii* are fully consistent with the higher plant work as all three γ-CAs have been found in association with Complex I. Cardol and colleagues have conducted proteomic studies on whole *C. reinhardtii* mitochondria (Cardol et al., 2005), as well as the mitochondrial electron transport complexes (Cardol et al., 2004). All three of the γ-CAs were found in the mitochondrial proteome and the Complex I fraction (Cardol et al., 2004; Cardol et al., 2005). This would place the CA domain exposed to the mitochondrial matrix, where most of the CO_2 would be generated by the processes of mitochondrial respiration and photorespiration.

4) Photorespiration

a) <u>Photorespiration</u>

Photorespiration is the light-dependent O_2 uptake and CO_2 release in all the photosynthetic organisms (Tolbert, 1997; Tural and Moroney, 2005). The oxidative photorespiration CO_2 release (C2 Cycle) combined with the reductive photosynthetic CO_2

assimilation (Calvin Cycle or C3 Cycle), contributes to a substantial portion of the carbon metabolism in the biosphere (Maurino and Peterhansel, 2010). This phenomenon was first known as the "Warburg effect" in which the presence of O_2 inhibits photosynthesis (Warburg, 1919). Biochemically, photorespiration is initiated by the oxygenation of the five carbon sugar RuBP, producing a two carbon compound phosphoglycolate, through the oxygenase activity of Rubisco. The process in which this two carbon compound is recycled is termed photorespiration and the pathway is called the C2 Cycle. This pathway is achieved by multiple enzymatic steps and coordinated between different subcellular locations. Ultimately the pathway metabolizes two molecules of phosphoglycolate into one molecule of 3-PGA that can re-enter the Calvin Cycle. Additionally, if the phosphoglycolate is not metabolized, it would inhibit the Calvin Cycle enzyme triosephosphate isomerase (Anderson, 1971) or the glycolytic enzyme phosphofructokinase (Kelly and Latzko, 1976). By detoxifying phosphoglycolate and recycling it, photorespiration serves an important role in photosynthesis especially in a low CO_2 environment.

Multiple organelles participate in photorespiration (Kisaki and Tolbert, 1969). The first step, phosphoglycolate dephosphorylation, occurs in the chloroplast, by the action of phosphoglycolate phosphatase (PGP). The resulting glycolate then can be relocated into the other organelles for further metabolism. In higher plants, glycolate is transported into the peroxisome and is converted to glyoxylate by glycolate oxidase (GOX). Glyoxylate is trans-aminated into glycine by the action of glyoxylate aminotransferases while the glycolate oxidation byproduct H_2O_2 is degraded by catalase (CAT). The newly formed glycine is then transported into the mitochondrion. Glycine

decarboxylase complex (GDC) splits one molecule of glycine into one molecule of CO_2 and one molecule of NH_3, which could be re-assimilated by Calvin Cycle and GS/GOGAT system respectively in the chloroplast. The byproduct of the glycine decarboxylation, 5,10-methylenetetra-hydrofolate is used by serine hydroxymetyltransferase (SHMT) to convert another molecule of glycine into serine. Serine is then returned into the peroxisome to be metabolized into hydroxypyruvate, and subsequently to glycerate. The transport of glycerate into the chloroplast and phosphorylation into 3-phosphoglycerate completes the photorespiration process.

b) Photorespiration in *C. reinhardtii*

One of the noteworthy differences between the photorespiratory pathways in higher plants and *C. reinhardtii* lies in the enzyme that converts glycolate into glyoxylate (Figure 2.3). In higher plants, glycolate oxidase catalyzes the conversion of glycolate into glyoxylate and H_2O_2 in the peroxisome. However, in *C. reinhardtii* where peroxisomes have not been identified to date, it is accepted that the cells convert glycolate to glyoxylate by the action of glycolate dehydrogenase (GDH) in the mitochondrion using NAD^+ as the electron acceptor. The rest of the reactions are in the mitochondria and chloroplast (Nelson and Tolbert, 1970; Beezley et al., 1976; Suzuki and Spalding, 1989; Nakamura et al., 2005; Tural and Moroney, 2005). In *C. reinhardtii*, glycolate dehydrogenase (GDH) activity was previously observed in the mitochondria fraction (Beezley et al., 1976). An insertional mutant (*hcr89*) lacking the glycolate dehydrogenase activity exhibited the classic sick on low CO_2 phenotype, and no glycolate oxidation from the mutant membrane fraction was detected (Nakamura et al., 2005). The mitochondrial localization of the glycolate dehydrogenase was further confirmed by a recent proteomics

Figure 2.3. Photorespiratory Pathway of *C.reinhardtii*.

In *C.reinhardtii,* photorespiration occurs in two subcellular locations, the chloroplast and the mitochonria. In the chloroplast, the Rubisco oxygenation product 2-PG is first dephosphorylated to glycolate by the activity of PGP. Glycolate is then translocated into the mitochondrion, where it is converted into Glycerate by the cooperation of series of enzymes. During this process, NH_3 is produced and is assimilated by the GS/GOGAT system in the chloroplast and CO_2 could be utilized by Rubisco. Glycerate is translocated into the chloroplast where it is phosphorylated by the action of GLYK yielding the final product of 3-PGA which re-enters the Calvin Cycle. For the key photorespiration enzymes, only PGP and GDH has its own corresponding mutants, and arer highlighted in purple. RubBP: Ribulose-1,5-bisphosphate; 3-PGA: 3-Phosphoglyceric acid; 2-PG, 2-phosphoglycerate (phosphoglycolate); CH2-THF: 5,10-Methylenetetrahydrofolate; PGP: Phosphoglycolate phosphatase; GDH: Glycolate Dehydrogenase; AAT1: Alanine: Glyoxylate aminotransferase; GDC: Glycine decarboxylase complex; SHMT: serine hydroxymethyltransferase; SGAT: serine:glyoxylate aminotransferase; HPR: hydroxypyruvate reducatse; GLYK: Glycerate kinase;

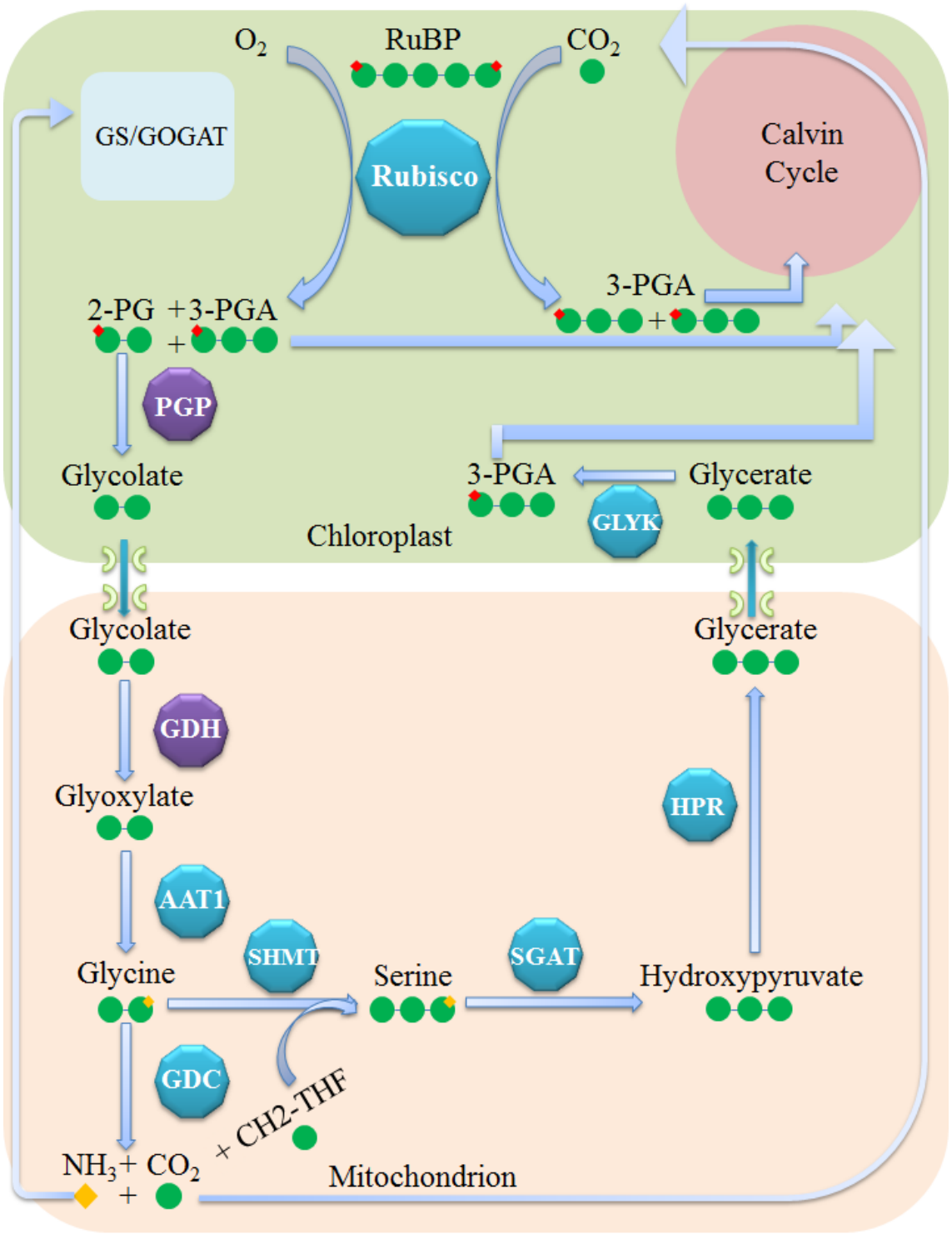
O2
RuBP
CO2
GS/GOGAT
Rubisco
Calvin
Cycle
2-PG +3-PGA
+
3-PGA
+
PGP
Glycolate
3-PGA
Glycerate
GLYK
Chloroplast
Glycolate
Glycerate
GDH
Glyoxylate
HPR
AAT1
SHMT
SGAT
Glycine
Serine
Hydroxypyruvate
GDC
+ CH2-THF
NH3+ CO2
+
Mitochondrion

study (Atteia et al., 2009). On the other hand, there is indication of the presence of glycolate oxidase homologues (GYX1) in the *C. reinhardtii* genome based on sequence similarities (Chauvin et al., 2008). However, studies by Hackenberg et al. showed that the GYX1 preferred lactate over glycolate as the oxidation substrate. Thus the *C. reinhardtii* glycolate oxidase homologue is likely to be a lactate oxidase (Hackenberg et al., 2011).

Most of the core enzymes involved in the photorespiratory pathway have been identified (Foyer et al., 2009; Bauwe et al., 2010) and most of the photorespritory pathway mutants identified showed a typical sick on low CO_2 phenotype. The first photorespritory mutant identified from Arabidopsis lacked the phosphoglycolate phosphatase activity, and exhibited a sick on low CO_2 phenotype. This indicated that the conversion from phosphoglycolate to glycolate is part of the photorespiration pathway, and photorespiration is needed for growth in a low CO_2 environment (Somerville and Ogren, 1979). Two decades later, the last photorespiratory enzyme glycerate kinase that connects the C2 cycle and C3 cycle, was identified and a mutant of glycerate kinase showed a typical photorespiratory mutant phenotype (Boldt et al., 2005).

In *C. reinhardtii*, most photorespiratory gene homologues could be found in the genome. For example, hyroxypyruvatereductase (HPR), serine:glyoxylateaminotransferase (SGAT) (Tural and Moroney, 2005), and the glycerate kinase (Boldt et al., 2005). However, the characterization of the photorespiratory genes is limited to a few genes including, phosphoglycolate phosphatase (Suzuki et al., 1990; Mamedov et al., 2001), glycolate dehydrogenase (Nakamura et al., 2005), alanine:α-ketogluterate aminotransferase (Chen et al., 1996) and serine hydroxymethyltransferase

(Im and Grossman, 2002). Among these, only mutants of *PGP1* and *GDH* have been characterized, and both mutants indeed showed the sick on low CO_2 phenotypes.

Photorespiration serves as an ancillary carbon recovery system for the primary photosynthesis process, especially when CO_2 is limiting. In *C. reinhardtii*, the expressions of *PGP1* (Mamedov et al., 2001), *AAT1* (Chen et al., 1996), *SHMT* (Im and Grossman, 2002) , *SGAT*, *HPR*, *GDH* (Tural and Moroney, 2005), GLYK, GYD1, and SGAT (Fang et al., 2012) were shown to increase under low CO_2 conditions, indicating the close relation with the induction of the CCM genes. However, the low CO_2 response pattern of the photorespiratory genes is different than the CCM genes. Most of the investigated photorespiratory genes showed a transient and rapid upregulation within the first two hours (Marek and Spalding, 1991; Chen et al., 1996; Tural and Moroney, 2005) while most of the CCM genes were observed to be long-lasting. The difference in the duration of upregulation is understandable, since photorespiration is required mainly to remove the Rubisco oxygenation product phosphoglycoate. When the CCM is fully induced, the oxygenation reaction of Rubisco could be minimized, thus reducing the requirement for the photorespiratory pathway enzymes. In *C. reinhardtii* and higher plants, although most of the core photorespiratory pathway enzymes have been identified and characterized, gaps such as the understanding the photorespiration regulation and signaling and transport of metabolites between different organelles still remain.

Endnotes

Descriptions from Carbonic Anhydrase (page 21-26) are adapted from Moroney et al., (2011).

Descriptions from Pyrenoid (page 16-17) are adapted from Ma et al., (2011a)

CHAPTER 3
MATERIALS AND METHODS

Cell Cultures and Growth

C. reinhardtii culture conditions were similar to those described previously (Rawat and Moroney, 1991). The wild-type strain D66 (CC-4425, *nit1-*, *nit2*$^{-}$, *cw15*, *mt*$^{+}$) was obtained from Rogene Schnell (University of Arkansas, Little Rock), and strain *cia5* was maintained by Dr. J. V. Moroney's laboratory (Moroney et al., 1989). The wild-type strain 137^{+} was obtained from Robert Togasaki (Indiana University, Bloomington). The *pgp1* mutant strain (CC-2648, pgp1-18-7F), wild-type strains 2137, CC-124 (*nit1*$^{-}$, *nit2*$^{-}$, *mt*$^{-}$) and CC-503(*nit1*$^{-}$, *nit2*$^{-}$, *cw92*, *mt*$^{+}$), were obtained from the *Chlamydomonas* Duke University Stock Center (http://www.chlamy.org/). The wild-type C9 was a gift from Dr. Hideya Fukuzawa (Kyoto University, Kyoto, Japan). For a complete genotype for the strains above, see Appendix I.

Tris–acetate–phosphate (TAP) and minimal (without acetate) liquid medium were prepared according to Sueoka (Sueoka, 1960). TAP plates and minimal media plates were prepared by adding 1.2% agar (w/v). Cells were first grown mixotrophically on TAP medium and then transferred to minimal medium for phototrophic growth and bubbled with either 0.01% (v/v) CO_2 for low CO_2 condition, or air containing 5% CO_2 (v/v), for high CO_2 conditions, with continuous shaking and light (100 µE m^{-2} s^{-1}).

For testing the growth phenotype at different pH, equal numbers of cells from each strain were spotted on agar plates containing minimal medium maintained at different pH levels with the help of the following buffers; 25 mM MES (for pH 5.8 and 6.2), 25 mM MOPS (pH 7.2) and 25 mM HEPES (pH 8.2). The plates were then exposed

to high CO_2 and low CO_2 conditions for 7 days under constant illumination of 100 µmol photons m^{-2} s^{-1}. To induce the CCM, one flask was switched from high CO_2 to low CO_2 (0.01% [v/v] CO_2 in air) bubbling for one day or otherwise as indicated in the text; the other flask was kept on high CO_2 as the control.

C. reinhardtii Mutagenesis and Electroporation

To generate the high CO_2 requiring mutant *cia6* described in Chapter 4, the wild-type strain D66 was mutagenized by transformation with a linearized pSP124s plasmid (Lumbreras et al., 1998) using the electroporation procedure described by Shimogawara et al. (1998) with modifications described by Colombo et al (2002). Transformants were first selected on TAP plates containing the antibiotic zeocin (7.5 µg mL^{-1}, Invitrogen, Carlsbad, CA). Antibiotic resistant strains were then screened for a CCM deficient phenotype in a low CO_2 chamber (0.01% [v/v] CO_2 in air) in light (100 µE m^{-2} s^{-1}).

To generate mutants for the PCR-based reverse genetics screen described in Chapter 7, the general procedure was similar with the above procedure. Strain D66 was mutagenized by transformation with the Paromomycin resistance gene cassette (*AphVIII*) from plasmid pSL18 (Depege et al., 2003) by electroporation (Shimogawara et al., 1998). The plasmid pSL18 was digested with KpnI-HF (High-Fidelity Enzymes, NEB, Ipswich, MA) and XhoI-HF (NEB, Ipswich, MA) to obtain the 1813bp *AphVIII* cassette, containing the *Hsp70+RbcSII* dual promoter, the *AphVIII* ORF, and the *RbcSII* terminator. Transformants were selected on TAP plates containing the antibiotic Paramomycin (5 µg mL^{-1}, Invitrogen, Carlsbad, CA). For the detailed mutagenesis protocol used in Chapter 7, see Appendix III.

Nucleic Acid Preparations

For small scale plasmid DNA isolation, either standard alkaline lysis followed by ethanol precipitation (Sambrook et al., 2001), or a commercial plasmid mini-prep kit (Qiagen, Chatsworth, CA) were used. For large scale plasmid DNA isolation, both the commercial plasmid max-prep kit (Qiagen, Chatsworth, CA) and a home-made preparation method were used (Refer to Appendix III for details).

Three different methods were used to prepare *C. reinhardtii* genomic DNA. The first two methods were used to obtain large amounts of DNA. The third method was used in Chapter 7 for colony DNA analysis. The first method used to isolate genomic DNA was according to Newman *et al*. (1990). The second method was developed in William Snell's laboratory at UT Southwestern Medical Center (personal communication). The details of the first method can be found in the Ph.D. dissertation of Ruby Ynalvez (Ynalvez, 2007). The details of the second method can be found in Appendix III. The second method is recommended for future experiments due to its relatively higher quality of DNA and ease in handling. The third method for *C. reinhardtii* colony DNA analysis was according to Steve Pollock's "Quick and Easy Genomic Prep" (http://www.chlamy.org/methods/quick_pcr.html) with a few modifications. Refer to Appendix III for details.

Total RNA was extracted from *C. reinhardtii* using Trizol reagent (Invitrogen, Carlsbad, CA), following the manufacture's protocol with a few modifications. Southern blots were carried out following the guidelines in Sambrook et al., (2001). Briefly, equal amounts of restriction enzyme digested DNA were loaded and separated on a 0.8% (w/v) agarose gel and blotted onto a nylon membrane (Schleicher & Schull, Keene, NH). ^{32}P-

dCTP-labeled probes were prepared using a random primer procedure (Sambrook et al., 2001).

For Quantitative RT-PCR analysis, RNA was first extracted using Trizol reagent following guidelines provided by the manufacture (Invitrogen, Carlsbad, CA). Contaminating DNA was removed by DNase treatment (Roche Applied Science, Indianapolis, IN) and total RNA was further purified using an RNeasy kit (Qiagen, Chatsworth, CA). Total RNA was used for cDNA synthesis following the manufacture's instruction (Roche Applied Science, Indianapolis, IN) using Poly (dT) primers. Synthesized cDNA was then subjected to Quantitative RT-PCR analysis using Sybr Green Premix (Takara, Shiga, Japan) and an ABI 7000 Real Time PCR System (Applied Biosystem, Foster City, CA).

Protein Analysis

To isolate total protein from *C. reinhardtii* cells for electrophoresis, the algal cultures were harvested and washed with TE buffer (10mM Tris-HCl, 10mM EDTA, pH=7.5). The protein content from the concentrated cell resuspension was then quantified based on chlorophyll a/b measurement, using 1:10 ratio of chlorophyll: protein.

Rubisco holoenzymes from *C. reinhardtii* cells were according to the method from Spreitzer and Mets (1980). Briefly, 1L TAP grown stationary cells were harvested, and were resuspended in freshly prepared sonication buffer (1mM DDT, 5mM $MgCl_2$, 10mM $NaHCO_3$, 50mM Tris, pH=7.5, with protease inhibitors). Cell resuspensions were sonicated and centrifuged at 27,000g (15,000rpm, JA18.1 rotor) for 15 minutes. The supernatant from all sonication tubes were combined and were layered onto a sucrose

gradient, followed by ultracentrifugation at 37,000rpm, overnight with the SW-41 rotor at 4 ℃. The overnight centrifuged sucrose gradient was then fractioned at 0.5-1mL fractions. The Rubisco enriched fraction was checked by SDS-PAGE. Further purification was performed using $(NH_4)_2SO_4$ precipitation followed by dialysis, or Amicon filter (30MLW, Millipore, Billerica, CA) device followed by acetone precipitation. The last purification method was used for preparing samples for 2-D electrophoresis. Rubisco protein content was measured by either Bradford assay (Biorad, Hercules, CA) or by using a bovine serum albumin as a standard on a coomassie blue stained SDS-PAGE gel.

For western blots, equal amounts of protein samples were loaded in each lane. Proteins were separated on 12% or 15% polyacrylamide gels (0.8% bisacrylamide) as described previously (Laemmli, 1970). Immunoblotting was performed as described in the protocol from BioRad Laboratories (Hercules, CA).

Identification of Flanking Regions and Genetic Linkage Analysis

Adaptor-mediated PCR was used to identify the DNA flanking the pSP124s insertion using a modified version of the Genome Walker TM kit (Clontech, Mountain View, CA). Homology searches were performed using the BLAST server (Altschul et al., 1997), and the Joint Genome Institute *C. reinhardtii* database V4.0 site (Merchant et al., 2007). Genetic crosses and tetrad analysis were performed as previously described (Sears et al., 1980; Moroney et al., 1986; Harris et al., 2009). Briefly *cia6* (mt^+) and CC124 (mt^-) cells cultures were subjected to nitrogen starvation in high light overnight and combined for mating for one hour. Aliquots (0.3mL) were plated on nitrogen-minus minimum medium containing 4% nitrogen-depleted agar and stored in the dark for zygote maturation for 10 days. The zygotes on the maturation plates were transferred to 1.2%

agar TAP medium plates and incubated overnight for meiotic germination. Tetrad dissections were then carried out and linkage was determined by association of the Bleomycin resistance with those progeny that grew poorly on low CO_2 levels.

Photosynthesis Assays

Cultures were started heterotrophically in 100 mL of TAP media. After reaching log phase, the cultures were then transferred to 1 L minimal medium and bubbled with 5% CO_2 until they reached a cell density of about $3x10^6$ cells mL^{-1}. The cultures were then subjected to CCM induction overnight. The affinity for external inorganic carbon, $K_{0.5}$ [DIC] was estimated as described by Pollock and Colman (2001). Briefly, cells containing 100µg chlorophyll were suspended in CO_2 free HEPES buffer (pH=7.3), which was previously bubbled with N_2. The cell suspension was transferred to the electrode chamber (Rank Brothers, Cambridge, UK) and was allowed to deplete any endogenous DIC until no net O_2 exchange was observed. The DIC concentrations of the medium were controlled by injecting $NaHCO_3$ solution into the chamber. The light intensity for photosynthesis assay was adjusted at 300 µE m^{-2} s^{-1}.The $K_{0.5}$ [DIC] value is calculated where the DIC concentration required for half-maximal rates of oxygen evolution (Badger, 1985).

Complementation

Complementation of the mutant strain *cia6* was achieved by transforming *cia6* cells with the entire *CIA6* genomic region using the glass bead method (Kindle, 1990). Briefly, cells were grown to $3x10^6$ cell mL^{-1} in 100 mL TAP before transferring to 1 L minimum medium bubbled with air till the cell density reaches $2x10^6$ cell mL^{-1}. Transformation was started by mixing 0.3 mL cell suspension ($3x10^8$ cell mL^{-1}), 300 mg

sterilized glass beads, 5 μg DNA and 0.1 mL 20% PEG. The mixture was then agitated at top speed in a 15 mL tube for 15 seconds. After beads settled to the bottom, the cell suspension was plated onto minimal media plates and maintained in low CO_2 chamber (70ppm CO_2 in air). Colonies that were able to grow heterotrophically under low CO_2 conditions were examined using light microscopy to screen for the strains with a pyrenoid. RNA was then extracted from putative complemented strains to confirm the reappearance of the full length *CIA6* mRNA.

CIA6 Overexpression and in vitro Methyltransferase Assay

CIA6 was cloned into the pMAL-c2x overexpression vector, downstream of the MalE gene that encodes for the maltose-binding protein (MBP) according to the manufacture's protocol (NEB, Ipswich, MA) and Ynalvez (2007). Primers 5'-BamHI-F 5'-*CGC GGA TCC* ATG GCT GAC -3' and 3'- HindIII-R 5'- *CCC AAG CTT* CTA CTT TCG CCC -3' were used to amplify the 2.1-kb CIA6 ORF, using the high fidelity enzyme Phusion (NEB, Ipswich, MA). The pMal-c2x plasmid was double digested with BamHI and HindIII sequentially followed by ligation and *E. coli* transformation. The transformation was performed using the DH5α host strain, by heat shock (Sambrook et al., 2001). Transformants were screened on 2XYT+Ampicillin (100 $\mu g \cdot mL^{-1}$) plates. In-frame insertion of the *CIA6* fused with MBP was verified by DNA sequencing.

The *E. coli* containing the pMal-CIA6 plasmid was grown under normal conditions (2XYT+Ampcilin, 37℃ overnight), with the supplement of glucose to repress the expression *E. coli* chromosomal amylase. Otherwise, the amylase would hydrolyze amylose used in the following amylose affinity resin purification procedure. The cells were induced for three hours with 1mM Isopropyl β-D-1-thiogalactopyranoside (IPTG)

when the culture OD_{600} is between 0.5-0.6. After induction, the cells were harvested and resuspended in column buffer (20mM Tris-HCl (pH=7.4), 200mM NaCl, 1mM EDTA, 1μg/mL leupeptin, 0.2mM PMSF (phenylmethanesulfonylfluoride)). The cell resuspension was then sonicated and centrifuged to remove the cell debris. The supernatant that contained the MBP-CIA6 protein was then diluted with 5X volume of the column buffer. Six milliliter of the amylose resin was washed with 30 mL column buffer and the diluted supernatant was then poured into the column, followed by washing with 72 mL column buffer. The purification procedure was completed by the final elution with 10 mL elution buffer (9 mL Column buffer + 1mL 100mM maltose), with 1 mL fraction size. Purified recombinant fusion proteins were further concentrated by passing through an Amicon filter (100MLW, Millipore, Billerica, CA). Protein concentration was measured by Bradford assay or by visualization on a SDS-PAGE gel.

For the *in vitro* methyltransferase assay, the Pea Rubisco large subunit methyltransferase (LSMT) was used as a positive control. This LSMT overexpressing strain was a gift from Dr. Spreitzer (Klein and Houtz, 1995; Ying et al., 1999; Raunser et al., 2009). The methyltransferase assay was performed according to the protocol from Dr. Spreitzer's laboratory. Briefly for one reaction, 2.75 μL 0.7mCi/mL ^{3}H AdoMet mix was made. The mix was prepared by mixing 0.19 μL of the radio labeled ^{3}H AdoMet (1.0mCi/mL, 12-18Ci/mmol, PerkinElmer, Waltham, MA), 0.23 μL of the unlabeled purified AdoMet (around 3mM, gift from Dr. Spreitzer's laboratory), plus 2.33 μL dH_2O. A 20μL reaction mix included 2μL of Bicine buffer (1M, pH=8.0), 2μL of $MgCl_2$ (20mM), 2μL of the above AdoMet mix, 45μg of *C. reinhardtii* Rubisco, and 5μg of the purified CIA6-MBP protein. For the control reaction, *C. reinhardtii* Rubisco was

replaced with equal amount of Spinach Rubisco and CIA6-MBP was replaced with equal amount of LSMT. The 20μL reaction mix was incubated at 37 °C water bath for 10 minutes before terminated by the addition of 500 μL 10% TCA (Trichloroacetic acid, Fisher Scientific, Waltham, MA). The reaction was mixed by vortexing and waited for 2-3 minutes on ice for protein to precipitate. It was then centrifuged in the bench-top centrifuge for 3 minutes in the cold room. The supernatant was carefully aspirated off. The pellet was dissolved in 150 μL 0.1M NaOH with shaking, followed by another cycle of TCA washing and precipitation. The reprecipitated pellet is then dissolved in 50 μL formic acid in the hood. Into this mix, 50 μL H_2O and 1.25 mL scintillation cocktail (National Diagnostics, Atlanta, GA) was added. The entire mix was mixed by vortexing until the cloudiness became clear. The remaining radio labeled ^3H AdoMet was counted by the scintillation counter (Beckman LS1801).

Immunolocalization Studies Using Electron Microscopy

Immunolocalization was performed as described previously {Mitra, 2004 #76}. Briefly, about 2 mL cell suspension was fixed with an equal volume of 1% OsO_4, 2% formaldehyde, 0.5% glutaraldehyde, and 0.1 mM sodium cacodylate buffer (pH=7.2) for 30 minutes. The solution was then extracted into a 10mL syringe with a Swinney filter holder fitted with a 13 mm diameter 5 μm pore polycarbonate filter and fixed for another 30 min, followed by five times of 15 minutes washes with 0.1 M cacodylate buffer containing 0.02 M glycine. Materials were rinsed with distilled water and stained with 0.5% uranyl acetate in the dark for 30 minutes. After this, excess cells were rinsed and the samples were dehydrated using an ethyl alcohol series. Samples were then infiltrated and embedded in LR White resin (EMS, PA). Embedded samples were sectioned with a

DuPont Sorvall microtome (Wilmington, DE) to 70 nm. TEM sections were mounted on collodion coated nickel grids.

The immunocytochemical procedure was similar to the method of Borkhsenious et al., (1998) with some modifications. Sections were pretreated with 2% sodium-meta-periodate (Sigma, St. Louis, MO) for 15 minutes to remove any residual glutaraldehyde, then blocked two times for 30 minutes in blocking solution (2% BSA and 0.1% Tween-20 in PBS). The sections were incubated for 90 minutes with Rubisco antibody (1:50) or with the preimmune serum with the same dilution. The grids were transferred to 1:50 dilution of gold labeled Protein-A (20nm, Sigma, St. Louis, MO) for one hour. Antibodies were all diluted in blocking solution. Finally, the sections were rinsed with distilled water and photographed under transmission electron microscopy.

The fraction of Rubisco in the pyrenoid and in the chloroplast stroma was measured as previously described (Borkhsenious et al., 1998). Except that the pyrenoid area was excluded from the total chloroplast stroma. The immunogold particle density in the pyrenoid (D_p, $\#\cdot\mu m^{-2}$) was first calculated by dividing the total number of immunogold particles in the pyrenoid by the area of pyrenoid. Similarly, the immunogold particle density in the chloroplast stroma (D_s, $\#\cdot\mu m^{-2}$) was calculated by dividing the total number of immunogold particles in the chloroplast stroma by the total area of chloroplast stroma. The total immunogold particles in the pyrenoid or stroma were then calculated by multiplying the immunogold density (D) averaged from 25 TEM thin sections and the average volume of each compartment (Lacoste-Royal and Gibbs, 1987). The fraction of Rubisco in the pyrenoid ($Fraction_p$) was further calculated by dividing the total particles

in the pyrenoid by the total number of particles from pyrenoid and chloroplast stroma. The final equation is shown below:

$Fraction_p = 100 \times [Dp \times 2.4 / (Dp \times 2.4 + Ds \times 35.6)]$; where D = (number of particles)/(area)

Other methods

The CO_2 concentration in the growth chambers was measured using an infrared gas analyzer (The Analytical Development Co. Ltd, Hoddesdon, England). The *C. reinhardtii* growth curve experiments were standardized based on chlorophyll content ($1.9 \mu g \cdot mL^{-1}$) and approximately the same cell density. Chlorophyll content was measured as the total content from chlorophyll a plus chlorophyll b (Arnon, 1949; Holden, 1976). Chlorophyll was extracted in 100% methanol and was quantified spectrophotometrically (Arnon, 1949) and calculated according to Holden (Holden, 1976). Cell density values were determined by direct counting in a hemacytometer chamber (Hausser Scientific, Horsham, PA). For pyrenoid staining and observation using light microscopy, *C. reinhardtii* cells were stained with 0.05% bromophenol blue (BPB) in 0.1% $HgCl_2$ (Kuchitsu et al., 1988).

CHAPTER 4
IDENTIFICATION AND CHARACTERIZATION OF A *CHLAMYDOMONAS REINHARDTII* PYRENOIDLESS MUTANT *CIA6*[1]

Introduction

Most aquatic photosynthetic organisms have a CO_2 concentrating mechanism (CCM) that increases the CO_2 concentration around the carboxylating enzyme Rubisco when CO_2 is limiting (Badger et al., 1998; Giordano et al., 2005; Moroney and Ynalvez, 2007). Two problems faced by organisms with CCMs are the potential leakage of CO_2, which can readily cross most biological membranes, and the rate of diffusion of CO_2 in water which is 10^4 times slower than in air. Since HCO_3^- crosses biological membranes at about 10^{-6} times the rate of CO_2(Gutknecht et al., 1977), a strategy that concentrates HCO_3^- would greatly minimize the loss of inorganic carbon. The cyanobacterial CCM adopts a system that concentrates HCO_3^- in the cytoplasm using a series of HCO_3^- transporters, and packages Rubisco in a proteinaceous structure called the carboxysome (Price et al., 2008). The HCO_3^- accumulated in the cytoplasm could then diffuse into the carboxysome through carboxysomal pores, be converted to CO_2 by carboxysomal carbonic anhydrases (CAs) and finally be fixed by Rubisco (Price et al., 2008). The importance of the carboxysome in the cyanobacterial CCM is illustrated by the fact that the ectopic expression of carbonic anhydrase in the cyanobacterial cytosol short circuits the CCM; the HCO_3^- in the cytosol is converted into CO_2 that diffuses out of the cell without fixation (Price and Badger, 1989).

In the eukaryotic green alga *C. reinhardtii*, the CCM appears to have strong similarities to the cyanobacterial system (Moroney and Ynalvez, 2007). In *C. reinhardtii*,

1. Copyright American Society of Plant Biologists. Reprinted by permission

bicarbonate is concentrated in the chloroplast stroma through the cooperation of multiple C_i transporters and carbonic anhydrases. Rubisco is packaged in a specialized chloroplast micro-compartment, called the pyrenoid, where active C_i fixation takes place (Borkhsenious et al., 1998). In the pyrenoid of *C. reinhardtii*, Rubisco is the predominant protein (Kuchitsu et al., 1988; Morita et al., 1997; Borkhsenious et al., 1998) and nonsense mutations in the Rubisco large subunit totally abolish the formation of the pyrenoid (Rawat et al., 1996). The pyrenoid in *C. reinhardtii* is also penetrated by a network of thylakoid tubules (Henk et al., 1995; Borkhsenious et al., 1998). The carbonic anhydrase, CAH3, in the thylakoid lumen is further enriched in the thylakoid tubules inside the pyrenoid (Karlsson et al., 1995; Karlsson et al., 1998; Mitra et al., 2005). Mutants that lack CAH3 have a non-functional CCM in which HCO_3^- accumulates intracellularly, but the mutant cells cannot grow on low or very low levels of CO_2 (Spalding et al., 1983a; Moroney et al., 1986; Pronina and Semenenko, 1992; Karlsson et al., 1998). In addition, a putative C_i transporter, LCIB, is localized around the pyrenoid (Yamano et al., 2010). Mutants with defects in LCIB's expression results in the unusual "air-dier" phenotype, that dies at air level of CO_2 but survives under low CO_2 (Wang and Spalding, 2006; Duanmu et al., 2009a).

A number of current models have proposed that the pyrenoid is critical to the optimal function of the CCM in *C. reinhardtii*, with the structure serving a role similar to the cyanobacterial carboxysomes (Morita et al., 1999; Moroney and Ynalvez, 2007; Spalding, 2008; Yamano et al., 2010). However, very few mutations affecting pyrenoid structure have been described. Among the few reports, Rawat *et al.* (1996) demonstrated that the loss of Rubsico in *C. reinhardtii* resulted in the loss of the pyrenoid. Recently,

Genkov and his colleagues described the creation of *C. reinhardtii* strains with hybrid Rubiscos (Genkov et al., 2010), in which a higher plant (spinach, Arabidopsis, and sunflower) small subunit gene (RbcS) was transformed into a *C. reinhardtii* RbcS mutant background. The resultant *C. reinhardtii* strain contained hybrid Rubisco with native RbcS and higher plant Rubisco large subunit (RbcL). However, strains containing the hybrid Rubisco could not grow as well as wild-type cells at low CO_2 levels. Strikingly, in the resultant *C. reinhardtii* strains, although the catalytic properties of the hybrid Rubisco were similar to wild-type Rubisco, and the Rubisco was expressed, it was found that these strains lacked pyrenoids as well as an active CCM.

In this report, we describe a novel mutant of *C. reinhardtii* in which a disruption in a nuclear gene other than in Rubisco resulted in a disrupted pyrenoid structure and a high-CO_2 requiring phenotype. This work provides further evidence that the organization of pyrenoid itself is important in the functioning of the CCM.

Results

cia6 Needs a High CO_2 Environment to Grow Optimally

C. reinhardtii strain D66 (Schnell and Lefebvre, 1993) was transformed with the pSP124s plasmid which contains the modified Ble^R cassette conferring bleomycin resistance (Lumbreras et al., 1998). 42,000 Ble^R insertional mutants were selected and screened for a high CO_2-requiring phenotype (Colombo et al., 2002; Pollock et al., 2003). Strains that could grow well on elevated CO_2 but grew slowly on low CO_2 were subsequently tested for their ability to accumulate inorganic carbon. One of those transformants also had a reduced ability to accumulate inorganic carbon and was named

cia6. Figure 4.1 shows the photoautotrophic growth characteristics in high (Figure 4.1A) and low (Figure 4.1B) CO_2 environments of the parent strain, D66; the insertional mutant, *cia6;* and a known high CO_2 requiring mutant, *cia5*, a strain defective in a transcription factor and fails to induce the CCM (Moroney et al., 1989). In high CO_2 conditions, all three strains displayed similar growth characteristics. However, in the low CO_2 environment, compared to the D66 strain which displayed growth pattern similar to the one under high CO_2 conditions, the *cia6* mutant grew poorly as did the CCM-defective strain, *cia5*. The results presented here showed that *cia6* requires an elevated CO_2 environment to grow photoautotrophically.

cia6 Has a Reduced Affinity for C_i

To determine the apparent affinity of *cia6* cells for inorganic carbon (C_i), the rate of photosynthesis as a function of the dissolved inorganic carbon (DIC) concentration was determined. When grown on high CO_2, D66, *cia5*, and *cia6* all had maximum photosynthesis rates of greater than 100 μmoles CO_2 fixed per mg chlorophyll per hour. However, *cia5* and *cia6* had affinities for DIC that were 1.5 to 2 times lower than D66 (Table 4.1, Figure 4.2A). Air-acclimated cells also exhibited similar maximum rates of photosynthesis, but in contrast, both *cia5* and *cia6* had an affinity for DIC approximately 10 times lower when compared to D66 cells (Table 4.1, Figure 4.2B). The rate of photosynthesis was also lower in air-grown *cia6* compared to wild type at low DIC concentrations. In order to measure the ability of *cia6* to accumulate inorganic carbon, light-dependent C_i uptake was estimated using the silicone oil centrifugation method (Figure 4.2C). The amount of C_i accumulation by *cia6* was one-fifth that of D66 during a60 second time course. In summary, these photosynthetic characteristics led to naming

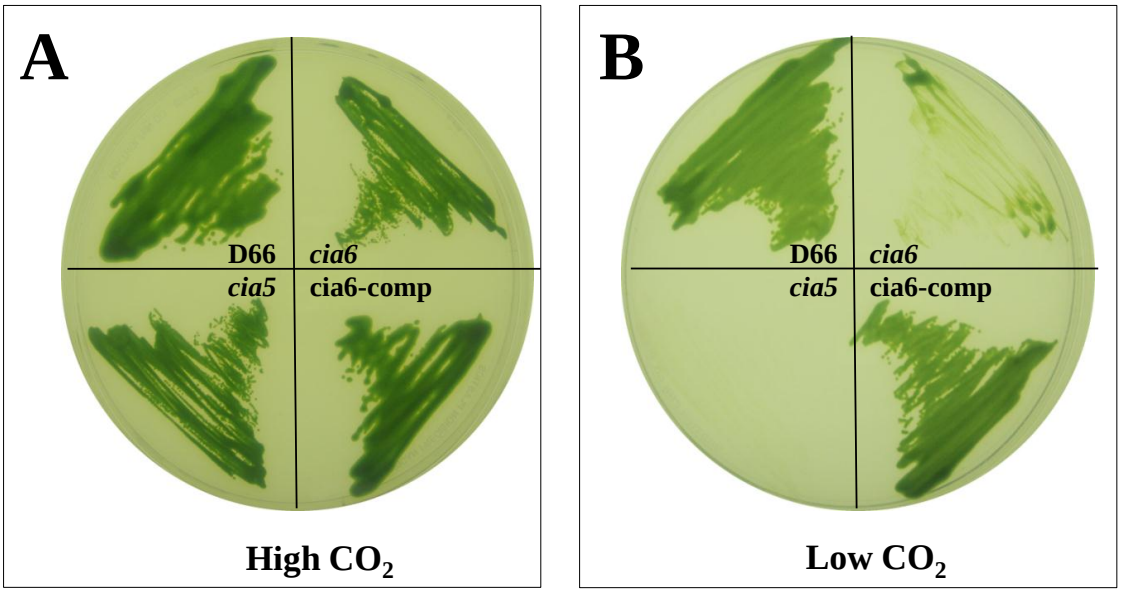

Figure 4.1. The mutant *cia6* demonstrated a typical CCM deficient phenotype.

The ability of *cia6* to grow photoautotrophically was tested by comparing its growth on minimum plates under high CO_2 (5% CO_2 [v/v], panel A) and very low CO_2 (0.01% CO_2 [v/v], panel B) conditions. A, *cia6* grew well in high CO_2 compared to its parental strain D66. B, *cia6* grew poorly under low CO_2 condition, similar to the CCM deficient mutant *cia5*. The complemented *cia6*, cia6-comp, in which the wild-type *CIA6* gene was put back into *cia6*, exhibited a phenotype similar to that of the wild-type D66.

Table 4.1. The $K_{1/2}$ (DIC) value of cia6-comp was recovered to the wild-type level.

Strain / Conditions	D66	*cia6*	*cia5*	cia6-comp
High CO_2	179±23	296± 24	444±46	106±8
Low CO_2	29±7	106±17	138±26	25±1

$K_{1/2}$(DIC) value is calculated by regression analysis from three individual experiments using Michaelis–Menten kinetics equation: $V=V_{max}[S]/(K_m+[S])$, in which [S] equals to the bicarbonate concentration, V equals to the oxygen evolution rate at each bicarbonate concentration, V_{max} equals to the maximum oxygen evolution rate when bicarbonate concentration is saturated, K_m equals to $K_{1/2}$(DIC).

this mutant *cia6* for inorganic carbon accumulation deficient mutant following the nomenclature described by Moroney *et al* (1986).

***cia6* Has an Insertion in a Novel Gene**

Southern blot analysis of *cia6* showed that a single insertion event had taken place during transformation as evidenced by a single intense hybridization band in *cia6* genomic DNA digested with different restriction enzymes that do not have cleavage sites within the predicted transgene (Figure 4.3A). Using an adaptor-mediated PCR strategy (Siebert et al., 1995), the DNA flanking one side of the pSP124s insert was cloned and sequenced. Comparison of this sequence with the Joint Genomics Initiative's *C. reinhardtii* genome sequence database (Merchant et al., 2007) yielded a match to a region on chromosome 10. No ESTs were aligned with this region. However, the gene structure prediction programs Genewise (http://www.ebi.ac.uk/Tools/Wise2/index.html) and GeneMark (http://exon.biology.gatech.edu/) identified putative open reading frames in this region of the chromosome. Using primers designed to bracket this region, a cDNA was amplified using RNA from wild-type cells as the template. RACE was employed to obtain a full length cDNA and DNA sequencing verified its identity. The *CIA6* gene consists of 5 exons spanning 2.9 kb (Figure 4.3B, GenBank Accession Number: JF288753). Subsequent sequence analysis demonstrated that the Ble^R cassette insertion disrupted the third exon. Primers spanning the Ble^R insertion (Figure 4.3B) were utilized to determine whether the *CIA6* mRNA was present in high and low CO_2 grown D66 and *cia6*, and primers amplifying glyceraldehyde 3-phosphate dehydrogenase (*GAPDH*) were used as an internal control (Figure 4.3C). In D66, the *CIA6* message was present in both high and low CO_2-grown cells, while the message was absent in *cia6*. Tetrad analysis

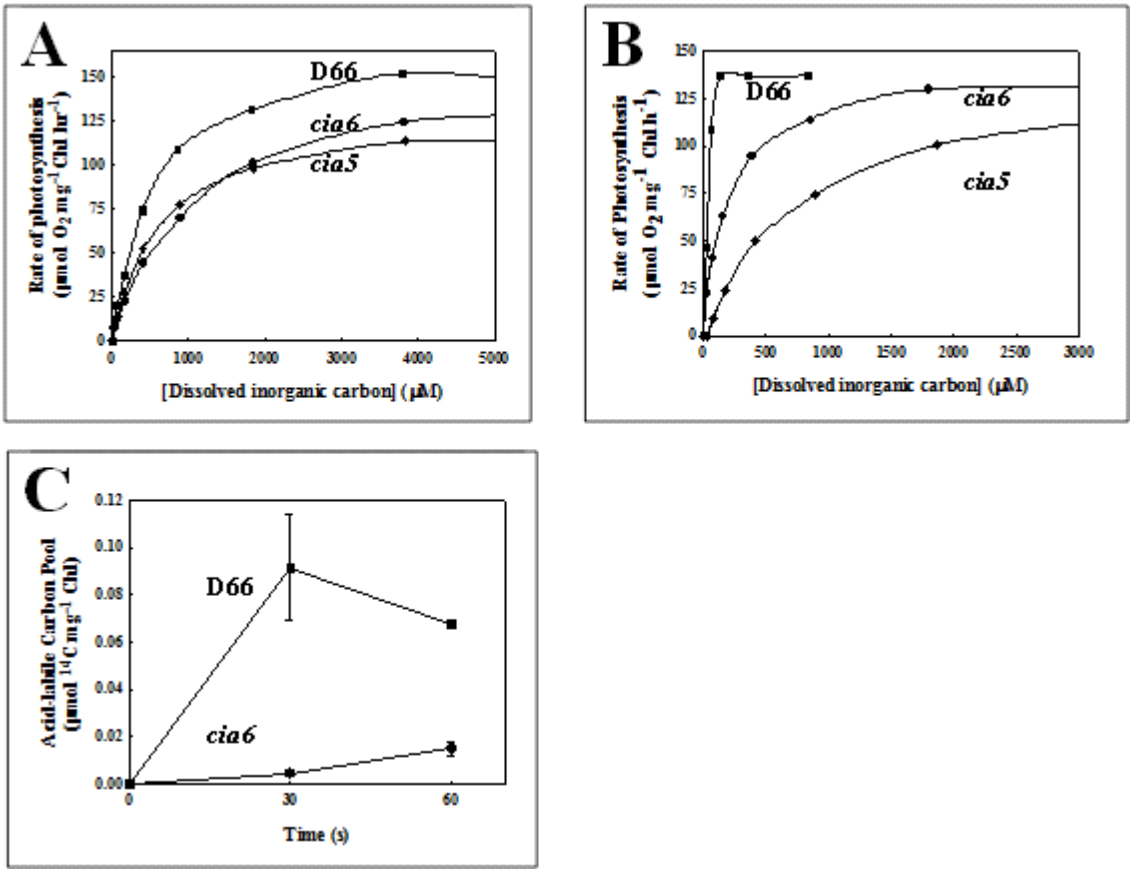

Figure 4.2. **The mutant *cia6* showed a reduced affinity for C_i.**

A and B, The rates of photosynthesis of D66 (■), *cia6* (●), and *cia5* (♦) as a function of the dissolved inorganic carbon concentration (DIC) for high CO_2 grown (A) and low CO_2 grown (B) cells were measured. C, The C_i accumulation in low CO_2 acclimated D66 (■) and *cia6* (●) was measured during the time course of ^{14}C-DIC accumulation. Each point represents the mean and standard error of three separate experiments.

confirmed the linkage between the CCM deficient phenotype and the *Ble*^{R} insertion (data not shown). These results are consistent with the hypothesis that the single pSP124s insertion disrupted the *CIA6* locus and abolished the transcription of *CIA6*.

cia6 Has a Disorganized Pyrenoid

In *C. reinhardtii*, the pyrenoid is a spheroid, electron-dense, Rubisco containing body inside the chloroplast (Figure 4.4A and 4.4B where the pyrenoid is labeled as "P"). The pyrenoid is penetrated by numerous thylakoid membranes and is estimated to occupy a volume of 2.4 μm^3, approximately 1/16 of the entire chloroplast (Griffiths, 1970; Lacoste-Royal and Gibbs, 1987). In Transmission Electron Microscopy (TEM) thin sections, a normal spherical pyrenoid is encountered in about 35% of wild-type cell thin sections (Henk et al., 1995). During the cell's acclimation to a low CO_2 environment, the pyrenoid undergoes dramatic structural changes as a ring of starch accumulates around the pyrenoid (Figure 4.4B where the starch sheath is labeled as "s"). Using TEM, *cia6* mutant cells were examined and were shown to have disorganized pyrenoids in both high CO_2-grown (Figure 4.4C where possible pyrenoid region was labeled as "*") and low CO_2 grown (Figure 4.4D where possible pyrenoid region was labeled as "*") cells. In contrast to the normal spheroid shaped, electron-dense pyrenoid with an average of 2.3μm^2 in area seen in wild-type cells (Figure 4.4A and 4.4B), it was revealed that the pyrenoid was either absent or highly disorganized in all the *cia6* ultra-thin cell sections examined. Although the electron-dense region could still be observed in the mutant cells, it was significantly smaller in size with an average of 1.2 μm^2, highly irregular in shape and often associated with the starch sheath. Over 100 *cia6* cell thin sections were observed, but no normal pyrenoid could be detected in *cia6*. Under light microscopy

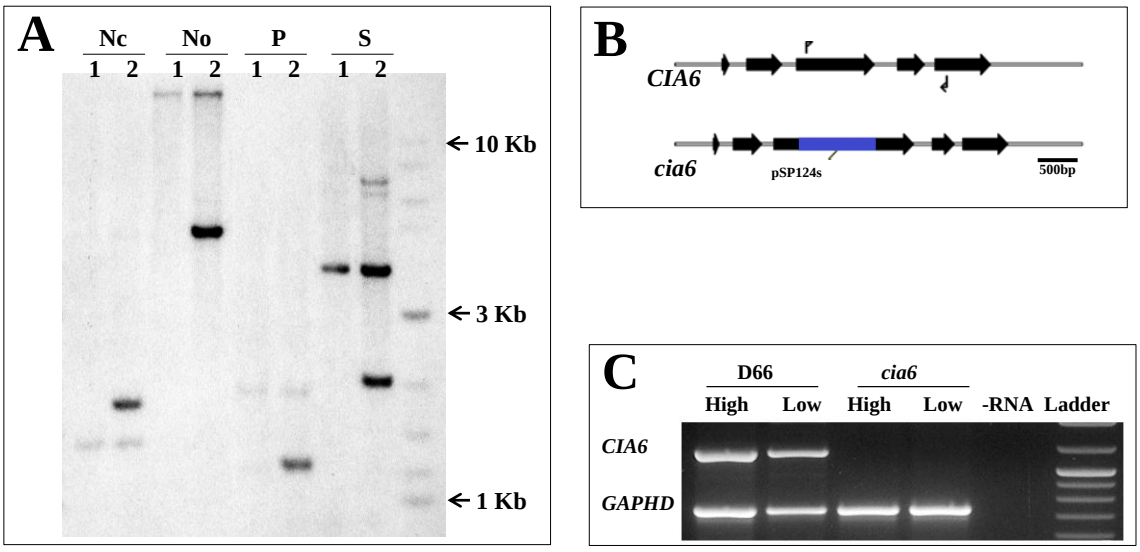

Figure 4.3. **The mutant *cia6* has an insertion in the *CIA6* locus.**

A, Southern blot analysis using the bleomycin resistance gene as a probe. D66 (1) and *cia6* (2) genomic DNA was digested with NcoI (Nc), NotI(No), PstI(P), and SacI(S) and blotted onto a nylon membrane. The membrane was then probed with a ^{32}P-labeled pSP124s specific fragment containing *Ble*^{R} DNA and the *RBCS2* intron. The weak bands present in both D66 and *cia6* correspond to the *RbcS2* intron, which is present in both the Ble^{R} mutant as well as the endogenous *RbcS2* gene. B, Genomic structure of the *CIA6* locus in wild-type and *cia6* showing the introns and exons, the site of the pSP124s insertion in *cia6*, and the cDNA primer sites (arrows) used for the RT-PCR analysis in figure 3C. C, RT-PCR analysis of the D66 and *cia6* strains using polyA RNA from high and low CO_2 grown cells as templates for reverse transcription. The primer-binding sites for *CIA6* are shown in figure 3B and amplify an 1100 bp product from cDNA. The internal control fragment (730 bp) is the product of primers designed to amplify Glyceraldehyde-3-phosphate dehydrogenase (GAPDH). The last lane contains the NEB 2-LOG ladder.

(100X), however, the possible presence of small pyrenoid-like structures was observed in the *cia6* mutant cells, and oftentimes multiple small pyrenoids were observed inside the chloroplast of a single cell (Figure 4.4E and 4.4F).

<u>*cia6* Can Be Complemented</u>

To confirm whether the *CIA6* mutation is responsible for the CCM deficient phenotype and the disorganized pyrenoid, complementation was attempted by transforming a 3.7kb genomic DNA fragment containing the wild type *CIA6* locus into the *cia6* mutant. *cia6* cells were transformed and selected under very low CO_2 conditions (70 ppm) on minimum plates. A total of 49 transformants that survived under very low CO_2 conditions were further examined for the restoration of the pyrenoid as observed under light microscopy. Twenty-two out of 49 transformants selected in this manner showed positive pyrenoid staining as indicated by strong staining using the $HgCl_2$-bromonophenol blue (BPB) reagent (Kuchitsu et al., 1988) in the pyrenoid and nucleus. One transformant, named cia6-comp was selected for analysis of growth and photosynthetic kinetics. Under both high and low CO_2 conditions, cia6-comp grew as well as the wild-type cells (Figure 4.1), showing that the growth defects had been complemented. Figure 4.5A shows that the complemented *cia6* had a higher affinity for C_i as compared to the mutant. The calculated affinity of cia6-comp for DIC ($K_{1/2}$(DIC)) was also close to the wild-type level (Table 4.1). In addition, the RNA sample isolated from cia6-comp also showed that the *CIA6* mRNA is recovered in the complemented strain, based on RT-PCR analysis (Figure 4.5B). The recovery of the WT pyrenoid structure (Figure 4.4G and 4.4H) together with the restoration of its C_i concentrating

Figure 4.4. **Pyrenoids in *C.reinhardtii* cells.**

Electron micrographs (A-D, F and H) and light micrographs (E and G) of *C.reinhardtii* cells grown in minimum medium in high (A and C) and low CO_2 (B and D, E-H) conditions. A, Wild-type D66 grown under high CO_2 conditions. B, Wild-type D66 grown under low CO_2 conditions. C, Mutant *cia6* grown under high CO_2 conditions. D, Mutant *cia6* grown under low CO_2 conditions. E, Light microscopes of *cia6* cells showing multiple pyrenoid or pyrenoid-like structure (labeled as "*") in the *cia6* observed under light microscope. F, Electron micrographs showing multiple pyrenoid or pyrenoid-like structures (labeled as "*") in the *cia6* observed under electron microscope. G, Pyrenoid (labeled as "P") and nucleus (labeled as "N") is observed as dark stainings in the complemented *cia6* grown under low CO_2 conditions. H, A positive pyrenoid in the complemented cia6 grown under low CO_2 conditions. P, pyrenoid; N, nucleus; s, starch; *, indicates the location of pyrenoid like bodies in mutant cells.

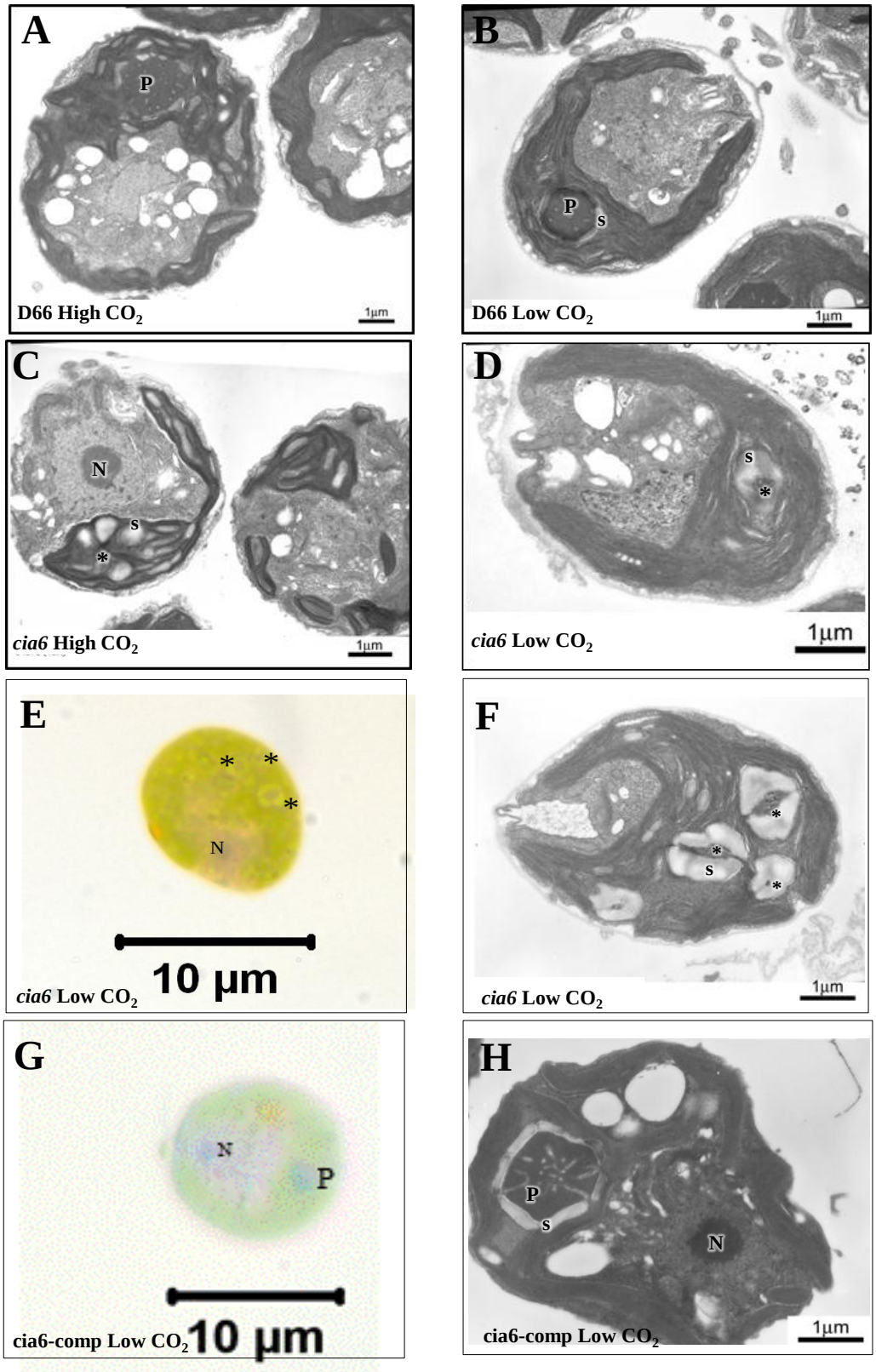
A
P
D66 High CO_2
1µm
B
P
S
D66 Low CO_2
1µm
C
N
S
*
cia6 High CO_2
1µm
D
S
*
cia6 Low CO_2
1µm
E
*
*
*
N
10 µm
cia6 Low CO_2
F
*
*
S
*
cia6 Low CO_2
1µm
G
N
P
10 µm
cia6-comp Low CO_2
H
P
S
N
cia6-comp Low CO_2
1µm

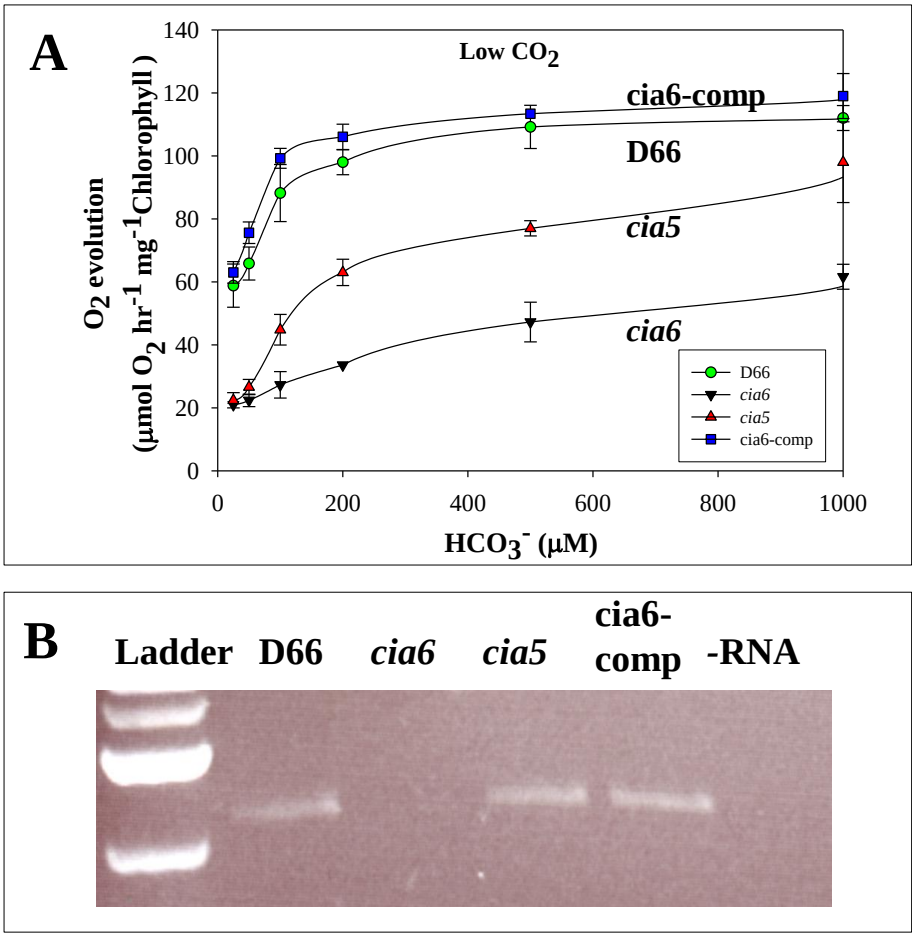

Figure 4.5. Complementation rescued the CCM deficiency in *cia6*.

By transforming genomic DNA containing the wild type *CIA6* gene into the *cia6* mutant, the resultant complemented strain cia6-comp exhibited a growth phenotype similar to the wild-type (See Figure 4.1). A, The rate of photosynthesis as a function of the dissolved inorganic carbon was measured using low CO_2 grown D66 (●), *cia6* (▼), *cia5* (▲) and the complemented strain cia6-comp (■). B, RT-PCR analysis of the D66, *cia6*, *cia5* and the complemented cia6 (cia6-comp) using RNA isolated from low CO_2 grown cells as templates for reverse transcription. Primers were designed to amplify the entire ORF. The reappearance of *CIA6* full length ORF in the complemented strain (cia6-comp) was observed on a DNA agarose gel. The last lane contained the no-RNA control.

ability demonstrated that the phenotype of the *cia6* mutant can be complemented with a 3.7 kb genomic fragment containing the WT *CIA6* locus.

***CIA6* Is Predicted to Encode a 72 kDa Protein Containing a SET Domain**

The predicted *CIA6* ORF encodes for a 72 kDa protein that has sequence similarity with a group of SET domain proteins. The SET domain was first recognized as a conserved sequence in three Drosophila melanogaster proteins (Su(var)3-9, E(z), Trithorax), characterized in 1998 now found in all eukaryotic organism studied. The substrates are mainly histone lysines (Qian et al., 2006; Dillon et al., 2005). Another family of SET domain proteins is Rubisco methyltransferases which functions by adding a methyl group on the flexible tail of the large or small subunit lysine residue (Qian et al., 2006; Dillon et al., 2005). Using the BlastP program searching the NCBI protein database, 14 homologs of CIA6 were identified (E-value $\leq 8e^{-20}$; Max score ≥ 100) (Figure 4.6). Among organisms possessing CIA6 homologs, the multicellular green alga *Volvox carteri f. nagariensis* has the highest similarity, followed by the unicellular photosynthetic green alga *Chlorella variabilis* NC64A and *Micromonas pusilla* CCMP1545 which also possess pyrenoid and an active CCM (Shiraiwa and Miyachi, 1983; Ikeda and Takeda, 1995; Worden et al., 2009). In addition, the non-vascular plant *Selaginella moellendorffii* has two genes similar to *CIA6*. The genomes of the early branching plant *Physcomitrella patens* as well as *Vitis vinifera*, *Populus trichocarpa*, *Arabidopsis thaliana* and *Oryza sativa*, all contained a gene predicted to encode a protein with significant homology to CIA6. To date, none of the CIA6 homologs identified in the NCBI database has been characterized.

Assessment of CIA6's Methyltransferase Activity in vitro

In order to test the putative methyltransferase activity of CIA6, the protein was overexpressed in *E.coli* using the pMALc2x overexpression system. The entire *CIA6* ORF was fused to the maltose binding protein (MBP) in the pMALc2x and overexpressed as a fusion protein in *E. coli* cells. *C. reinhardtii* Rubisco, calf thymus histone, and *C. reinhardtii* whole cell extracts were used as possible substrates. Positive controls in which pea Rubisco large subunit methyltransferase (RLsMT) (Klein and Houtz, 1995) was incubated with either the spinach or the *C. reinhardtii* Rubisco isolated from both the wild-type and the *cia6* mutant showed significant methyltransferase activity. In contrast, no *in vitro* methyltransferase activity was detected when the purified CIA6 fusion protein was incubated with the same array of substrates. The detected activity of pea RLsMT with the *C. reinhardtii* Rubisco is probably achieved by methylating on the Lys_{14} site as the pea RLsMT does *in vivo* with pea Rubisco. The observation is consistent with previous reports that the isolated Rubisco could be an *in vitro* substrate even though their Lys_{14} is not methylated *in vivo* (Houtz et al., 1992; Raunser et al., 2009).

***cia6* Has Normal Levels of Rubisco but Rubisco Fails to Associate and form a Pyrenoid**

Rawat *et al*. (1996) demonstrated that the pyrenoid could not be found in the RbcL nonsense strain 18-7G (Spreitzer et al., 1985), which indicates that pyrenoid formation requires the presence of Rubisco. Thus, to address why the *cia6* mutant cells lacked a pyrenoid, Rubisco protein levels from D66 and *cia6* were compared using western blot (Figure 4.7). However, when using anti-Rubisco polyclonal antibody

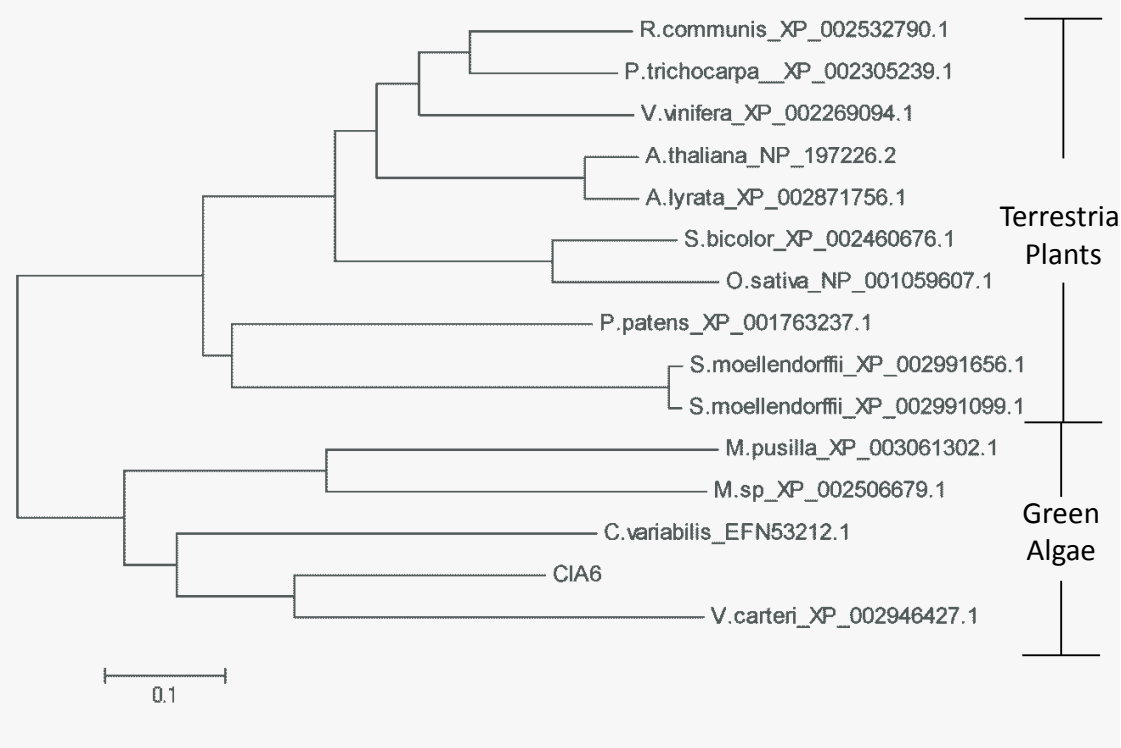

Figure 4.6. Evolutionary relationships of CIA6 amongst 14 taxa.

Phylogenetic analyses were conducted in MEGA4 (Tamura et al., 2007). Each protein name begins with the abbreviation of its scientific name, and followed by its NCBI accession number. The species are: *Volvox carteri f. nagariensis*; *Chlorella variabilis*; *Micromonas pusilla CCMP1545*; *Micromonas sp. RCC299; Physcomitrella patens subsp. patens; Vitis vinifera; Ricinus communis; Selaginella moellendorffii; Selaginella moellendorffii; Populus trichocarpa; Arabidopsis thaliana; Arabidopsis lyrata subsp. lyrata; Sorghum bicolor; Oryza sativa.* The evolutionary history was inferred using the Neighbor-Joining method.

(Borkhsenious et al., 1998) that recognize both the RbcL and the RbcS, it was found that the protein levels of both Rubisco subunits from both strains were not different. Another possible explanation regarding the disruption of pyrenoid in the mutant cells could be that, even though the amount of Rubisco protein was not changed, the directing of the Rubisco holoenzyme into the correct position (pyrenoid) in the mutant chloroplast was impaired. Immunolocalization of Rubisco was performed in cells from the wild-type and mutant strains, under both high and low CO_2 conditions. As seen for the high CO_2 grown (Figure 4.8A and 4.8B) and low CO_2 grown (Figure 4.8C and 4.8D) wild-type cells, the pyrenoid contained the majority of immunogold particles with almost all the immunological particles found inside of the wild-type pyrenoid upon low CO_2 induction (Figure 4.8B). This result agrees with earlier published reports from Morita's laboratory (Morita et al., 1997), and our laboratory (Borkhsenious et al., 1998) that more than 90% of the Rubisco resides inside the pyrenoid in wild-type cells grown under low CO_2 conditions. In *cia6* however, Rubisco particles were no longer accumulating inside the pyrenoid in either high CO_2 (Figure 4.8E and 4.8F) or low CO_2 (Figure 4.8G and 4.8H) grown cells. Using the estimated volume of the stroma and pyrenoid (Lacoste-Royal and Gibbs, 1987), it was estimated that the fraction of Rubisco in the pyrenoid-like structures was about 35% in *cia6*, which is similar to the percentage seen in wild-type cells grown in high CO_2 conditions (Table 4.2). Hence, the total Rubisco concentration in the mutant *cia6* was not changed while the localization of this CO_2 fixation enzyme was greatly altered as a result of the pyrenoid disruption.

***cia6* Has a Higher Chlorophyll Content Per Cell**

In *C. reinhardtii* wild-type cells, the chlorophyll per cell ratio remains constant

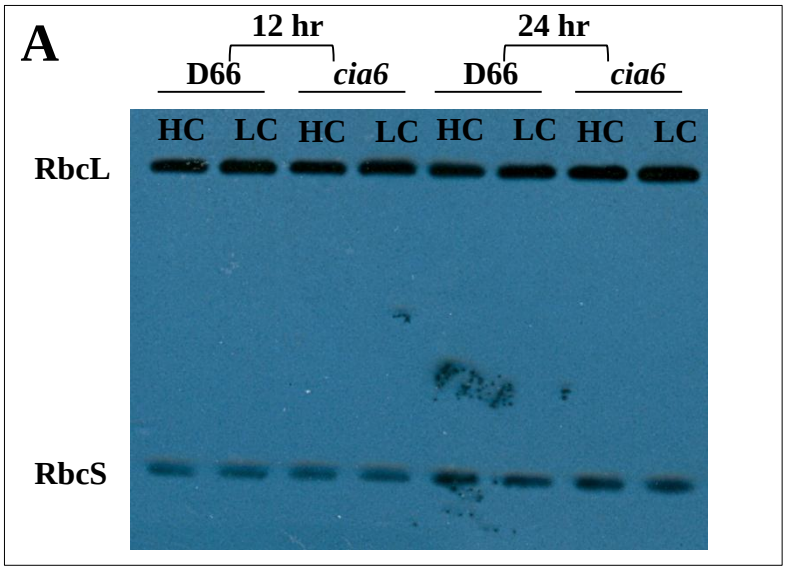

Figure 4.7. **Rubisco level is not altered in *cia6*.**

Rubisco content in the wild-type D66 and mutant *cia6* cells were investigated using western blot against anti-Rubisco antibody. Total protein isolated from D66 and *cia6* grown under high and low-CO_2 conditions for 12 hours and 24 hours. Using western blot, the amount of dissociated Rubisco large and small subunits (RbcL & RbcS) were estimated to be normal in the mutant compared to the wild-type.

Figure 4.8. Rubisco is dispersed throughout the chloroplast stroma in *cia6*.

Rubisco content in the wild-type D66 and mutant *cia6* cells were investigated immunoglod labeling (A-H) against anti-Rubisco antibody. A and B, High-CO_2-grown wild-type cells D66 grown on minimal medium probed with an antibody raised against Rubisco. C and D, Low-CO_2-grown wild-type cells D66 grown on minimal medium probed with an antibody raised against Rubisco. E and F, high-CO_2-grown *cia6* grown on minimal medium probed with an antibody raised against Rubisco. G and H, low-CO_2-grown *cia6* grown on minimal medium probed with an antibody raised against Rubisco. Bars indicate 1 μm. P, Pyrenoid; N, nucleus; Th, thylakoid; *, pyrenoid-like structures in *cia6.*

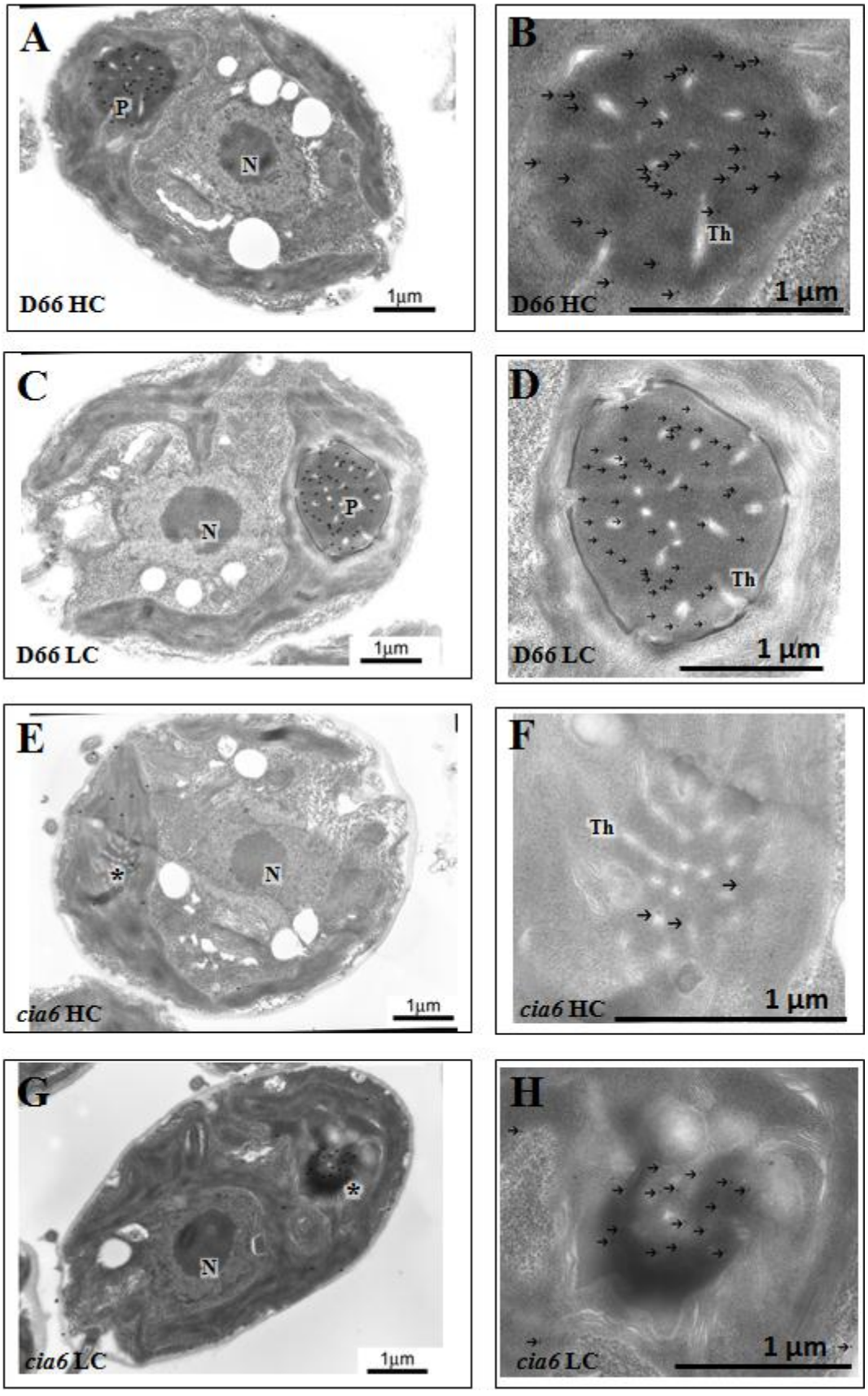
A
P
N
D66 HC
1µm
B
Th
D66 HC
1 µm
C
N
P
D66 LC
1µm
D
Th
D66 LC
1 µm
E
*
N
cia6 HC
1µm
F
Th
cia6 HC
1 µm
G
*
N
cia6 LC
1µm
H
cia6 LC
1 µm

Table 4.2. Comparison of the Rubisco fraction between wild-type and *cia6*.

C. reinhardtii strain	Immunogold density (particles/μm^2)		% Rubisco in the pyrenoid
	Pyrenoid	Stroma	
D66	23.3	0.00	100%
cia6	7.5	1.3	35.8%

Comparison of the Rubisco fraction found in the pyrenoid and in the chloroplast stroma between wild-type and *cia6*. The data shown are the averages of 25 *Chlamydomonas* EM thin sections and a total of 300 particles counted.

during the log phase growth, at around 2.8×10^{-6} µgChl cell^{-1} and 1.7×10^{-6} µgChl cell^{-1} under photoautotrophic and heterotrophic conditions respectively (Figure 4.9 and Figure 4.10). However, in the mutant *cia6*, it was observed that the chlorophyll per cell ratio is significantly higher in photoautotrophic grown cells (minimal medium bubbled with air, Figure 4.9). In addition, the chlorophyll per cell ratio is also higher in minimal medium even under high CO_2 concentrations (Figure 4.10). When *cia6* was grown under photoheterotrophic conditions where acetate was used as a carbon source, the chlorophyll per cell ratio was similar to wild-type D66 cells. The complemented strain cia6-comp exhibited the same growth characteristics and chlorophyll per cell ratio as the wild-type strain in all growth conditions.

cia6 Acclimates Slowly to Low CO_2 Conditions

To test whether the disruption of pyrenoid structure in *cia6* might have other pleiotropic effects on the expression of the CCM, changes in the expression of other key CCM components including *LCIB*, *CAH4* and *CCP1* were investigated by performing Q-RT analysis using RNA samples collected during a low CO_2 induction time course (Figure 4.11A and 4.11B). As shown in Figure 4.10A, the relative transcript abundance of those key CCM genes was lower in the mutant cells than in the wild-type cells. In addition, protein samples collected at the same time points were probed with CCP1, LCIB and CAH4 antibodies to estimate the protein levels by western blotting (Figure 4.11C). For most of the CCM related proteins, the amount of the protein was close to wild-type levels after 4 hours (Figure 4.11C). However, the abundance of CCP1, a chloroplast envelope protein, was reduced the most among the CCM proteins that were examined, and remained at low levels even after 4 hours.

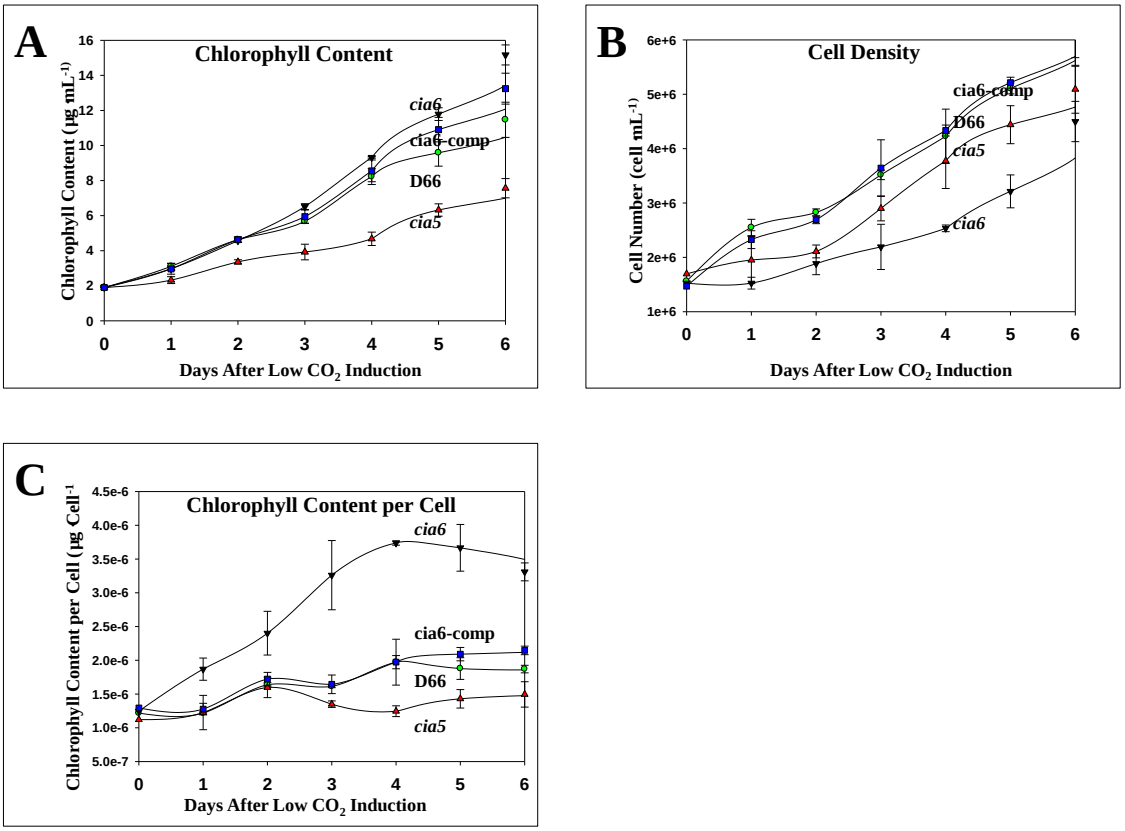

Figure 4.9. A higher chlorophyll content per cell was observed in *cia6* grown in minimal medium.

Cultures of D66 (●), *cia6* (▼), *cia5* (▲) and cia6-comp (■) were started at the same chlorophyll concentration, and was grown in minimal medium bubbling with air. For the subsequent 6 days, samples were collected every 24 hours and chlorophyll concentration (A) and cell density (B) were measured, and the chlorophyll concentration per cell were calculated (C). A, Cell density was determined by direct counting using a hemocytometer. B, Chlorophyll concentration was measured and the mutant *cia6* had the highest chlorophyll concentration at the end of the time course. C, Chlorophyll content per cell values were plotted so that it was clear that the mutant *cia6* had an increased chlorophyll content per cell compared to the other tested strains. Each point represents the mean and standard deviation of three separate experiments.

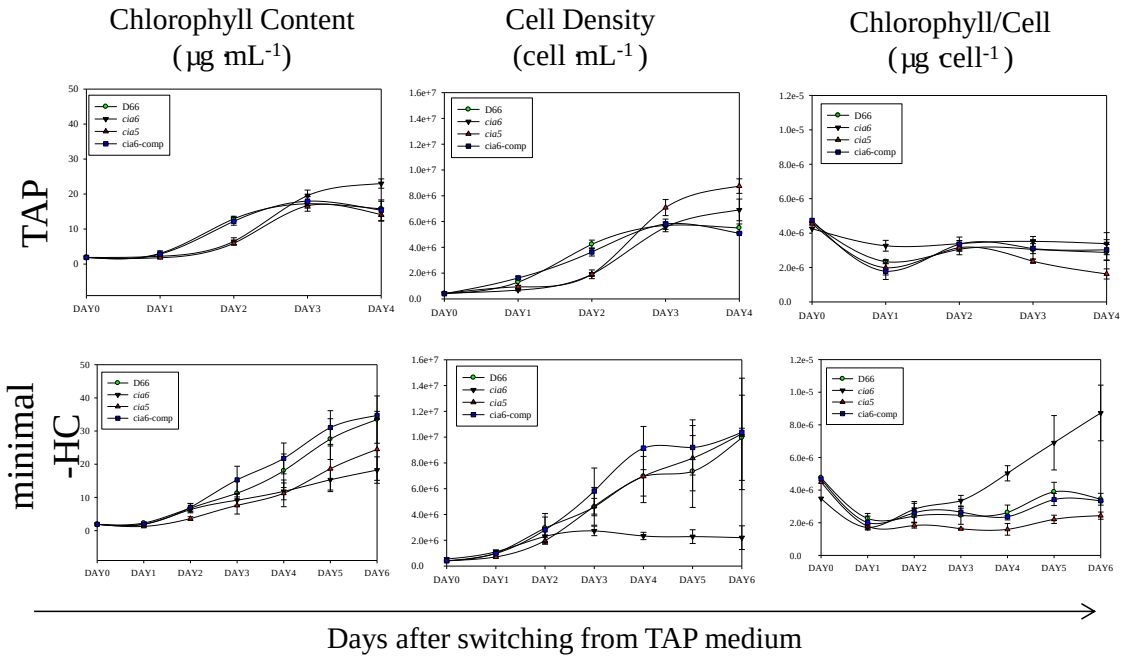

Figure 4.10. A higher chlorophyll content per cell was observed in *cia6* when grown heterotrophically.

Cultures of D66 (●), *cia6* (▼), *cia5* (▲) and cia6-comp (■) were initially started in TAP medium, and then switched to minimal or TAP medium at the same chlorophyll concentration of 1.9 μg·mL^{-1} till the stationary phase is reached. Samples were collected every 24 hours and chlorophyll concentration and cell density were measured, and the chlorophyll concentration per cell were calculated. Each point represents the mean and standard error of three separate experiments.

Discussion

In this report, we described the isolation and characterization of a novel *C. reinhardtii* mutant, in which a nuclear gene named *CIA6* was disrupted. The mutation in CIA6 resulted in the dysfunction of the CCM (Figure 4.1 and Figure 4.2), the disruption of the chloroplast pyrenoid (Figure 4.4 and Figure 4.8) and a higher than normal chlorophyll concentration (Figure 4.9 and Figure, 4.10). Transformation of the *cia6* mutant with a functional wild-type *CIA6* gene restored a functional CCM (Figure 4.1, Figure 4.5B and Table 4.1), a normal pyrenoid phenotype (Figure 4.4G and 4.4H) and its normal levels of chlorophyll (Figure 4.9 and Figure 4.10). This work revealed that the nuclear gene product CIA6 is required for the normal formation of the pyrenoid, and also provides evidence that the presence of pyrenoid is essential for the functioning of CCM in *C. reinhardtii*.

Most eukaryotic photosynthetic algae have pyrenoids (Griffiths, 1970; Bold and Wynne, 1985), while pyrenoids are mostly absent from higher plants with the exception of some species of hornworts (*Anthocerotophyta*) (Griffiths, 1970). In electron micrographs of a *C. reinhardtii* cell, the pyrenoid appears as an electron-dense microcompartment embedded inside the chloroplast stroma. A network of modified thylakoid tubules is present inside the pyrenoid body (Griffiths, 1970), and the accumulation of the starch plates surrounding the pyrenoid is often observed especially when the environmental CO_2 level is low (Ramazanov et al., 1994; Henk et al., 1995). The dense matrix of the pyrenoid mainly consists of Rubisco (Kuchitsu et al., 1988; Ramazanov et al., 1994; Rawat et al., 1996; Morita et al., 1997; Borkhsenious et al.,

1998). Rubisco activase has also been shown to be present in the pyrenoid (McKay et al., 1991).

The specific localization of Rubisco to the pyrenoid in *C. reinhardtii* is considered to be a key element in the optimal functioning of its CCM (Moroney and Ynalvez, 2007; Spalding, 2008; Yamano et al., 2010). Analogous to the packaging of Rubisco in cyanobacterial carboxysomes (Badger et al., 1998), the pyrenoid in *C. reinhardtii* could likewise be the location of the high CO_2 concentration generated by CCM. Since this high CO_2 concentration is in the vicinity of Rubisco, the carboxylation reaction will be enhanced at the expense of the oxygenation reaction, hence reducing photorespiration. In the pyrenoid-containing hornworts, there is also good correlation between the operation of a CCM and the presence of a pyrenoid (Vaughn et al., 1990; Hemsley and Poole, 2004). Besides the role in physical compartmentalization of Rubisco away from the rest of chloroplast stroma, the dynamic nature of pyrenoid in response to environmental changes adds extra complexity to the CCM. One notable observation made using immunolocalization was that in response to a switch from high CO_2 to low CO_2 environment, the Rubisco in the wild-type chloroplast started to redistribute and accumulate in the pyrenoid after 2 h in low CO_2 (Borkhsenious et al., 1998). The percentage of the pyrenoid-Rubisco labeling over the total labeling rose from 40% on high CO_2 to a maximum of 90% within 4 h on low CO_2. This process is tightly correlated with the time required for the appearance of a starch plate surrounding the pyrenoid (Henk et al., 1995), for the induction of most of the CCM genes (Miura et al., 2004) and for the maximal increase in C_i affinity (Borkhsenious et al., 1998). The rapid biochemical and morphological rearrangement indicates that the pyrenoid is a dynamic structure and

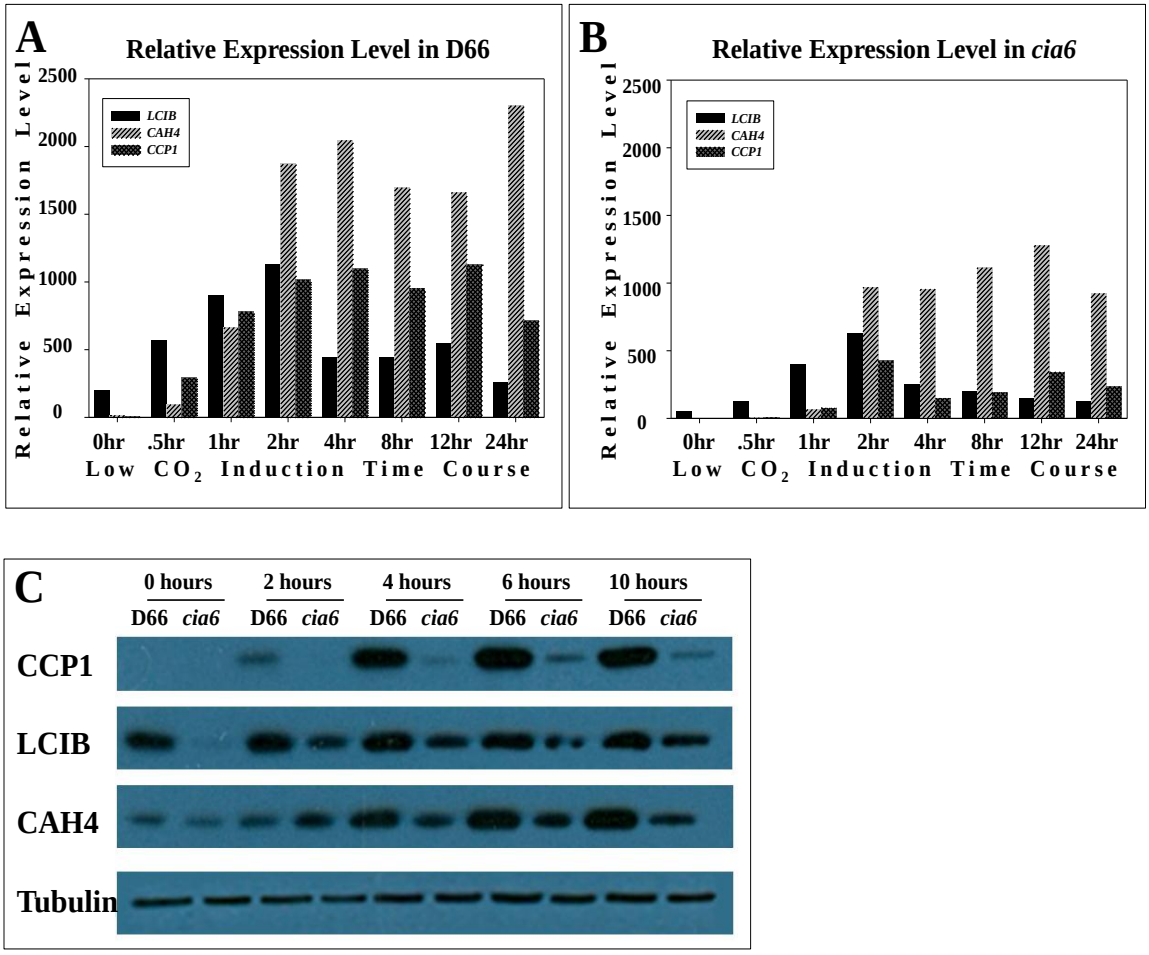

Figure 4.11. *cia6* Acclimates Slowly to Low CO_2 Conditions.

Time course of *LCIB*, *CAH4* and *CCP1* levels during low CO_2 induction process as measured by Q-RT PCR (A and B) and western blotting (C). A, Wild-type D66 cells subjected to low CO_2 induction were sampled at the time points as indicated in the figure. The *CBLP* gene was used as the internal control. (B) Mutant *cia6* cells subjected to low CO_2 induction were sampled at time points as indicated in the figure. *CBLP* gene was used as the internal control. (C) Wild-type D66 and mutant *cia6* protein samples were collected at the time points as indicated in the figure, and were then subjected to Western blot analysis using antibody raised against CCP1, LCIB, and CAH4. Anti-α-Tubulin antibody was used as a loading control.

is actively involved in the cell's acclimation to low CO_2 conditions.

One prediction based on the present CCM models is that, if the pyrenoid structure is disrupted, the CCM should also be adversely affected. However, among the few mutants with disrupted pyrenoid, either Rubisco was not present (Rawat et al., 1996), or chloroplast ribosomes were mutated leading to the absence of Rubisco (Goodenough, 1970), or the entire chloroplast structure is highly disrupted (Inwood et al., 2008). One piece of direct evidence supporting the role of the pyrenoid in an active CCM comes from a recent study by Genkov and his colleagues (Genkov et al., 2010). In their work, the *C. reinhardtii* Rubisco holoenzyme was engineered so that the *C. reinhardtii* native RbcL assembled with higher plants RbcS. Although the hybrid Rubisco had similar kinetic properties and was present in amounts equivalent to wild-type Rubisco, the resultant *C. reinhardtii* cells were found to lack the chloroplast pyrenoid, and failed to grow on low CO_2. This is strong evidence that the pyrenoid is playing an important role in the CCM.

In this current study, the characterization of the *cia6* mutant with disorganized pyrenoids provides additional evidence that the pyrenoid is a necessary part of the CCM. The *CIA6* mutation is the first mutation in a gene other than the Rubisco large or small subunit genes that disrupts the pyrenoid structure, while not affecting the entire chloroplast. Here, we show that the pyrenoid is disorganized in the *cia6* mutant cells. We also show that Rubisco is mislocalized in *cia6*, as approximately 65% of the Rubisco was found in the stroma rather than in the "pyrenoid-like" structures. This result is reminiscent of the *Synechococcus* sp. PCC 7942 strain, EK6, described by Schwarz et al. (Schwarz et al., 1995) where a 30 amino acid extension in the RbcS caused the Rubisco

to mislocalize to the cytoplasm. The EK6 strain had empty carboxysomes and was unable to grow under low CO_2 conditions. However, the mutation in *cia6* is not within RbcS as in the EK6 strain, but rather in the *CIA6* gene on chromosome ten. By using both denaturing gels and non-denaturing gels, the Rubisco holoenzymes in wild-type and mutant cells have been examined. Cell extracts from both the wild-type and mutant cells were analyzed by western blot on a denaturing gel using an anti-Rubisco antibody, but no significant concentration differences in the two subunits could be revealed between the strains (Figure 4.7). Rubisco isolated from both the wild-type and mutant cells were also subjected to electrophoresis on a non-denaturing gel and stained with Coomassie blue. However, no significant differences were noticed between the two Rubisco preparations, as evidenced by the appearance of the same three high molecular weight bands, which were all recognized by anti-Rubisco antibody after using western blotting (data not shown). The combination of both the denaturing and the non-denaturing gel electrophoresis analysis indicated the normal composition of the Rubisco holoenzyme in the mutant cells. On the other hand, the appearance of the four high molecular weight bands in both *C. reinhardtii* Rubiscos on a non-denaturing gel, is similar to the four bands observed when the pea RLsMT bound spinach Rubisco was subjected to non-denaturing gel (Raunser et al., 2009), with each band representing the addition of one RLsMT onto the Rubisco while the lowest band represents the native Rubisco.

In both cyanobacteria and the green algae, the arrangement of the CCM components within the cell or chloroplast is critical to the functioning of the CCM. In a current model of the *C. reinhardtii* CCM (Moroney and Ynalvez, 2007; Spalding, 2008; Yamano et al., 2010), a higher than ambient concentration of CO_2 inside the thylakoid

lumen is predicted to be generated by CAH3. Since the thylakoid lumen is acidified in the light, most inorganic carbon in the lumen will be converted to CO_2. This CO_2 will either diffuse into the pyrenoid region to be fixed by Rubisco, or diffuse back into the stroma. Since the stroma becomes more basic in the light, any CO_2 that leaks out of the pyrenoid have a chance to be converted back to HCO_3^- by CAH6, thus reducing CO_2 leakage. In *cia6* cells, net C_i accumulation was reduced (Figure 4.2C). This reduced accumulation could be due to a lower rate of C_i uptake or due to a reduction in the ability of the cells to retain C_i, but we cannot discriminate between these two possibilities. It is clear that any disruption of the pyrenoid potentially disconnects the arrangement of these CCM components and reducing CO_2 assimilation efficiency.

Recently there has been increasing interest in the possible interaction between the LCIB/LCIC complex and the pyrenoid (Yamano et al., 2010). Two roles for such a localization have been proposed, including a role in re-capturing CO_2 using stromal carbonic anhydrase (CAH6); and a role as a structural barrier in avoiding CO_2 leakage from the pyrenoid. It would be intriguing to investigate how the LCIB/LCIC complex would localize in the *cia6* mutant background in which the pyrenoid is absent and Rubisco is no longer concentrated in this specialized region of the chloroplast. For example, would low CO_2 still induce the migration of LCIB/LCIC complex to the vicinity of the pyrenoid-like structure in the mutant *cia6* cell? These results might shed light on whether the aggregation of LCIB/LCIC complex needs the presence of pyrenoid or not; or whether the complex is actually associating with the thylakoids tubules or the pyrenoid.

Apparently CIA6 is required for the formation of pyrenoid in *C. reinhardtii*, however, the exact function of CIA6 in the CCM or pyrenoid formation is not clear. Predicted to contain a SET domain by Pfam (Bateman et al., 2002), the CIA6 protein is likely to act as a lysine methyltransferase (Dillon et al., 2005; Qian and Zhou, 2006; Ng et al., 2007). In plants, other than modifying histones, SET domain containing proteins were also found to methylate Lys_{14} on Rubisco large subunit (Klein and Houtz, 1995; Ying et al., 1999; Trievel et al., 2002; Trievel et al., 2003). Since in the *cia6* mutant cells the Rubisco containing pyrenoid is not well developed, it could be speculated that one possible function of CIA6 could be acting as the *C. reinhardtii* Rubisco methyltransferase, modifying the conformation of this holoenzyme in some way allowing it to organize or self-assemble into a pyrenoid. However, the Rubisco methylating activity of CIA6 could not be found *in vitro*. It should be noted that unlike the pea RbcL with methylated Lys_{14} on the N-terminal tail, the *C. reinhardtii* RbcL's Lys_{14} is un-methylated. Instead, crystal structure data from *C. reinhardtii* Rubisco indicated the presence of methyl-Cys_{256} and methyl-Cys_{369} (Taylor et al., 2001), with the first Cys buried at the interface of RbcL and RbcS, and the latter Cys positioned on the external surface of RbcL. Notwithstanding the potential electrostatic problem of a cysteine fitting in the narrow cleft of the SET domain's catalytic site, neither cysteines is thought to easily enter the catalytic channel of RLsMT, as compared to the Lys_{14} on the flexible N-terminal tail. On the other hand, by examining the amino acid sequences of CIA6 and its 13 homologs, it was found that the invariant tyrosine residue on the SET domain N terminus is present, indicating the possible presence of the target lysine binding site. However, in all 13 CIA6 homologs, the highly conserved catalytic site motif NHS could not be found, which could argue that

these proteins may belong to a sub-class of SET domain containing proteins that do not have catalytic functions but emphasize on structural roles in relation to Rubisco aggregation and pyrenoid formation. Alternatively, based on the fact that CIA6 homologs are only found in green algae and higher plants but not in cyanobacteria or the sequenced diatom genomes, it could be speculated that the function of CIA6 may not be limited to or directly linked to the formation of pyrenoid structure or CCM function.

A notable phenotype of *cia6 C. reinhardtii* cells was its increased chlorophyll content under photoautotrophic conditions (Figure 4.9 and Figure 4.10). This observation implies that the function of CIA6 might be related to chloroplast organization or nuclear/chloroplast coordination. Like the chloroplast, the pyrenoid reproduces by binary fission during cell division (Goodenough, 1970; Goodenough and Levine, 1970; Harris et al., 2009). The disruption of the pyrenoid might occur if chloroplast structure or division is not well coordinated in the *CIA6* deficient cell. We are presently working on obtaining an Arabidopsis knockout line with *CIA6* homolog gene disrupted to see whether the chloroplast structure is affected in that plant. Given the fact that multiple small pyrenoids were sometimes observed in a single mutant chloroplast, the possibility that the mutant pyrenoid division problem led to the altered chlorophyll concentration can not be excluded.

In summary, *CIA6* is a member of a new gene family found in green algae and in higher plants. When this gene is knocked out in *C. reinhardtii*, the cell has a disrupted pyrenoid and a dysfunctional CCM. When the wild-type gene is returned to *cia6* mutant cells, the normal pyrenoid morphology and CCM function are restored. This is the first report of a gene outside of the Rubisco-structure genes that affects pyrenoid structure.

The linkage of the pyrenoid structure and the CCM provides strong support for CCM models in which the localization of Rubisco to the pyrenoid is essential.

Endnotes

[1] The cloning of the CIA6 gene as well as the data in Table 4.1 and Figures 4.1, 4.4, 4.5, 4.6, 4.7, 4.8, 4.9, 4.10, 4.11 were contributed by the author of this dissertation.

[2] **Ma, Y.,** Pollock, S.V., Xiao, Y., Cunnusamy, K., and Moroney, J.V. (2011). Identification of a novel gene, CIA6, required for normal pyrenoid formation in *Chlamydomonas reinhardtii*. Plant Physiol **156**, 884-896.

CHAPTER 5
TRANSCRIPTIONAL ANALYSIS OF THE THREE PHOSPHOGLYCOLATE PHOSPHATASE GENES IN WILD-TYPE AND THE *PGP1* MUTANT OF *CHLAMYDOMONAS REINHARDTII*

Introduction

Photorespiration contributes substantially to metabolism in every photosynthetic organism. This process, resulting from the dual catalytic properties of Rubisco, detoxifying the RuBP oxygenation product phosphoglycolate, which would inhibit the Calvin Cycle (Anderson, 1971) if not removed efficiently. To recycle phosphoglycolate through photorespiration, the first step is to convert it to glycolate by the action of the phosphoglycolate phosphatase (PGPase, EC 3.1.3.18, Equation 5.1) inside the chloroplast. The dephosphorylated glycolate then can be translocated into other organelles to be metabolized into glycerate, NH_3 and CO_2. Inside the chloroplast, the NH_3 and CO_2 are reassimilated by the GS/GOGAT system and Calvin Cycle respectively. Glycerate is converted to Glyceraldehyde 3-phosphate (G-3P) through phosphorylation and re-enters the Calvin Cycle (Refer to Figure 2.3).

Equation 5.1 $$\mathbf{Phosphoglycolate} \overset{\mathbf{PGPase}}{\Longleftrightarrow} \mathbf{Glycolate} + \mathbf{P_i}$$

As the entry enzyme for photorespiration, PGPase is arguably one of the most important enzymes in photorespiration. The first photorespiration mutant (CS119) was isolated through mutagenesis screens in Arabidopsis (Somerville and Ogren, 1979), and was found to lack PGPase activity and exhibited a sick on low CO_2 phenotype. The mutation identity was revealed nearly 30 years later (Schwarte and Bauwe, 2007). Among the 13 PGP-like genes found in the Arabidopsis genome, the *AtPGLP1*

(At5g36700) in the C2119 mutant was shown to have a point mutation on the exon 8 splice donor site. In Arabidopsis, two *AtPGLP* (*AtPGLP1* and *AtPGLP2*) genes were shown to encode active PGPases, but only the *AtPGLP1* knock-out mutant showed a severe growth reduction in a low CO_2 environment (Schwarte and Bauwe, 2007).

In *C. reinhardtii*, the genome sequence revealed three genes encoding putative PGPase: *PGP1*, *PGP2*, and *PGP3*, on chromosomes 3, 10 and 6 respectively. The three PGP isozymes show high sequence similarity, with PGP1 and PGP2 share the highest similarity (47% score) on the protein level, and all consensus motifs of p-nitrophenyl phosphatases were present (Mamedov et al., 2001; Suzuki et al., 2005). Sequence alignment of the three isoforms also indicates that PGP1 and PGP3 both have an extra N-terminal signal peptide while the signal peptide is missing in the PGP2 isoform. The N-terminal peptide in PGP1 was proposed to be a chloroplast stroma leader sequence based on *in silico* analysis (Mamedov et al., 2001). All three *PGP* genes have similar representation in the EST database (refer to Table 7.3), indicating that they are expressed *in vivo*.

PGPase has been purified from *C. reinhardtii* (Husic and Tolbert, 1985; Mamedov et al., 2001) with the highest activity observed from the chloroplast fraction (Husic and Tolbert, 1985). It has also been shown that the maximum PGPase activity was 86.5 μmol $P_i \cdot mg^{-1}protein \cdot min^{-1}$, using phosphoglycolate as the substrate (Mamedov et al., 2001). During a switch from high CO_2 to low CO_2 condition, a transient increase in the activity and the expression level of the PGPase was reported (Marek and Spalding, 1991; Tural and Moroney, 2005). The rapid and short-lived increase in PGPase is proposed to function as a quick-response approach for the cell to cope with low CO_2 environment

before the entire CCM is fully induced. Five common motifs in the upstream sequence of the *PGP1* were identified by comparison of the upstream sequence of the *PGP1* gene and the *CAH1* gene (Suzuki et al., 2005). In the mutant *cia5*, which lacks the functional CCM master regulator (Moroney et al., 1989; Fukuzawa et al., 2001; Xiang et al., 2001), the *PGP1* transcription was not upregulateda (Tural and Moroney, 2005), suggesting that the expression of the *PGP1* gene is controlled by the CCM master regulator.

One mutant (18-7F) with a mutated *PGP1* in *C. reinhardtii* was isolated as a high CO_2 requiring mutant (Spreitzer and Mets, 1981) and was demonstrated to have very minimal PGPase activity under either high or low CO_2 conditions (Suzuki et al., 1990). In this mutant, a G to A point mutation created by EMS (ethylmethane sulfonate) was found to reside in beginning of the first intron (Suzuki et al., 2005). The mutation was proposed to destroy the "GT" splice donor site, thus resulting in the fusion of the first exon, the first intron, and the second exon in the transcript (Figure 5.1). Furthermore, this missense mutation resulted in the incorporation of a stop codon from the first intron in the transcript, leading to a truncated PGP1 protein (Suzuki et al., 2005). The *pgp1* mutant (18-7F) was reported to have a conditional lethal phenotype that required elevated concentrations of CO_2 for growth (Spreitzer and Mets, 1981; Suzuki et al., 1990; Suzuki, 1995). However, a few decades after its first characterization, we found that this strain maintained in our lab (referred to *pgp1-1-old*) had regained the ability to grow under low CO_2 conditions. The same phenotype reversion was also observed from the mutant strain maintained in the Duke University Stock Center (CC-2648, referred to *pgp1-1-new*). Three hypotheses were made to address the loss of phenotype in the *pgp1* mutant. First, single isolates from the *pgp1* mutant stock might still possess the conditional lethal

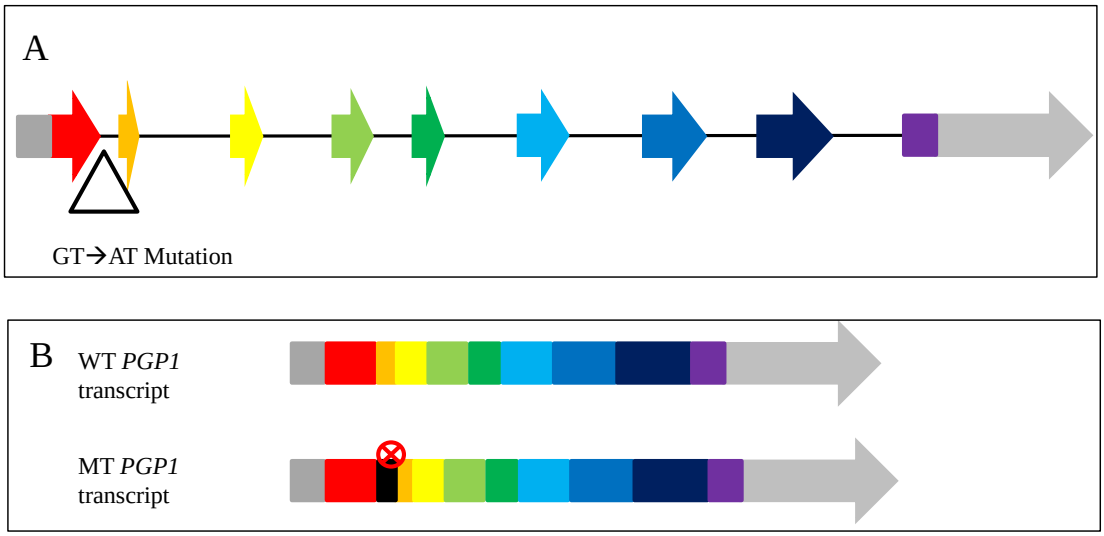

Figure 5.1. Gene model of the *PGP1* locus in the wild-type and the mutant strains.

(A): The GT to AT point mutation was created by EMS on the first exon and intron splice donor site. (B) This point mutation led to the production of a longer PGP1 transcript in the mutant since the first intron was no longer spliced out. The first intron contains a stop codon (indicated by the ⊗ sign), resulting in a truncated PGP1 protein in the mutant.

phenotype. Second, the original splice mutation might be lost in the *pgp1* mutant. Third, the other two PGPase isozymes (PGP2 and PGP3) might compensate for the loss of the PGP1 in the *pgp1* mutant. Based on this study, the first two hypotheses were rejected. Using Quantitative-RT PCR, the third hypothesis was tested and showed that the *PGP2* gene was upregulated and might be one of the factors contributing to the phenotypic reversion in the *pgp1* mutant.

Results

There is a reversion in the *pgp1* phenotype

The harmful product phosphoglycolate must be recycled through the photorespiratory pathway (Tolbert 1997), otherwise its build-up would exert a potent inhibitory effect on triose phosphate isomerase and carbon recycling in the Calvin Cycle (Anderson 1971). The *pgp1* mutant lacked a functional PGP1 was reported not able to grow under low CO_2 conditions (Spreitzer and Mets, 1981; Suzuki et al., 1990; Suzuki, 1995). However, both the *pgp1-1-old* strain and the *pgp1-1-new* strain can now survive as well as their parental strain 2137, under low CO_2 on minimum medium (Figure 5.2). Phenotypes of the isolates from both the *pgp1* mutants (*pgp1-1-old* and *pgp1-1-new*) were examined under low CO_2 conditions. One of the isolates named *pgp1-1-18* showed a small reduction in growth when compared to the *pgp1-1-old* and *pgp1-1-new* strains. However, this phenotype still could not be counted as "conditional lethal" as recorded previously.

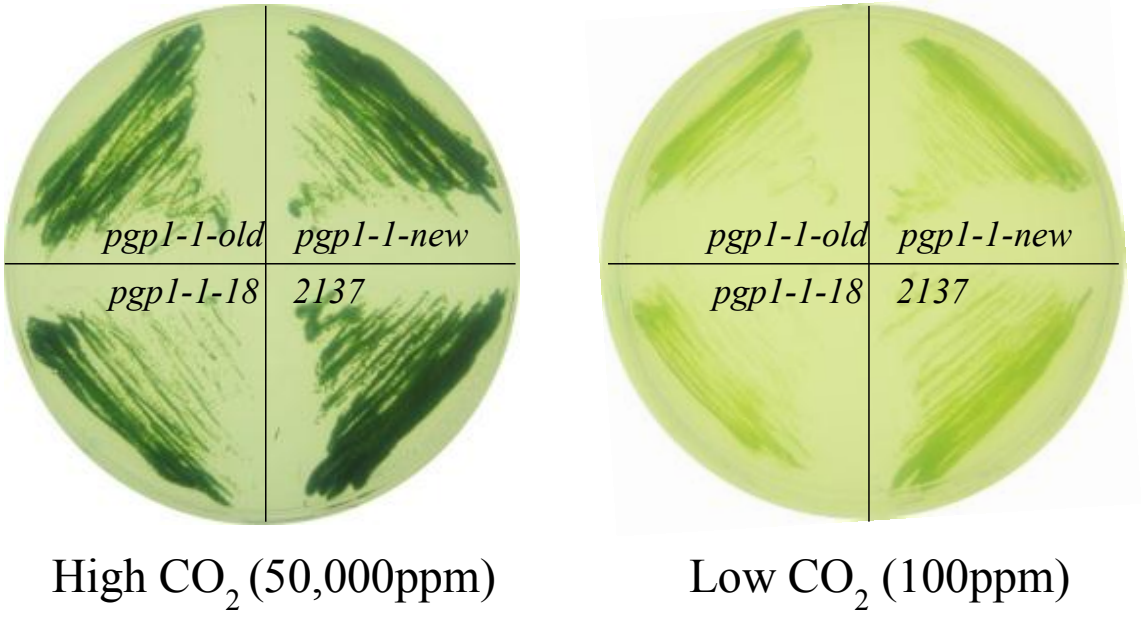

Figure 5.2. Growth phenotype of the *pgp1* mutants.

Growth phenotype of the *pgp1* mutants under high (left panel) and low CO_2 (right panel) conditions. Although the three *pgp1-1* mutants exhibited relatively lower growth compared to the parent strain 2137, they could still survive under low CO_2 conditions, as opposed to "lethal phenotype" originally reported (Suzuki et al., 1990).

The mutation at the splice junction is still present

The second hypothesis to explain the phenotype reversion that occurred in the *pgp1* mutant was that the genetic identity of the original strain has changed. To be specific, the G to A mutation on the exon-intron splice junction might have reverted, resulting in the normal full length *PGP1* message. Previously, it was proposed that the G to A splice mutation caused the fusion of the first two exons without splicing out the first intron in the *pgp1* mutant (Figure 5.1). If this point mutation is still present in the *pgp1* mutants, the mutant transcript would be bigger in size due to the addition of the first intron. To verify whether the splice mutation is still present in the *pgp1* mutant, PCR primers (PGP1-F and PGP1-R) were designed to span the original point mutation and the 81-bp first intron (Figure 5.3A). The presence of the splice mutation could be tested by the PCR product size comparison. The wild-type PCR product would be smaller than the mutant PCR product since the mutant transcript possesses the extra 81-bp first intron.

RNA samples from all three *pgp1* strains (*pgp1-1-old, pgp1-1-new* and *pgp1-1-18*) and the 2137 wild-type strain were isolated under both high CO_2 condition and the two hour low CO_2 induced condition. cDNA was synthesized using oligod(T) primers and PCR using PGP1-F and PGP1-R was performed (Figure 5.3B). Based on the PCR analysis, it showed that the original mutation was still present in all three *pgp1* mutants as evidenced by the extended exon size in the mutants. The addition of the 1st intron in the mutant cDNA (Figure 5.3B, Lane 2-4) added an extra 81-bp to the wild-type cDNA (Figure 5.3B, Lane1).

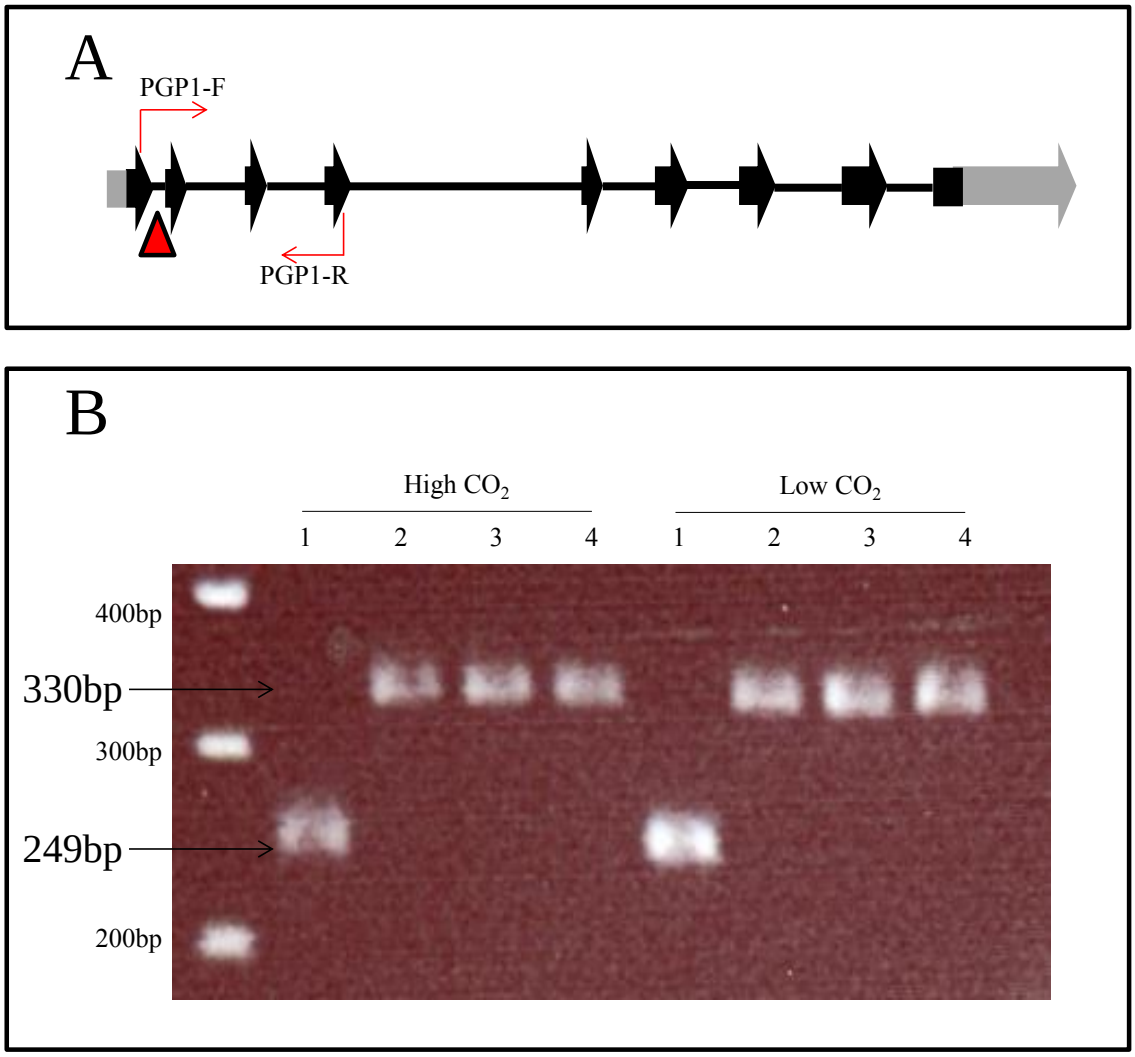

Figure 5.3. The *PGP1* mutation is still present in the mutant.

(A): PCR primers (indicated by the red arrorw) were designed to span the splice mutation (indicated by the red triangle) in the mutant. (B): The extended 1st exon caused by the point mutation at the splice donor site was present in all the *pgp1-1* mutants investigated. 1: wild-type strain 2137; 2: *pgp1-1-old*; 3: *pgp1-1-new*; 4: *pgp1-1-old-18*.

The reverted phenotype is possibly due to the increased expression from *PGP2*

Since the original *PGP1* splice mutation was still present, the third hypothesis was tested to see whether the other PGP isoenzymes (PGP2 and/or PGP3) were compensating for the loss of PGP1. Q-RT-PCR was performed to determine the relative expression level of the three PGPase isozymes among the five wild-type strains (including the parental strain 2137; D66, a strain often used in our laboratory; CC-503, the genome sequence reference strain; and two other wild-type strains C9, and 137), as well as three *pgp1* mutant strains (*pgp1-1-old*, *pgp1-1-new* and *pgp1-1-18*). The CCM transcriptional regulator deficient strain *cia5* was used as a negative control, since genes of the photorespiratory pathways would not be expected to be induced in this mutant background (Tural and Moroney, 2005).

The Q-RT PCR results (Figure 5.4) revealed that in all of the wild-type strains tested, *PGP1* was the most highly expressed of the *PGP* genes, consistent with the previous observation that the PGP1 is the primary PGPase in *C. reinhardtii*. The other two PGP isoforms were shown to be suppressed under both high and low CO_2 conditions. In addition, *PGP1* expression was significantly upregulated under low CO_2 conditions, typically about 2 fold on average. The increased expression of *PGP1* under low CO_2 conditions is consistent with the earlier report of Marek and Spalding (1991), and of Tural and Moroney (2005). In the CCM mutant, *cia5*, the up-regulation of *PGP1* was not seen. This was also observed by Tural and Moroney (2005) that the expression of the many photorespiratory genes under low CO_2 was apparently under the control of the CIA5 transcriptional regulator. All strains with the exception of *cia5* showed a strong

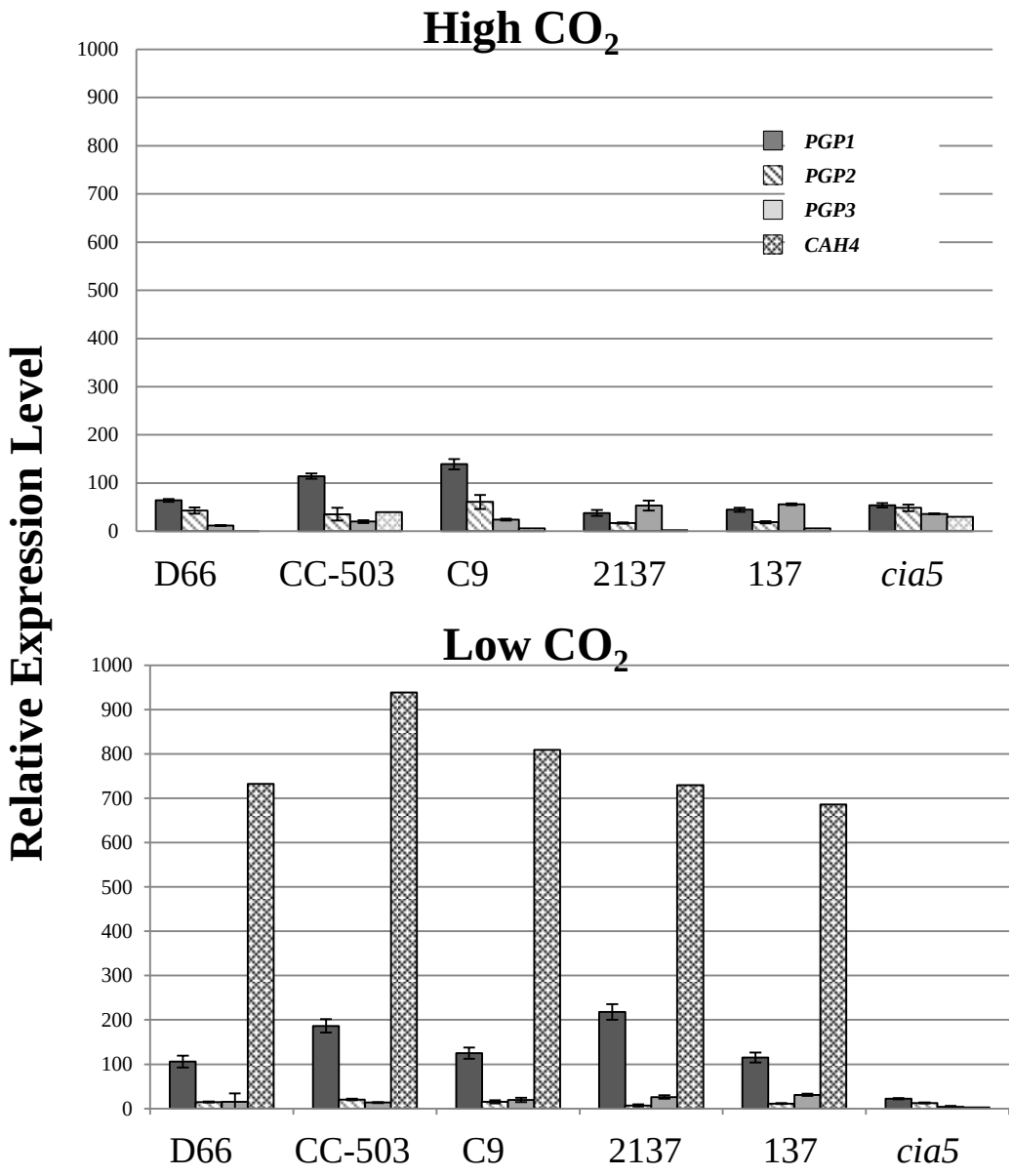

Figure 5.4. Phosphoglycolate phosphatase genes in wild-types.

Quantitative RT-PCR results for phosphoglycolate phosphatase genes under high (upper panel) and low CO_2 (lower panel) conditions in a variety of wild-type strains listed. The carbonic anhydrase *CAH4* was used as a positive control for effective CCM induction. Relative expression level is expressed as the $1000/2^{\Delta Ct}$, in which $\Delta Ct = Ct_{gene} - Ct_{CBLP}$.

induction of the CCM under low CO_2 conditions as judged by the induction of expression of the mitochondria carbonic anhydrase gene *CAH4*.

Next, the expression of the three *PGP* genes was investigated in the three *pgp1* mutants. Among the three *pgp1* mutants, the expression level of the *PGP1* isoform appeared to be upregulated, but to a much lesser extent when it's compared to the level in the wild-type (Figure 5.5). This down-regulation could possibly be explained by the decreased stability of the mutant mRNA secondary structure if not properly processed. Additionally, the *CAH4* expression level in the three *pgp1* mutants was not affected, indicating the presence of an active CCM even when the photorespiratory pathway is not functioning effectively. This observation was consistent with the previous report that the induction in the C_i uptake and carbonic anhydrase activity was not significantly affected in the absence of the PGP1 (Suzuki et al., 1990).

Most importantly, based on the Q-RT analysis, it appeared that the *PGP2*, instead of the *PGP1* is upregulated to a greater magnitude in the *pgp1* mutants. The expression of *PGP2* did not change appreciably under low CO_2 conditions and remained relatively high under both high and low CO_2 growth conditions. However, the up-regulation of the *PGP2* could likely contribute to the restored growth phenotype when a functional PGP1 is not present.

Discussion

Originally characterized by Suzuki et al. (1990), the *pgp1-1* mutant was reported to have a defect in growth under low CO_2 conditions. The G to A mutation on the splice donor site was proposed to create an extended exon and an early translation stop, which

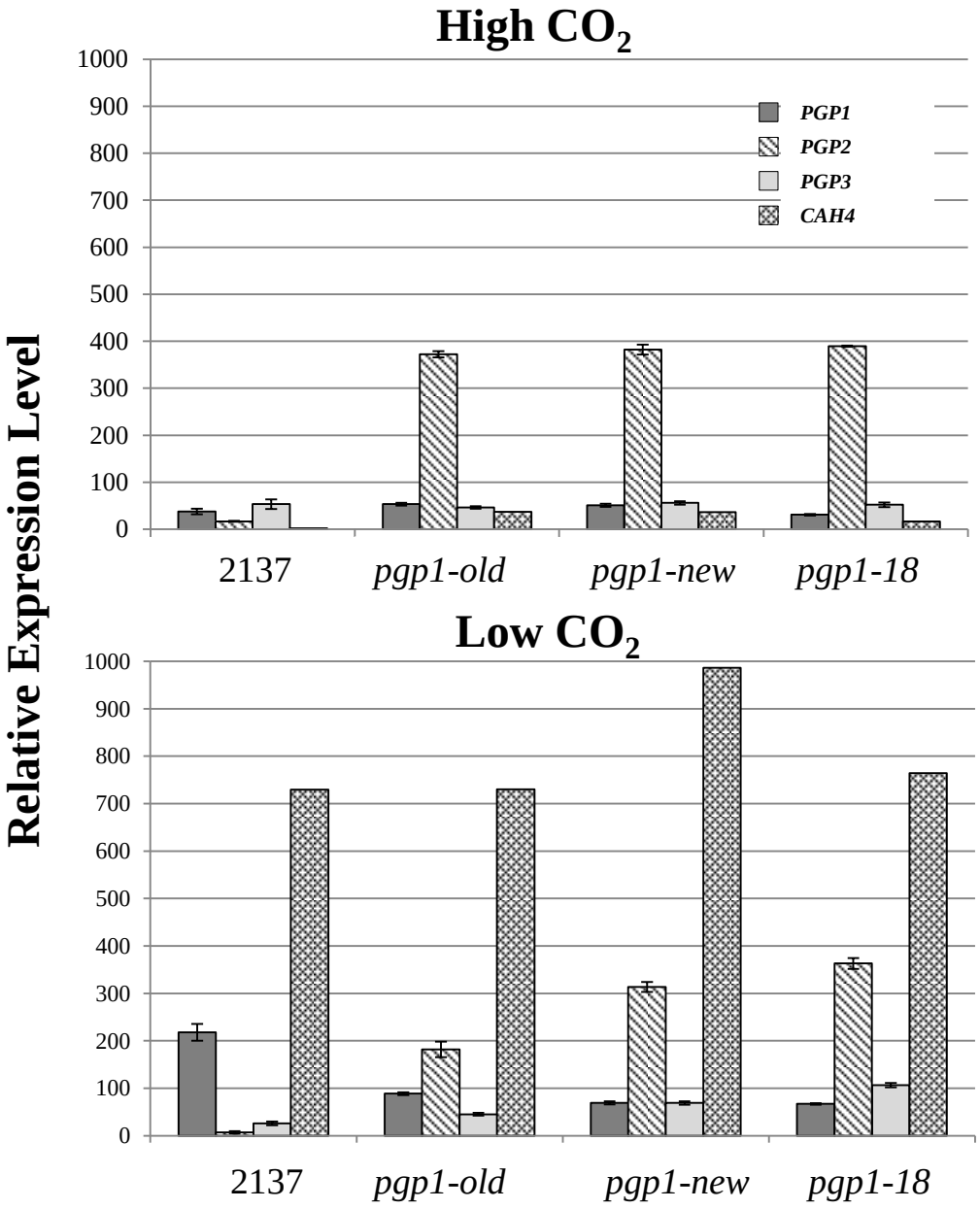

Figure 5.5. Phosphoglycolate phosphatase genes in the mutants.

Quantitative RT-PCR results for phosphoglycolate phosphatase genes under high (upper panel) and low CO_2 (lower panel) conditions in a variety of wild-type strains listed. The carbonic anhydrase *CAH4* was used as a positive control for effective CCM induction. Relative expression level is expressed as the $1000/2^{\Delta Ct}$, in which $\Delta Ct = Ct_{gene} - Ct_{CBLP.}$

resulted in a non-functional truncated PGPase (Suzuki et al., 2005). However, after nearly thirty years since its first isolation (Spreitzer and Mets, 1981; Suzuki et al., 1990; Suzuki, 1995), this mutant was observed to regain the ability to grow in the limited CO_2 environment, although the original splice mutation was still present in all the isolates tested.

In an attempt to explain this observation, the transcription profile of the three PGPase was examined after a 2-hour low CO_2 induction. Among all the wild-type strains investigated, the *PGP1* level showed a 2-fold induction under low CO_2 conditions. The level of *PGP2* and *PGP3* appeared to remain the same under both conditions, suggesting that the PGP1 is the primary PGPase active in response to the low CO_2 stress. This is consistent with previous report that *PGP1* and *CAH1* both shared the same low CO_2 responsive motifs in the 5' upstream region (Suzuki et al., 2005). However, these motifs could not be identified in either PGP2 or PGP3 DNA sequences (this study). Additionally, in the original *pgp1* mutant, PGPase activity was barely measurable compared to the one from the wild-type strain (Suzuki et al., 1990).

In contrast to the up-regulation of *PGP1* in the wild-type strains under low CO_2 conditions, the *PGP1* message was relatively unchanged in all three *pgp1* isolates. This was not expected since the mutation in the *pgp1* mutant found on the splice donor site of the coding region is not likely to affect the low CO_2 responsive motifs in the 5' upstream region of the *PGP1* gene. However, the altered response pattern of the *PGP1* transcript seen in the *pgp1* mutants might result from the aberrant RNA splice and its associated unstable secondary structure. Additionally, this observation could also be explained by the accumulation of a nonfunctional PGPase or the other Calvin Cycle intermediates that

could serve as a feedback signal that inhibits the induction of the *PGP1* gene in the mutants.

Most importantly, despite the minimal level of *PGP1*, the *PGP2* message was significantly upregulated in all three *pgp1* isolates. This up-regulation could likely be regarded as a compensation mechanism for the loss of the PGPase activity in the mutants. Unlike the *PGP1* that is up-regulated when subjected to low CO_2 stress in the wild-type, the *PGP2* message remained unaffected by the CO_2 levels in the *pgp1* mutants, being expressed at relatively high level. This could possibly be explained by the absence of the low CO_2 responsive motifs in the *PGP2* 5' upstream region. However, the theory that the up-regulation of the *PGP2* isoform compensates for the loss of PGP1 needs to be tested in detail. For example, if the upregulation of *PGP2* indeed resulted in the phenotype reversion in the *pgp1* mutant, the crossing of the *pgp1* with the wild-type would be expected to yield a 3:1 separation in the tetrads. Assume the genotype of the wild-type is *PGP1pgp2* (meaning *PGP1* is upregulated while *PGP2* is not) and the genotype of the mutant is *pgp1PGP2* (meaning PGP1 is mutated while *PGP2* is proposed to compensate for *PGP1*). Among the four haploid tetrads, three would show the wild-type phenotype (*PGP1PGP2*, *pgp1PGP2*, *PGP1pgp2*) and one would show the mutant phenotype (*pgp1pgp2*).

The current method for maintaining most of the strains, including the *pgp1* mutants, is to keep on tris-acetate plates in the light in room air. In this situation, most of the time cells are growing mixotrophically, especially considering the acetate in the plates can be depleted over time. Without the functioning of the phosphoglycolate phosphatases, the phosphoglycolate produced from Rubisco oxygenation would have

accumulated to an extent that *pgp1* mutants could not survive under routine laboratory maintenance conditions. Under this pressure, it can be speculated that the *PGP2* was upregulated through unknown mechanism to serve as a back-up enzyme to recycle the phosphoglycolate and complement the *pgp1* mutation. Nevertheless, the *PGP2* upregulation might not be the only contributing factor to the phenotype reversion in the *pgp1* mutants.

CHAPTER 6
THE PERIPLASMIC CARBONIC ANHYDRASE, CAH1, IS ABSENT IN THE SEQUENCED *CHLAMYDOMONAS REINHARDTII* STRAIN, CC-503[1]

Introduction

The photosynthetic green alga, *C. reinhardtii*, can successfully acclimate to fluctuating levels of external C_i, without compromising its photosynthetic efficiency. It does so by the induction of an efficient C_i uptake and utilization process that elevates the CO_2 levels around Rubisco, better known as the Carbon Concentrating Mechanism or CCM (Badger et al., 1980). Important components of the CCM are the pyrenoid (Chapter 4), C_i transporters, and carbonic anhydrases (CAs; carbonate dehydratase; EC 4.2.1.1). CAs are zinc-metalloenzymes that catalyze the reversible inter-conversion of CO_2 and HCO_3^-, and they exhibit multiple physiological roles at different cellular locations. Early studies with *C. reinhardtii* showed that photosynthesis rate as well as C_i affinity were severely impaired by CA inhibitors, indicating that CAs directly participated in the CCM of *C. reinhardtii* (Berry et al., 1978; Tsuzuki and Miyachi, 1979; Badger et al., 1980; Moroney et al., 1985; Tsuzuki et al., 1980; Tsuzuki and Miyachi, 1989).

Twelve CAs have been identified so far in *C. reinhardtii* (Moroney and Ynalvez, 2007; Moroney et al., 2011; Mukherjee and Moroney, 2011). As mentioned earlier (Chapter 2), the twelve CA genes are made up of three α-, six β- and three γ-CAs. CAH1, one of the α-CAs, was the first CA isoform to be isolated from *C. reinhardtii*. Work from Miyachi's group and others showed that CAH1 was found in the periplasmic space of *C. reinhardtii* (Fukuzawa et al., 1990a; Fukuzawa et al., 1990b). In fact, if cells from a low-CO_2-grown culture were pelleted by centrifugation, CA activity could easily be detected

in the supernatant (Rawat and Moroney, 1991). Furthermore, the CAH1 protein can be detected in the cell wall fraction using immunoblots (Ishida et al., 1993). Immunogold localization studies using anti-CAH1 antibodies also clearly showed labeling in the cell wall region (Moroney and Ynalvez, 2007). In addition, the primary sequence of CAH1 has a leader sequence that is consistent with a secretory pathway signal (Fujiwara et al., 1990; Ishida et al., 1993).

CAH1 is an unusual CA that has two large and two small subunits. The assembly of CAH1 is a multi-step process. Work in the early and mid-nineties showed that CAH1 is extensively processed after it is translated (Ishida et al., 1993). During translation, the CAH1 is directed to the ER lumen and the leader sequence is cleaved. Subsequently, an internal region of the protein is excised, leaving a large and a small subunit that remain associated in the periplasmic space through disulfide bridges. In addition, the protein is glycosylated (Fukuzawa et al., 1990b). After all of these post-translational modifications, the protein is sent to the periplasmic space. The final protein is a heterotetramer consisting of two large and two small subunits connected by disulfide bridges (Kamo et al., 1990; Ishida et al., 1993).

Like many other key CCM proteins, CAH1 is highly induced under limiting CO_2 conditions, under the control of the CCM master regulator gene *CCM1(CIA5)* (Moroney et al., 1989; Fukuzawa et al., 2001; Xiang et al., 2001). Additionally, LCR1, a MYB-type transcriptional factor, was reported to regulate CAH1, LCI1 and LCI6 via CCM1 under low CO_2 conditions (Yoshioka et al., 2004). Many studies have focused on the role of this CA in the *C. reinhardtii* CCM (Fujiwara et al., 1990; Fukuzawa et al., 1990a, 1990b; Ishida et al., 1993). Studies using acetazolamide, a soluable CA inhibitor, caused a small

decrease in the affinity of the cells for C_i (Berry et al., 1978; Tsuzuki and Miyachi, 1979; Badger et al., 1980; Tsuzuki et al., 1980; Tsuzuki and Miyachi, 1989). The work was extended by making dextran bound sulfonamide (DBS), a membrane impermeant CA inhibitor (Moroney et al., 1985), demonstrating that DBS inhibited C_i-dependent O_2 evolution to the same extent as acetazolamide. This led to the conclusion that inhibiting the periplasmic CAs also reduces the ability of *C. reinhardtii* to obtain C_i from the medium (Moroney et al., 1985). However, later mutant studies have not supported the inhibitor work. In 1999, Van and Spalding characterized a strain, *cah1*, which has a deletion in the *CAH1* gene (Van and Spalding, 1999). By growing the cells at different external pH and measuring C_i-dependent O_2 evolution at different pH, no significant physiological differences between *cah1* and wild-type cells could be detected.

The strain CC-503 ($nit1^-$, $nit2^-$, cw-92, mt^+), together with the other wild-type strains D66 (CC-4425, $nit1^-$, $nit2^-$, cw15, mt^+) and C9 (CC-408, mt^-), are common laboratory strains used for experimental studies in the *C. reinhardtii* field. The cw-92 cell wall deficiency (Hyams and Davies, 1972; Harris et al., 2009) in CC-503 facilitates the isolation of genomic DNA, thus making this strain the reference strain for *C. reinhardtii* genome sequencing (Merchant et al., 2007). For the same reason, nuclear transformation becomes more efficient when using this strain due to its minimal barrier from the cell wall. However, in the course of CCM related experiments performed with CC-503 as a wild-type strain, it was discovered that the CAH1 protein could not be found in the strain CC-503. This observation was quite surprising when one considers the great abundance of CAH1 when other wild-type strains are under the low CO_2 stress (Moroney et al., 2011). Attempts were made to explain the lack of CAH1 protein in CC-503, as well as to

explore the possible physiological consequences from missing CAH1. Most importantly, this chapter highlights the fact that the sequenced strain CC-503 is a natural mutant for the periplasmic CA, CAH1.

Results

The CAH1 protein is not present in CC-503

The *CAH1* gene is known to be highly transcribed upon induction of the *C. reinhardtii* CCM (Moroney et al., 2011). For the wild-type strains D66 and C9, the presence of the CAH1 protein could be easily detected by immunoblotting in low CO_2 acclimated cells (Figure 6.1), which is consistent with previous observations (Kucho et al., 1999; Mitra et al., 2004). However, in CC-503, the CAH1 protein could not be detected (Figure 6.1). The lack of CAH1 in CC-503 resembles the situation in the two control mutants here, *cia5* and *cah1*. The *CAH1* gene is either not responsive to low CO_2 stress due to the *CIA5* mutation, or the *CAH1* gene itself is defective as seen in the *cah1* mutant (Van and Spalding, 1999). While level of CAH1 was undetectable in CC-503, the level of the other important CCM components CAH4 and CCP1 was not affected. The CAH1 transcriptional regulator LCR1, (Yoshioka et al., 2004), is presumably functional in CC-503 as evident by the normal levels of LCI1, another protein that is regulated by the same gene (Figure 6.1).

CC-503 has an extra repeat region in the CAH1 promoter

The absence of CAH1 may be due to the presence of a mutation in the *CAH1* locus, which results in a lack of inductionof *CAH1* in CC-503. In the *CAH1* promoter nucleotide transcription start site that was sufficient for the CO_2 responsive transcription

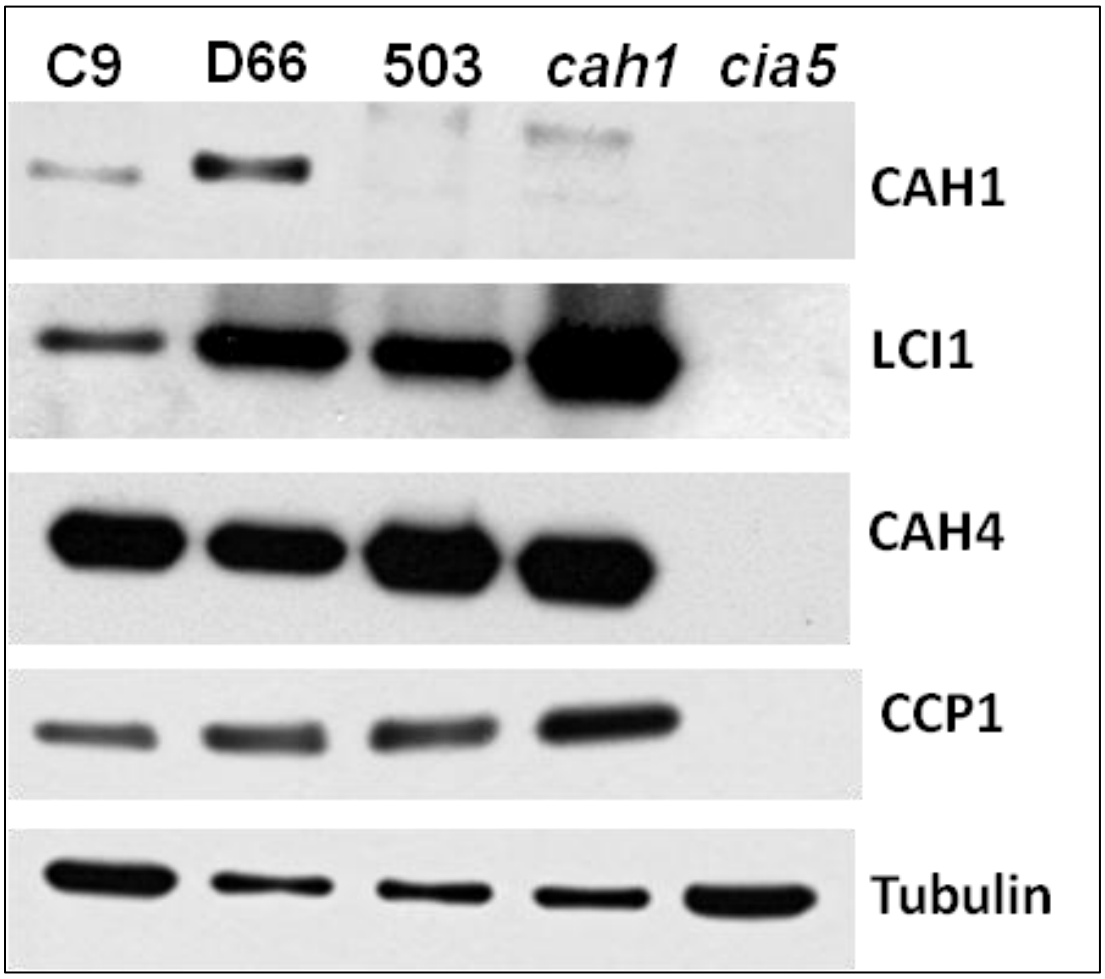

Figure 6.1. CAH1 is missing in CC-503

Western blot analysis using a CAH1 specific antibody shows the absence of CAH1 in CC-503. LCI1, CAH4 and CCP1 are CCM proteins that are induced under low CO_2 conditions. *cah1*: CAH1 mutant strain; *cia5*: CCM mutant strain.

of the *CAH1* gene (Kucho et al., 1999). This region was found to consist of two parts, a 358-bp silencer region from -651 to -294 and a 185-bp enhancer element from -293 to -109 with respect to the transcriptional start site. The silencer region was shown to repress the gene under high CO_2 conditions whereas the enhancer region induced gene expression under low CO_2 conditions in the presence of light (Kucho et al., 1999). DNA sequence comparison was performed between the *CAH1* sequence in the CC-503 (available from the *C. reinhardtii* genome database, Version 4.0) and the published sequence from C9 (Kucho et al., 1999; Kohinata et al., 2005). It was found that both the 358-bp silencer region and the 185-bp enhancer region, as well as the coding sequence were identical in both CC-503 and C9. However, there was one significant difference upstream of the 358-bp silencer region. In C9, there was a 78-bp region consisting of about 13 tandem repeats of the sequence AGGGGC. In CC-503, however, this repeat region was about 582-bp long, with 97 tandem repeats (Figure 6.2).

Attempts to verify the presence of the repeat region by PCR amplification using primers flanking the repeat region failed in case of the CC-503 and revealed a slightly longer fragment than expected in the case of C9 (data not shown). The repeat could form what is called a G-quartet, which could pose a difficulty in the PCR amplification from the CC-503 genomic DNA. The presence of these repeats might also have interfered with the proper sequencing of this region which would mean that the actual number of AGGGGC repeats might vary from the values inferred from the sequences available from CC-503 and C9.

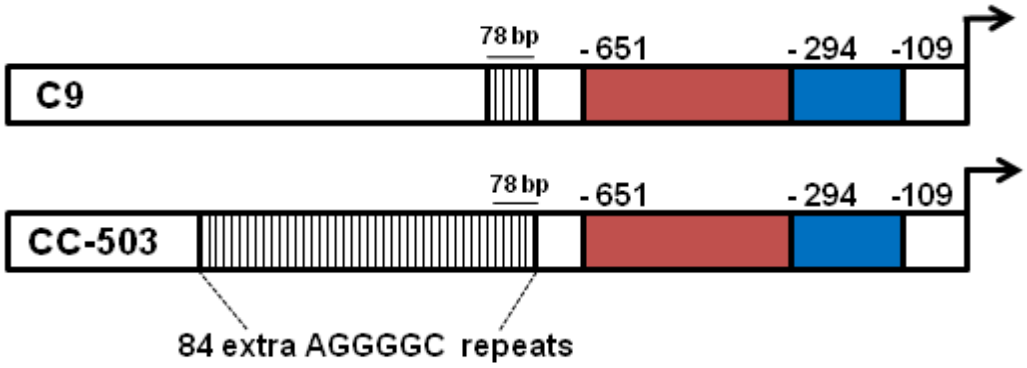

Figure 6.2. CC-503 has an extra repeat region in the CAH1 promoter

A schematic diagram of the region upstream of the *CAH1* transcriptional start site, from the two strains CC-503 and C9. The silencer region (red) and the enhancer region (blue) are identical between the two strains. However, there are 84 extra AGGGGC repeats upstream of the (-651 to -294) region in CC-503.

The CAH1 transcript was not affected in CC-503

The presence of the extra 79 repeats close to the *CAH1* transcriptional regulator region could be a possible contributing factor to the absence of the protein by reducing or eliminating the transcription of the *CAH1* gene. To test this hypothesis, an attempt was made to see if the gene was transcribed at the expected levels in CC-503.

CAH1 transcript levels measured by qRT-PCR, revealed that there was no significant difference in between the CC-503 strain and the other wild-type strains, D66 and C9 (Figure. 6.3). The presence of the whole transcript was also confirmed with PCR, using primers covering the first nine exons (data not shown). These data suggest that even though CAH1 protein is absent in CC-503, the *CAH1* gene is still transcribed at a comparable level to wild-type strains. Since the absence of the protein cannot be accounted for by a reduction in transcript levels, determining the cause for the absence of CAH1 will remain a focal point for future investigations.

CC-503 showed reduced growth at low pH

Previously, it was reported that in the absence of *CAH1*, *C. reinhardtii* cells failed to produce any significant differences in either the growth phenotype or the ability to induce a fully functional CCM at low CO_2, even when pH levels were varied (Van and Spalding, 1999). When the growth phenotype of CC-503 under different pH levels was tested in this study, it was noticed that the cells showed reduced growth at lower pH levels (pH 5.8) and a somewhat lesser reduction in growth at a high pH level (pH 8.2) (Figure 6.4). This growth phenotype was often more reduced when compared to the *cah1* mutant. While the *cah1* mutant cells could still grow at a low pH of 5.8, most of the CC-503 cells died at this low pH.

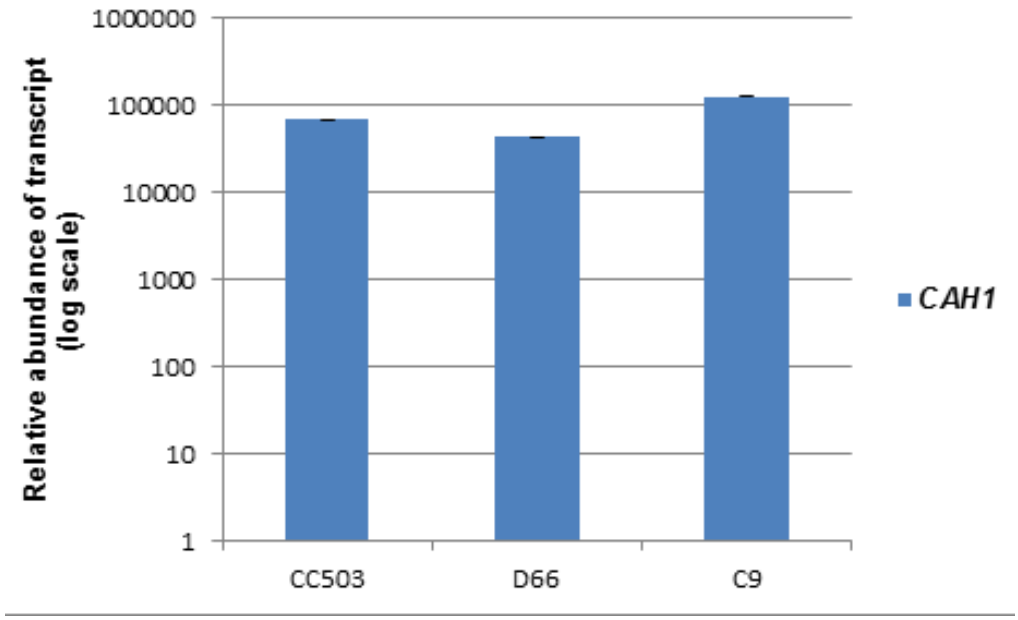

Figure 6.3. The *CAH1* transcript was not affected in CC-503

qRT-PCR measurements of the relative abundance of the *CAH1* transcript in CC-503, compared to D66 and C9 in low CO_2. The *CBLP* gene was used as an internal reference gene as it is of high abundance and its expression remains unchanged under varying CO_2 conditions.

The relative transcript level is expressed as the $2^{\Delta_{\Delta CT}}$, in which $\Delta_{\Delta CT} = \Delta CT_{\text{High } CO_2} - \Delta CT_{\text{Low } CO_2}$, and $\Delta CT_{\text{High/Low } CO_2} = \Delta CT_{CAH1} - \Delta CT_{CBLP}$

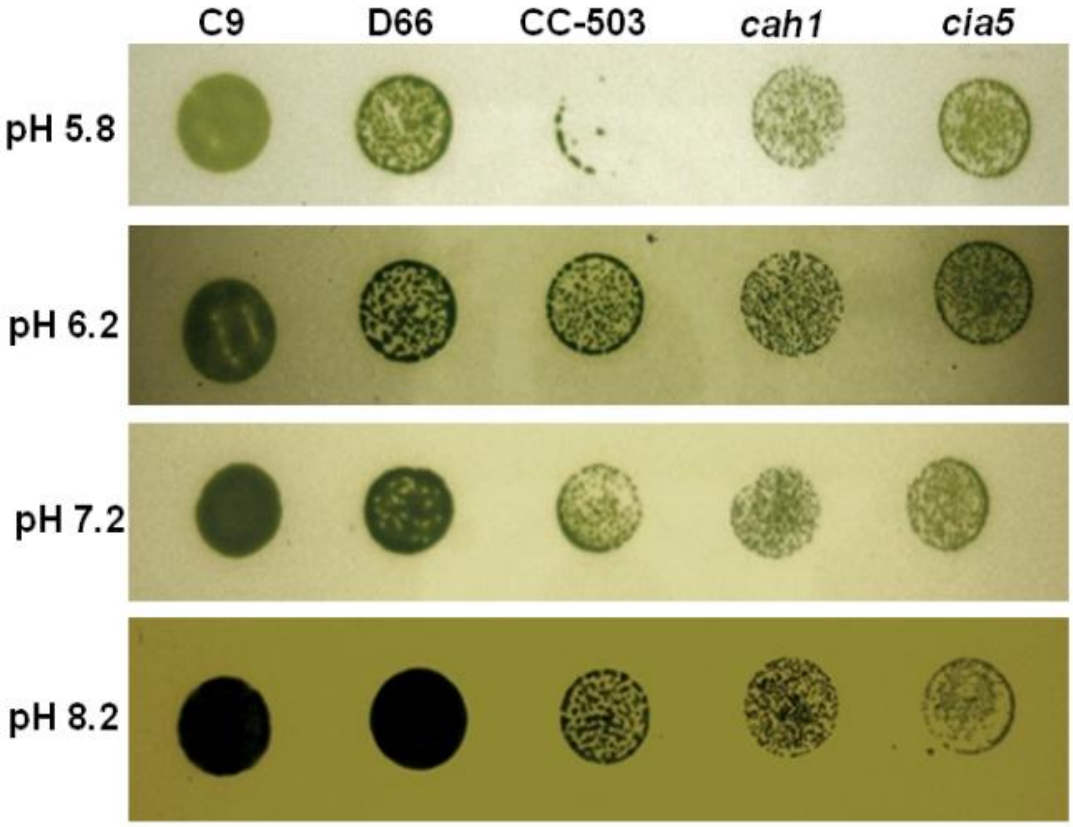

Figure 6.4. Growth phenotype of CC-503.

Growth phenotype of CC-503, compared to other wild-type cells C9 and D66, when grown under low CO_2 conditions at different pH levels. *cah1*: *CAH1* mutant, *cia5*: CCM mutant. For spot tests, 4000 cells of each strain were pipetted onto minimum agar plates. The plates were incubated in low CO_2 conditions (100 ppm) for 10 days.

CC-503 showed no reduction in photosynthesis rate

The ability of the CC-503 strain to induce an otherwise normal CCM was indicated by the presence of other key CCM proteins at levels comparable to those in other wild-type strains (Figure 6.1), as shown in all laboratory generated *CAH1* mutant strains. The rate of O_2 evolution in CC-503 at different pH levels did not deviate much from the other cell wall deficient wild-type strain, D66 (Figure 6.5). At a low pH level of 6.2, CC-503 cells showed a photosynthetic response similar to the mutant *cah1*. This trend was consistent at pH levels of 7.2 and 8.2 (data not shown).

Discussion

CAs are important components of the CCM in *C. reinhardtii* in catalyzing the conversion between CO_2 and bicarbonate and plays a critical role in directly or indirectly delivering CO_2 to Rubicso. For example, the thylakoid lumen CA, CAH3, is proposed to assume the important role in directly delivering CO_2 to Rubisco in the pyrenoid region. This CA converts the accumulated bicarbonate into CO_2, which then diffuses out of the thylakoid lumen (Moroney and Ynalvez, 2007; Moroney et al., 2011; Mukherjee and Moroney, 2011). Mutants that lack the CAH3 exhibited a severe growth reduction in low CO_2 conditions (Spalding et al., 1983a; Moroney et al., 1986; Funke et al., 1997; Karlsson et al., 1998). In these mutants, bicarbonate over-accumulates intracellularly, but cannot be assimilated due to the lack of CAH3 activity. The role of the periplasmic CA, CAH1, is not entirely clear. Localized in the cell wall region of a *C. reinhardtii* cell, CAH1 is proposed to play a role in assisting the delivery of external C_i into the cell, especially when cells are under alkaline conditions (Moroney et al., 1985; Giordano et al., 2005; Mitra et al., 2005; Spalding, 2008).

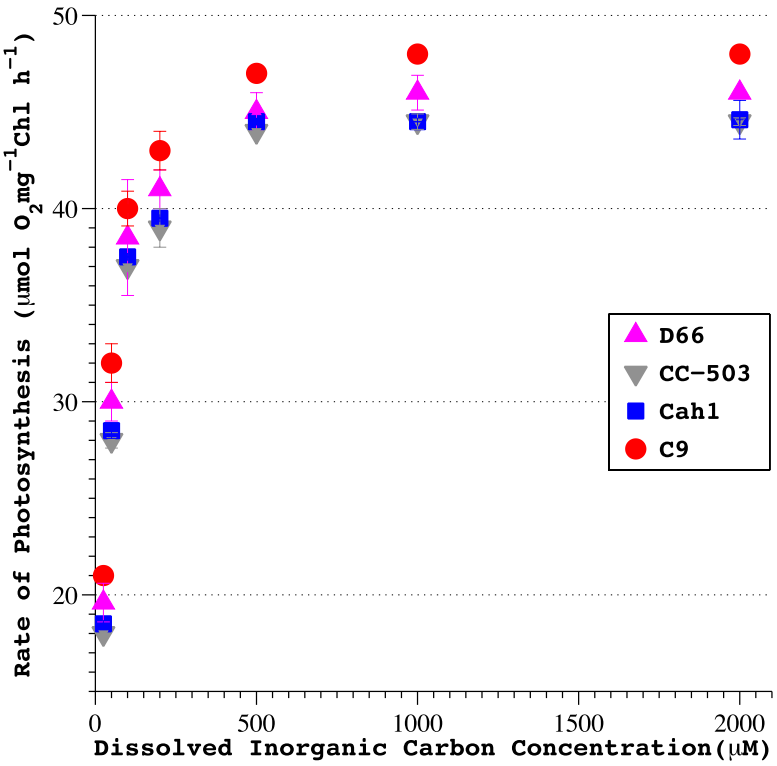

Figure 6.5. CC-503 showed no changes in photosynthesis rate

The rates of photosynthesis in low CO_2 grown cells of D66 (▲), CC-503 (▼), *cah1* (■) and C9 (●) measured as a function of the dissolved inorganic carbon concentration (provided by solutions of $NaHCO_3$ ranging from 25μM to 2 mM). Experiments were carried out an external pH of 6.2 and each point represents the mean and standard deviation of three replicates.

Early studies using both membrane permeable and membrane impermeable CA inhibitors had demonstrated that the reduction in CA activity was correlated with the impaired C_i affinity for the cell, suggesting the periplasmic CA is essential for the CCM in *C. reinhardtii* (Berry et al., 1978; Tsuzuki and Miyachi, 1979; Badger et al., 1980; Tsuzuki et al., 1980; Moroney et al., 1985; Tsuzuki and Miyachi, 1989). However, studies by Van and Spalding (1999) using the *cah1* mutant, suggested that the functioning of the CCM and the photosynthesis efficiency were not affected in the *cah1* mutant.

In this study, we found that a *C. reinhardtii* strain CC-503, the strain sequenced in the *C. reinhardtii* genome project (Merchant et al., 2007), does not contain CAH1. By inspecting the genome sequence of CC-503, it was found that it has about 92 copies of the DNA repeat, AGGGGC, at about 700 base pairs upstream of the transcription start of *CAH1*. Other *C. reinhardtii* strains have only a few copies of the DNA repeat in the same region (Kucho et al., 1999; Kucho et al., 2003; Kohinata et al., 2005; Merchant et al., 2007). The presence of the extra repeat appears not to affect transcription of *CAH1*, but might contribute to the reduction in the amount of CAH1 protein in CC-503. Even though CC-503 has no detectable CAH1, it grows normally on low CO_2 concentrations and does not show a reduction in photosynthesis. In the case of both CC-503 and *cah1*, it is indicated that CAH1 is not essential to photosynthesis at low CO_2. This is in contrast to the inhibitor studies which indicated that the periplasmic CA was needed for efficient delivery of C_i to the cell.

How might the two different results be reconciled? One difference between the two approaches is there may be some remaining CA activity in the periplasmic space of the mutant strains. In both the cases of *cah1* and CC-503, it has not been determined

whether the other periplasmic α-CA, CAH2, is present. CAH1 and CAH2 are extremely closely similar, showing only a few amino acid differences (Fujiwara et al., 1990; Fukuzawa et al., 1990a; Fukuzawa et al., 1990b). In addition, these two genes are adjacent to each other on chromosome 4, forming a tandem repeat (http://genome.jgi-psf.org/Chlre4/Chlre4.home.html). It appears that *CAH2* might be the result of a gene duplication event, as it is not highly expressed under any tested growth condition. It is possible that enough CAH2 is present in both strains to facilitate C_i diffusion to the plasma membrane. In addition, since CAH1 was not deleted in CC-503, a small percentage of the protein might be made since the DNA difference is in the promoter region and not the coding region. Inhibitor studies may be a better indicator of the role of the periplasmic proteins because the inhibitor would block both isoforms, while in the mutants only CAH1 is knocked out or reduced.

An additional complication is the presence of CAH8 (Ynalvez et al., 2008). This protein also appears to be located on the plasma membrane or in the periplasmic space close to the plasma membrane. One question is whether the active site of CAH8 is on the outside or inside of the cell. The TMpred program predicts that the active site would be on the outside of the cell membrane. If it is outside of the cell, then it would be expected that CAH8 activity is partially redundant with that of CAH1 and CAH2. The phrase "partially redundant" is used as CAH1 and CAH2 are found in layers of the cell wall quite far from the plasma membrane and are actually shed by *C. reinhardtii* during cell division. If CAH8 is outside of the cell, its presence could explain why CAH1 deletion strains show no reduction in C_i-dependent O_2 evolution. In this case the acetazolamide could be inhibiting three different isoforms while the deletion strains are only missing

CAH1. If, however, the active site of CAH8 is inside the cell, then its role would be quite different than that of CAH1 and CAH2. In this case, CAH8 might be facilitating the entry of CO_2 into the cell by rapidly converting the CO_2 to HCO_3^- as it enters the cell, maintaining the concentration gradient across the membrane.

Almost all research in the *C. reinhardtii* field has utilized three major stock lines (Sager, Cambridge and Ebersold/Levine) as wild-type strains, which are assumed to be descendants of a single zygote isolated by Smith in 1945 (Harris et al., 2009). The strain C9 was descended from the stock sent to Japan by Sager in 1945, and was used as the wild-type strain for EST sequences at Kazusa DNA Research Institute in Japan (Asamizu et al., 1999; Asamizu et al., 2000; Asamizu et al., 2004). The strain CC-503 and D66 both belong to the Ebersold/Levine line, in which the gene encoding nitrate reductases were mutated ($nit1^-$, $nit2^-$). These two strains appeared to deviate from each other. And this separate probably could be dated back when Davies first make the categorization of *C. reinhardtii* strains based on cell wall mutations (Davies and Plaskitt, 1971; Hyams and Davies, 1972; Schnell and Lefebvre, 1993; Harris et al., 2009). D66 carries the cw-15 mutation while CC-503 carries the cw-92 mutation, which resulted in minimal wall material. Given the normal levels of photosynthesis and CCM induction in CC-503, the growth phenotypes seen at lower pH values may be a result of the extreme cell wall deficiency in CC-503. The multilayers of cell wall in a normal situation might act as a physical matrix in the retention of CO_2 molecules which is the dominant C_i species under low pH. The presence of a CA in the periplasmic region can actively convert the retained CO_2 into bicarbonate to be transported into the cell. In the case of CC-503, where this physical matrix is minimal and CA activity is greatly lost, it could be expected that the C_i

affinity is impaired and growth is altered. With the minimal cell wall in the CC-503, it could also be possible some cell-wall associating H^+/ATPase is also missing in this strain. Furthermore, cw-92 mutation in the CC-503 might associate with mutations in other alleles. For example, the enzyme required for the glycosylation of CAH1 may be defective, which would result in the lost of CAH1 protein after translation. Nevertheless, it would of great interest to investigate whether other strains that carry this cw-92 mutation are equally susceptible to low external pH levels.

The aim of this work was to highlight the fact that CC-503 might be a natural *C. reinhardtii* mutant for CAH1. For example, it would be recommended to avoid using this strain as the wild-type to study CCM especially using transcriptomics approaches in a genome-wide scale. Although no obvious expression differences were observed in the CCM genes examined in this study, there is no guarantee that other untested or yet to be identified CCM genes are not affected in the absence of CAH1 in CC-503. Regardless of its lack of CAH1, this strain could prove valuable if used together with the already existing mutants of this gene in further elucidation of CAH1 function and regulation in *C. reinhardtii*. Now that we have a few *cah8* mutants obtained from a recent mutagenesis screen (Chapter 7), the crossing of the *cah8* mutant with either the *cah1* mutant or the CC-503 strain could be help to further characterize the role of the CAH1 in the *C. reinhardtii* CCM.

Endnotes

[1] All the figures are contributed by Bratati Mukherjee. The presence of the transcript of CAH1, and the phenotype differences at different pH conditions were observed by the author of this dissertation.

CHAPTER 7
PCR-BASED REVERSE GENETICS MUTAGENESIS SCREEN[1]

Introduction

Since its first isolation from a potato field near Amherst, Massachusetts by GM Smith in 1945 (Harris et al., 2009), *C. reinhardtii* has been serving as a model organism in the study of many photosynthesis processes, including the studies on the CCM. Considerable progress has been made towards understanding of expression, regulation and function of the CCM components in *C. reinhardtii* (Moroney and Ynalvez, 2007; Spalding, 2008; Yamano and Fukuzawa, 2009; Mukherjee and Moroney, 2011). The use of forward genetic screens has been the primary method used to identify and characterize essential CCM genes (Spreitzer and Mets, 1981; Moroney et al., 1989; Suzuki et al., 1990; Colombo et al., 2002; Pollock et al., 2003). This process involves a random mutagenesis (*via* UV, chemical mutagen, or insertion of a foreign DNA), a subsequent screen for a conditional phenotype (for example, the "sick on low CO_2 phenotype" described in Chapter 4), and a final genetic identification of the mutated locus. The first CCM deficient mutant named *ca-1-12*-1C (designated as CC-1219 in the *Chlamydomonas* Center) was isolated nearly thirty years ago (Spreitzer and Mets, 1981; Spalding et al., 1983a). Later on, it was revealed the mutant lacked the thylakoid lumen carbonic anhydrase CAH3 (Funke et al., 1997; Karlsson et al., 1998). Subsequently, three other independent *CAH3* mutants (*cia1*, *cia2*, *cia3*) (Moroney et al., 1989), two *CCM1* mutants (*cia5*, C16) (Moroney et al., 1989; Fukuzawa et al., 1998; Van et al., 2001), two *LCIB* mutants (*pmp1*, *ad1*) (Wang and Spalding, 2006) and a few other CCM mutants were identified through mutagenesis screens (Table 7.1). The identification and

characterization of these mutants has contributed in large part to the understanding of the *C. reinhardtii* CCM. However, forward genetics screens have their limitations since only mutants with a noticeable phenotype can be isolated and characterized. But not all mutants would exhibit a certain phenotype, especially in a general mutagenesis phenotype screen. For example, the *CAH1* mutants (*cah1* as well as CC-503) do not have dramatic phenotypes especially under normal pH growth conditions (Van and Spalding, 1999; Mukherjee et al., 2011).

On the other hand, with the *C. reinhardtii* genome now fully sequenced, using reverse genetics is becoming more practical and powerful. The use of the conserved RNA silencing mechanism (Ecker and Davis, 1986; Fire et al., 1998) has been developed in *C. reinhardtii* to elucidate the biological function of particular genes via both siRNA and miRNA (Rohr et al., 2004; Kim and Cerutti, 2009; Molnár et al., 2009; Petroutsos et al., 2009; Zhao et al., 2009; Remacle et al., 2010). Using this approach, a few CCM components have been studied and their roles in the CCM were elucidated (Pollock et al., 2004; Duanmu et al., 2009b). Regardless of its profound contribution to the understanding of biological processes in *C. reinhardtii*, RNAi is notorious for its off-target effects (Xu et al., 2006; Gilchrist and Haughn, 2010). An alternative way for gene specific mutagenesis is through zinc-finger nucleases (Durai et al., 2005; Porteus and Carroll, 2005; Urnov et al., 2010), which provides more specificity in genome editing. This approach has been used effectively in Arabidopsis, tobacco, soybean and other plants (De Pater et al., 2009; Osakabe et al., 2009; Petolino et al., 2010; Curtin et al., 2011; Tzfira et al., 2012). However, to date there is no successful report of knocking out a specific gene in *C. reinhardtii* using zinc-finger nucleases.

Over the decades, by using both forward and reverse genetics, a collection of CCM mutants was generated and characterized (Table 7.1). These mutants can often be acquired from the *C. reinhardtii* Center, substantially contributing to the studies in this field and the deeper understanding of CCM. However, a large number of the proposed CCM genes do not have a corresponding mutant, which hinders understanding the specific role of each component, and the development of the entire CCM network. For example, the chloroplast stroma carbonic anhydrase CAH6 has been postulated to play an important role in CO_2 fixation by reducing the leakage of CO_2 out of the chloroplast or by maintaining the elevated CO_2 concentration around Rubisco (Yamano and Fukuzawa, 2009). CAH6 has also been proposed to be associated with the Rubisco containing body, the pyrenoid, and a chloroplast stroma protein LCIB (Yamano et al., 2010). If a *CAH6* mutant were available, the biological role of this carbonic anhydrase could be better assigned, and the interaction among the CCM components could be further studied.

In light of the recently published work by Gonzales-Ballester et al. (2011), a large scale insertional mutagenesis screen employing a PCR-based reverse genetics approach was planned to obtain more mutants in which potential CCM genes are disrupted. In their work, by incorporating the concept of both DNA pooling from a number of transformants and development of a primer cocktail from one specific gene, the speed and efficiency of the PCR-based mutant screening was dramatically increased. Starting with a 100,000-mutant library, a total of 45 mutants were identified with insertions in 37 different genes out of 63 screened.

This chapter described a pilot project to identify more potential CCM components using this approach. Furthermore, this pilot project aimed to optimize the workflow and

Table 7.1. **A list of the CCM mutants and the methods used in mutant generation.**

Gene	Gene functions	Mutant	Mutant Generation	References
CCM1	Master regulator for CCM induction	*cia5, C16*	EMS	Moroney et al. (1989); Fukuzawa et al., (1998)
LCR1	Myb-type TF controlled by *CCM1*	*lcr1*	NIA insertion	Yoshioka et al., (2004)
CAH1	Periplasmic carbonic anhydrase	*cah1*	Tagging	Fukuzawa et al (1998); Van and Spalding (1999)
CAH3	Thylakoid lumen carbonic anhydrase	*ca1, cia1, cia2, cia3*	EMS	Spalding et al (1983a); Moroney et al., (1989)
LCIB	chloroplast soluble protein	*pmp1, ad1*	EMS	Wang & Spalding (2006)
HLA3	putative plasma membrane ABC-type Ci transporter,		RNAi	Duanmu et al., (2009b)
CCP1/ CCP2	putative mitochondria carrier proteins		RNAi	Pollock et al., (2004)
ycf10	chlroplast encoded, inner chloroplast envelope membrane Ci transporter		HR	Rolland et al (1997)
GYD1	glycolate dehydrogenase;	*gdh1*	ARG insertion	Nakamura et al (2005)
PGP1	Phosphoglyco-phosphatase	*pgp1*	EMS	Mamedov et al (2001); Suzuki et al (1990); Ma et al (2011b)
RCA1	Rubisco activase	*rca1*	Ble Insertion	Pollock et al (2003)
CIA6	Required for pyrenoid formation	*cia6*	Ble Insertion	Ma et al (2011a)

The majority of the generation methods were based on forward genetics, in which random mutagenesis followed by subsequent phenotype screens to isolate mutants with aberrant phenotypes. The generations of the *HLA3* and *CCP1/CCP2* mutants are currently the only two exceptions using the reverse genetics to illuminate gene functions. EMS: Ethyl methanesulfonate; NIA: Nitrate reductase; HR: homologous recombination.

procedures during this process, and to provide the foundation for a future large-scale mutagenesis to obtain more mutants for studies in the CCM.

Results

With the goal to identify more CCM components and to illuminate the biological functions of proposed CCM genes, a PCR-based reverse genetics mutant screen was performed, inspired by the work from Gonzales-Ballester et al (Referred to as Gonzales-Ballester's method hereinafter). The overall screening strategy used was similar. After mutagenesis, the genomic DNA from the positive transformants was pooled together to serve as the PCR template; the antibiotic resistance gene (*AphVIII*) cassette insertion locus could be identified via PCR using one primer inside the *AphVIII* cassette and one primer from the gene locus where the *AphVIII* cassette inserted. Over the course of five months, a total of 22,860 insertional mutants were generated, and 71 genes that are possibly involved in the CCM were screened. Insertions in eight different genes were identified and validated by sequencing. A total of eleven mutants were obtained at the end of the mutagenesis screen.

The general workflow is described in Figure 7.1 through Figure 7.3. Figure 7.1 and Figure 7.2 illustrate the DNA pooling strategy used early in the screen and the single colony identification method used later in this study. Figure 7.3 illustrates the overall primer design for all the CCM related genes, and gives more detail about the PCR tactics used in the early stage of the screening process. Figures 7.4 through 7.6 show the control PCRs performed before the actual PCR screens. Figures 7.7 through 7.13 present the detailed PCR data, using the identification of two mutants with insertion in the *Bestrophin* (referred to 516309 in the text), and *RHP1* as examples.

Generating Mutants

Mutant selection was performed using Paromomycin as the selective antibiotic, mainly due to its non-mutagenic nature, making it more favorable than Bleomycin, an antibiotic that induces DNA damage if the transgene is not active immediately (Chen et al., 2008). The Paromomycin resistance cassette was obtained from the plasmid pSL18 (Depege et al., 2003). Using restriction enzymes, a DNA fragment comprising the *Hsp70+RbcSII* dual promoter, the ORF of the Paromomycin resistance gene: aminoglycoside 3'-phosphotransferase (*AphVIII*) (Sizova et al., 2001), and the *RbcSII* terminator was obtained. The purified $Paro^R$ cassette was transformed into the wild-type strain D66 by electroporation (Shimogawara et al., 1998). Considering abiotic stressors like low CO_2 concentrations might lead to dramatic chromatin structural changes especially around active CCM genes, the CCM was induced in D66 cultures for 4 hours before electroporation, presumably making the CCM related genes more accessible to the foreign DNA. The choice of the parental strain D66 (*nit2*$^-$, *cw15*, *mt*$^+$) (Schnell and Lefebvre, 1993) was based on its high efficiency in transformation due to its type-C cell wall deficiency (Harris et al., 2009). Overall, 197 individual transformations were conducted, and a total of 22,860 Paromomycin resistant mutants were obtained corresponding to an approximate $2x10^{-6}$ transformation efficiency. Meanwhile, all paromomycin positive colonies were screened in low CO_2 conditions. Nearly 522 colonies were judged to have a sick on low CO_2 phenotype in an initial screen and ultimately 37 colonies showed a definite sick on low CO_2 phenotype. The detailed results of the second screen are summarized in Appendix IV.

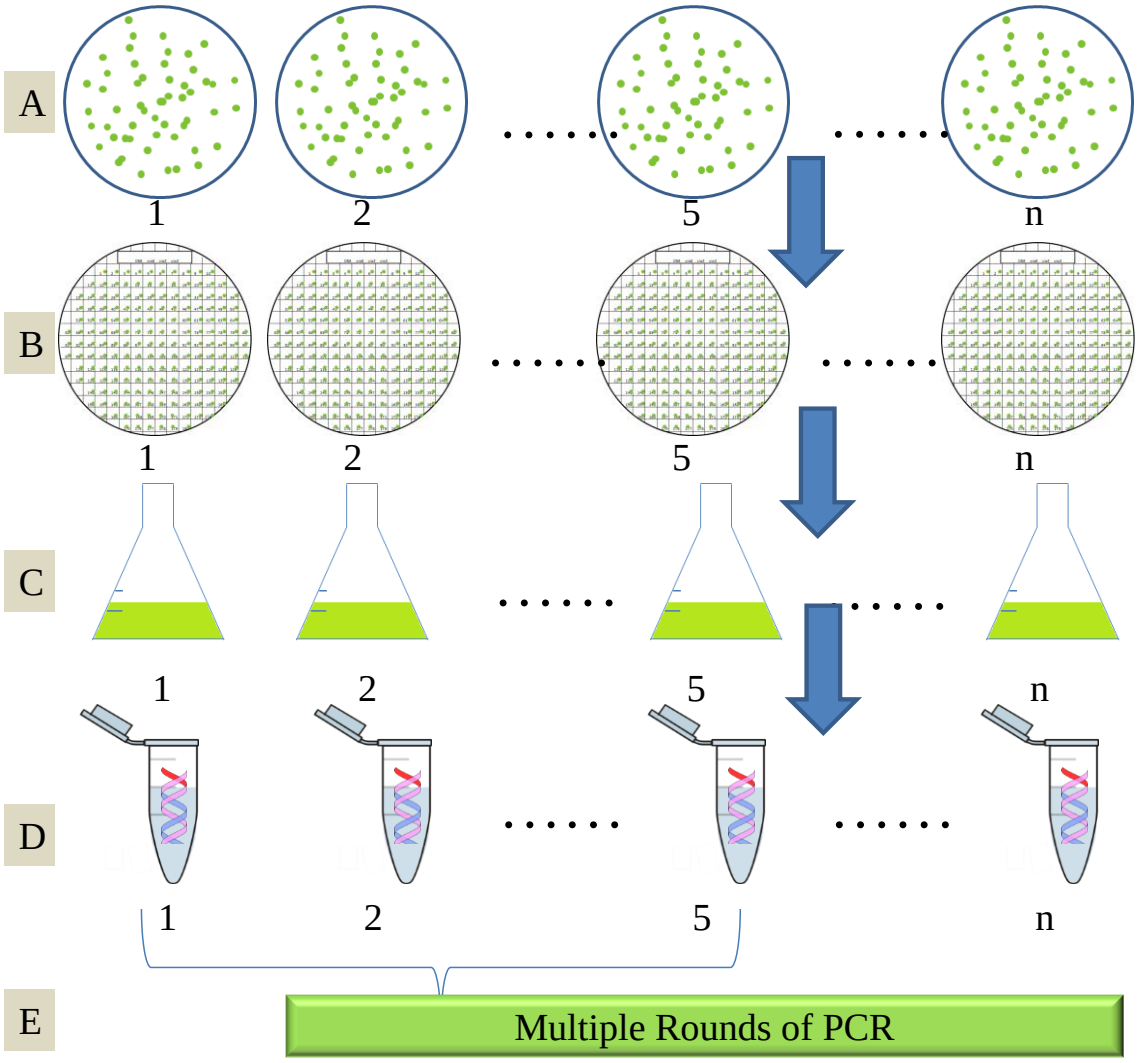

Figure 7.1. Culture maintenance and DNA preparations.

Mutants generated by transforming with the *AphVIII* cassette were first selected on TAP-paro plates (A). Every 180 colonies were then transferred onto TAP-paro grid plates (B). For every plate, all 180 colonies were scrapped into a TAP containing flask for culture growth (C) and DNA preparation (D). DNA from five individual plates were pooled together (referred to as "pooled DNA") serving as a PCR template (E).

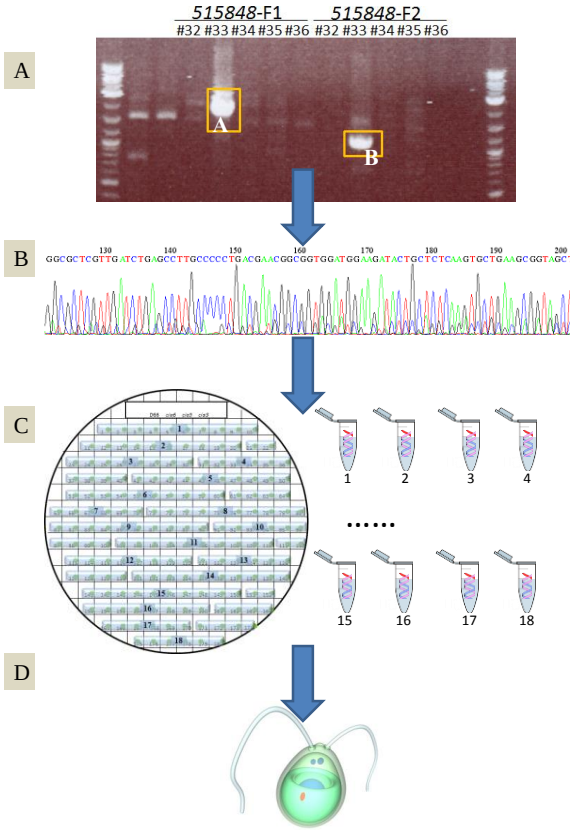

Figure 7.2. Sequencing and Identifying Single Colonies.

After the PCR signal is confirmed by multiple rounds of PCR (Figure 7.1) using pooled DNA, the DNA from the five individual plates composing the pooled DNA were used as the PCR templates to identify where the PCR signal originated. In this figure, F1 from the gene (*515848*) paired with primer RB1 from the *AphVIII* insertion yielded a fragment around 2-kb (band A). Additionally, F2 from *515848* yields a fragment around 1-kb (band B), corresponding to the 1-kb gap between the two primers F1 and F2. These two PCR signals originally observed from DNA pool #5 consisted of plate #32, # 33, #34, #35 and #36 could be traced back to a single plate #33 (A).

After the verification of the PCR signal from a single plate DNA, the PCR product is sequenced to validate the gene specific insertion (B). Subsequently, the mutations verified by sequencing could be traced back to individual colonies by two steps. Firstly, every ten colonies are pooled together for PCR analysis (C). Secondly, ten individual colony PCRs are performed to identify one single colony with *AphVIII* insertion (D).

Culture Maintenance and DNA preparation

Unlike the Gonzales-Ballester's method that uses 96-well microtiter plates for colony propagation and DNA preparations, we used agar plates for *C. reinhardtii* maintenance and DNA extractions (Figure 7.1 and Figure 7.2). The advantages that 96-well microtiter plates might offer are the quick indexing of generated mutants, better space usage for storage and growth of mutants, and compatibility with robot systems. However, the 96-well microtiter plates have disadvantages for the growth of *C. reinhardtii*. Unlike mammalian cells, *C. reinhardtii* cells do not adhere to the tube. This could create the potential cross-contamination problems within a microtiter plate after repetitive handling of the plate. Secondly, *C. reinhardtii* in microtiter plates might be more exposed to bacterial and fungal contamination. When *C. reinhardtii* is maintained on a plate, the contamination can be easily monitored and controlled. However, the contaminations in one well of the microtiter plate might spoil the entire microtiter plate. Thirdly, according to observations in our lab, the growth of *C. reinhardtii* in a microtiter plate is not as robust as on a plate, possibly due to the limited gas exchange inside the plate wells. Thus during this round of mutagenesis screen, we used the traditional agar plate with a 180-colony grid, for transformants maintenance and all other related procedures. A total of 152 180-colony plates were generated at the end of the mutagenesis. Those plates were stored in 4℃ cold room for 30-60 days. From the 152 plates, 135 plates were maintained throughout the screening process. Five plates were lost during the cold room storage and 12 others due to contamination.

The Gonzales-Ballester's method utilized a system in which every 96 colonies (one microtiter plate) were pooled together for one DNA preparation and every ten DNA

preparations were pooled together for one set of PCR screens. Therefore, 960 individual colonies were screened simultaneously. With our system, all 180 colonies from one plate were pooled together for one DNA preparation and every five DNA preparations were further combined (referred to "pooled DNA" hereinafter) for one set of PCR screens. Likewise, in our system, all 900 individual colonies were screened simultaneously. From the 135 plates maintained, 135 DNA preparations were performed and 27 DNA pools were generated for PCR screens.

PCR Screens

Taking advantage of primer cocktails, a PCR-based reverse genetics screen (Figure 7.3) was used to identify mutants with lesions in specific genes possibly involved in the CCM (Table 7.2). Briefly, potential CCM genes were selected based on previous knowledge and published bioinformatics data (Table 7.2). Primers were designed (Figure 7.3A, Appendix V), and PCR screens using primer mixes were performed on DNA pools (Figure 7.3B). PCR signals were validated first by multiple rounds of PCR and then by sequencing (Figure 7.1, Figure 7.2). Finally, single colonies that possessed the positive signals were identified (Figure 7.2).

1. Gene Selection

Three classes of genes were selected as PCR targets (Table 7.2). The first two groups consist of genes that had been previously characterized and/or proposed as essential CCM components in *C. reinhardtii*. The third group was chosen from nearly 2000 genes identified as upregulated by low CO_2 studied by two recent RNA-seq publications (Brueggeman et al., 2012; Fang et al., 2012). For a quick index, the target

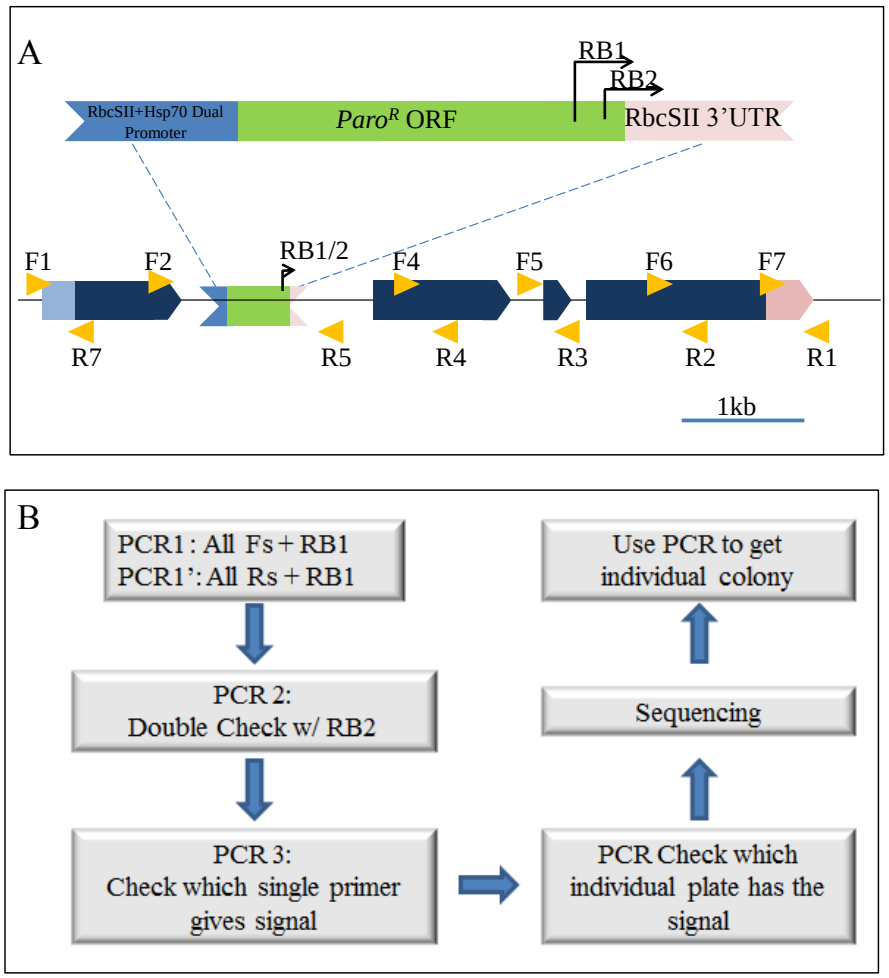

Figure 7.3. Primer design and PCRs.

(A): An example of a hypothetical Chlamydomonas nuclear gene with an *AphVIII* insertion. Primers are placed every 1-kb from each other and are designed in both directions. The first forward primer (▶, F1) is several base pairs beyond the 5'UTR (■), and the first reverse primer (◀, R1) is several base pairs beyond the 3'UTR (▶). Seven pairs of primers were designed for a 7-kb gene. For PCR, all forward primers are mixed together (referred to as "F") and all reverse primers are mixed together (referred to as "R"). (B): In this model, with the first round of PCR (PCR1, PCR1'), a positive PCR signal would be generated from PCR1', presumably by the amplification from RB1 paired with R5 and/or R4. A second round of PCR (PCR2) is used to verify the signal from the previous step using RB2 paired with R. PCR 3 is then performed to identify the single primer(s) responsible for the signal(s) seen in previous steps. The three PCR steps are followed another PCR to sheck which individual plate has the PCR signal. Subsequently, the PCR signal is verified by DNA sequencing, which verifies the gene specific insertion. Finally, individual colonies could be identified from the plates through a few rounds of PCR.

Table 7.2. A list of the 71 genes screened.

Protein ID	Name	Chromosome Location	Cluster	F.C.	EST
510853	NAR 1.6	chromosome_1:2015037-2018721(+)	n/a	2.4	0
511233	CGL41/RbcX	chromosome_1:4292836-4296074(-)	n/a	3.34	~40
511332	4660.C	chromosome_1:4886649-4894847(-)	9	n/a	13
510680	ABCt	chromosome_1:733666-752174 (-)	15	5.79	16
518934	HLA3	chromosome_2:3208217-3215491(+)	15	5.33	~40
▲ 519635	LCI9	chromosome_2:7341013-7348511(-)	n/a	3.36	~50
519637	LCI9 paralogue	chromosome_2:7356802-7362006(+)	8	2.08	20
519760	LCR1	chromosome_2:8320304-8324302(-)	15	5.72	16
520703	LCI1	chromosome_3:1912474-1915352(-)	15	11.57	~100
520827	PGP1	chromosome_3:2663806-2668960(+)	n/a	n/a	~30
520884	GYX1	chromosome_3:2940092-2943406(+)	n/a	n/a	2
520458	MTase	chromosome_3:521758-525622 (+)	15	4.51	4
521673	RDRP	chromosome_3:7132224-7143998(+)	8	5.22	1
▲▲▲ 521721	NAR1.3	chromosome_3:7664317-7672585(-)	3	n/a	~20
522029	THB4	chromosome_4:1182047-1186095(-)	8	n/a	9
522030	THB3	chromosome_4:1186937-1191795(-)	n/a	n/a	17
522119	CCP2	chromosome_4:1804462-1807550(-)	14	6.9	~40
522120	LCID	chromosome_4:1807721-1810885(+)	14	6.48	1
522126	CAH1	chromosome_4:1849022-1853330(-)	15	9.38	~150
522129	LCIE	chromosome_4:1874916-1877584(-)	15	7.56	0
522130	CCP1	chromosome_4:1877695-1880829(+)	15	10.99	~50
521926	SRC	chromosome_4:389097-400711 (+)	n/a	5.28	0
521927	SRC	chromosome_4:401538-413146 (-)	8	3.07	0
522486	Guanylate cyclase	chromosome_5:1403264-1414228(+)	15	7.41	3
522626 + 524141	CAH9	chromosome_5:2467646-2468704(-) scaffold_61:22427-34555(-)	13 n/a	n/a	6 7
522732	CAH4	chromosome_5:3320139-3322687(-)	15	9.34	200-300
522733	CAH5	chromosome_5:3324418-3327142(+)			
523044	CEM1	chromosome_6:1544794-1547328(+)	16	n/a	~20
523284+523283	PGP3	chromosome_6:2792436-2796394(-) chromosome_6:2792436-2796274(-)	n/a	n/a	10
523507	LCI23	chromosome_6:3840357-3845935(-)	15	10.59	15
▲ 523557	RHP1	chromosome_6:4082786-4087794(-)	3	n/a	35
536268	RHP2	chromosome_6:4088321-4094462(-)	n/a		4
▲ 523796	MITC11	chromosome_6:5558933-5562561(-)	8	2.94	2
524046	LCIC	chromosome_6:7141544-7144642(-)	14	4.52	~100
524076	NAR1.2	chromosome_6:7279856-7282824(-)	15	12.05	~60

Table 7.2. (Continued)

	August ID	Name	Chromosome Location	Cluster	F.C.	EST
	524387	Adenylyl cyclase	chromosome_7:1263093-1265027 (+)	15	5.02	~30
	524677	NAR1.4	chromosome_7:3197820-3202384 (+)	n/a	n/a	7
▲▲	526207	CAH8	chromosome_9:3001549-3007313 (+)	11	n/a	6
	526296	ECA1	chromosome_9:3621094-3628678 (+)	n/a	6.76	0
▲	526295	ECA1	chromosome_9:3651805-3663233 (-)	n/a	4.96	~30
	526316	NAR1.1	chromosome_9:3796483-3799657 (+)	n/a	n/a	2
	509757	Acetyltransferase	chromosome_10:1250148-1255142 (+)	15	7.16	11
	509959	LCI5	chromosome_10:2491110-2493454 (+)	8	2.3	~40
	144255	CIA6	chromosome_10:2640236-2642514 (-)	n/a	n/a	0
	509989	PGP2	chromosome_10:2668746-2671880 (+)	n/a	n/a	22
	510019	CGL28/CID11	chromosome_10:2809450-2814524 (+)	15	5.09	20
	510111	BOR1	chromosome_10:3307458-3316722 (+)	16	n/a	0
	510414	GPX5	chromosome_10:5434433-5436481 (-)	n/a	n/a	~50
	512404	MHX	chromosome_11:2142976-2152044 (-)	14	3.43	15
	512520	CAH6	chromosome_12:210288-213222 (+)	12	n/a	~30
	513120	Chromate Transp	chromosome_12:3365716-3370610 (+)	8	4.13	4
	513361	RMT2	chromosome_12:4690021-4695579 (-)	n/a	n/a	8
	513715	NAR1.5	chromosome_12:6839303-6844411 (-)	9	n/a	17
	513788	HP	chromosome_12:7237733-7239117 (+)	15	10.62	0
	513839	CGL2	chromosome_12:7473725-7477099 (+)	8	2.59	2
	513843	ABCt	chromosome_12:7496709-7504083 (+)	n/a	1.34	3
	513967	LCI6	chromosome_12:8266638-8269582 (+)	n/a	2.04	~20
	515107/515108	CAH7	chromosome_13:6481814-6487302 (-) chromosome_13:6481814-6487302 (-)	n/a	n/a	23
	515280	THB2	chromosome_14:1124707-1127451 (+)	2	n/a	2
	515281	THB1	chromosome_14:1128937-1131301 (+)	n/a	n/a	~40
	515848	ORF158	chromosome_15:1581786-1589614 (-)	15	10.93	0
	516263	RMT1	chromosome_16:1739402-1744326 (+)	n/a	n/a	17
	516273	NTF2	chromosome_16:1807672-1810726 (+)	14	7.35	1
	516290	Bestrophin	chromosome_16:1921202-1924200 (-)	15	8.17	18
	516308	3' part of LCI11	chromosome_16:2022322-2026260 (-)	n/a	2.23	~30
▲	516309	5' part of LCI11	chromosome_16:2027232-2031650 (-)	14	7.25	~40
	516770	PTAC17	chromosome_16:5072356-5074980 (+)	15	7.62	24
	517053	LCI31	chromosome_17:339215-342359 (+)	14	4.09	17
▲	517880	ORF158	chromosome_17:5553807-5565545 (-)	8	9.33	0
	520182	Na^+/H^+ t	scaffold_24:124886-139650 (+)	8	4.67	1
	522781	HP	scaffold_59:20576-24870 (+)	15	11.62	26

Table 7.2 (continued)
The genes are listed in the order of the chromosome locations. The data of Cluster and Fold Change (F.C.) information were from Brueggeman et al. (2012). EST information were based on the data from the Chlamydomonas genome site (http://genome.jgi-psf.org/Chlre4/Chlre4.home.html). The triangles indicate the identification of the mutant in which this gene locus is disrupted by the *AphVIII* insertion. The red triangle (▲) indicated that the insertion was found in the ORF region of the gene. The green triangle (▲) indicated a 5'UTR insertion and the blue triangle (▲) indicated a 3'UTR insertion.

genes were listed in the order of their relative physical locations on the chromosomes, instead of the biological functions which could be overlapping to some extent (Table 7.2).

The first two groups of genes have 40 genes in total, including all seven *α-CA*s and *β-CA*s (except for *CAH3*, since there are already more than three *cah3* mutants available), seventeen genes potentially involved in C_i transport (*CEM1*, *BOR1*, *RHP1*, *RHP2*, *NAR1.1*, *NAR1.2*, *NAR1.3*, *NAR1.4*, *NAR1.5*, *NAR1.6*, *CCP1*, *CCP2*, *Lci1*, *HLA3*, *LCIC*, *LCID*, and *LCIE*), five genes of the photorespiratory pathway or cellular homeostasis (*PGP1*, *PGP2*, *PGP3*, *GYX1* and *GPX5*), four Rubisco or pyrenoid associated genes (*CIA6*, *CGL41/RBCX*, *RMT1* and *RMT2*), the truncated hemoglobin gene family (*THB1*, *THB2*, *THB3* and *THB4*), two low CO_2 inducible genes (*LCI5* and *LCI6*), the CCM regulatory gene *LCR1* and one hypothetical ABC transporter gene identified in a microarray experiment to be the third most down regulated gene when subjected to low CO_2 stress in D66 (original probe id: 4660.C; Pollock and Grossman, unpublished data).

Two recent papers using the RNA-seq approach documented the detailed transcriptional changes that occur under different external environment stress, and in different genotypes (Brueggeman et al., 2012; Fang et al., 2012). In the first study, the authors identified 16 clusters of genes based on their expression profiles under different CO_2 levels with or without the presence of the *CCM1*/*CIA5* transcriptional regulator. Among the 16 gene clusters, interesting expression patterns were displayed in cluster 8, 14 and 15 indicating the genes in these clusters could be closely related to the CCM and low CO_2 responses (Fang et al., 2012). The second study presented extensive data about the transcriptional fold changes of the analyzed genes. By cross-referencing results from

the two laboratories, possible CCM related genes could be identified. For example, one of the important CCM components *NAR1.2*, was categorized into the gene Cluster 15 (Fang et al., 2012). The expression fold changes under the low CO_2 condition was 12.05 (value expressed in ΔCt, Brueggeman et al., 2012; Table 7.2). To select genes as PCR targets for mutagenesis screen in our laboratory, the information from both papers were combined and analyzed *in silico*.

The criteria for the third group of PCR target genes include the possible chloroplast localization, predicted transmembrane domains, and either belonging to one of the three CCM-related clusters, or exhibiting high fold change under the low CO_2 condition. The reason behind such criteria was that one of the goals for the mutagenesis was trying to discover a thylakoid located membrane protein that could transport C_i between the thylakoid lumen and the rest of the chloroplast stroma. Thus, to search for genes that could fulfill those criteria, all 1869 genes (Brueggeman et al., 2012) were analyzed by TMHMM for transmembrane predictions (http://www.cbs.dtu.dk/services/TMHMM/), ChloroP for chloroplast localization predictions (http://www.cbs.dtu.dk/services/ChloroP/), and TargetP for general localization predictions (http://www.cbs.dtu.dk/services/TargetP/). Information generated by *in silico* analysis as well as from the two RNA-seq papers was combined together. 30 genes were selected as PCR targets for mutagenesis screening as the third group PCR targets.

2. Primer designs for the selected genes

To design primers for one specific gene (all the gene models used were based on Phytozome v7.0), two directions of primers were designed along the locus, spaced

approximately 1-kb from each other (Figure 7.3). The guiding rule for primer design followed the Gonzalez-Ballester's method with a few modifications. First of all, the first forward (F1) and the first reverse (R1) primer was positioned 20-bp to 200-bp beyond the 5'UTR or 3'UTR region respectively. In some cases where a gene had an extra-long 3'UTR, R1 was positioned within the 3'UTR. Secondly, repeat regions within a gene (eg. *CAH8*) were avoided for primer designs. Overall, all the 789 primers (Appendix V) were designed using the online tool, IDT Oligo Analyzer (http://www.idtdna.com/analyzer/Applications/OligoAnalyzer/). All the primers were designed to have a similar Tm (60.0±0.8℃) and a low self-dimer ΔG (-4.63±-1.38kcal/mole).

3. PCR procedure

For a specific gene, all the forward primers were combined together (designated as "F") and all the reverse primers were combined together (designated as "R"). For each gene, two PCRs were performed by paring the *AphVIII* internal primer RB1 (Gonzalez-Ballester et al., 2011) with either F or R. Therefore, for a total of 71 genes, 142 PCRs are performed with one DNA pool, and 3834 PCRs are performed with all 27 DNA pools for an initial PCR screen using F and R primers.

a) Control PCRs

Before the actual PCR screens, control PCRs were performed for quality assurance (Figures 7.4 to 7.6). First of all, primers designed for all the 71 genes were checked by PCR to show the functionality of all primers using a wild-type DNA. An example is given in Figure 7.4. Secondly, the sensitivity of PCR using the pooled DNA

was checked by diluting one single wild-type DNA to mimic the dilution effect by pooling individual DNAs (Figure 7.5). The PCR was performed to amplify a 1-kb DNA fragment from the *NAR1.2* locus at different dilutions of the wild-type DNA. In Figure 7.5, it was shown that the 1-kb signal from the *NAR1.2* gene could be detected with up to 2000 fold diluted DNA template. This indicated that any potential PCR target from the pooled DNA should be detected by PCR since the potential signal in the pooled DNA was only 900 fold diluted. Additionally, the background of the screening PCR was checked by adding F (or R), RB1, all the other PCR components, but leaving out the DNA template (Figure 7.6). It was shown that the primers did not form a distinguishable PCR signal when the DNA template was absent.

b) Screening PCRs

Following the control PCRs, the actual PCR screens were performed. As mentioned previously, for each gene two PCRs were performed (F primer or R primer paired with RB1, respectively). For a total of 71 genes, 142 PCRs were performed with one DNA pool, and 3834 PCRs were performed with all 27 DNA pools for an initial PCR screen. For simplicity, only the data that led to the identification of the *516309* and *rhp1* mutants is presented here (Figure 7.7 through Figure 7.13). The *516309* mutant was identified from pool #13 and the *rhp1* mutant was identified from pool #15.

First of all, multiple pools were screened in parallel, helping focus on the unique signal(s) existing in only one of the pools (Figure 7.7). In this figure, DNAs from Pool #13, #14, #15 were screened simultaneously. Out of the 71 genes (Table 7.2), 26 genes were assigned to the author and were listed in the table on the right (Figure 7.7). The

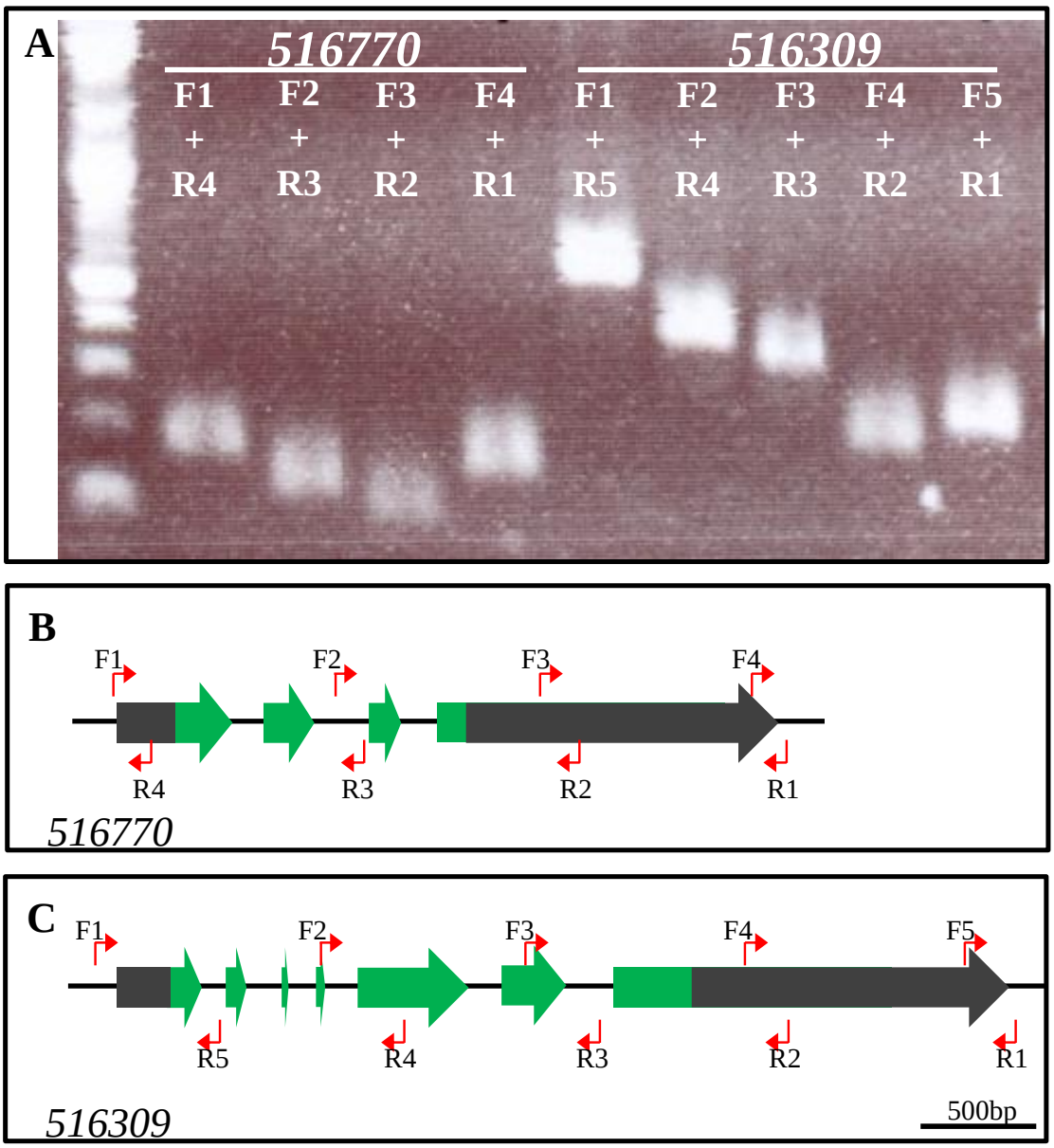

Figure 7.4. Two examples of the initial PCR controls.

For each gene, the optimal amplicon size ranged from 100bp to 1.5-kb. These initial PCRs ensured the functionality of all gene specific primers. (A): showing the successful amplification of the fragments from gene *516770* and *516309*. The primer pairs used in the PCR are diagramed in (B) and (C).

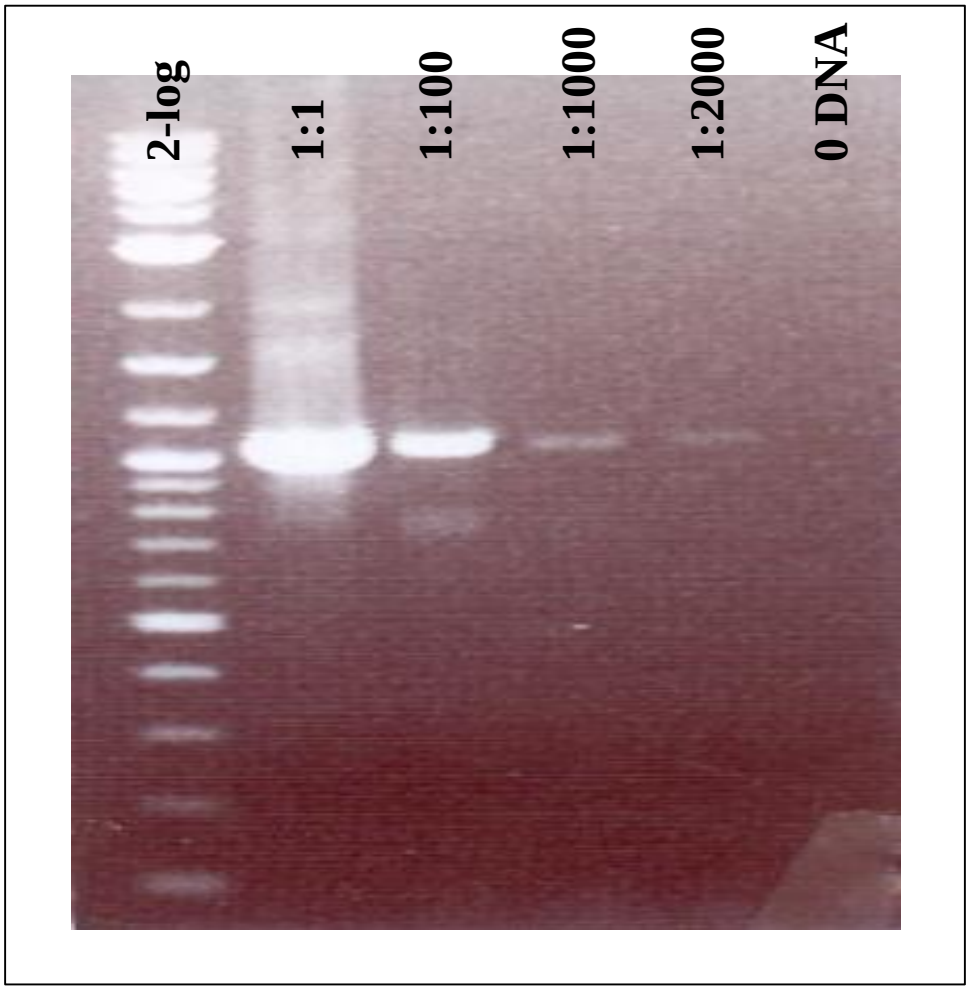

Figure 7.5. PCR sensitivity.

Wild-type DNA was diluted with H_2O to 1:100, 1:1000 and 1:2000 fold to test the sensitivity of the PCR procedure. Primers flanking a 1-kb fragment of the *NAR1.2* locus were used throughout the PCR screens as a positive control. It was shown that at 1:1000 dilution, which approximates the 900-colony pooling system in this screen, the PCR procedure used was able to detect the presence of the target gene. The average DNA concentration during the pooled DNA screen was around 100 ng/μL.

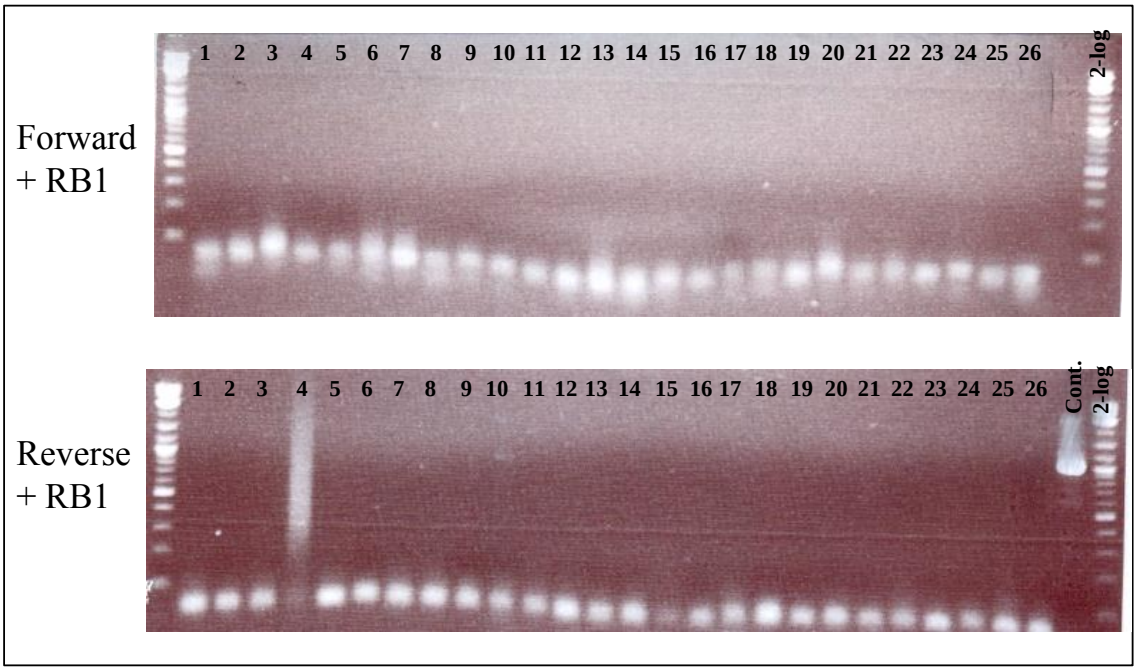

Figure 7.6. No DNA control.

No DNA control PCR was performed to ensure that the gene specific primers mix and the RB1 primer do not form amplifiable primer dimers which will complicate the interpretation of the PCR results. For a list of genes tested in this PCR, refer to the table in Figure 7.7. The smear observed in Lane 4 (Reverse +RB1) probably represented a non-specific amplification and no interference with the potential possible bands were observed during the mutagenesis PCR screen.

amplification of the 1-kb fragment of *NAR1.2* was used as a positive control for the PCR. By comparing all the signals from the three pools, combined with previous PCR data, the bands unique in the individual pools were identified and highlighted with the blue circles in the gel pictures, as well as in the gene list. The *516309* from pool #13 and *RHP1* from pool #15 were highlighted with the red squares. This step is the first round of PCR screening (shown as PCR1 and PCR1'in Figure 7.3B)

Nine unique signals (eight different genes) detected with the first round PCR using the RB1 primer were repeated (Figure 7.8A) with another *AphVIII* internal primer RB2 (Gonzalez-Ballester et al., 2011; Figure 7.8B) to test the the reproducibility of the previously identified PCR signals. From the nine signals, five were verified (Figure 7.8A). This step is the second round of PCR (PCR2, Figure 7.3B).

The five signals verified in PCR2 (Figure 7.8A) were pursued using individual primers to identify which single primer within the primer mix yielded the signal (Figure 7.8C). For each PCR set-up here, the first lane was the primer mix control (either F or R). The next few lanes were the expansion of the single primers within the primer mix. In pool #13, the genes *513120* and *RHP1* were tested by single primers. In the gene *513120*, the first lane shows the reproducibility from the reverse primer mix (Figure 7.8C, Pool #13, gene *513120*, Lane R). The next five lanes were the PCRs from using the five single reverse primers (R1 to R5). Among the five primers, the R5 primer rendered the same signal as seen in the primer mix (R). However, this type of match was considered as a false positive throughout the screen, mainly because one single primer was not supposed to form multiple bands if the amplification was specific. Hence, this type of "match" was discarded throughout the screen. On the other hand, in the *RHP1* PCR set, the 400-bp

Figure 7.7. PCR Screen (PCR1).

An example of the first round of PCR screening in which pool #13, pool #14, and pool #15 were screened simultaneously using primer RB1. By comparing the signals among the three pools, as well as with previous pool PCR patterns, nine unique bands (highlighted with blue circles) for 10-R, 14-R from pool #13, 4-F, 22-R, 16-F from pool #14, 14-F, 15-R, 19-R, 25-F from pool #15 were further investigated (See Figure 7.8-7.10). The corresponding gene names are listed in the table on the right, in which the potential interesting genes are also highlighted. From this batch, the *RHP1* mutant was identified from pool #13 and the *516309* mutant was identified from pool #15. The PCR bands of *RPH1* and *516309* were highlighted with red squares.

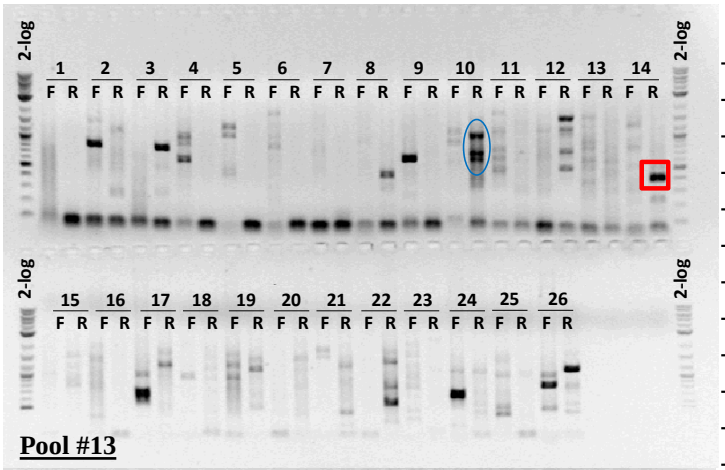

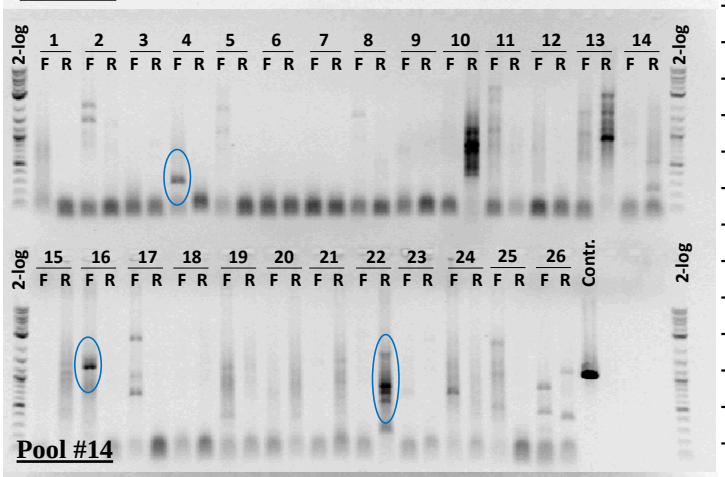

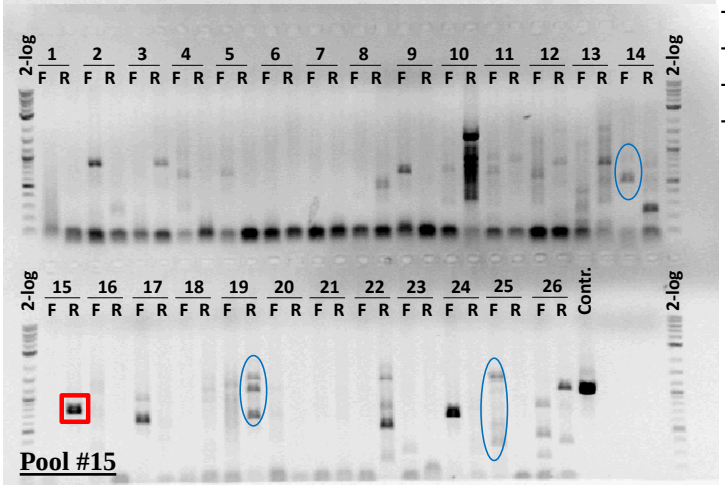

No.	Gene
1	*GCL41*
2	*PGP2*
3	*NAR1.5*
4	*516770*
5	*517053*
6	*523796*
7	*513839*
8	*NAR1.4*
9	*NAR1.6*
10	*513120*
11	*CAH1*
12	*PGP3*
13	*LCR1*
14	*RHP1*
15	*516309*
16	*520458*
17	*522781*
18	*RHP2*
19	*509757*
20	*CAH7*
21	*THB3*
22	*RMT1*
23	*RMT2*
24	*519637*
25	*523507*
26	*515848*
Control	*NAR1.2*

band from primer R5 matched the signal from the primer mix (Figure 7.8C, Pool #13, gene *RHP1*, Lane R5). Additionally, a 1.4-kb band from using the neighboring primer (R4) was also observed. This further indicates the presence of the *AphVIII* insertion in the *RHP1* locus. The same situation was observed in the *516309* PCR set from pool #15. Here the 800-bp band from R5 matched the signal from the primer mix and the neighboring primer (R4) presented a band with approximately1-kb bigger. All the positive signals were highlighted with red squares. This step is the third round of PCR (PCR3, Figure 7.3B).

Following PCR3, any signals that could be tracked back to individual primers were further pursued using the five individual plate DNA preprations to identify which plate within the pooled DNA yielded the signal (Figure 7.9). In the example of pool #13 with a potential *rhp1* mutant, the template consisted of the DNAs from plates #108, #109, #110, #113, and #115. To determine which plate had the colony of interest, DNA from those five plates were used as PCR templates and it was shown that plate #109 (Figure 7.9A) had a signal around 400-bp corresponding to the one from the pool DNA. The presence of the *rhp1* mutant in plate #109 was further verified by using another primer (R4) that amplified a band around 1.4-kb (Figure 7.9B). In the case of the *516309* gene in pool #15, the mutation appeared to exist in plate #134 as evidenced by the identical 800-bp band in both the pool and plate DNA (Figure 7.9B).

Sequencing

When the signals could be tracked back to individual primers and individual plate DNAs, the PCR products were sequenced using the common primer RB1. Sequencing results were compared with the published *C. reinhardtii* genome (Merchant et al., 2007)

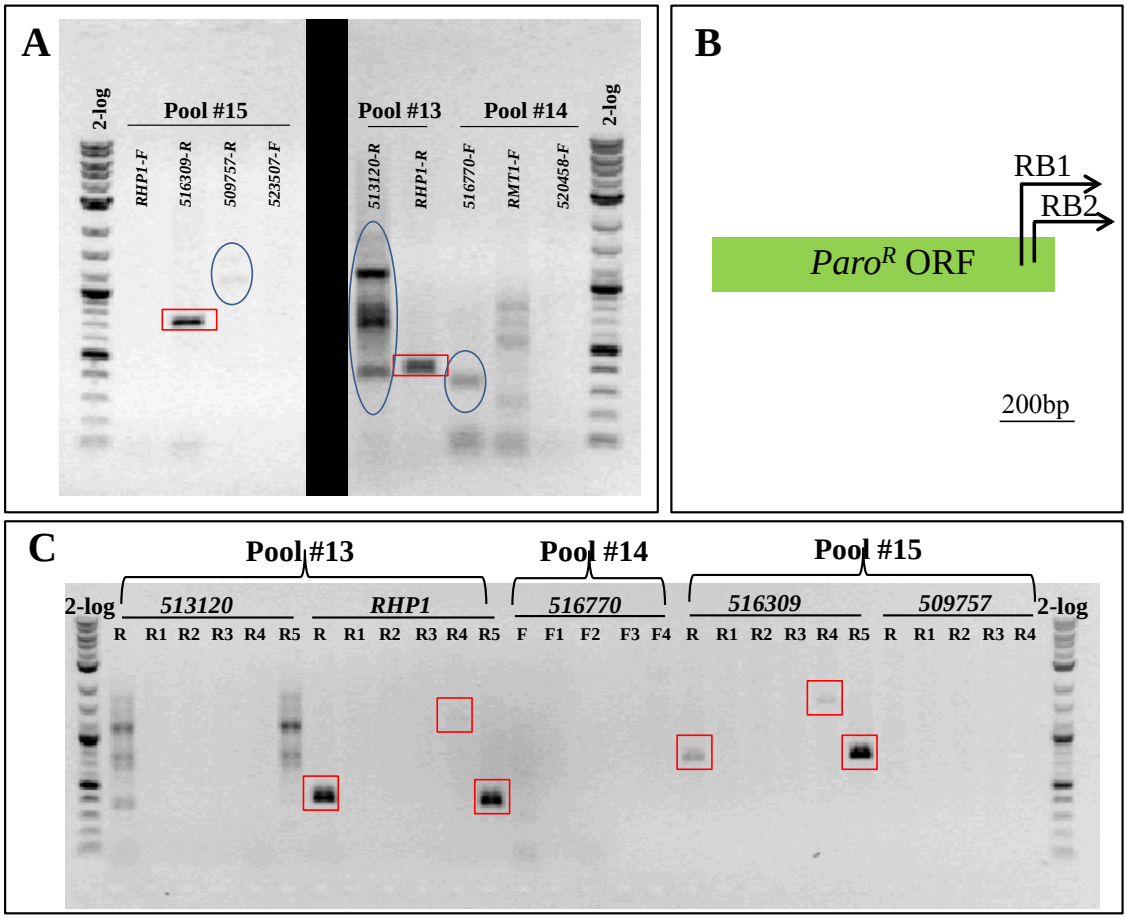

Figure 7.8. PCR Screen (PCR2 and PCR3).

An example of the second round of PCR screening (PCR2, Figure 7.8A) in which the nine PCR signals from PCR1 were verified by using another *AphVIII* internal primer RB2 (Figure 7.8B). Out of the nine PCR bands, five could be reproduced by the RB2 primer (highlighted with the blue circles, and the *RHP1* and *516309* were highlighted with the red squares). The third round of PCR (PCR3, Figure 7.8C) was performed to further identify which single primer from the primer mix contributes to the band formation. In the *RHP1* PCR set (consisting of the reverse primer mix (R), single reverse primer R1, R2, R3, R4, R5), the band around 400-bp using primer R5 corresponded to the band from the primer mix R. Also, PCR from using primer R4 resulted in a band at around 1.4-kb, matching the designed 1-kb gap between R4 and R5 primers. The same situation for *516309* PRC set, in which the R5 corresponded to the band seen in the primer mix and R4 PCR product was around 1-kb bigger than the R5 PCR product.

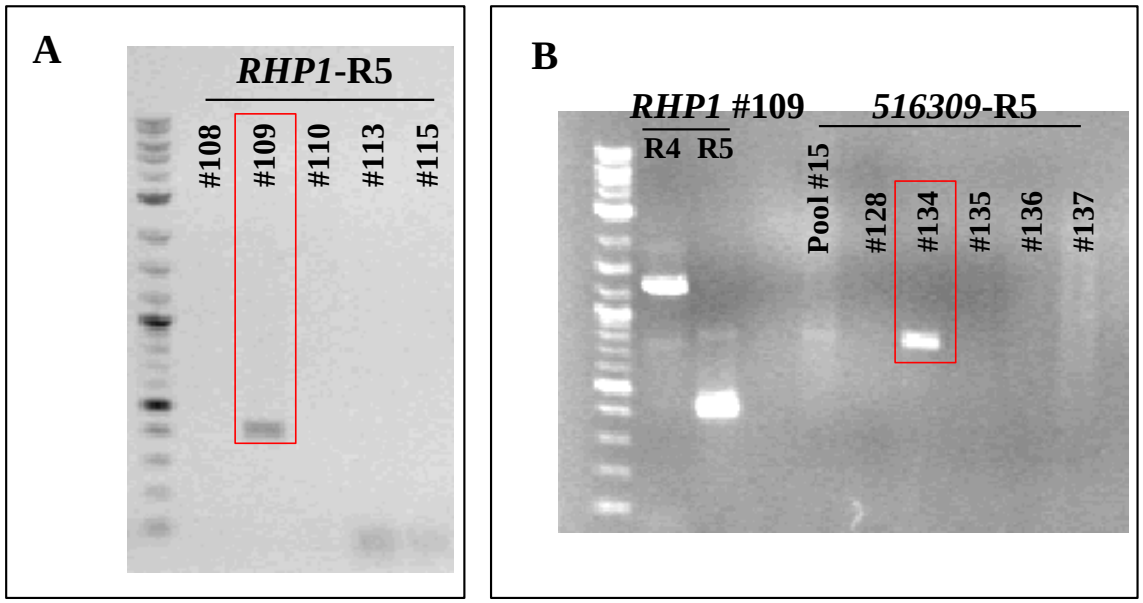

Figure 7.9. Individual Plates.

When the presence of the *RHP1* and *516309* mutation in DNA pool #13 and #15 were verified by single primers, the fourth round of PCR was performed to identify the exact individual plate that contains the mutants. The *RHP1*-R5 and RB1 primer pair was used to amplify the 400-bp PCR product from the 180-colony plate #109 from DNA pool #13 (A). Similarly, the 516309-R5 and RB1 primer pair was used to amplify the 800-bp PCR product from the 180-colony plate #134 from DNA pool #15 (B). The presence of the *RHP1* mutation in plate #109 was further verified by the 1.4-kb PCR product using *RHP1*-R4 primer (B).

(http://genome.jgi-psf.org/Chlre4/Chlre4.home.html) using the Blastn program. The genes with the *AphVIII* insertions were identified. Among the 36 sequenced potential mutations, ten mutants in seven genes were found to have an *AphVIII* insertion in the corresponding locus. These include: *RHP1* (chromosome_6:4082534-4087507), *Bestrophin* (chromosome_16:2027232-2031650), *LCI9* (chromosome_2:7341013-7348511), *MitC11* (chromosome_6:5558933-5562561), 526295 (chromosome_9:3651805-3663233), 517880 (chromosome_17:5553807-5565545), two *CAH8* (chromosome_9: 3001516-3007085) and three *NAR1.3* (chromosome_3:7664323-7672577) mutations. Among these, the mutations in *RHP1* and *Bestrophin* were both in the 5'UTR region (Figure 7.10). Three individual *nar1.3* mutations all have the *AphVIII* inserted in the 3'UTR region. A summary of the identified gene specific mutations is listed in Table 7.2.

Identifying Single Colonies

Eleven possible mutants corresponding to ten 180-colony plates were identified to contain the *AphVIII* insertional mutants. In order to pinpoint which single colony from the 180 colonies had the mutation, another round of PCR screen was performed. For one 180-colony plate, every ten single colonies were pooled together for one PCR analysis. Ideally, one out of a total 18 PCR reactions would have a positive signal indicating the presence of the single mutant colony in one of the tens. Finally, the single mutant colony could be identified by another ten individual PCR reactions. Using this system, *rhp1*, *516309*, *526295*, *517880*, two *cah8*, and three *nar1.3* mutants were identified. The mutant *MitC11* could not be recovered possibly due to the loss of colonies during maintenance.

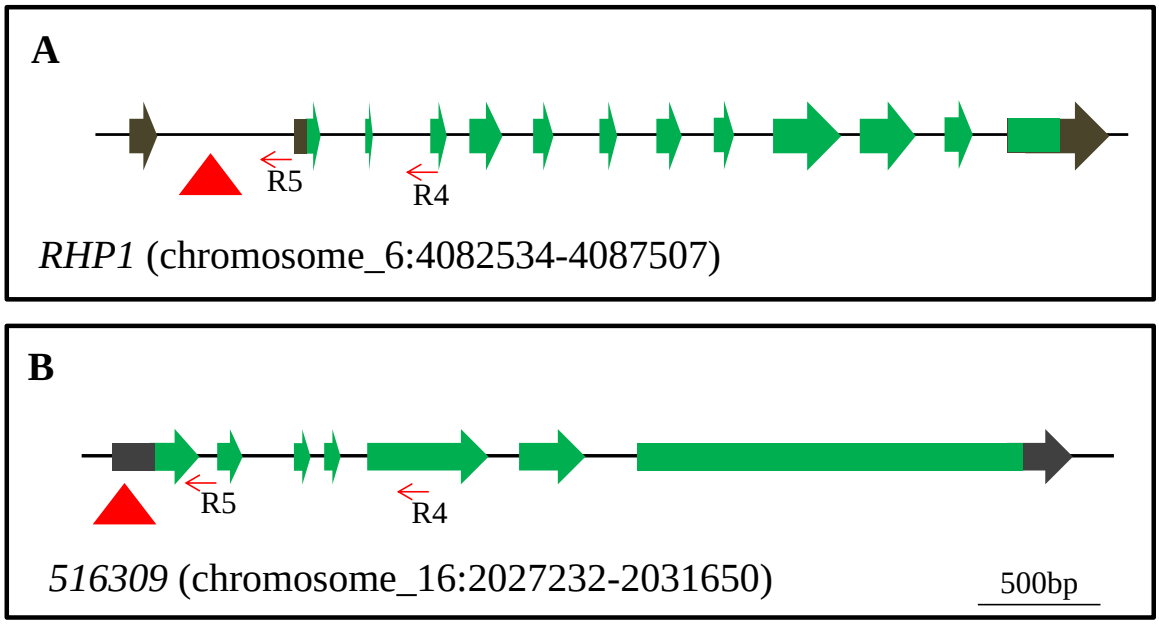

Figure 7.10. Gene models showing the location of the *AphVIII* insertion in *RHP1* and *516309*.

Exons are depicted with green arrows and introns are depicted with small black solid lines. Black regions represent the UTRs. Possible *AphVIII* insertions are denoted by red solid triangles and primers used to identify the insertions are displayed.

The PCR data examples for the identification of the *516309* and the *rhp1* mutants are presented in Figures 7.11 through 7.13. To pinpoint the *rhp1* mutant from 180 colonies on plate #13, every 10 colonies were pooled together for one DNA preparation and subsequent PCR analysis. In Figure 7.11A, among the 18 PCR reactions, the 15th lane contained a band corresponding to the same size as the one from the control PCR, indicating the presence of the *rhp1* mutant in the ten colonies from colony #141 through colony #150. The final identification of the *rhp1* mutant was illustrated in Figure 7.12 (left), where the colony #141 was found to contain the *RHP1* mutation. This is shown by the presence of the same sized-band as compared to the control reaction. The procedure to identify the *516309* mutant was the same, in which the mutation was first identified in a pool of ten colonies (colony #91 to colony #100, Figure 7.11B), and was finally pinpointed as the colony #94 on plate #15 (Figure 7.12, right).

After the mutant was determined on the single colony level, single colonies from each mutant colony further isolated. PCR analysis from five random colonies was performed to insure the homogeneity of the mutant colony to be maintained for future studies. For example, the culture from the *516309* mutant was streaked onto a TAP plate to allow the formation of single colonies. Five random colonies were chosen for PCR analysis for the presence of the insertion. In Figure 7.13, it showed that all the five single colonies possessed the *AphVIII* insertion in the *516309* locus.

Discussion

With the purpose to identify more genes or gene mutations that play essential roles in the *C. reinhardtii* CCM, a small scale preliminary PCR-based mutagenesis screen was carried out, adopting the method developed by Gonzales-Ballester et al. (2011). The

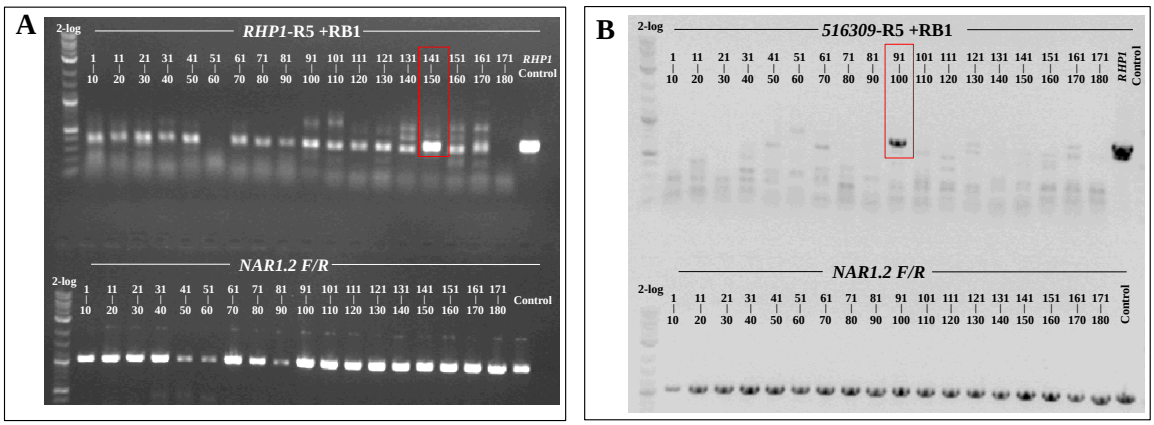

Figure 7.11. Identifying single colonies (step 1).

To determinate the single mutant colony from the 180 colonies, every ten colonies were pooled together for a PCR analysis. (A): The *RHP1* mutation was found to be among the 10 colonies (#141 to #150) as evidenced by the identical band observed in both the test sample (highlighted by the red square) and the control. (B): The *516309* mutation was found to be among the 10 colonies (#91 to #100) as evidenced by the identical band observed in both the test sample (highlighted by the red square) and the control. For both PCRs, the amplification of the 1-kb fragment from *NAR1.2* was used as a positive control.

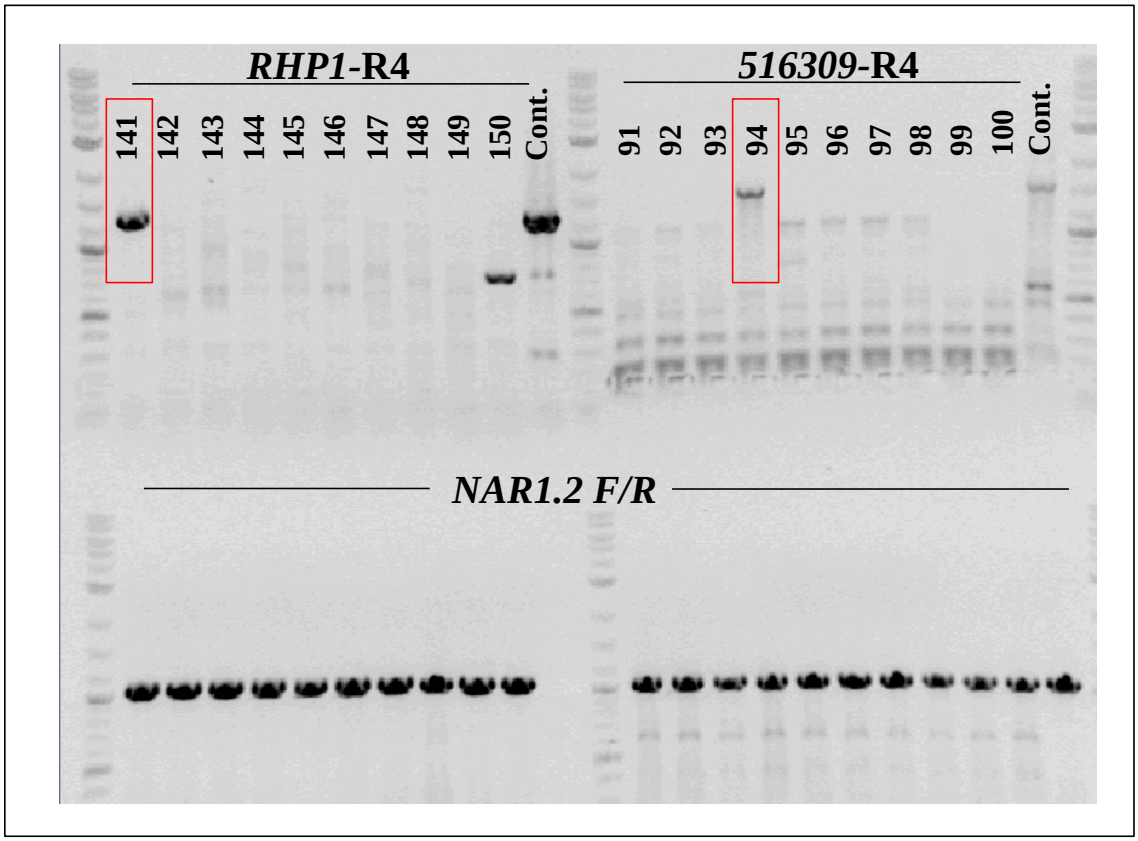

Figure 7.12. Identifying single colonies (step 2).

Among the previously identified ten colonies possessing the gene specific mutations, colony#141 in plate #109 was found to be the *RHP1* mutant while colony #94 was found to be the *516309* mutant.

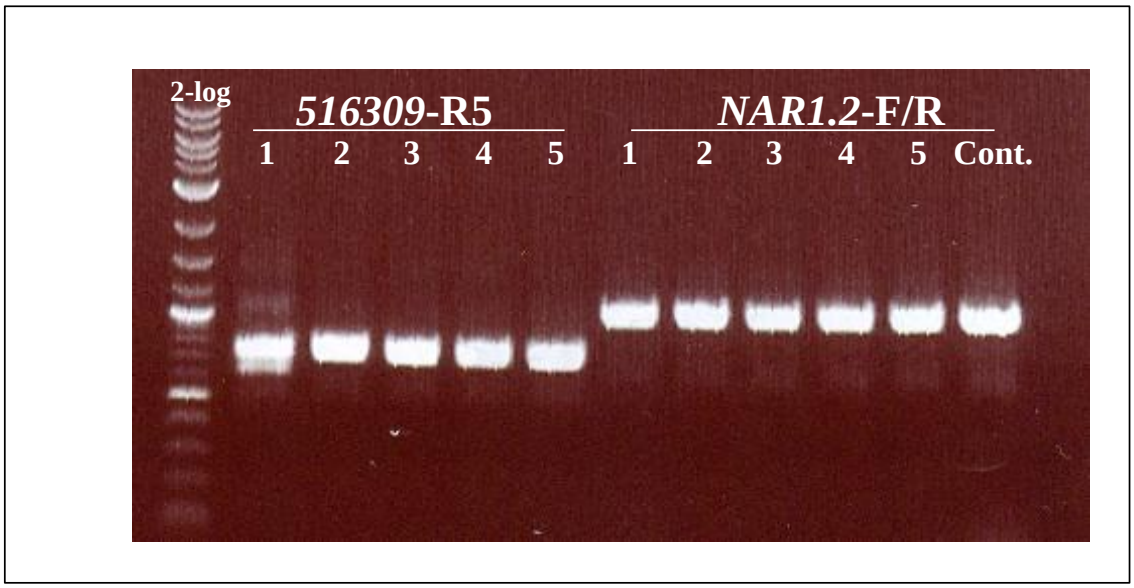

Figure 7.13. Identifying single colonies (step 3).

Five single colonies were further isolated from the previously identified mutant. PCR was conducted to analyze the presence of the gene specific mutation in each of the five colonies. For the *516309* mutant, all the five examined had the same 800-bp band indicating the *AphVIII* insertion in the *516309* locus.

study in this chapter served as a pilot experiment to test the logistics and gather information before a larger mutagenesis screen. Overall, in a seven-month time frame, a total of ~22,000 insertional mutants were generated, 71 potentially CCM associating genes were screened by PCR, and eleven mutants were obtained at the end of the mutagenesis screen (Table 7.2, Figure 7.14). The possibility of adapting the PCR-based mutagenesis approach to identify CCM mutants was validated.

In the work by Gonzales-Ballester et al. (2011), the mutant screens were conducted in two different mutant libraries, containing ~100,000 transformants and ~20,000 transformants respectively. For the ~100,000 transformants library, 63 genes were screened by PCR and 37 different mutants were obtained. For the smaller library, 7 genes were screened and 2 different mutants were isolated. It could be noticed that with the increasing number of transformants screened, the probability of obtaining relative mutants also increases. Therefore, to obtain more mutants with possible CCM genes disrupted, a full scale mutagenesis aiming at a ~100,000 transformants would be reasonable.

During this intitial project, a few deficiencies regarding the culture maintenance and PCR screenings were revealed and could be avoided or optimized in the future. First of all, culture contamination was a big problem during the mutagenesis screen. This could be avoided or at least alleviated by a few approaches. Keeping everything sterilized is a must. Adding the fungicide (Carbendazim) to all the plates for transformant selection and maintenance is recommended, since there was no observed negative effect on *C. reinhardtii* while certain species of fungus could be effectively removed. Prolonged

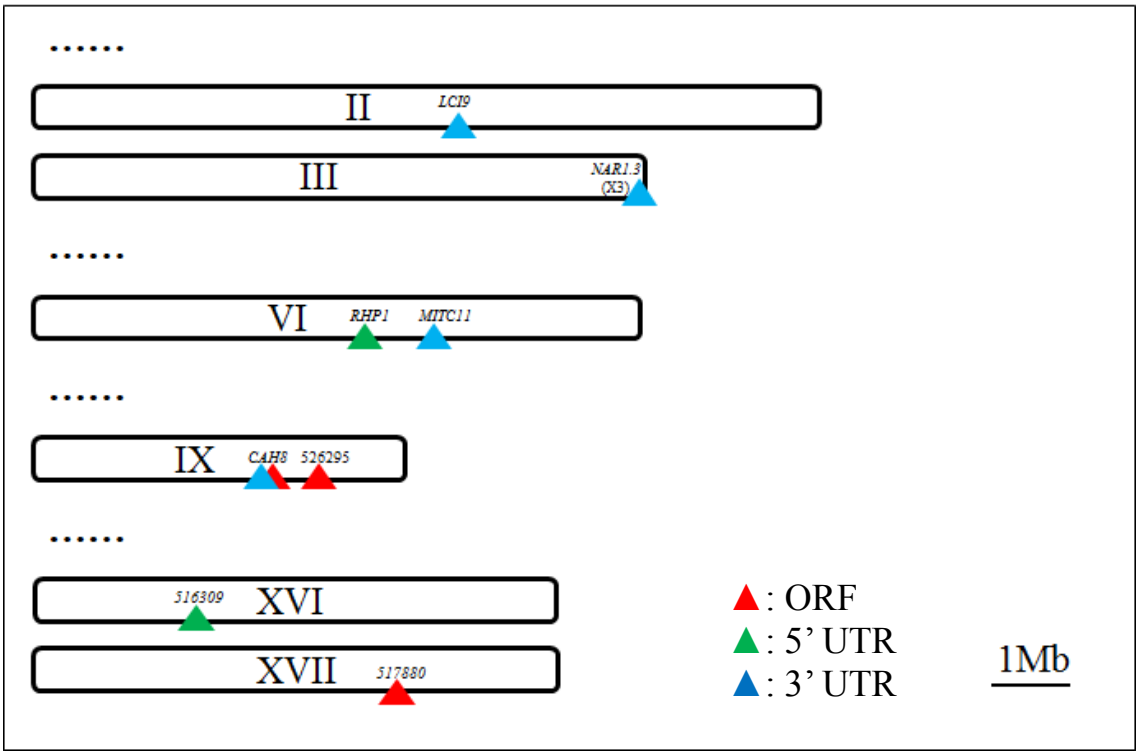

Figure 7.14. A summary of the identified *AphVIII* insertion loci.

The PCR-based mutagenesis screen resulted in the identifications of eleven insertional mutants with nine different genes. The relative locations of the mutated genes are depicted by triangles in the context of the chromosomes in *Chlamydomonas*. The red triangle (▲) indicated that the insertion was found in the ORF region of the gene. The green triangle (▲) indicated a 5'UTR insertion and the blue triangle (▲) indicated a 3'UTR insertion. Three individual *NAR1.3* mutants were identified, all of which had insertions in the 3'UTR region.

storage especially in the cold should also be avoided, which means the entire screening process should be planned, conducted and organized in a timely manner. This would become particularly essential in a large scale mutant library screen. Secondly, during the pilot experiment, all the transformants plates were sealed with Parafilm (Penchiney, Menasha, WI) and were kept in the 4℃ dark room for around one month. Although the majority of the transformants survived after transferring to a fresh plate, a few earlier plates died. In the opinion of the author, keeping plates in the 4℃ dark room is feasible but the storage length should not exceed a month. Additionally, it appeared that the survivability of the transformants could be increased by recovering the 4℃/dark incubated transformants at room temperature in the dim light for 1-2 days before moving to a normal light condition. Sealing plates with parafilm is still under debate. Since parafilming could protect the agar plates from drying but it could also decrease gas exchange substantially.

The most difficult part of the mutagenesis screening seemed to lie in the culture maintenance logistics. However, the PCR screening process itself also has room for improvement. For example, during this trial experiment, the full set of target genes were screened using one pooled DNA. Multiple pooled DNAs were analyzed simultaneously with the purpose to compare multiple PCR results to identify unique signals present in one pool. However, the opposite approach in which the full set of pooled DNAs is screened using one target gene would be much more efficient and straightforward. Using this alternative approach, any unique signal from only one pooled DNA could be spotted easily, even in a relatively noisy background. This PCR approach would be recommended for a future screen.

Endnotes

[1] All figures and tables except for Figure 7.13 and Figure 7.14 are contributed by the author of this dissertation. Figure 7.13 is contributed by Bratati Mukherjee. The table in Appendix IV is contributed by Nadine Jungnick. Figure 7.14 is contributed equally by Bratati Mukherjee, Nadine Jungnick and the author of this dissertation

The author and Bratati Mukherjee contributed equally in the PCR target selection, primer design, primer check, *C. reinhardtii* mutagenesis and initial PCR screening.

The author, Bratati Mukherjee and Nadine Jungnick contributed equally in the later stage of PCR screening and mutants identifications.

CHAPTER 8
CONCLUSIONS

The proteinaceous microcompartment, the chloroplast pyrenoid, has been proposed as an important structural component for the CCM in *C. reinhardtii*. A recent study by Genkov and his colleagues (Genkov et al., 2010) illustrated the importance of the pyrenoid in the CCM. In their work, the *C. reinhardtii* Rubisco holoenzyme was modified so that the *C. reinhardtii* endogenous RbcL assembled with RbcS from higher plants. Although the hybrid Rubisco had similar *in vitro* enzymatic kinetics and was present in amounts equivalent to wild-type Rubisco, the resultant *C. reinhardtii* cells were found to lack the chloroplast pyrenoid, and had a reduced growth under low CO_2 conditions. This is strong evidence that the pyrenoid is playing an important role in the CCM.

However, evidence directly linking the CCM and the pyrenoid was lacking, since all the previous mutants identified so far were deficient in Rubisco, with mutations in either small subunit (Genkov et al., 2011), or the large subunit (Rawat et al., 1996). Since Rubisco is missing and the cells had no pyrenoid and also no function CCM, we could not test the link between the pyrenoid and CCM. Chapter 4 described the identification and characterization of a novel pyrenoid mutant (*cia6*), providing the first piece of direct evidence that the presence of the pyrenoid is essential for the functioning of the CCM. This mutant was initially isolated as a sick on low CO_2 mutant generated in a mutagenesis screen and the gene disrupted by the Ble^R was identified on chromosome 10. The most interesting feature about this mutant is that the pyrenoid region in this mutant is highly disorganized, which led us to think that this mutant could shed light on the

importance of the pyrenoid relative to CCM. Indeed, without the pyrenoid, the C_i affinity was greatly reduced in the mutant. The correlation of the presence of the pyrenoid and the proper function of the CCM was further evidenced by the complementation experiment. The expression levels of the other key CCM components were also observed to deviate from the wild-type in response to low CO_2 stress. Regarding the biological function of *CIA6*, it is still unknown. However, the discovery of this mutant provides strong evidence that the presence of the pyrenoid is essential to the functionality of the CCM. Additionally, this mutant could be used for studies investigating in the biogenesis of pyrenoid.

Another important facet of the *C. reinhardtii* CCM is photorespiration, of which the enzymes serve essential roles during the initial transition phase before the entire CCM is fully induced and functioning. The entry enzyme for the photorespiration cycle, is the phosphoglycophosphatase (PGPase) that converts the phosphoglycolate into glycolate. A PGPase mutant *pgp1* was isolated and characterized showing a sick on low CO_2 phenotype nearly thirty decades ago. However, this phenotype is no longer observed and this situation was investigated in Chapter 5. In this Chapter, the transcription levels of three PGPase isoforms in *C. reinhardtii* were investigated. It was found that the *PGP2* transcription level was increased in the *pgp1* mutant, which might explain the phenotypic reversion in the *pgp1* mutants. This finding was interesting, but still needs to be validated by other approaches such as genetic crossing, to see whether the increase of *PGP2* is the reason for the reversion, or just one of the consequences resulted from the phenotypic reversion in the *pgp1* mutants.

Besides the *pgp1* mutant, another interesting natural mutant, *C. reinhardtii* wild-type strain CC-503 was investigated. In this strain, it was found that one of the periplasmic CAs, CAH1 was missing. CAH1 has been proposed to be one of the important candidates essential for CCM, since large amount of CAH1 could be observed when the CCM is induced. However, with the discovery of this natural CAH1 mutant, and its fully functional CCM under low CO_2 conditions, the importance of the periplasmic CA in CCM remains unclear. However, it could also be speculated that other CAs in the periplasmic region, such as CAH2 and possibly CAH8 could compensate for the loss of CAH1 in CC-503. Besides, it is still unclear whether the cw-92 mutation in CC-503 is the reason for the lack of CAH1, although strains with another cell-wall mutation cw-15 still have CAH1. Nevertheless, it is also intriguing to investigate whether the type of cell wall mutation in the CC-503 strain results in the pleiotropic effects while maintaining the rest of the functional CCM.

Mutant identifications and characterizations have been a great driving force for the course of my Ph.D. study in Dr. Moroney's lab. By working with the *cia6* mutant, the important function of pyrenoid was strengthened, especially relative to CCM in *C. reinhardtii*. By working with the *pgp1* mutant and its interesting phenotypic reversion, I truly begin to appreciate that nature has a mind of its own. By creating something new (as simple as the upregulation in *PGP2*, or something else that is more complicated that we don't know yet), the phenotype could be rescued even in the presence of the existing mutation. The same is true for the third mutant we looked at, the CC-503. With the absence of the long proposed important CCM component, the strain CC-503 generally behaved as well as the other wild-types. One could argue that CAH1 is not needed for the

functioning of the CCM, or other CCM components are compensating for the loss of the CAH1 or some other unknown mechanism specific to CC-503 helps it survive under low CO_2 conditions.

The idea for another mutagenesis screen to identify more CCM components has been in our laboratory for years. With the recent publication using a PCR based reverse genetics screen as the guiding tool, and two recent publications with extensive RNA-seq data regarding the CO_2 responsive gene transcriptional patterns that provides us with potential targets, we were encouraged for another round of mutagenesis in search for more interesting CCM mutants. A trial project was performed on a relatively small scale using Gonzales-Ballester's method. Overall, a total of 22,860 insertional mutants were generated, 71 genes that are possibly involved in the CCM were screened. A total of eleven mutants were obtained at the end of the mutagenesis screen, and they are currently under careful characterizations. It was demonstrated that this method could be adapted into our laboratory, and most importantly, lessons were learned and the procedures were optimized.

REFERENCES

Alber, B.E., and Ferry, J.G. (1994). A carbonic anhydrase from the archaeon Methanosarcina thermophila. Proc Natl Acad Sci USA **91,** 6909-6913.

Altschul, S.F., Madden, T.L., Schaffer, A.A., Zhang, J., Zhang, Z., Miller, W., and Lipman, D.J. (1997). Gapped BLAST and PSI-BLAST: a new generation of protein database search programs. Nucleic Acids Res **25,** 3389-3402.

Anderson, L.E. (1971). Chloroplast and cytoplasmic enzymes. II. Pea leaf triose phosphate isomerases. Biochim Biophys Acta **235,** 237-244.

Arnon, D.I. (1949). Copper Enzymes in Isolated Chloroplasts. Polyphenoloxidase in Beta Vulgaris. Plant Physiol **24,** 1-15.

Asamizu, E., Nakamura, Y., Sato, S., Fukuzawa, H., and Tabata, S. (1999). A large scale structural analysis of cDNAs in a unicellular green alga, *Chlamydomonas reinhardtii*. I. Generation of 3433 non-redundant expressed sequence tags. DNA research **6,** 369-373.

Asamizu, E., Miura, K., Kucho, K., Inoue, Y., Fukuzawa, H., Ohyama, K., Nakamura, Y., and Tabata, S. (2000). Generation of expressed sequence tags from low-CO_2 and high-CO_2 adapted cells of *Chlamydomonas reinhardtii*. DNA Research **7,** 305-307.

Asamizu, E., Nakamura, Y., Miura, K., Fukuzawa, H., Fujiwara, S., Hirono, M., Iwamoto, K., Matsuda, Y., Minagawa, J., and Shimogawara, K. (2004). Establishment of publicly available cDNA material and information resource of *Chlamydomonas reinhardtii* (Chlorophyta) to facilitate gene function analysis. Phycologia **43,** 722-726.

Atteia, A., Adrait, A., Brugière, S., Tardif, M., Van Lis, R., Deusch, O., Dagan, T., Kuhn, L., Gontero, B., and Martin, W. (2009). A Proteomic Survey of *Chlamydomonas reinhardtii* Mitochondria Sheds New Light on the Metabolic Plasticity of the Organelle and on the Nature of the α-Proteobacterial Mitochondrial Ancestor. Mol Biol and Evol **26,** 1533-1548.

Badger, M., and Spalding, M. (2004). CO_2 acquisition, concentration and fixation in cyanobacteria and algae. Photosynthesis **9,** 369-397.

Badger, M.R. (1985). Photosynthetic Oxygen Exchange. Ann Rev of Plant Physiol **36,** 27-53.

Badger, M.R., and Price, G.D. (1992). The CO_2 concentrating mechanism in cyanobactiria and microalgae. Physiol Plant **84,** 606-615.

Badger, M.R., Kaplan, A., and Berry, J.A. (1980). Internal Inorganic Carbon Pool of *Chlamydomonas reinhardtii* - Evidence for a Carbon-Dioxide Concentrating Mechanism. Plant Physiol **66,** 407-413.

Badger, M.R., Andrews, T.J., Whitney, S.M., Ludwig, M., Yellowlees, D.C., Leggat, W., and Price, G.D. (1998). The diversity and coevolution of Rubisco, plastids, pyrenoids, and chloroplast-based CO_2-concentrating mechanisms in algae. Can J Bot **76,** 1052-1071.

Bainbridge, G., Madgwick, P., Parmar, S., Mitchell, R., Paul, M., Pitts, J., Keys, A.J., and Parry, M.A.J. (1995). Engineering Rubisco to change its catalytic properties. J Exp Bot **46,** 1269-1276.

Bartlett, S.G., Mitra, M., Moroney, J.V., Wise, R.R., and Hoober, J.K. (2006). CO_2 Concentrating Mechanisms. The Structure and Function of Plastids (Springer Netherlands), pp. 253-271.

Bateman, A., Birney, E., Cerruti, L., Durbin, R., Etwiller, L., Eddy, Sean R., Griffiths-Jones, S., Howe, K.L., Marshall, M., and Sonnhammer, E.L.L. (2002). The Pfam Protein Families Database. Nucleic Acids Res **30,** 276-280.

Bauwe, H., Hagemann, M., and Fernie, A.R. (2010). Photorespiration: players, partners and origin. Trends in Plant Sci **15,** 330-336.

Beezley, B.B., Gruber, P.J., and Frederick, S.E. (1976). Cytochemical localization of glycolate dehydrogenase in mitochondria of Chlamydomonas. Plant Physiol **58,** 315.

Berry, J.A., Kaplan, A., and Badger, M. (1978). Evidence for a CO_2 Concentrating Mechanism in Alga *Chlamydomonas reinhardtii*. Plant Physiol **61,** 38-38.

Bold, H., and Wynne, M. (1985). Introduction to the Algae (Englewood, NJ: Prentice-Hall), pp. 720.

Boldt, R., Edner, C., Kolukisaoglu, Ü., Hagemann, M., Weckwerth, W., Wienkoop, S., Morgenthal, K., and Bauwe, H. (2005). D-GLYCERATE 3-KINASE, the last unknown enzyme in the photorespiratory cycle in Arabidopsis, belongs to a novel kinase family. Plant Cell **17,** 2413-2420.

Borkhsenious, O.N., Mason, C.B., and Moroney, J.V. (1998). The intracellular localization of ribulose-1,5-bisphosphate carboxylase/oxygenase in *Chlamydomonas reinhardtii*. Plant Physiol **116,** 1585-1591.

Bracey, M.H., Christiansen, J., Tovar, P., Cramer, S.P., and Bartlett, S.G. (1994). Spinach carbonic anhydrase: investigation of the zinc-binding ligands by site-

directed mutagenesis, elemental analysis, and EXAFS. Biochemistry **33,** 13126-13131.

Braun, H.P., and Zabaleta, E. (2007). Carbonic anhydrase subunits of the mitochondrial NADH dehydrogenase complex (complex I) in plants. Physiol Plant **129,** 114-122.

Brueggeman, A.J., Gangadharaiah, D.S., Cserhati, M.F., Casero, D., Weeks, D.P., and Ladunga, I. (2012). Activation of the Carbon Concentrating Mechanism by CO_2 Deprivation Coincides with Massive Transcriptional Restructuring in *Chlamydomonas reinhardtii*. Plant Cell **24,** 1860–1875.

Burnell, J.N., Gibbs, M.J., and Mason, J.G. (1990). Spinach chloroplastic carbonic anhydrase: nucleotide sequence analysis of cDNA. Plant Physiol **92,** 37-40.

Burow, M., Chen, Z., Mouton, T., and Moroney, J. (1996). Isolation of cDNA clones of genes induced upon transfer of *Chlamydomonas reinhardtii* cells to low CO_2. Plant Mol Biol **31,** 443-448.

Cardol, P., Vanrobaeys, F., Devreese, B., Van Beeumen, J., Matagne, R.F., and Remacle, C. (2004). Higher plant-like subunit composition of mitochondrial complex I from *Chlamydomonas reinhardtii*: 31 conserved components among eukaryotes. Biochim Biophys Acta **1658,** 212-224.

Cardol, P., Gonzalez-Halphen, D., Reyes-Prieto, A., Baurain, D., Matagne, R.F., and Remacle, C. (2005). The mitochondrial oxidative phosphorylation proteome of *Chlamydomonas reinhardtii* deduced from the Genome Sequencing Project. Plant Physiol **137,** 447-459.

Chauvin, L., Tural, B., and Moroney, J.V. (2008). *Chlamydomonas reinhardtii* has genes for both glycolate oxidase and glycolate dehydrogenase. In Photosynthesis: Energy from the sun. Proceedings of the 14th International Congress on Photosynthesis, J. Allen, B. Osmond, J.K. Golbeck, and E. Gantt, eds (Springer), pp. 823-827.

Chen, J., Ghorai, M.K., Kenney, G., and Stubbe, J.A. (2008). Mechanistic studies on bleomycin-mediated DNA damage: multiple binding modes can result in double-stranded DNA cleavage. Nucleic Acids Research **36,** 3781-3790.

Chen, Z., Lavigne, L., Mason, C., and Moroney, J. (1997). Cloning and Overexpression of Two cDNAs Encoding the Low-CO_2-lnducible Chloroplast Envelope Protein LIP-36 from *Chlamydomonas reinhardtii*. Plant Physiol **114,** 265-273.

Chen, Z.Y., Burow, M.D., Mason, C.B., and Moroney, J.V. (1996). A low-CO_2-inducible gene encoding an alanine: alpha-ketoglutarate aminotransferase in *Chlamydomonas reinhardtii*. Plant Physiol **112,** 677-684.

Chirica, L.C., Elleby, B., and Lindskog, S. (2001). Cloning, expression and some properties of alpha-carbonic anhydrase from Helicobacter pylori. Biochim Biophys Acta **1544,** 55-63.

Colombo, S.L., Pollock, S.V., Eger, K.A., Godfrey, A.C., Adams, J.E., Mason, C.B., and Moroney, J.V. (2002). Use of the bleomycin resistance gene to generate tagged insertional mutants of *Chlamydomonas reinhardtii* that require elevated CO_2 for optimal growth. Funct Plant Biol **29,** 231-241.

Curtin, S.J., Zhang, F., Sander, J.D., Haun, W.J., Starker, C., Baltes, N.J., Reyon, D., Dahlborg, E.J., Goodwin, M.J., and Coffman, A.P. (2011). Targeted mutagenesis of duplicated genes in soybean with zinc-finger nucleases. Plant Physiol **156,** 466-473.

Davies, D.R., and Plaskitt, A. (1971). Genetical and structural analyses of cell-wall formation in *Chlamydomonas reinhardtii*. Genet. Res **17,** 33-43.

De Pater, S., Neuteboom, L.W., Pinas, J.E., Hooykaas, P.J.J., and Van Der Zaal, B.J. (2009). ZFN-induced mutagenesis and gene-targeting in Arabidopsis through Agrobacterium-mediated floral dip transformation. Plant Biotech J **7,** 821-835.

Depege, N., Bellafiore, S., and Rochaix, J.D. (2003). Role of chloroplast protein kinase Stt7 in LHCII phosphorylation and state transition in Chlamydomonas. Science's STKE **299,** 1572.

Dillon, S., Zhang, X., Trievel, R., and Cheng, X. (2005). The SET-domain protein superfamily: protein lysine methyltransferases. Genome Biol **6,** 227.1-227.10.

Drum, R., and Pankratz, H. (1964). Pyrenoids, raphes, and other fine structure in diatoms. Am J Bot **51,** 405-418.

Duanmu, D., Wang, Y., and Spalding, M.H. (2009a). Thylakoid lumen carbonic anhydrase (CAH3) mutation suppresses air-Dier phenotype of LCIB mutant in *Chlamydomonas reinhardtii*. Plant Physiol **149,** 929-937.

Duanmu, D., Miller, A.R., Horken, K.M., Weeks, D.P., and Spalding, M.H. (2009b). Knockdown of limiting-CO_2 induced gene HLA3 decreases HCO_3^- transport and photosynthetic C_i affinity in *Chlamydomonas reinhardtii*. Proc Natl Acad Sci USA **106,** 5990.

Durai, S., Mani, M., Kandavelou, K., Wu, J., Porteus, M.H., and Chandrasegaran, S. (2005). Zinc finger nucleases: custom-designed molecular scissors for genome engineering of plant and mammalian cells. Nucleic Acids Res **33,** 5978-5990.

Ecker, J.R., and Davis, R.W. (1986). Inhibition of gene expression in plant cells by expression of antisense RNA. Proc Natl Acad Sci USA **83,** 5372-5376.

Elleby, B., Chirica, L.C., Tu, C., Zeppezauer, M., and Lindskog, S. (2001). Characterization of carbonic anhydrase from Neisseria gonorrhoeae. Eur J Biochem **268,** 1613-1619.

Ellis, R.J. (1979). The most abundant protein in the world. Trends in Biochem Sci **4,** 241-244.

Eriksson, M., Gardestrom, P., and Samuelsson, G. (1995). Isolation, Purification, and Characterization of Mitochondria from *Chlamydomonas reinhardtii*. Plant Physiol **107,** 479-483.

Eriksson, M., Karlsson, J., Ramazanov, Z., Gardestrom, P., and Samuelsson, G. (1996). Discovery of an algal mitochondrial carbonic anhydrase: Molecular cloning and characterization of a low-CO_2-induced polypeptide in *Chlamydomonas reinhardtii*. Proc Natl Acad Sci USA **93,** 12031-12034.

Fang, W., Si, Y., Douglass, S., Casero, D., Merchant, S.S., Pellegrini, M., Ladunga, I., Liu, P., and Spalding, M.H. (2012). Transcriptome-Wide Changes in *Chlamydomonas reinhardtii* Gene Expression Regulated by Carbon Dioxide and the CO_2-Concentrating Mechanism Regulator CIA5/CCM1. Plant Cell **24,** 1876-1893.

Fawcett, T.W., Browse, J.A., Volokita, M., and Bartlett, S.G. (1990). Spinach carbonic anhydrase primary structure deduced from the sequence of a cDNA clone. J Biol Chem **265,** 5414-5417.

Fire, A., Xu, S.Q., Montgomery, M.K., Kostas, S.A., Driver, S.E., and Mello, C.C. (1998). Potent and specific genetic interference by double-stranded RNA in Caenorhabditis elegans. Nature **391,** 806-811.

Foyer, C.H., Bloom, A.J., Queval, G., and Noctor, G. (2009). Photorespiratory metabolism: genes, mutants, energetics, and redox signaling. Ann Rev Plant Biol **60,** 455-484.

Fujiwara, S., Fukuzawa, H., Tachiki, A., and Miyachi, S. (1990). Structure and differential expression of two genes encoding carbonic anhydrase in *Chlamydomonas reinhardtii*. Proc Natl Acad Sci USA **87,** 9779-9783.

Fukuzawa, H., Fujiwara, S., Tachiki, A., and Miyachi, S. (1990a). Nucleotide sequences of two genes *CAH1* and *CAH2* which encode carbonic anhydrase polypeptides in *Chlamydomonas reinhardtii*. Nucleic Acids Res **18,** 6441-6442.

Fukuzawa, H., Fujiwara, S., Yamamoto, Y., Dionisiosese, M.L., and Miyachi, S. (1990b). cDNA Cloning, Sequence, And Expression Of Carbonic-Anhydrase In *Chlamydomonas reinhardti*i - Regulation By Environmental CO_2 Concentration. Proc Natl Acad Sci USA **87,** 4383-4387.

Fukuzawa, H., Ishizaki, K., Miura, K., Matsueda, S., Ino-ue, T., Kucho, K., and Ohyama, K. (1998). Isolation and characterization of high-CO_2 requiring mutants from *Chlamydomonas reinhardtii* by gene tagging. Can J Bot **76,** 1092-1097.

Fukuzawa, H., Miura, K., Ishizaki, K., Kucho, K., Saito, T., Kohinata, T., and Ohyama, K. (2001). Ccm1, a regulatory gene controlling the induction of a carbon-concentrating mechanism in *Chlamydomonas reinhardtii* by sensing CO_2 availability. Proc Natl Acad Sci USA **98,** 5347-5352.

Funke, R.P., Kovar, J.L., and Weeks, D.P. (1997). Intracellular carbonic anhydrase is essential to photosynthesis in *Chlamydomonas reinhardtii* at atmospheric levels of CO_2 - Demonstration via genomic complementation of the high-CO_2-requiring mutant *ca-1*. Plant Physiol **114,** 237-244.

Genkov, T., Meyer, M., Griffiths, H., and Spreitzer, R.J. (2010). Functional Hybrid Rubisco Enzymes with Plant Small Subunits and Algal Large Subunits. J Biol Chem **285,** 19833-19841.

Geraghty, A.M., Anderson, J.C., and Spalding, M.H. (1990). A 36 Kilodalton Limiting-CO_2 Induced Polypeptide of Chlamydomonas Is Distinct from the 37 Kilodalton Periplasmic Carbonic Anhydrase. Plant Physiol. **93,** 116-121.

Gilchrist, E., and Haughn, G. (2010). Reverse genetics techniques: engineering loss and gain of gene function in plants. Briefings in Functional Genomics **9,** 103-110.

Giordano, M., Beardall, J., and Raven, J.A. (2005). CO_2 Concentrating Mechanisms in Algae: Mechanisms, Environmental Modulation, and Evolution. Ann Rev Plant Biol **56,** 99-131.

Gonzalez-Ballester, D., Pootakham, W., Mus, F., Yang, W., Catalanotti, C., Magneschi, L., de Montaigu, A., Higuera, J., Prior, M., Galvan, A., Fernandez, E., and Grossman, A. (2011). Reverse genetics in Chlamydomonas: a platform for isolating insertional mutants. Plant Methods **7:** 24.

Goodenough, U.W. (1970). Chloroplast Division And Pyrenoid Formation In *Chlamydomonas reinhardii*. J Phycol **6,** 1-6.

Goodenough, U.W., and Levine, R.P. (1970). Chloroplast structure and function in ac-20, a mutant strain of *Chlamydomonas reinhardii*. 3. Chloroplast ribosomes and membrane organization. J Cell Biol **44,** 547-562.

Götz, R., Gnann, A., and Zimmermann, F.K. (1999). Deletion of the carbonic anhydrase-like gene NCE103 of the yeast Saccharomyces cerevisiae causes an oxygen-sensitive growth defect. Yeast **15,** 855-864.

Govindjee. (2000). Milestones in photosynthesis research. In Probing Photosynthesis: Mechanism, Regulation & Adaptation, M. Yunus, U. Pathre, and P. Mohanty, eds (London: Taylor & Francis), pp. 9-39.

Gray, M., and Boer, P. (1988). Organization and expression of algal (Chlamydomonas reinhardtii) mitochondrial DNA. Philos Trans Royal Society of London. B, Biol Sci **319,** 135-147.

Griffiths, D. (1970). The pyrenoid. The Botanical Review **36,** 29-58.

Grossman, A., Croft, M., Gladyshev, V., Merchant, S., Posewitz, M., Prochnik, S., and Spalding, M. (2007). Novel metabolism in Chlamydomonas through the lens of genomics. Current Opinion in Plant Biology **10,** 190-198.

Gutknecht, J., Bisson, M.A., and Tosteson, F.C. (1977). Diffusion of carbon dioxide through lipid bilayer membranes: effects of carbonic anhydrase, bicarbonate, and unstirred layers. J Gen Physiol **69,** 779-794.

Hackenberg, C., Kern, R., Hüge, J., Stal, L.J., Tsuji, Y., Kopka, J., Shiraiwa, Y., Bauwe, H., and Hagemann, M. (2011). Cyanobacterial Lactate Oxidases Serve as Essential Partners in N_2 Fixation and Evolved into Photorespiratory Glycolate Oxidases in Plants. Plant Cell **23,** 2978-2990.

Hanba, Y.T., Shibasaka, M., Hayashi, Y., Hayakawa, T., Kasamo, K., Terashima, I., and Katsuhara, M. (2004). Overexpression of the barley aquaporin HvPIP2; 1 increases internal CO_2 conductance and CO_2 assimilation in the leaves of transgenic rice plants. Plant Cell Physiol **45,** 521-529.

Harris, E.H., Stern, D.B., and Witman, G. (2009). The Chlamydomonas sourcebook. (Amsterdam ; Boston: Academic Press).

Hemsley, A., and Poole, I. (2004). The evolution of plant physiology: from whole plants to ecosystems. (Academic Press).

Henk, M., Rawat, M., Hugghins, S., Lavigne, L., Ramazanov, Z., Mason, C., and Moroney, J. (1995). Pyrenoid morphology in Rubisco and CO_2 concentrating mutants of *Chlamydomonas reinhardtii*. In Proceedings of the Xth International

Photosynthesis Congress, P. Mathis, ed (Montpellier, France: Springer), pp. 595-598.

Hewett-Emmett, D., and Tashian, R.E. (1996). Functional diversity, conservation, and convergence in the evolution of the alpha-, beta-, and gamma-carbonic anhydrase gene families. Mol Phylogenet Evol **5,** 50-77.

Hibberd, J.M., Sheehy, J.E., and Langdale, J.A. (2008). Using C4 photosynthesis to increase the yield of rice--rationale and feasibility. Current Opinion Plant Biol **11,** 228-231.

Holden, M. (1976). Chlorophylls. In: Chemistry and biochemistry of plant pigments, T.W. Goodwin, ed (Academic Press, Inc., London), pp. 1-37.

Holdsworth, R.H. (1968). The presence of a crystalline matrix in pyrenoids of the diatom, *Achnanthes brevipes*. J Cell Biol **37,** 831-837.

Houtz, R.L., Magnani, R., Nayak, N.R., and Dirk, L.M.A. (2008). Co-and post-translational modifications in Rubisco: unanswered questions. J Exp Bot **59,** 1635-1645.

Houtz, R.L., Poneleit, L., Jones, S.B., Royer, M., and Stults, J.T. (1992). Posttranslational Modifications in the Amino- Terminal Region of the Large Subunit of Ribulose- 1,5-Bisphosphate Carboxylase/Oxygenase from Several Plant Species. Plant Physiol. **98,** 1170-1174.

Husic, H.D., and Tolbert, N.E. (1985). Properties of Phosphoglycolate Phosphatase from *Chlamydomonas reinhardtii* and *Anacystis nidulans*. Plant Physiol. **79,** 394-399.

Hyams, J., and Davies, D.R. (1972). The induction and characterisation of cell wall mutants of *Chlamydomonas reinhardii*. Mutation Research/Fundamental and Molecular Mechanisms of Mutagenesis **14,** 381-389.

Ikeda, T., and Takeda, H. (1995). Species-Specific Differences of Pyrenoids In Chlorella (Chlorophyta). J Phycol **31,** 813-818.

Im, C., and Grossman, A. (2002). Identification and regulation of high light induced genes in *Chlamydomonas reinhardtii*. The Plant Journal **30,** 301-313.

Inwood, W., Yoshihara, C., Zalpuri, R., Kim, K.S., and Kustu, S. (2008). The ultrastructure of a *Chlamydomonas reinhardtii* mutant strain lacking phytoene synthase resembles that of a colorless alga. Mol Plant **1,** 925-937.

Ishida, S., Muto, S., and Miyachi, S. (1993). Structural analysis of periplasmic carbonic anhydrase 1 of *Chlamydomonas reinhardtii*. Eur J Biochem **214,** 9-16.

Jordan, D.B., and Ogren, W.L. (1981). Species variation in the specificity of ribulose biphosphate carboxylase/oxygenase. Nature **291,** 513-515.

Kamo, T., Shimogawara, K., Fukuzawa, H., Muto, S., and Miyachi, S. (1990). Subunit constitution of carbonic-anhydrase from *Chlamydomonas-reinhardtii*. Eur J Biochem **192,** 557-562.

Kaplan, A., and Reinhold, L. (1999). CO_2 concentrating mechanisms in photosynthetic microorganisms. Ann Rev of Plant Physiol Plant Mol Biol **50,** 539-570.

Karlsson, J., Hiltonen, T., Husic, H.D., Ramazanov, Z., and Samuelsson, G. (1995). Intracellular Carbonic-Anhydrase Of *Chlamydomonas reinhardtii*. Plant Physiol **109,** 533-539.

Karlsson, J., Clarke, A.K., Chen, Z.Y., Hugghins, S.Y., Park, Y.I., Husic, H.D., Moroney, J.V., and Samuelsson, G. (1998). A novel alpha-type carbonic anhydrase associated with the thylakoid membrane in *Chlamydomonas reinhardtii* is required for growth at ambient CO_2. EMBO J **17,** 1208-1216.

Kelly, G., and Latzko, E. (1976). Inhibition of spinach-leaf phosphofructokinase by 2-phosphoglycolate. FEBS Lett **68,** 55-58.

Khalifah, R.G. (1973). Carbon dioxide hydration activity of carbonic anhydrase: paradoxical consequences of the unusually rapid catalysis. Proc Natl Acad Sci U S A **70,** 1986-1989.

Kim, E.J., and Cerutti, H. (2009). Targeted Gene Silencing by RNA Interference in *Chlamydomonas*. Meth Cell Biol **93,** 99-110.

Kimber, M.S., and Pai, E.F. (2000). The active site architecture of *Pisum sativum* beta-carbonic anhydrase is a mirror image of that of alpha-carbonic anhydrases. EMBO J **19,** 1407-1418.

Kindle, K.L. (1990). High-frequency nuclear transformation of *Chlamydomonas reinhardtii*. Proc Natl Acad Sci U S A **87,** 1228-1232.

Kisaki, T., and Tolbert, N. (1969). Glycolate and glyoxylate metabolism by isolated peroxisomes or chloroplasts. Plant Physiol **44,** 242-250.

Klein, R.R., and Houtz, R.L. (1995). Cloning and developmental expression of pea ribulose-1,5-bisphosphate carboxylase/oxygenase large subunit N-methyltransferase. Plant Mol Biol **27,** 249-261.

Klodmann, J., Sunderhaus, S., Nimtz, M., Jansch, L., and Braun, H.P. (2010). Internal Architecture of Mitochondrial Complex I from *Arabidopsis thaliana*. Plant Cell **22,** 797-810.

Kohinata, T., Nishino, H., Miura, K., and Fukuzawa, H. (2005). Functional regions of the regulatory factor CCM1 indispensable to the CO_2-limiting stress responses in *Chlamydomonas reinhardtii*. Plant Cell Physiol **46,** S108-S108.

Kuchitsu, K., Tsuzuki, M., and Miyachi, S. (1988). Characterization of the Pyrenoid Isolated from Unicellular Green-Alga *Chlamydomonas reinhardtii* - Particulate Form of Rubisco Protein. Protoplasma **144,** 17-24.

Kucho, K., Ohyama, K., and Fukuzawa, H. (1999). CO_2-responsive transcriptional regulation of *CAH1* encoding carbonic anhydrase is mediated by enhancer and silencer regions in *Chlamydomonas reinhardtii*. Plant Physiol **121,** 1329-1337.

Kucho, K., Yoshioka, S., Taniguchi, F., Ohyama, K., and Fukuzawa, H. (2003). Cis-acting elements and DNA-binding proteins involved in CO_2-responsive transcriptional activation of *Cah1* encoding a periplasmic carbonic anhydrase *Chlamydomonas reinhardtii*. Plant Physiology **133,** 783-793.

Kustu, S., and Inwood, W. (2006). Biological gas channels for NH_3 and CO_2: evidence that Rh (Rhesus) proteins are CO_2 channels. Transfusion Clinique et Biologique **13,** 103-110.

Lacoste-Royal, G., and Gibbs, S.P. (1987). Immunocytochemical Localization of Ribulose-1,5-Bisphosphate Carboxylase in the Pyrenoid and Thylakoid Region of the Chloroplast of *Chlamydomonas reinhardtii*. Plant Physiol. **83,** 602-606.

Laemmli, U.K. (1970). Cleavage of structural proteins during the assembly of the head of bacteriophage T4. Nature **227,** 680-685.

Lane, T.W., and Morel, F.M.M. (2000). Regulation of carbonic anhydrase expression by zinc, cobalt, and carbon dioxide in the marine diatom Thalassiosira weissflogii. Plant Physiol **123,** 345-352.

Lane, T.W., Saito, M.A., George, G.N., Pickering, I.J., Prince, R.C., and Morel, F.M.M. (2005). Biochemistry: A cadmium enzyme from a marine diatom. Nature **435,** 42-42.

Lindskog, S. (1997). Structure and mechanism of carbonic anhydrase. Pharmacol Ther **74,** 1-20.

Lumbreras, V., Stevens, D.R., and Purton, S. (1998). Efficient foreign gene expression in *Chlamydomonas reinhardtii* mediated by an endogenous intron. Plant J **14,** 441-447.

Ma, Y., Pollock, S.V., Xiao, Y., Cunnusamy, K., and Moroney, J.V. (2011a). Identification of a novel gene, *CIA6*, required for normal pyrenoid formation in *Chlamydomonas reinhardtii*. Plant Physiol **156,** 884-896.

Ma, Y., Hartman, M., and Moroney, J.V. (2011b). Transcriptional analysis of the three phosphoglycolate phosphatase genes in wild type and the *pgp1* mutant of *Chlamydomonas reinhardtii*. In Proceedings of the 15th International Congress on Photosynthesis (In press) (Beijing, China: Springer).

Makino, A. (2003). Rubisco and nitrogen relationships in rice: leaf photosynthesis and plant growth. Soil Sci Plant Nutrition **49,** 319-327.

Mamedov, T.G., Suzuki, K., Miura, K., Kucho Ki, K., and Fukuzawa, H. (2001). Characteristics and sequence of phosphoglycolate phosphatase from a eukaryotic green alga *Chlamydomonas reinhardtii*. J Biol Chem **276,** 45573-45579.

Marek, L.F., and Spalding, M.H. (1991). Changes in photorespiratory enzyme activity in response to limiting CO_2 in *Chlamydomonas reinhardtii*. Plant Physiol **97,** 420-425.

Mariscal, V., Moulin, P., Orsel, M., Miller, A.J., Fernández, E., and Galván, A. (2006). Differential Regulation of the Chlamydomonas *Nar1* Gene Family by Carbon and Nitrogen. Protist **157,** 421-433.

Maurino, V.G., and Peterhansel, C. (2010). Photorespiration: current status and approaches for metabolic engineering. Curr Opinion Plant Biolo **13,** 248-256.

McKay, R.M.L., Gibbs, S.P., and Vaughn, K.C. (1991). RuBisCo activase is present in the pyrenoid of green algae. Protoplasma **162,** 38-45.

Meldrum, N.U., and Roughton, F.J. (1933). Carbonic anhydrase. Its preparation and properties. J Physiol **80,** 113-142.

Merchant, S.S., Prochnik, S.E., Vallon, O., Harris, E.H., Karpowicz, S.J., Witman, G.B., Terry, A., Salamov, A., Fritz-Laylin, L.K., Marechal-Drouard, L., Marshall, W.F., Qu, L.H., Nelson, D.R., Sanderfoot, A.A., Spalding, M.H., Kapitonov, V.V., Ren, Q., Ferris, P., Lindquist, E., Shapiro, H., Lucas, S.M., Grimwood, J., Schmutz, J., Cardol, P., Cerutti, H., Chanfreau, G., Chen, C.L., Cognat, V., Croft, M.T., Dent, R., Dutcher, S., Fernandez, E., Fukuzawa, H., Gonzalez-Ballester, D., Gonzalez-Halphen, D., Hallmann, A., Hanikenne, M., Hippler, M., Inwood, W., Jabbari, K., Kalanon, M., Kuras, R., Lefebvre, P.A., Lemaire, S.D., Lobanov, A.V., Lohr, M., Manuell, A., Meier, I., Mets, L., Mittag, M., Mittelmeier, T., Moroney, J.V., Moseley, J., Napoli, C., Nedelcu, A.M., Niyogi, K., Novoselov, S.V., Paulsen, I.T., Pazour, G., Purton, S., Ral, J.P., Riano-Pachon, D.M., Riekhof, W., Rymarquis, L., Schroda, M., Stern, D., Umen, J., Willows, R., Wilson, N., Zimmer, S.L., Allmer, J., Balk, J., Bisova, K., Chen, C.J., Elias, M., Gendler, K., Hauser, C., Lamb, M.R., Ledford, H., Long, J.C., Minagawa, J., Page, M.D., Pan, J., Pootakham, W., Roje, S., Rose, A., Stahlberg, E., Terauchi, A.M., Yang, P., Ball, S., Bowler, C., Dieckmann, C.L., Gladyshev, V.N., Green, P., Jorgensen, R., Mayfield, S., Mueller-Roeber, B., Rajamani, S., Sayre, R.T., Brokstein, P.,

Dubchak, I., Goodstein, D., Hornick, L., Huang, Y.W., Jhaveri, J., Luo, Y., Martinez, D., Ngau, W.C., Otillar, B., Poliakov, A., Porter, A., Szajkowski, L., Werner, G., Zhou, K., Grigoriev, I.V., Rokhsar, D.S., and Grossman, A.R. (2007). The Chlamydomonas genome reveals the evolution of key animal and plant functions. Science **318,** 245-250.

Michaelis, G., Vahrenholz, C., and Pratje, E. (1990). Mitochondrial DNA of *Chlamydomonas reinhardtii*: the gene for apocytochrome b and the complete functional map of the 15.8 kb DNA. Mol Gen Genetics **223,** 211-216.

Mitra, M., Lato, S.M., Ynalvez, R.A., Xiao, Y., and Moroney, J.V. (2004). Identification of a new chloroplast carbonic anhydrase in *Chlamydomonas reinhardtii*. Plant Physiol **135,** 173-182.

Mitra, M., Mason, C.B., Xiao, Y., Ynalvez, R.A., Lato, S.M., and Moroney, J.V. (2005). The carbonic anhydrase gene families of *Chlamydomonas reinhardtii*. Can J Bot **83,** 780-795.

Miura, K., Yamano, T., Yoshioka, S., Kohinata, T., Inoue, Y., Taniguchi, F., Asamizu, E., Nakamura, Y., Tabata, S., Yamato, K.T., Ohyama, K., and Fukuzawa, H. (2004). Expression profiling-based identification of CO_2-responsive genes regulated by CCM1 controlling a carbon-concentrating mechanism in *Chlamydomonas reinhardtii*. Plant Physiol **135,** 1595-1607.

Mizohata, E., Matsumura, H., Okano, Y., Kumei, M., Takuma, H., Onodera, J., Kato, K., Shibata, N., Inoue, T., and Yokota, A. (2002). Crystal structure of activated ribulose-1, 5-bisphosphate carboxylase/oxygenase from green alga Chlamydomonas reinhardtii complexed with 2-carboxyarabinitol-1, 5-bisphosphate1. J Mol Biol **316,** 679-691.

Molnár, A., Bassett, A., Thuenemann, E., Schwach, F., Karkare, S., Ossowski, S., Weigel, D., and Baulcombe, D. (2009). Highly specific gene silencing by artificial microRNAs in the unicellular alga *Chlamydomonas reinhardtii*. Plant J **58,** 165-174.

Morita, E., Kuroiwa, H., Kuroiwa, T., and Nozaki, H. (1997). High localization of ribulose-1,5-bisphosphate carboxylase/oxygenase in the pyrenoids of *Chlamydomonas reinhardtii* (Chlorophyta), as revealed by cryofixation and immunogold electron microscopy. Journal of Phycology **33,** 68-72.

Morita, E., Abe, T., Tsuzuki, M., Fujiwara, S., Sato, N., Hirata, A., Sonoike, K., and Nozaki, H. (1999). Role of pyrenoids in CO_2 concentrating mechanism: comparative morphology, physiology and molecular phylogenetic analysis of closely related strains of *Chlamydomonas* and *Chloromonas* (Volvocales). Planta **208,** 365-372.

Moroney, J., Ma, Y., Frey, W., Fusilier, K., Pham, T., Simms, T., DiMario, R., Yang, J., and Mukherjee, B. (2011). The carbonic anhydrase isoforms of *Chlamydomonas reinhardtii*: intracellular location, expression, and physiological roles. Photosynthesis Research **109,** 133-149.

Moroney, J.V., and Tolbert, N.E. (1985). Inorganic Carbon Uptake by *Chlamydomonas reinhardtii*. Plant Physiol **77,** 253-258.

Moroney, J.V., and Mason, C.B. (1991). The role of the chloroplast in inorganic carbon acquisition by *Chlamydomonas reinhardtii*. Can J Bot **69,** 1017-1024.

Moroney, J.V., and Ynalvez, R.A. (2007). Proposed carbon dioxide concentrating mechanism in *Chlamydomonas reinhardtii*. Eukaryot Cell **6,** 1251-1259.

Moroney, J.V., Husic, H.D., and Tolbert, N.E. (1985). Effect of Carbonic Anhydrase Inhibitors on Inorganic Carbon Accumulation by *Chlamydomonas reinhardtii*. Plant Physiol **79,** 177-183.

Moroney, J.V., Tolbert, N.E., and Sears, B.B. (1986). Complementation analysis of the inorganic carbon concentrating mechanism of *Chlamydomonas reinhardtii*. Mol Gen Genetics **204,** 199-203.

Moroney, J.V., Bartlett, S.G., and Samuelsson, G. (2001). Carbonic anhydrases in plants and algae. Plant Cell Environ **24,** 141-153.

Moroney, J.V., Husic, H.D., Tolbert, N.E., Kitayama, M., Manuel, L.J., and Togasaki, R.K. (1989). Isolation and Characterization of a Mutant of *Chlamydomonas reinhardtii* Deficient in the CO_2 Concentrating Mechanism. Plant Physiol **89,** 897-903.

Mukherjee, B., and Moroney, J.V. (2011). Algal Carbon Dioxide Concentrating Mechanisms. In eLS (John Wiley & Sons Ltd, Chichester).

Mukherjee, B., TT., P., Ma, Y., Simms, T., and Moroney, J. (2011). The absence of the periplasmic carbonic anhydrase, CAH1, in the sequenced *Chlamydomonas reinhardtii* strain, CC-503. In Proceedings of the 15th International Congress on Photosynthesis (In press) (Beijing, China: Springer).

Nakamura, Y., Kanakagiri, S., Van, K., He, W., and Spalding, M. (2005). Disruption of the glycolate dehydrogenase gene in the high-CO_2-requiring mutant *HCR89* of *Chlamydomonas reinhardtii*. Can J Bot **83,** 820-833.

Nelson, E.B., and Tolbert, N. (1970). Glycolate dehydrogenase in green algae. Arch Biochem Biophys **141,** 102-110.

Newman, E.A. (1994). A physiological measure of carbonic anhydrase in Muller cells. Glia **11,** 291-299.

Newman, S.M., Boynton, J.E., Gillham, N.W., Randolph-Anderson, B.L., Johnson, A.M., and Harris, E.H. (1990). Transformation of Chloroplast Ribosomal RNA Genes in Chlamydomonas: Molecular and Genetic Characterization of Integration Events. Genetics **126,** 875-888.

Ng, D.W., Wang, T., Chandrasekharan, M.B., Aramayo, R., Kertbundit, S., and Hall, T.C. (2007). Plant SET domain-containing proteins: structure, function and regulation. Biochim Biophys Acta **1769,** 316-329.

Ohnishi, N., Mukherjee, B., Tsujikawa, T., Yanase, M., Nakano, H., Moroney, J.V., and Fukuzawa, H. (2010). Expression of a Low CO_2 nducible Protein, LCI1, Increases Inorganic Carbon Uptake in the Green Alga *Chlamydomonas reinhardtii*. Plant Cell **22,** 3105-3117.

Osakabe, K., Osakabe, Y., and Toki, S. (2009). Site-directed mutagenesis in Arabidopsis using custom-designed zinc finger nucleases. Proceedings of the National Academy of Sciences **107,** 12034.

Park, H., Song, B., and Morel, F.M.M. (2007). Diversity of the cadmium-containing carbonic anhydrase in marine diatoms and natural waters. Environ Microbiol **9,** 403-413.

Petolino, J.F., Worden, A., Curlee, K., Connell, J., Strange Moynahan, T.L., Larsen, C., and Russell, S. (2010). Zinc finger nuclease-mediated transgene deletion. Plant Mol Biol **73,** 617-628.

Petroutsos, D., Terauchi, A.M., Busch, A., Hirschmann, I., Merchant, S.S., Finazzi, G., and Hippler, M. (2009). PGRL1 participates in iron-induced remodeling of the photosynthetic apparatus and in energy metabolism in *Chlamydomonas reinhardtii*. J Biol Chem **284,** 32770-32781.

Pollock, S.V., and Colman, B. (2001). The inhibition of the carbon concentrating mechanism of the green alga *Chlorella saccharophila* by acetazolamide. Physiol Plant **111,** 527-532.

Pollock, S.V., Colombo, S.L., Prout, D.L., Jr., Godfrey, A.C., and Moroney, J.V. (2003). Rubisco activase is required for optimal photosynthesis in the green alga *Chlamydomonas reinhardtii* in a low-CO_2 atmosphere. Plant Physiol **133,** 1854-1861.

Pollock, S.V., Prout, D.L., Godfrey, A.C., Lemaire, S.D., and Moroney, J.V. (2004). The *Chlamydomonas reinhardti*i proteins CCP1 and CCP2 are required for long-

term growth, but are not necessary for efficient photosynthesis, in a low-CO_2 environment. Plant Mol Biol **56,** 125-132.

Porteus, M.H., and Carroll, D. (2005). Gene targeting using zinc finger nucleases. Nature Biotech **23,** 967-973.

Portis, A.R., and Parry, M.A.J. (2001). Rubisco. In eLS (John Wiley & Sons, Ltd).

Price, G.D., and Badger, M.R. (1989). Expression of Human Carbonic Anhydrase in the Cyanobacterium *Synechococcus* PCC7942 Creates a High CO_2-Requiring Phenotype : Evidence for a Central Role for Carboxysomes in the CO_2 Concentrating Mechanism. Plant Physiol **91,** 505-513.

Price, G.D., Badger, M.R., Woodger, F.J., and Long, B.M. (2008). Advances in understanding the cyanobacterial CO_2-concentrating-mechanism (CCM): functional components, Ci transporters, diversity, genetic regulation and prospects for engineering into plants. J Exp Bot **59,** 1441-1461.

Pronina, N.A., and Semenenko, V.E. (1992). Carbonic Anhydrase Activity and Fatty-Acid Composition of Photosystem Deficient and High CO_2 Required Mutants of *Chlamydomonas reinhardtii*. Photosynthesis Res **34,** 201-201.

Qian, C., and Zhou, M.M. (2006). SET domain protein lysine methyltransferases: Structure, specificity and catalysis. Cell Mol Life Sci **63,** 2755-2763.

Ramazanov, Z., Mason, C.B., Geraghty, A.M., Spalding, M.H., and Moroney, J.V. (1993). The Low CO_2-Inducible 36-Kilodalton Protein Is Localized to the Chloroplast Envelope of *Chlamydomonas reinhardtii*. Plant Physiol **101,** 1195-1199.

Ramazanov, Z., Rawat, M., Henk, M.C., Mason, C.B., Matthews, S.W., and Moroney, J.V. (1994). The induction of the CO_2-concentrating mechanism is correlated with the formation of the starch sheath around the pyrenoid of *Chlamydomonas reinhardtii*. Planta **195,** 210-216.

Raunser, S., Magnani, R., Huang, Z., Houtz, R.L., Trievel, R.C., Penczek, P.A., and Walz, T. (2009). Rubisco in complex with Rubisco large subunit methyltransferase. Proc Natl Acad Sci USA **106,** 3160-3165.

Raven, J.A. (1997). CO2-concentrating mechanisms: A direct role for thylakoid lumen acidification? Plant Cell Environ **20,** 147-154.

Rawat, M., and Moroney, J.V. (1991). Partial characterization of a new isoenzyme of carbonic anhydrase isolated from *Chlamydomonas reinhardtii*. J Biol Chem **266,** 9719-9723.

Rawat, M., Henk, M.C., Lavigne, L.L., and Moroney, J.V. (1996). Chlamydomonas reinhardtii mutants without ribulose-1,5-bisphosphate carboxylase-oxygenase lack a detectable pyrenoid. Planta **198,** 263-270.

Remacle, C., Coosemans, N., Jans, F., Hanikenne, M., Motte, P., and Cardol, P. (2010). Knock-down of the COX3 and COX17 gene expression of cytochrome c oxidase in the unicellular green alga *Chlamydomonas reinhardtii*. Plant Mol Biol **74,** 223-233.

Roberts, S.B., Lane, T.W., and Morel, F.M.M. (1997). Carbonic anhydrase in the marine diatom *Thalassiosira weissflogii* (Bacillariophyceae). J Phycol **33,** 845-850.

Rohr, J., Sarkar, N., Balenger, S., Jeong, B.-r., and Cerutti, H. (2004). Tandem inverted repeat system for selection of effective transgenic RNAi strains in Chlamydomonas. The Plant Journal **40,** 611-621.

Rojdestvenski, I., Park, Y.I., Karlsson, J., Oquist, G., and Samuelsson, G. (2000). A carbonic anhydrase catalyzed CO_2 pump in Chlamydomonas reinhardtii: In vivo experiments, computer modelling, and theory. Russian J Plant Physiol **47,** 613-621.

Rolland, N., Dorne, A.-J., Amoroso, G., Sultemeyer, D.F., Joyard, J., and Rochaix, J.-D. (1997). Disruption of the plastid *ycf10* open reading frame affects uptake of inorganic carbon in the chloroplast of *Chlamydomonas*. EMBO J **16,** 6713-6726.

Rowlett, R.S., Chance, M.R., Wirt, M.D., Sidelinger, D.E., Royal, J.R., Woodroffe, M., Wang, Y.F., Saha, R.P., and Lam, M.G. (1994). Kinetic and structural characterization of spinach carbonic anhydrase. Biochem **33,** 13967-13976.

Sage, R.F. (2002). Variation in the kcat of Rubisco in C3 and C4 plants and some implications for photosynthetic performance at high and low temperature. J Exp Bot **53,** 609-620.

Sambrook, J., Maniatis, T., Russell, D.W., and Fritsch, E.F. (2001). Molecular cloning: a laboratory manual. (Cold Spring Harbor, N.Y.,: Cold Spring Harbor Laboratory Press).

Sasaki, Y., Sekiguchi, K., Nagano, Y., and Matsuno, R. (1993). Chloroplast envelope protein encoded by chloroplast genome. FEBS Lett **316,** 93-98.

Schneider, G., Lindqvist, Y., and Branden, C.I. (1992). RUBISCO: structure and mechanism. Ann Rev Biophy Biomol Struct **21,** 119-143.

Schnell, R.A., and Lefebvre, P.A. (1993). Isolation of the Chlamydomonas regulatory gene NIT2 by transposon tagging. Genetics **134,** 737-747.

Schroda, M., Vallon, O., Wollman, F.A., and Beck, C.F. (1999). A chloroplast-targeted heat shock protein 70 (HSP70) contributes to the photoprotection and repair of photosystem II during and after photoinhibition. Plant Cell **11,** 1165-1178.

Schwarte, S., and Bauwe, H. (2007). Identification of the photorespiratory 2-phosphoglycolate phosphatase, PGLP1, in Arabidopsis. Plant Physiol **144,** 1580-1586.

Schwarz, R., Reinhold, L., and Kaplan, A. (1995). Low Activation State of Ribulose-1,5-Bisphosphate Carboxylase/Oxygenase in Carboxysome-Defective *Synechococcus* Mutants. Plant Physiol **108,** 183-190.

Sears, B.B., Boynton, J.E., and Gillham, N.W. (1980). The Effect of Gametogenesis Regimes on the Chloroplast Genetic System of *Chlamydomonas reinhardtii*. Genetics **96,** 95-114.

Shimogawara, K., Fujiwara, S., Grossman, A., and Usuda, H. (1998). High-Efficiency Transformation of *Chlamydomonas reinhardtii* by Electroporation. Genetics **148,** 1821-1828.

Shiraiwa, Y., and Miyachi, S. (1983). Factors Controlling Induction of Carbonic Anhydrase and Efficiency of Photosynthesis in *Chlorella vulgaris* llh Cells. Plant Cell Physiol **24,** 919-923.

Siebert, P.D., Chenchik, A., Kellogg, D.E., Lukyanov, K.A., and Lukyanov, S.A. (1995). An improved PCR method for walking in uncloned genomic DNA. Nucleic Acids Res **23,** 1087-1088.

Sizova, I., Fuhrmann, M., and Hegemann, P. (2001). A *Streptomyces rimosus aphVIII* gene coding for a new type phosphotransferase provides stable antibiotic resistance to *Chlamydomonas reinhardtii*. Gene **277,** 221-229.

Smith, K.S., and Ferry, J.G. (1999). A plant-type (beta-class) carbonic anhydrase in the thermophilic methanoarchaeon *Methanobacterium thermoautotrophicum*. J Bacteriol **181,** 6247-6253.

So, A.K., Espie, G.S., Williams, E.B., Shively, J.M., Heinhorst, S., and Cannon, G.C. (2004). A novel evolutionary lineage of carbonic anhydrase (epsilon class) is a component of the carboxysome shell. J Bacteriol **186,** 623-630.

So, A.K.C., and Espie, G.S. (2005). Cyanobacterial carbonic anhydrases. Can J Bot **83,** 721-734.

Soltes-Rak, E., Mulligan, M.E., and Coleman, J.R. (1997). Identification and characterization of a gene encoding a vertebrate-type carbonic anhydrase in cyanobacteria. J Bacteriol **179,** 769-774.

Somerville, C.R., and Ogren, W.L. (1979). A phosphoglycolate phosphatase-deficient mutant of Arabidopsis. Nature **280,** 833-836.

Soupene, E., Inwood, W., and Kustu, S. (2004). Lack of the Rhesus protein Rh1 impairs growth of the green alga *Chlamydomonas reinhardtii* at high CO_2. Proc Natl Acad Sci USA **101,** 7787.

Soupene, E., King, N., Feild, E., Liu, P., Niyogi, K.K., Huang, C.-H., and Kustu, S. (2002). Rhesus expression in a green alga is regulated by CO_2. Proc Natl Acad Sci USA **99,** 7769-7773.

Spalding, M. (2009). CO_2-concentrating mechanism and carbon assimilation. In The Chlamydomonas Sourcebook, E.H. Harris, ed (Amsterdam, The Netherlands: Elsevier Publishers), pp. 257-301.

Spalding, M.H. (2008). Microalgal carbon-dioxide-concentrating mechanisms: Chlamydomonas inorganic carbon transporters. J Exp Bot **59,** 1463-1473.

Spalding, M.H., Spreitzer, R.J., and Ogren, W.L. (1983a). Carbonic Anhydrase-Deficient Mutant of *Chlamydomonas reinhardii* Requires Elevated Carbon Dioxide Concentration for Photoautotrophic Growth. Plant Physiol **73,** 268-272.

Spalding, M.H., Spreitzer, R.J., and Ogren, W.L. (1983b). Reduced inorganic carbon transport in a CO_2-requiring mutant of *Chlamydomonas reinhardii*. Plant Physiol **73,** 273.

Spreitzer, R., and Mets, L. (1980). Non-mendelian mutation affecting ribulose-1, 5-bisphosphate carboxylase structure and activity. Nature **285,** 114-115.

Spreitzer, R.J., and Mets, L. (1981). Photosynthesis-deficient mutants of *Chlamydomonas reinhardii* with associated light-sensitive phenotypes. Plant Physiology **67,** 565.

Spreitzer, R.J., Goldschmidt-Clermont, M., Rahire, M., and Rochaix, J.-D. (1985). Nonsense mutations in the Chlamydomonas chloroplast gene that codes for the large subunit of ribulosebisphosphate carboxylase/oxygenase. Proceedings of the National Academy of Sciences of the United States of America **82,** 5460-5464.

Sueoka, N. (1960). Mitotic Replication of Deoxyribonucleic Acid in *Chlamydomonas reinhardtii*. Proc Natl Acad Sci USA **46,** 83-91.

Sunderhaus, S., Dudkina, N.V., Jansch, L., Klodmann, J., Heinemeyer, J., Perales, M., Zabaleta, E., Boekema, E.J., and Braun, H.P. (2006). Carbonic anhydrase subunits form a matrix-exposed domain attached to the membrane arm of mitochondrial complex I in plants. J Biol Chem **281,** 6482-6488.

Suzuki, K. (1995). Phosphoglycolate Phosphatase-Defident Mutants of *Chlamydomonas reinhardtii* Capable of Growth under Air. Plant Cell Physiol **36,** 95-100.

Suzuki, K., and Spalding, M.H. (1989). Adaptation of *Chlamydomonas reinhardtii* High-CO_2-Requiring Mutants to Limiting CO_2. Plant Physiol **90,** 1195-1200.

Suzuki, K., Marek, L.F., and Spalding, M.H. (1990). A Photorespiratory Mutant of *Chlamydomonas reinhardtii*. Plant Physiol **93,** 231-237.

Suzuki, K., Uchida, H., and Mamedov, T.G. (2005). The phosphoglycolate phosphatase gene and the mutation in the phosphoglycolate phosphatase-deficient mutant (*pgp1-1*) of *Chlamydomonas reinhardtii*. Can J Bot **83,** 842-849.

Tabita, F.R. (1999). Microbial ribulose 1, 5-bisphosphate carboxylase/oxygenase: a different perspective. Photosynthesis Research **60,** 1-28.

Tabita, F.R., Satagopan, S., Hanson, T.E., Kreel, N.E., and Scott, S.S. (2008). Distinct form I, II, III, and IV Rubisco proteins from the three kingdoms of life provide clues about Rubisco evolution and structure/function relationships. J Exp Bot **59,** 1515-1524.

Tamura, K., Dudley, J., Nei, M., and Kumar, S. (2007). MEGA4: Molecular evolutionary genetics analysis (MEGA) software version 4.0. Mol Biol Evol **24,** 1596-1599.

Tanaka, S., Kerfeld, C.A., Sawaya, M.R., Cai, F., Heinhorst, S., Cannon, G.C., and Yeates, T.O. (2008). Atomic-level models of the bacterial carboxysome shell. Science **319,** 1083-1086.

Taylor, T.C., Backlund, A., Bjorhall, K., Spreitzer, R.J., and Andersson, I. (2001). First Crystal Structure of Rubisco from a Green Alga,*Chlamydomonas reinhardtii*. J Biol Chem **276,** 48159-48164.

The Arabidopsis Genome Intiative (2000). Analysis of the genome sequence of the flowering plant *Arabidopsis thaliana*. Nature **408,** 796-815.

Tolbert, N.E. (1997). The C2 Oxidative Photosynthetic Carbon Cycle. Annu Rev Plant Physiol Plant Mol Biol **48,** 1-25.

Trievel, R., Flynn, E., Houtz, R., and Hurley, J. (2003). Mechanism of multiple lysine methylation by the SET domain enzyme Rubisco LSMT. Nature Structural & Molecul Biol **10,** 545-552.

Trievel, R.C., Beach, B.M., Dirk, L.M.A., Houtz, R.L., and Hurley, J.H. (2002). Structure and Catalytic Mechanism of a SET Domain Protein Methyltransferase. Cell **111,** 91-103.

Tsuzuki, M., and Miyachi, S. (1979). Effects of CO_2 Concentration during Growth and of Ethoxyzolamide on CO_2 Compensation Point in Chlorella. FEBS Lett **103,** 221-223.

Tsuzuki, M., and Miyachi, S. (1989). The Function of Carbonic-Anhydrase in Aquatic Photosynthesis. Aquatic Bot **34,** 85-104.

Tsuzuki, M., Shiraiwa, Y., and Miyachi, S. (1980). Role of Carbonic-Anhydrase in Photosynthesis in Chlorella Derived from Kinetic-Analysis of $^{14}CO_2$ Fixation. Plant Cell Physiol **21,** 677-688.

Tural, B., and Moroney, J.V. (2005). Regulation of the expression of photorespiratory genes in *Chlamydomonas reinhardtii*. Can J Bot **83,** 810-819.

Tuskan, G.A., Difazio, S., Jansson, S., Bohlmann, J., Grigoriev, I., Hellsten, U., Putnam, N., Ralph, S., Rombauts, S., Salamov, A., Schein, J., Sterck, L., Aerts, A., Bhalerao, R.R., Bhalerao, R.P., Blaudez, D., Boerjan, W., Brun, A., Brunner, A., Busov, V., Campbell, M., Carlson, J., Chalot, M., Chapman, J., Chen, G.L., Cooper, D., Coutinho, P.M., Couturier, J., Covert, S., Cronk, Q., Cunningham, R., Davis, J., Degroeve, S., Dejardin, A., Depamphilis, C., Detter, J., Dirks, B., Dubchak, I., Duplessis, S., Ehlting, J., Ellis, B., Gendler, K., Goodstein, D., Gribskov, M., Grimwood, J., Groover, A., Gunter, L., Hamberger, B., Heinze, B., Helariutta, Y., Henrissat, B., Holligan, D., Holt, R., Huang, W., Islam-Faridi, N., Jones, S., Jones-Rhoades, M., Jorgensen, R., Joshi, C., Kangasjarvi, J., Karlsson, J., Kelleher, C., Kirkpatrick, R., Kirst, M., Kohler, A., Kalluri, U., Larimer, F., Leebens-Mack, J., Leple, J.C., Locascio, P., Lou, Y., Lucas, S., Martin, F., Montanini, B., Napoli, C., Nelson, D.R., Nelson, C., Nieminen, K., Nilsson, O., Pereda, V., Peter, G., Philippe, R., Pilate, G., Poliakov, A., Razumovskaya, J., Richardson, P., Rinaldi, C., Ritland, K., Rouze, P., Ryaboy, D., Schmutz, J., Schrader, J., Segerman, B., Shin, H., Siddiqui, A., Sterky, F., Terry, A., Tsai, C.J., Uberbacher, E., Unneberg, P., Vahala, J., Wall, K., Wessler, S., Yang, G., Yin, T., Douglas, C., Marra, M., Sandberg, G., Van de Peer, Y., and Rokhsar, D. (2006). The genome of black cottonwood, Populus trichocarpa (Torr. & Gray). Science **313,** 1596-1604.

Tzfira, T., Weinthal, D., Marton, I., Zeevi, V., Zuker, A., and Vainstein, A. (2012). Genome modifications in plant cells by custom-made restriction enzymes. Plant Biotech J **10,** 373-389.

Urnov, F.D., Rebar, E.J., Holmes, M.C., Zhang, H.S., and Gregory, P.D. (2010). Genome editing with engineered zinc finger nucleases. Nature Rev Gene **11,** 636-646.

Van, K., and Spalding, M.H. (1999). Periplasmic carbonic anhydrase structural gene (*Cah1*) mutant in *Chlamydomonas reinhardtii*. Plant Physiol **120,** 757-764.

Van, K., Wang, Y., Nakamura, Y., and Spalding, M.H. (2001). Insertional mutants of *Chlamydomonas reinhardtii* that require elevated CO_2 for survival. Plant Physiol **127,** 607-614.

Vaughn, K.C., Campbell, E.O., Hasegawa, J., Owen, H.A., and Renzaglia, K.S. (1990). The pyrenoid is the site of ribulose 1,5-bisphosphate carboxylase/oxygenase accumulation in the hornwort (Bryophyta: Anthocerotae) chloroplast. Protoplasma **156,** 117-129.

Wang, Y., and Spalding, M.H. (2006). An inorganic carbon transport system responsible for acclimation specific to air levels of CO_2 in *Chlamydomonas reinhardtii*. Proc Natl Acad Sci U S A **103,** 10110-10115.

Wang, Y., and Spalding, M. (2007). LCIB functions in a multi-subunit complex essential for inorganic carbon transport in *Chlamydomonas reinhardtii*. Photosynthesis Res **91,** 221-222.

Warburg, O. (1919). The rate of photochemical decomposition of carbonic acid in living cells. Biochem. Z. **100,** 230-270.

Worden, A.Z., Lee, J.-H., Mock, T., Rouze, P., Simmons, M.P., Aerts, A.L., Allen, A.E., Cuvelier, M.L., Derelle, E., Everett, M.V., Foulon, E., Grimwood, J., Gundlach, H., Henrissat, B., Napoli, C., McDonald, S.M., Parker, M.S., Rombauts, S., Salamov, A., Von Dassow, P., Badger, J.H., Coutinho, P.M., Demir, E., Dubchak, I., Gentemann, C., Eikrem, W., Gready, J.E., John, U., Lanier, W., Lindquist, E.A., Lucas, S., Mayer, K.F.X., Moreau, H., Not, F., Otillar, R., Panaud, O., Pangilinan, J., Paulsen, I., Piegu, B., Poliakov, A., Robbens, S., Schmutz, J., Toulza, E., Wyss, T., Zelensky, A., Zhou, K., Armbrust, E.V., Bhattacharya, D., Goodenough, U.W., Van de Peer, Y., and Grigoriev, I.V. (2009). Green Evolution and Dynamic Adaptations Revealed by Genomes of the Marine Picoeukaryotes Micromonas. Science **324,** 268-272.

Xiang, Y., Zhang, J., and Weeks, D.P. (2001). The *Cia5* gene controls formation of the carbon concentrating mechanism in *Chlamydomonas reinhardtii*. Proc Natl Acad Sci USA **98,** 5341-5346.

Xu, P., Zhang, Y., Kang, L., Roossinck, M.J., and Mysore, K.S. (2006). Computational estimation and experimental verification of off-target silencing during posttranscriptional gene silencing in plants. Plant Physiol **142,** 429-440.

Yamano, T., and Fukuzawa, H. (2009). Carbon-concentrating mechanism in a green alga, *Chlamydomonas reinhardtii*, revealed by transcriptome analyses. J Basic Microbiol **49,** 42-51.

Yamano, T., Tsujikawa, T., Hatano, K., Ozawa, S., Takahashi, Y., and Fukuzawa, H. (2010). Light and Low-CO_2-Dependent LCIB-LCIC Complex Localization in the Chloroplast Supports the Carbon-Concentrating Mechanism in *Chlamydomonas reinhardtii*. Plant Cell Physiol **51,** 1453-1468.

Ying, Z., Mulligan, R.M., Janney, N., and Houtz, R.L. (1999). Rubisco small and large subunit N-methyltransferases. Bi- and mono-functional methyltransferases that methylate the small and large subunits of Rubisco. J Biol Chem **274,** 36750-36756.

Ynalvez, R.A. (2007). Isolation and Characterization of Two Closely Related Beta-Carbonic Anhydrases of *Chlamydomonas reinhardtii* In Biological Sciences (Baton Rouge: Louisiana State University).

Ynalvez, R.A., Xiao, Y., Ward, A.S., Cunnusamy, K., and Moroney, J.V. (2008). Identification and characterization of two closely related beta-carbonic anhydrases from *Chlamydomonas reinhardtii*. Physiol Plant **133,** 15-26.

Yoshioka, S., Taniguchi, F., Miura, K., Inoue, T., Yamano, T., and Fukuzawa, H. (2004). The novel Myb transcription factor LCR1 regulates the CO_2-responsive gene *Cah1*, encoding a periplasmic carbonic anhydrase in *Chlamydomonas reinhardtii*. Plant Cell **16,** 1466-1477.

Zhao, T., Wang, W., Bai, X., and Qi, Y. (2009). Gene silencing by artificial microRNAs in Chlamydomonas. Plant J **58,** 157-164.

APPENDIX I
C. REINHARDTII STRAINS USED IN THIS DISSERTATION

Strain	CC Number[a]	Reference	Genotype
D66	CC-4425	Schnell and Lefebvre (1993); Pollock et al. (2003)	$nit1^-$, $nit2^-$, cw15, mt^+
CC-124	CC-124		$agg1^-$, $nit1^-$, $nit2^-$, mt^-
2137	CC-3269	Spreitzer and Mets (1981)	mt^+
137^+			mt^+, $nit1^-$, $nit2^-$
CC-503	CC-503	Hyams and Davies (1972)	cw92, mt^+
C9	CC-408		mt^-
cia5	CC-2702	Moroney et al. (1989)	parental strain: 137
pgp1	CC-2648	Suzuki et al. (1990)	parental strain: 2137

a: Chlamydomonas Resource Center Number

APPENDIX II
LIST OF PRIMERS IN CHAPTER 4 – CHAPTER 6

CCP1	(F): CAAGATGCAGATGCAGCGCC (R): TGTCACGCAGGATGGTGGAG
CAH4-QRT	(F): TCTACTACAGCATCAGCCCG (R): ACGATCTTGAGCTTGCCCTCC
LCIB-QRT	(F): AGAAGTCCTGCAAGGTGCCC (R): TGACGGCGTAGTCGGCAAC
PGP1-QRT	(F): GCAGAGTGTGTATCGGGTGTCG (R): TGGCCTTTGCACGCTTAAACCA
PGP2-QRT	(F): TTTGTGTGGAGGCTGCGTCA (R): ACATGGTGCAACTTGTGGCGT
PGP3-QRT	(F): TCTTGTTGTAGCGGCTCAGCTT (R): ATCTACAAGGTGCTCAAGCAGGTG
CBLP-QRT	(F): ATTGCCATGCTGTGGGACC (R): CCACGATGCTCTTGCTCTCC
CAH1-QRT	(F): ACCCCGATGCCTACACCTG (R): CCTGGAAAATGGAATGCCTGCT
PGP1-check splice	(F): GTTCGCAGGATGGTTGCT (R): CAGGGACTGGAACTTGGA
CIA6 complementation	(F): GGGCGGGCAGACTGTTAACTGTA (R): CGGTTCAATACTCGCAGCTC
CIA6 Overexpression	(F): CGCGGATCCATGGCTGAC (R): CCCAAGCTTCTACTTTCGCCC

APPENDIX III
PCR BASED MUTAGENESIS SCREEN PROTOCOL

A. Mutagenesis

Insertional mutagenesis was achieved by transforming the *AphVIII* cassette that confers paromomycin resistance into *C. reinhardtii* D66 cells. Electroporation was performed as described previously with a few modifications (Shimogawara et al., 1998).

1). Before starting:

a). Material preparations:

- Each step should be performed under sterile conditions.
- Start a D66 culture on a YA plate to eliminate any possible contamination at an early stage. Start a liquid culture in TAP using the culture from the YA plate as an inoculation.
- Autoclave 500mL Nalgene centrifuge bottles and 4X 500mL 60mM TAP-sorbitol.
- Prepare TAP plates containing Paromomycin antibiotic (final concentration: 5µg/mL). Agar concentration could be 1-1.2% (w/v). Use 100-mm size plates for the initial transformant screen. Use 150-mm size plates for everything else.
- 10mL aliquots of 60mM TAP-sorbitol can be prepared in bulk in 15mL conical tubes and stored at 4 ℃.
- 10µL pipet tips could be used for colony picking in place of tooth picks.
- The electroporation cuvette holder should be stored at -20 ℃ to ensure cooling (make sure to wipe off any condensation on the holder before electroporation).

- Soak electroporation cuvettes in 75% ethanol the night before electroporation. On the day of electroporation, arrange all cuvettes in a rack with lids open. Place the rack in a hood with UV lights on to completely sterilize the cuvettes and the working area.
- A no DNA control is always needed during electroporation.

b). Preparation of the DNA insert:

1. Harvest 200mL *E.coli* culture (DH5α) containing pSL18, and perform a plasmid prep (See the "home-made midi-prep" at the end of this Appendix).
2. Digest the pSL18 plasmid using KpnI-HF and XhoI-HF to obtain only the 1813bp AphVIII cassette, which consists of the *Hsp70+RbcSII* dual promoter, the *AphVIII* ORF, and the *RbcSII* terminator.
3. Separate the *AphVIII* cassette from the rest of the plasmid by gel electrophoresis. Purify the *AphVIII* cassette band using a gel extraction kit (Qiagen, Chatsworth, CA).
4. Quantify the amount of *AphVIII* cassette DNA by gel electrophoresis.

2). To start:

1. Inoculate a portion of the previously TAP grown D66 into a 1.5L minimum medium bubbled with high CO_2 under 80 $\mu E \cdot m^{-2} \cdot sec$ continuous light. The rest of the TAP grown D66 can be maintained as a continuous culture by adding fresh TAP medium.
2. When the D66 grown in minimum medium reaches early log-phase (1.2-1.8x10^6cell/mL), switch high CO_2 to low CO_2 (100-200 ppm) for 4 hours.
3. On the day of electroporation, harvest cells by centrifugation at 3,000 rpm at 4℃ in the autoclaved 500mL Nalgene centrifuge bottles for 10 minutes. Resuspend cell pellets first by adding 2mL of 60mM TAP-sorbitol, followed by transferring into a 50mL conical tube. Count the cell number using a hemocytometer (proper dilution is

needed). Based on the cell number, further dilute the cell suspension to a final cell density of $2x10^8$ cells/mL by adding the proper amount of TAP-sorbitol.

4. Arrange all electroporation cuvettes in a rack. In each cuvette, pipet 300 µL of diluted cells and 1-5 µg DNA. Chill in a 15 ℃ water bath 5-15 minutes. Before electroporation, transfer the rack to icy water.
5. Electroporation (Biorad,GenePulserII) :

   Immediately before electroporation, wipe off any condensation on the cuvette.

   Capacitance: 25 µF Pulse Control: ∝ Shunt Resistor: None

   Voltage: 0.8kV =2000V/cm, in a 0.4cm cuvette (red capped).

   Immediately after electroporation, put back each cuvette into the icy water.

   Record the time, best results are achieved between 9 and 13 msec.
6. Place all cuvettes in 15 ℃ water bath for a 10-15 minutes recovery period.
7. Transfer all cells of each cuvette by pipetting into pre-aliquoted tubes containing 10mL TAP-sorbitol.
8. Place all tubes on a shaker with gentle horizontal movement. Recover overnight (not more than 12 hours) in darkness.
9. The next day, centrifuge cells at 3,000 rpm for 5 minutes and carefully pour off the medium. Resuspend pellet in the remaining medium and spread the suspension onto TAP-paro plates (100mm). Whenever the liquid soaks into the medium, invert the plates. Let grow under 50 $\mu E \cdot m^{-2} \cdot sec$ illumination.
10. Allow 5-7 days for positive colonies to appear.
11. Transfer 180 colonies onto a 150mm TAP-paro plate. A careful log should be maintained to indicate different batches of transformation on one plate. (In case you

isolated two mutants in the same gene, in the same position, if you the two mutants are from the same batch of transformation, these two mutants are probably two progenies from one mutant. If not, there are probably two independent hits. Under any circumstances, logs are always helpful.)

B. Culture Maintenance

1). Type of medium used

a) TAP-Paro plates are used for maintaining the transformants.

b) TAP-carbendazim (70μg/mL) plates were used in the later stage when fungal contamination caused problems. However, TAP-carbendazim plates are recommended for future experiments since no harmful effect on *C. reinhardtii* growth were observed on TAP-carbendazim plates and most of the fungus contaminations could be eliminated.

c) TAP slants could also be prepared in bulk to serve as back-ups for TAP plates. (see below)

d) Minimum plates are used for colony sick-on-low CO_2 phenotype screens. It is recommended to incorporate the fungicide into the medium since it was observed that the minimum medium is more prone to fungal contamination.

2). Culture maintenance

a) Culture plates could be parafilmed and stored in the 4℃ cold room for not longer than a month. However, this should be tested again by putting a plate in the cold for a month and transfer to room temperature.

b) After moving plates from the cold room, plates are recommended to stay in dim light for a day or two before moving to bright light.

c) After a dim light recovery, colonies from the old plates need to be transferred to fresh plates immediately.

C. DNA Preparation

1). Culture growth

a) To start a culture, pour 5-10mL of TAP medium onto the plate containing 180 well grown (nice juicy) colonies. Scrape off all 180 colonies from the plate using a bent pasteur pipet. Pour the scraped cells into a flask containing 100mL TAP medium.

b) After 2-3 days of growth on a shaker under continuous illumination, harvest cells in 50-mL tubes by centrifugation at 3,000 rpm, 4℃ for 10 minutes. Pour off the supernatant and immediately freeze the pellet at -20℃.

2). DNA extraction

We followed Dr. Snell's protocol (personal communication) with a few modifications (all the water used here was autoclaved MiliQ water).

a) Vigorously resuspend the cell pellet in 5mL water, transfer to a new centrifuge tube (Nalgene #3119-0050). Add 5mL 2x Lysis buffer (100mM Tris-Cl: pH 7.5, 300mM NaCl, 30mM EDTA, pH8.0, 4% SDS, 80μg/ml Proteinase K (NEB #P8102S, freshly add before DNA isolation))and stir at Speed 5 on the Orbital Shaker immediately for 30 minutes.

b) In the fume hood: add 10 ml Phenol-chloroform(1:1), mix well, centrifuge at 20,000g for 10 min at 4℃ in a fixed-angle rotor (JA20). Once centrifugation is done,

immediately take supernatant (~ 8mL) to a new centrifuge tube (Nalgene #3119-0050), be careful, don't disturb the interface.

c) Add 9 mL 100% isopropanol to the supernatant at room temperature, centrifuge at 20,000g for 15 minutes, 4 ℃ in a fixed-angle rotor. Discard the supernatant solution.

d) Resuspend the pellet in 500µL water with 100µg RNase A. Incubate at room temperature for 2 hours.

e) Transfer to a new 2mL Eppendorf tube, then add 500 µL Phenol-chloroform(1:1), mix well, centrifuge at 20,000g for 10 minutes at 4 ℃ in a fixed-angle rotor. Take the supernatant to a new 2mL Eppendorf tube, with 500µl 100% isopropanol at room temperature, centrifuge at 20,000g for 15 minutes, 4 ℃ in a fixed-angle rotor. Discard the supernatant solution.

f) Wash the pellet once with 1mL 80% ethanol, centrifuge at 13,000rpm for 5 minutes in a bench-top centrifuge. Remove the supernatant completely by careful aspiration. Dry the pellet for approximately 20 minutes in the hood till the edge of the DNA pellet turns transparent.

g) Into the pellet add 300µL water and let the pellet rehydrate for 30 minutes. Add 1mL isopropanol, 30µL 3M NaAC (pH=5.5). Incubate the tube at -20 ℃ overnight.

h) Next day centrifuge the tube at 13,000rpm at 4 ℃ for 30 minutes.

i) Aspire the supernatant carefully. Wash the pellet twice with 80% ethanol. Remove the supernatant completely by careful aspiration. Dry the pellet for around 20 minutes in the hood till the edge of the DNA pellet turns transparent.

j) Add 300µL water and let it rehydrate for 30 minutes. Aliquot the DNA solution in desired amount, and store at -20 ℃.

k) All DNA prepared should be checked by gel electrophoresis, and especially by PCR amplifying a control gene to ensure the DNA quality.

l) For the purpose of the PCR screen, combine 5 individual DNA preparations together. For example, pipet 150μL from each single DNA tube to make a final 750μL DNA pool. Aliquot the 750μL DNA pool into 6 tubes with 100μL each. (A careful log is needed for the DNA quality check, as well as for the pooling of single DNAs).

D. PCR Screen

A PCR based reverse genetics screen is used to identify mutants with a lesion in specific genes possibly involved in CCM. Briefly, potential CCM genes were selected based on previous knowledge and bioinformatics data. Primers were designed, and PCRs screens using a primer mix were performed on DNA pools. PCR signals were verified by sequencing, and were further pursued to identify the single colony with the *AphIII* cassette insertion

1). Gene Selection

See Chapter 7 for details for this section. For a list of genes selected, see Table 7.2.

2). Primer Design

Essentially, for one specific gene, two directions of primers were designed along the locus approximately 1kb from each other. The guiding rule for primer design follows the Gonzalez-Ballester (Gonzalez-Ballester et al., 2011) paper with a few modifications:

a. The first forward primer (F1) is positioned 20-200bp upstream the 5'UTR region.

b. The first reverse primer (R1) is positioned 20-200bp downstream of the 3'UTR region (In some cases where a gene has an extra-long 3'UTR, R1 is positioned within the 3'UTR).
c. Repeat regions within a gene (eg. CAH8) are avoided for primer designs.
d. Primers were designed using IDT Oligo Analyzer (http://www.idtdna.com/analyzer/Applications/OligoAnalyzer/). All the primers were designed to have close Tm (60.0±0.8℃) and low self-dimer ΔG (-4.63±-1.38kcal/mole).
e. The sequences of all the primers are listed in Appendix V.

3). PCR

OneTaq (NEB, #M0480X) was used as the DNA polymerase for the initial PCR screen. For one gene, all the forward primers were combined together (designated as "F") and all the reverse primers were combined together (designated as "R"). For each gene, two PCRs were performed: F+RB1 and R+RB1.

a). PCR Controls

Before running PCR on pooled DNA (containing 900 colonies), a few control PCRs were performed (See below). For the detailed PCR conditions used here are summarized in Protocol-PCR A at the end of this appendix.

a. The primers for all 71 genes were first checked by PCR to test the functionality of all primers using wild-type DNA.
b. The PCR background was checked by using F+ RB1, R +RB1, without DNA.

c. The sensitivity of PCR using pooled DNA was checked by diluting one single wild-type DNA in water to mimic the pooling effect.

d. All the above PCR controls would not be necessary if future experiments are done using the same set of 71 genes and primers.

b). PCR Screen

The actual PCR screens were performed following the guidelines below. Protocol-PCR B gives the detailed information.

a. Multiple pools could be screened in parallel, which helps to focus on the unique signal present in a pool with a potential positive PCR band.

b. For every 20μL PCR reaction, 0.2μL RB1 is used. The amount for primer mix (for example, F) equals to the N fold of 0.2 μL, in which N means the number of forward primers in this gene.

c. When the unique signals were detected with RB1, those PCR reactions were repeated with RB2 replacing RB1.

d. Any signal that could be reproduced by RB2 was pursued further using individual primers to identify which single primer within the primer mix yielded the signal. This step PCR was done with RB1.

e. Any signals that could be tracked back to individual primers were further pursued using the five individual plate DNAs (containing 180 colonies) to identify which plate within the pool DNA yielded the signal. This step PCR was done with RB1.

f. Any signals that could be tracked back to individual primers and individual plate DNA were sequenced.

c). Sequencing

The goal of this stage was to validate any positive PCR signal by sequencing to see whether it is gene specific.

a. Positive signals that could be identified with gene specific individual primer in individual plate DNA were re-amplified.
b. Single bands were gel extracted and purified according to manufacturer's protocol (Qiagen, Chatsworth, CA).
c. Purified DNA are quantified by gel electrophoresis
d. Sequencing reactions were performed at Macrogen (Rockville, MD), with RB1 as the sequencing primer.
e. Sequencing results were compared to the *C. reinhardtii* genome using BlastN, and the genes with the *AphVIII* insertion were verified.

d). Identifying Single Colonies

The goal of this stage was to identify the single colony that has the *AphVIII* insertion from the previously determined 180-colony-plate.

a. Every 10 colonies (designated as "10-pool") were inoculated together in a 0.5mL tube with 50-150 μL 10mM Na-EDTA.
b. Centrifuge the cultures in a bench-top centrifuge at 13,000 rpm, for 2 minutes at room temperature. Carefully aspirate the supernatant.
c. Add 50-100μL 10mM Na-EDTA. Homogenize by either pipetting or vortexing.
d. Incubate at 100 ℃ for 5 minutes.

e. Vortex to mix. Centrifuge at 13,000 rpm for 3 minutes in a bench-top microcentrifuge. Transfer the supernatant (containing the DNA) into a fresh 500μL tube. Take 0.4-0.8 μL for PCR. (See PCR protocol C)

f. Using the method above, the positive PCR signal should be identified from one out of the 18 tubes.

g. From the identified 10-pool, DNA from the 10 individual colonies are extracted by simply resuspending a paste of each single colony from the plate into 50 μL 10mM Na-EDTA, followed by boiling and centrifuge action as above.

h. The single colony is then streaked onto a TAP plate to isolate single isolates. Five random isolates from the positive colony were then checked using PCR to ensure were the homogeneity of this mutant.

E. Other Protocols

1). Home-made plasmid midi-prep

Solution I

per 500mL	Stock	Final Conc.
25mL	1M Tris-HCl	50mM
10mL	0.5M EDTA	10mM

Add 10uL RNase (30ug/uL) for every 10mL Solution I

Solution II

per 100mL	Stock	Final Conc.
2mL	10M NaOH	200mM
10mL	10% SDS	1%

Solution III

per 200mL		Final Conc.
58.88g	Potassium Acetate	3M
Adjust pH to 5.5 with about 22 mL glacial acetic acid		

1) 200mL overnight culture, spin down.
2) Wash the pellet with 20mL Solution I w/o RNase.
3) Resuspend the pellet in 3mL Solution I w/RNase.
4) Add 6mL Solution II. Incubate at RT for 5 min.
5) Add 4mL Solution III. Incubate on ice for 10 min.
6) Centrifuge at >20,000g for 30min at 4C;
7) Add 26mL ethanol. Mix and centrifuge at> 15,000g for 30min at 4 ℃.
8) Resuspend in 400uL TE. Load on gel check yield. (~50ng/μL. Total yield=20μg)
9) Run through PCR-purification column* according to the manufacture's instruction (Qiagen, Chatsworth, CA) to clean up gDNA and protein.

    *Only apply to plasmid smaller than 10-kb.

    *Maximum capacity of the column is 10μg.

2). PCR Protocols (OneTaq)

PCR A: Initial PCR primer checks

Ingredient	Final Conc.	1X
ddH_2O		10.3µL
PCR Buffer [5x]	1x	4µL
Enhancer	20%	4µL
dNTPs [10mM]	200µM ea.	0.4µL
Gene Primer [20µM]	0.2µM	0.2µL
RB1 [20µM]	0.2µM	0.2µL
OneTaq [5U/µL]	2.5U	0.5µL
DNA	20-200ng	0.4µL
Total		20µL

94°C 1 min
94°C 30 sec
60°C 30 sec
68°C 1 min
} 30-40 Cycles
68°C 5 min
4°C ∞

PCR B: Actual Screening PCR

Ingredient	Final Conc.	1X
ddH_2O		
PCR Buffer [5x]	1x	4µL
Enhancer	20%	4µL
dNTPs [10mM]	200µM ea.	0.4µL
Gene Primer [20µM]	.2µM	0.2µL
RB1 [20µM]	.2µM	0.2NµL
OneTaq [5U/µL]	2.5U	0.5µL
DNA	20-200ng	0.4µL
Total		20µL

94°C 1 min
94°C 30 sec
60°C 30 sec
68°C 3 min
} 40 Cycles
68°C 5 min
4°C ∞

PCR C: Identifying Single Colony

Ingredient	Final Conc.	1X
ddH_2O		10.3µL
GC Buffer [5x]	1x	4µL
dNTPs [10mM]	200µM ea.	0.4µL
Gene Primer [20µM]	.2µM	0.2µL
RB1 [20µM]	.2µM	0.2µL
DMSO	10%	2µL
Phusion [2U/µL]	0.4U	0.2µL
DNA	20-200ng	0.4µL
Total		20µL

98°C 1 min
98°C 30 sec
61°C 30 sec
72°C 2 min
} 35-40 Cycles
72°C 5 min
4°C ∞

APPENDIX IV
A SUMMARY OF THE MUTANTS IDENTIFIED UNDER DIFFERENT CO_2 GROWTH CONDITIONS

A

	Low CO_2	High CO_2	Ambient CO_2
Plate #1	15	0	0
Plate #2	14	0	0
Plate #3	8	1	0
Total	37	1	0

B

Minimum-Plate 1			Minimum-Plate 2			Minimum-Plate 3		
Clone #	Original plate		Clone #	Original plate		Clone #	Original plate	
	Plate #	Clone #		Plate #	Clone #		Plate #	Clone #
26	28	13	13	71	156	67	152	20
28	31	89	41	99	128	4	137	130
30	33	116	51	100	171	6	138	57
44	37	145	52	102	16	7	138	68
65	42/43	71	57	102	144	12	138	177
66	42/43	100	67	105	156	25	141	162
67	42/43	101	68	106	21	27	143	48
93	50	33	70	106	61	38	146	65
104	52	127	71	106	78	46	147	99
117	55	70	87	109	34			
118	55	158	97	113	18			
129	59	21	112	115	85			
130	59	32	134	120	165			
165	64	13	153	128	19			
176	66	162	154	128	37			
178	67	92						

During the initial sick on low CO_2 phenotype screening, nearly 522 colonies out of 22,000 transformants were selected to have the possible phenotype, maintained on three 180-colony plates. (A): After the second round of phenotype screening under low CO_2 on minimum medium, a total of 37 colonies showed the definite sick on low CO_2 phenotype, with fifteen colonies from Plate #1, fourteen from Plate #2 and eight from Plate #3. (B): This list showed the detailed origins of the colonies showing a sick on low CO_2 phenotype with a few exceptions. Clone #165 had a reduced growth in the presence all levels of CO_2 even on a TAP plate (Highlighted with a red square). Clone #134 had a reduced growth under both high and low CO_2 when grown on a minimum plate (Highlighted with a .blue square). Clone #67 is the colony that showed a reduced phenotype under high CO_2 condition (Highlighted with a .green square). The colonies in grey font were not maintained due to contaminations.

APPENDIX V
LIST OF PRIMERS IN CHAPTER 7

NAR1.6	NAR1.6 mut_scr F1[(a)]	CAGCGGAAGGCATTGATGTCCT
	NAR1.6 mut_scr F2	TGTTCCGTTTGTTCATCACGCCC
	NAR1.6 mut_scr F3	ATGCGTGGCTGAGAGGTTGATT
	NAR1.6 mut_scr F4	ATGTACGCATGTGGTGGTGACTGT
	NAR1.6 mut_scr R1	TGGGCGGGTTTGTGGAAATTGT
	NAR1.6 mut_scr R2	GTGCTCTTGCCTCCATTACGCATT
	NAR1.6 mut_scr R3	TGATGTCACCAATGAACTTGCCCG
	NAR1.6 mut_scr R4	TACACCCACAAACTTGCCCGTGA
	NAR1.6 mut_scr R5	GAAAGCAAACGCCATGCCGAATGA
CGL41	CGL41-F1	CCCATTCAGGTGCACAGCTTGT
	CGL41-F2	TCCTTTCTTCCGTTGCGTGCCT
	CGL41-F3	TGGTGTGTTGTCATGCAGCCG
	CGL41-F4	TGGGTGAAATCATGTCGCCGTG
	CGL41-R1	ACG AAG CTG AGG ACG ACC ACA T
	CGL41-R2	CGG CGT CAT ACC AAC GCA TGT T
	CGL41-R3	TGC TAC ACG CAC CAG CCA AT
	CGL41-R4	AGT CCC GAA ACA GTC GTC GGT A
466.c ABCt (511332)	ABCt mut_scr F1	CGCTTGAAATTCTGTGATTGCATTTCGC
	ABCt mut_scr F2	TTCTGACGGCATTCCTTCTGGGTT
	ABCt mut_scr F3	AAGGGTAAGCTGCTGCTGGAGAA
	ABCt mut_scr F4	GGCAAAGCTGGTGACTGAGATGGG
	ABCt mut_scr F5	GCTGTCGAGGTGGGAGTTTAGAGA
	ABCt mut_scr F6	ATGGGCATGGGCACGGTGG
	ABCt mut_scr F7	ACATGCTGTGCCTAATGTTGTGCC
	ABCt mut_scr F8	TCTCTCTGAGCCAAGCCAATCCAA
	ABCt mut_scr R1	TTCTGTTTAGTGGTGAGGGCATGG
	ABCt mut_scr R2	ATCGGTTGGAATGACGGTGTTCGT
	ABCt mut_scr R3	TCAGAGAGACAGTGGTGACGAGGT
	ABCt mut_scr R4	AGCGAATGGTCATCATCACACAGC
	ABCt mut_scr R5	TAGCAGTTACCTTGTTGACCTCGC
	ABCt mut_scr R6	TCCATGAGGTCCTTCTCCTCGG
	ABCt mut_scr R7	CCACCACACCATGCTGTGCG
	ABCt mut_scr R8	CAAACTCCTCCTCCTCCTCGCTG

PAS(510 680)	PAS mut_scr F1	CATTTGATTTGGGTGCGAACGGA
	PAS mut_scr F2	GTTACCTGAATGGTGTTGGCTGCT
	PAS mut_scr F3	TATTTCAGCCCAGCAAGAAAGCCG
	PAS mut_scr F4	TGATCTTGATGTGTCGCCCGTG
	PAS mut_scr F5	TAAGCCCGTCTGTCGTTCCCTTC
	PAS mut_scr F6	TGTTTGGCTGGCGGCTTAGT
	PAS mut_scr F7	GGCAAAGACCGACCTCCATTCAT
	PAS mut_scr F8	GCAGCGTTTGTTGTCAGGTTCAATGG
	PAS mut_scr F9	TCAAGACCAAGCAGAAGGATGTGG
	PAS mut_scr F10	AGATGATGATGACAAGGCGGACAG
	PAS mut_scr F11	TGGCTTGCATGTGTGTTTGCATG
	PAS mut_scr F12	TCTCCATGCCCATGACGATGTG
	PAS mut_scr F13	ACATTCCTGGTCATACCCGTGGTG
	PAS mut_scr F14	TTCTTATGTGCCCACGACCTCCG
	PAS mut_scr F15	AACGCACTAAACCACTCGCACAAC
	PAS mut_scr F16	TAGAACGTGGGCTACAAGGTACGG
	PAS mut_scr R1	CCCTGATAAGAATTGAGGAACCGAGG
	PAS mut_scr R2	TACCTTAGTCATCGGTTGTAGCCG
	PAS mut_scr R3	ATGACCCACAGCATCAGGAACAGG
	PAS mut_scr R4	TCGCTGCTGACGTAGCTCACC
	PAS mut_scr R5	AACAGTCAACTCACCCGCATCTCA
	PAS mut_scr R6	ACGGAACACCAACGCACTACATCT
	PAS mut_scr R7	CACACCGCAGTATAGCATCAGGTCA
	PAS mut_scr R8	ACAGAGTTGGCAGGGTCTTGTTCT
	PAS mut_scr R9	TTGATCTCGTTGTGCTGTCTTGCG
	PAS mut_scr R10	TTGCCGTCAGTGTGGGTAGC
	PAS mut_scr R11	TCCATGTGCTCCATTAGCGAACGA
	PAS mut_scr R12	TCTCACCTCTTGACTGTGTCGCT
	PAS mut_scr R13	TCCTCTCCAGAAACTTGCCGTACA
	PAS mut_scr R14	TAAAGGCACACGCACATACACACC
	PAS mut_scr R15	CAGCAATAACGCACCTCTGCCATA
	PAS mut_scr R16	ACGGAGCGTTTATGAGTGAGGTAC
HLA3	HLA3 mut_scr F1	GCATTTCGTGTCAACACCAAGCCT
	HLA3 mut_scr F2	TTGCTTGTGGCTTCTCATGCTCAC
	HLA3 mut_scr F3	ATGTGGTTGTTTAGAGGCTTGGCG
	HLA3 mut_scr F4	CCATCCTCGGCAACATGGTCAA
	HLA3 mut_scr F5	GTGGGTGAACGACGAGTACAAGAA
	HLA3 mut_scr F6	ATGCTTGTGTTCTACACCTGGGTG

	HLA3 mut_scr R1	AGCCACAGCACAGCAAGCATTAAG
	HLA3 mut_scr R2	CATCACTTTCGCTCCACTCCACTCA
	HLA3 mut_scr R3	GCTCACCTTGAACTCGCCGAAG
	HLA3 mut_scr R4	GTTGATGGTGACGGACACGGTG
	HLA3 mut_scr R5	CTCGTTCCACTTGCCGAAGTACAG
	HLA3 mut_scr R6	CACCTCCTCCAGCAGGTAGGC
	HLA3 mut_scr R7	TGGGATGGAAGGATAGGTGGCTAT
519635 (LCI9)	519635-F1	TCAGAGTGAAGTGCCCAAAGCC
	519635-F2	ACGCCCTTCTAATGTCCTGCCT
	519635-F3	TGCTGCTTGTGGACACACCA
	519635-F4	TGACACCGCAACAACTGAACCC
	519635-F5	TGCGACTGACACTCCCAGACTT
	519635-F6	TCACCAAGAAGGAGGCGATGGA
	519635-F7	AGGCGGCTCCTGGTGGATATT
	519635-F8	TTGCGGCTTGACCAACTCCT
	519635-R1	AGT GCC ACT GTT GGT CCC G
	519635-R2	GCA CAC CGT CAC ACG CAA AGT T
	519635-R3	GGT CGC TTC CGT TGC CGA TTT A
	519635-R4	AGG TGA ACC ATC TCA AAG CGG C
	519635-R5	ACG CAG CAG AGG AGT GGA AGT
	519635-R6	GGG TTC AGT TGT TGC GGT GTC A
	519635-R7	CCT GGG AAT CTG TCA TGG CGA A
	519635-R8	TAG TTG GCG GAA TCA GGG CAA G
519637	519637-F1	GATATGGCAAATGGGTTGGCGG
	519637-F2	CCCCTTCATGTTCTCGGCTCTCT
	519637-F3	GCCTCGCTCAACAGCATGG
	519637-F4	ATCTTCGTGTGCCGCTGGA
	519637-F5	AGTCTGTCCACGCTTTGCTGT
	519637-F6	TCCTTCGCATGAAGTGTGGACG
	519637-R1	TGT GTG TTA AGG AAG AGG GCT GC
	519637-R2	ACA AAC TCC GTC TCC CGC TC
	519637-R3	TCA CAA CCC GCT TCC ACT GTC T
	519637-R4	GAA CTC GCA CAA CAA CGC TCC T
	519637-R5	TTA GCA ATC CAC TCC TGC CAC G
	519637-R6	GGC AAC ATA ACT GCG AGG GTG A
LCR1	LCR1-F1	GTCCATCCTTCATCGGGCAGTC
	LCR1-F2	ACAACCTGGTCTACGCCTACGC
	LCR1-F3	AGCAGCAGCACCACCTCAT

	LCR1-F4	ACCAGCAGGATCACCAGCTTCT
	LCR1-F5	GTGAAGGTGCAAACGGCACGAA
	LCR1-R1	GCT GCT CTG AGC CCA ATG TGA C
	LCR1-R2	ATG TGG AGT TTG CAT GGT GGC G
	LCR1-R3	TGA GCC CTG GAC GTG GTG
	LCR1-R4	ACT GAC ACA CTG CTA CTG CGG
	LCR1-R5	ACT GGG CGT CCT AGC GGT ATA T
LCI1	LCI1 mut_scr F1	CGCATCCGCAAATCCACACACAAA
	LCI1 mut_scr F2	GCAGCGAAAATGTGACCAGGACG
	LCI1 mut_scr F3	CATCGCCACCGCTCAGGTAC
	LCI1 mut_scr R1	AGCATGTGAGTGCCAGAGGTAAGT
	LCI1 mut_scr R2	CATTGCCCATTTGTGCCCTGTCA
	LCI1 mut_scr R3	ACCGTGAAGACCTCCTTGTAAACG
PGP1	PGP1-F1' [b]	TGGCAGTTCCTTAGTGACCGCT
	PGP1-F2	TGGCGGTGGTAGGGTGAAGGT
	PGP1-F3	ACCAGACCCATGTCGGACAC
	PGP1-F4	TGTGTGCGACCGTGTGTGAG
	PGP1-F5	GTGTGGTGTGCGTGTGTCAGTG
	PGP1-F6	CCGACCTGTTGTCCGTCAAGGA
	PGP1-F7	TCAGCACTACCTGCGTCTCTTG
	PGP1-R1	AAG CCG ACG TGA CAA GGC TG
	PGP1-R2	CAC AGC ACC ACC CTC ACA CAA G
	PGP1-R3	GAT GTG CCC TGT CGA AGG ATG G
	PGP1-R4	GGG TCT TTG CCG TGA CTT CAG G
	PGP1-R5	TGG TGC TGT CGG ACA CGT CT
	PGP1-R6	CGT GCG ACA CAC ACA CAC ACA C
	PGP1-R7	GCA CAG AGC AGC ATC GGG AT
GYX1	GYX1 mut_scr F1	ATCAAGCTCCAGTCGAGACGGAAA
	GYX1 mut_scr F2	AGGCATCCGCTCCTCCAT
	GYX1 mut_scr F3	ATGAAGTTGTTCACGTCAGGTGCG
	GYX1 mut_scr R1	TACCTGCTTGTCAGGGTTTCCC
	GYX1 mut_scr R2	ACCTGAGTGTCATGGAGCTGTGTT
	GYX1 mut_scr R3	AACGAGAGAACACTTCGCCACCA
	GYX1 mut_scr R4	ACTCAAGCACTGAAGGCTCACAGA
520458	520458-F1	CAACGACCCAACCGTCGC
	520458-F2	AGCCCTTCCAACCCTTCCAA
	520458-F3	TCTGACTCTGGCGGCGTTC
	520458-F4	GTGCCTTCCGCCTGTGTCA

	520458-F5	TCGTGTCCATCCTCCTCGTACA
	520458-R1	CGG TCA CAG CAT TCC AAC GCA T
	520458-R2	GTG CGT CAT GTG GTC GTC CA
	520458-R3	CCC CAC CCT CTA CAT CCG TAC A
	520458-R4	CCG CAA ACT TCA GCC CGA TGA T
	520458-R5	GCT GTG TCC AAG CAC TTT GTA GCA
521673	521673 mut_scr F1	TGCTGCTTTCGGTTCGGTTGTC
	521673 mut_scr F2	AGTCCTTCTGGTGGGTGCC
	521673 mut_scr F3	TGGGCAGGATCAGGAGCAGA
	521673 mut_scr F4	AGCAGCATCCCTCTTCACAGCA
	521673 mut_scr F5	TCGCCTACCTCCGTGACCA
	521673 mut_scr F6	TCGCCTACCTCCGTGACCA
	521673 mut_scr F7	CGGGTGCTTGTTGTCGGT
	521673 mut_scr F8	TGTCTGTACGGTGTCGCAGC
	521673 mut_scr F9	TCCTGATGGCGGCAGTACA
	521673 mut_scr R1	TCTTCAAAGGTCCACAGGTGCC
	521673 mut_scr R2	TCAGAGAGCATCCCGTTCACACA
	521673 mut_scr R3	GAAGAACTTGTCCGCCTCCCATT
	521673 mut_scr R4	GTTGCTGCTGTGGCGTTTGC
	521673 mut_scr R5	GCTCCTGCTGCTGCTGTTG
	521673 mut_scr R6	TGTGGTCAACTATGTCAACACGTTGC
	521673 mut_scr R7	TGAGACCACATAAGCACACGCCA
	521673 mut_scr R8	GCCGAGATGTTGAAATGCCGACAA
NAR1.3	NAR1.3 mut_scr F1	CGGTATTAGGTGATGGGCGTTCG
	NAR1.3 mut_scr F2	ACATCGTGGCTACGGGTGAGTT
	NAR1.3 mut_scr F3	GTGCTGGCGGGTTTCTACATCT
	NAR1.3 mut_scr F4	GCGGATCTGTTCACAAGCAGC
	NAR1.3 mut_scr F5	GTGACGGGTGAGAGCGTGAG
	NAR1.3 mut_scr F6	ACCATCGGCAACATCATCGGC
	NAR1.3 mut_scr F7	CGCCACACACCTCTCTCTTACACTC
	NAR1.3 mut_scr R1	TCCGCAAATCTCACGGCATGTG
	NAR1.3 mut_scr R2	ACTGGTTGTGTACTCGCAGCAT
	NAR1.3 mut_scr R3	ACACTGCTGGGAGTCGCTCT
	NAR1.3 mut_scr R4	TCACTTCTCGTACACGGCTGTG
	NAR1.3 mut_scr R5	GGCACCCAGTTGTCACGAATGA
	NAR1.3 mut_scr R6	AAATGATGCCCTGTGCGTGC
	NAR1.3 mut_scr R7	GCCTGCTTGGCAATGACACGA
	NAR1.3 mut_scr R8	CATTCCTGCACCTGCTTCGACA

THB4	THB4 mut_scr F1	TTGGGAACTGCTGAGAGACTGTTG
	THB4 mut_scr F2	CTTACGCACGCACATCCTGTTT
	THB4 mut_scr F3	GCTCAATCTGACGCACTTCGACAA
	THB4 mut_scr R1	AATGGGTTCAAGTCAAGCACAGCC
	THB4 mut_scr R2	GCCGTGTTGCCAATTTGCCATG
	THB4 mut_scr R3	TTGCCCAGTACAATGCGAACAGG
	THB4 mut_scr R4	GTTCTGCTTGGCGATGAGCGTTAC
THB3	THB3-F1	GGGTATGTGGGATGTAGAGCGT
	THB3-F2	TGAGCGTTGTGGACGTGTTCAC
	THB3-F3	ACATGGTGAGTGGAAGCGTGG
	THB3-F4	GCTGCCTCGTATACCACTCGAAC
	THB3-F5	TGAGGTGTGAGTCAACGCAGGA
	THB3-F6	CTTGGGAACGGTGAGCAGAGT
	THB3-R1	GTC AGA GCT TTC AGA TGG GCG T
	THB3-R2	CAT AGA CCC ATA GCC GAA CAG CC
	THB3-R3	CTG CTA TCG ACC GCA CTA CAG AG
	THB3-R4	GGG TTA TGT GCC CAT GCC CA
	THB3-R5	TCC CAA CTC CCA ATG CCC AAC
	THB3-R6	GCA ACA AAC ACG GCG TTC CA
CCP2	CCP2 mut_scr F1	TACGAGACCTCCTACAATGCCGAG
	CCP2 mut_scr F2	CGATGGATTGCGTCCGTAAGATGA
	CCP2 mut_scr F3	GCAGAGAGAATGGGCGTAGCA
	CCP2 mut_scr R1	GTGTCCCACCAAACTCCTCCATTT
	CCP2 mut_scr R2	CGTTCTCCTCGTACCACTTGATGC
	CCP2 mut_scr R3	GGCAGGTTTGGTTTCAGCAAAGG
LCID	LCID mut_scr F1	CTCGGCATTGTAGGAGGTCTCG
	LCID mut_scr F2	GCTGCTGTCTAATGCTGCCC
	LCID mut_scr F3	CGCAGGACCTGGAGTACCTGATC
	LCID mut_scr R1	AGACTTGACCACAACAATGCGTGC
	LCID mut_scr R2	TACTGGGTGCAAGCTAATGCAACG
	LCID mut_scr R3	AAAGCATTGCCAAGCGAAGCGTCT
	LCID mut_scr R4	TGGCTGGGTCAGTAATGGAAGGAA
CAH1	CAH1-F1	TCCACACCCTGCGTTGAGTCAT
	CAH1-F2	AGGGTTCCAAGATTGCCAACGG
	CAH1-F3	CAGCCATGCACAACCAGACCAA
	CAH1-F4'	AAGAAGAGCGAGGTGTCGGGT
	CAH1-F5	GAGCGGAATAAAGTCAGTGGGC
	CAH1-R1	ATG AGG TAG ACA CTT GCG GCC T

	CAH1-R2'	CAC CAA ACC GTG AAG CAA AGC C
	CAH1-R4	ACT GCT TGG CGC TAT GAA TCC T
	CAH1-R5	ACC AGT TCT CGC CGT TGA GG
LCIE	LCIE mut_scr F1	ATATTGCGATGTGCCATGAGGGC
	LCIE mut_scr F2	ACCTGCGGTGTGATTGGCATG
	LCIE mut_scr F3	TTGGTAGGGCACTGTTGGAAGGAA
	LCIE mut_scr R1	TTGAGGCAGTTGCTTGAGCTGTTC
	LCIE mut_scr R2	AAGCATTGTTAGCGGAGTGCTGTC
	LCIE mut_scr R3	TACATGGAGAGAAGCAAGCGTGGA
CCP1	CCP1 mut_scr F1	AACACTGGTTGCGTTACTCGATGC
	CCP1 mut_scr F2	TGCTATTCTCCCTTCCCTCACCTT
	CCP1 mut_scr F3	CAAACCTGACCGTGCCATCC
	CCP1 mut_scr R1	GTTGGAGCATGGCGAGTGTG
	CCP1 mut_scr R2	CTTGAGGCAGTCCATCGTGGA
	CCP1 mut_scr R3	TGGGAGAAGTTGGAGTAGTGGTCA
521926	521926-F1	AGCACAGCCATCTGTAGCCAAG
	521926-F2	TCCCTGAATCGCACGCTCAA
	521926-F3	TGCTGTCGTTGCTAGAGGAGGA
	521926-F4	AACGGAGACCTTGGGAGCATCT
	521926-F5	ACCACGCCAGACCCTAGC
	521926-F6	TGACTGCCACTACGGGTGC
	521926-F7	ATCCCGCTCCACACTCATCCT
	521926-F8	TTCACACACACCGCCGACTTC
	521926-F9	GACGGTGGTCGTGGCTGTC
	521926-F10	CCGCCATCGCAGTCATCATCATC
	521926-F11	TCAGCATGGAAGACAGCGACGA
	521926-F12	GCTGAATACTACACGCCCGC
	521926-F13	TGCCTCACTTGGAGCCCAGAT
	521926-R1	TTG TTT GCC ATC TGC TCG GGT C
	521926-R2	GGG CAT AGA TAC GCA GCA CCT AC
	521926-R3	AAG CCA TCC GTG AAC CTG GA
	521926-R4	GCA GGT AGG CAC CAG CAG TA
	521926-R5	GAG ATG AGG TCC ACC CAG TAC AGG
	521926-R6	CGT GTT GCG GTG TGG TGA TGA
	521926-R7	TGG AGC TGT GGC GGT GAT
	521926-R8	AGT ACA ACA GCT CCG TCT CCG T
	521926-R9	TCG GGC TGC TGA TGT TGG ATC T
	521926-R10	ATG TTG CTC TCC AAG CCT GTG C

	521926-R11	GCT GGC AAG TAG GCA AGT AGA TAC
	521926-R12	TAA TAC CAG CCA CCA CTG CCG A
	521926-R13	ACA GCC CAT AGT AGA GCA GGT C
521927	521927-F1	CCGTTCTCACGCTGCACTTGTT
	521927-F2	ACCTGCTCTACTATGGGCTGCT
	521927-F3	ATAGTGAGGTTGGGTCGGCG
	521927-F4	AACGGGTACGGTTACAGCAGCA
	521927-F5	ATCGCTGACGGTGCCCACAA
	521927-F6	TAGTCACAAGGATTGGTGGCGG
	521927-F7	TACGTCCGCAGCAGCAACG
	521927-F8	ACGGAGACGGAGCTGTTGTACT
	521927-F9	ATACCGCCGACTTCAGCACTCT
	521927-F10	GCTCGTACTGCTGCGTTGCTT
	521927-F11	TGGAGTGGTTGTGGAACGGCTT
	521927-F12	CGAGCCACGACATCTTCTGTGT
	521927-F13	CACTATCGGTGCGTGTCTGAGCA
	521927-F14	GCCCTGCTGGACCCTTGATT
	521927-R1	CCC GCC CAC AAA CAT GCC AAT A
	521927-R2	CAC GCA AAG CAT CTC CGA AGT C
	521927-R3	ATC TGC TGC TGC TGG TTC AGG
	521927-R4	AGC AGC CGA TCA ACC CAC TAG A
	521927-R5	ATG GCA AGG GAA GTG GGT GGA T
	521927-R6	AAG CAT GGC TGG GAG CAG G
	521927-R7	TGC GAG AGT GGG ACA GAC AAG T
	521927-R8	CGC CAG AGA TGG ACG AGT TGA A
	521927-R9	ATG TTG CTC TCC AAG CCT GTG C
	521927-R10	ATC GGC TAG ATC GGC TAG ATC G
	521927-R11	GTG CCA AGA CAC CTA ACC ACC A
	521927-R12	CCC AGC AGA CGA CAA CAT TCC T
	521927-R13	AGG AGA AGG CGA CAG AGT AGC A
	521927-R14	ACT GTG CCA GAT TCG TAC CC
522486	522486-F1	AAGCACCACACCTACCACTCCT
	522486-F2	CCAACGACCACGTCAAGAGCA
	522486-F3	ATTGGACCTGGGCACACTAGGA
	522486-F4	CCCAGGCTTCATACACGGCTA
	522486-F5	TGAATACTTGGGTCTCGCAGGC
	522486-F6	TCGTGAAGTGGTGAGGTGGTCA
	522486-F7	CACATCCACCCACCCACTGTA

	522486-F8	TGCGAGTGTGCGTACCGT
	522486-F9	TGCCGTACACTTCATCACACCC
	522486-F10	AGTTGATAGGTGAAGGCTGCGG
	522486-R1	AGC AGC GAA CCC ATT CTT CCA C
	522486-R2	CAG AGA CAG GGA CAT CGG GAT T
	522486-R3	AAC CAC CCA ACC CTA CCT CGT
	522486-R4	CCA GCC CTA ATC AAT GCG AAC C
	522486-R5	GCT GCT GGA GAC GCA CAC ATA
	522486-R6	AGG TAC ACA GTA ATC GTC GTC GGG
	522486-R7	TGG GCG GCA GAT AAT GAG GTG A
	522486-R8	TTG TGG CAA GCG GTG ATT GTG G
	522486-R9	TGC GAG GGA CTT GTA AAT GCG G
	522486-R10	AGA ACA GGA GTA GGA GGC AAG G
CAH9	CAH9-F1	CAAAGCATCCTGCCTCAGCCAT
	CAH9-F2'	CCAACGAGACACACCATCCC
	CAH9-F3	CACCTTCACCAACGAGCAGGT
	CAH9-F4	CTCCAGGTGTTTGGGTACGTGT
	CAH9-R1	GAC TGA TTG TGT GTG CCC CTA GC
	CAH9-R2	GGT GGC AGT CGG CAT TAA CTC C
	CAH9-R3	CAC GAC AAG CCC AGA GCA GTT T
	CAH9-R4	AAT GCC CAG CAC CTT CTC AAC G
CAH4	CAH4-F1	ACGACTAACTTGCGACTTGCCT
	CAH4-F2	TCGAGATCATCTTCGACCAGGG
	CAH4-F3	AGGAGGGCAAGCTCAAGATCGT
	CAH4-R1	CGG AAG CAT GAC CGT TTG GGA A
	CAH4-R2	TCT TGT TAC CCA GGC CCA TTG C
	CAH4-R3	AAG CCA ACC AAC CAA CAC ACG G
CAH5	CAH4-F1	ACGACTAACTTGCGACTTGCCT
	CAH4-F2	TCGAGATCATCTTCGACCAGGG
	CAH4-R1	CGG AAG CAT GAC CGT TTG GGA A
	CAH4-R2	TCT TGT TAC CCA GGC CCA TTG C
	CAH5-F	GGCTTGGTACATACTCGTCGGAT
	CAH5-R	ATC CGA CGA GTA TGT ACC AAG CC
CEM1	CEM1-F1	AAACTTGCGTGCGTGTAGGTGG
	CEM1-F2	CCAGTGATGCCAGCGATGGTT
	CEM1-F3	GCCTTCGAGCTGAGCGAGATG
	CEM1-R1	GAA ACG GGT CCC AAA GGG TCT G
	CEM1-R2	AAC GCA CCG CAA TCT GTG TGT C

	CEM1-R3	TGC ACG CAC TTG CCT TCC T
PGP3	PGP3-F1	ACCGTGAAGCGGAATTGGTGTG
	PGP3-F2	GGGCAAGCGGCTATTGTTCGTC
	PGP3-F3	TTCTCATGTGAGTGCGTGCGTG
	PGP3-F4	CATACCACCCACCTGACCACAC
	PGP3-F5	CGGTCATTAGGCTGGCGTACAG
	PGP3-R1	CAA GGG CGA TGG CGA GAA GAA G
	PGP3-R2	GAC TAC CAC GTC TGG GTG CT
	PGP3-R3	GCC TGC ATG GAC CTC AAG CCA T
	PGP3-R4	CTC AGG GCA CCT GCA TGT GGT
	PGP3-R5	CAG GGT GGA TGT TTC CCG CA
523507	523507-F1	GCACGATCCACCATTATCACGC
	523507-F2	AAGTCCCGCTTCATCGCCA
	523507-F3	CGCAATAGTCACGAGCAGCAGT
	523507-F4	AGTTCCCTGAGCGTGCTGG
	523507-F5	GTGGTCAGTGCGATTGAGGAGA
	523507-F6	GCTGAGTGGCATTTGCGAGCAT
	523507-R1	TGC CTC AAT GTC CGA ATC CCA C
	523507-R2	ATC ATA GCT CCC GTC TCT CCC T
	523507-R3	TCT CCT CAA TCG CAC TGA CCA C
	523507-R4	GCC ATC GCA ACG CTT TCG CTA
	523507-R5	GCA GAG AAG GTT CAG GAC TGG CT
	523507-R6	GTA GGG AGA GGT TGA GAC GCA G
RHP1	RHP1 mut_scr F1	TGTAAGACACAACGTCACAACCGC
	RHP1 mut_scr F2	ACAGCCTGGACTGGTCGCATATT
	RHP1 mut_scr F3	TCCTGTCCTCCCACAGCAAGTG
	RHP1 mut_scr F4	CTCCATGATCGGAACCATCTTCCTCT
	RHP1 mut_scr F5	ACCTTCTTGCGTCCTTCTTGTTGC
	RHP1 mut_scr R1	CATTCATCAGTTCACGCAGTCGGC
	RHP1 mut_scr R2	ACCACGAAGCCGCCTAGCA
	RHP1 mut_scr R3	TGCGTATCTCACTTGCGGCTGAT
	RHP1 mut_scr R4	CGAAACCGATCCACACCATGATGT
	RHP1 mut_scr R5	CTCGCCCGACTGAATTTAAGCCCA
RHP2	RHP2 mut_scr F1	TCCCGTCAATTTACCAGCTTTGGC
	RHP2 mut_scr F2	ATTCCATGATTGCCTTGGTAGCGG
	RHP2 mut_scr F3	ATGTGCTAGGTCGTGTCACTGTCT
	RHP2 mut_scr F4	TTCACGTCCCTCACCACGTACC
	RHP2 mut_scr F5	GCTTCGTGGTGTCGTGGTTCAA

	RHP2 mut_scr R1	GGCACACCTGAAGCATTGGCTAAA
	RHP2 mut_scr R2	TGCCACAATCCTACCCTAGTACCA
	RHP2 mut_scr R3	TGAATTGAGGGTGCTGAGGTGGAT
	RHP2 mut_scr R4	AGAGGAGGGTGTTGACAATGGCTA
	RHP2 mut_scr R5	GGTTGAGCATACGGCTGATACGG
	RHP2 mut_scr R6	ATACTTGTAGTACCGCTCCACCTGC
MITC11	MITC11 F1	GGTCCCTCTCGTTTATTCACCTGC
	MITC11 F2	GCTGTGGAAGCTGGCACAAG
	MITC11 F3	TGCCTTCTAGCTCACACTTGGACA
	MITC11 F4	AGGCGTTGGGAAGAGGTACTAATG
	MITC11 R1	AGGTTTGGTGATAGGACTTGCCGT
	MITC11 R2	TTCCACACACACCAGCAGCATCAT
	MITC11 R3	GGCGTAGCAGGGCATGTTCA
	MITC11 R4	TCGCCGCCACTCACGCTTGTAGTT
LCIC	LCIC mut_scr F1	AACAAGTGATTTCTTCGCTCCGCC
	LCIC mut_scr F2	ACCCAGGTGGTGAAGGACAAG
	LCIC mut_scr F3	TTGGTGCTGTGTTGCTTCTTGGAG
	LCIC mut_scr R1	CGCACTACGCAAAGCCCTTCATTT
	LCIC mut_scr R2	CGCTTAGTTCATGTTGGCGAGC
	LCIC mut_scr R3	AGGATGCTGTACTCGGGCTCAAT
NAR1.2	NAR1.2 mut_scr F1	TAGGGCGGTTGTGTACGGAACA
	NAR1.2 mut_scr F2	CCTTCCTCGCCATCTCCGTG
	NAR1.2 mut_scr F3	ACCGACCCATAGGCAACTTCGT
	NAR1.2 mut_scr R1	TGGTCAGTTGGAGCATGGCTTG
	NAR1.2 mut_scr R2	AGGTTCGTGATTCCTCTGGGCA
	NAR1.2 mut_scr R3	GTGAGGGAGGGAAGAAGCACA
524387	524387 mut_scr F1	TACGTTGTAGCGAGAAGCGAAGC
	524387 mut_scr F2	ACCAAGCACGACTTCATGCTGG
	524387 mut_scr R1	CCCGAGACCAGGAGAACCTGAAA
	524387 mut_scr R2	TCTGGATTAGATGTCTTGCGGCGT
NAR1.4	NAR1.4 mut_scr F1	CCCAACCCTGTCTCTGTTTACGGA
	NAR1.4 mut_scr F2	CGCACCAGCACATCCCATGTTT
	NAR1.4 mut_scr F3	CGGAGGAGGAGAACTACGGTCTG
	NAR1.4 mut_scr F4	TACCTGACAACCGCCATGTTGC
	NAR1.4 mut_scr R1	CGATTGACACCGACCTGGCTA
	NAR1.4 mut_scr R2	AACAGTCCGTGCCGTAACAACG
	NAR1.4 mut_scr R3	AACAGCGTGGTGGTCTTGTGAC
	NAR1.4 mut_scr R4	GAGTATGCCGAGTCCTCCTGTCC

	NAR1.4 mut_scr R5	CAGCATTGAACGTCACCTTTCGC
CAH8	CAH8-F1	GGGTTAAAGCGAGGCAGGTGT
	CAH8-F2	AACCCGCTTCGCTACGTACTAGTT
	CAH8-F3	ACTTGACTGTCCGTTTCCCGTCTT
	CAH8-F4'	GACACTGACGCAAGCAGGGTTT
	CAH8-F5	AGGTGGTTGCTGTATTTGGGTGTG
	CAH8-F6	GCAAAGGACGCATAAGGTCATGC
	CAH8-F7	TCTTACTATTGCGTGACGGAGCGT
	CAH8-R1	ACA CCT CCC CAG GAT GCG T
	CAH8-R2	GTA AAG CGG GTG CGT GCC TTA T
	CAH8-R3	GCG GAC ACC ACG TTG AGG TT
	CAH8-R4'	TCC ACC TGC ACG GTA TGC AAG A
	CAH8-R5	GGC TAC CGT TTC CTG TTT CGC T
	CAH8-R6	GCT CAC AAA GCC GCT CGA AGA A
	CAH8-R7	AGA CGA CGG TGC CAT CTT AGC T
526296	526296-F1	TACGGTCAATGCGGAACAGTGC
	526296-F2	ACACCATACTCAACCAGGGCGA
	526296-F3	CTGCTGCGGATGCTCAATGCAA
	526296-F4	TGGTGCTGGCGATTGGACTC
	526296-F5	TGCCCAATAAGCACTACGCAGC
	526296-F6	TTTGGGTAATGGTGCTGGTGCG
	526296-F7	AGTGTGTCACAAGCCCGAGCTA
	526296-F8	TTCTCGGCAGCAGGTCACTG
	526296-F9	AAGTTGTCCTGTTTCCACCCGC
	526296-F10	ATTGCTGAGTTGGGAGTACCGC
	526296-R1	TTA TAC CGC CAG CCA CGC AAT C
	526296-R2	TCC ACC AGC ACG AAC ACG ATT G
	526296-R3	TGG CTT CAT CGG GTA GGG TGT T
	526296-R4	TTT CGG ATG TTG TCC CAC ACG C
	526296-R5	ACG CCA TGT AAC AGG GTT GG
	526296-R6	GGC AGC GGA TAC AGT GCA ATC A
	526296-R7	TGA CTG GAA CGA CAG CAG GTG A
	526296-R8	CCG TGC CGA CCA TCT TGT TGA T
	526296-R9	AGT GAG AGG TGT TGC TGG AGG A
	526296-R10	GCT GAT CTT CTC CAC CTC GGT T
526295	526295-F1	GTTGTCCGTCCGAATCGCCAT
	526295-F2	TGCCCAACACCCTTCACCAAAG
	526295-F3	GTTTGCGATGCGTGATGTGTGC

	526295-F4	ATGCTCACAGGCGAGTCCGT
	526295-F5	GGGTGTAGCGAACCATACCAGT
	526295-F6	AGTACACCGTTAGTGGCGTGG
	526295-F7	GGCTGCTGGTGACATAGGTTGT
	526295-F8	AATGCTGGGAATCGTGCCGG
	526295-F9	ACACACCTTCGCAGGACACTCA
	526295-F10	TGGTGCTAGGGCTCTTCTACTGG
	526295-F11	CACACGCCCGACTTCCTGT
	526295-F12	GCGGCAGAACGGCATAGAATGA
	526295-R1	TTC CGT TTG AGA GGG ACT GAG GG
	526295-R2	AGT GCC GTA ATA TGC TTC GGG C
	526295-R3	GCT GCT TCC CTC TGG CAC T
	526295-R4	GCT GAC GAA GTA GGC GAC CTG
	526295-R5	ACC ACC CAA CCC ATT GCC TC
	526295-R6	GCC GCC AAA GTC AAC CCA GAT A
	526295-R7	GCA CCA GCA CCA AGA CCC AAA T
	526295-R8	TTG ACC AGG GAT GAG TCG TTG C
	526295-R9	TCT CTG ACG CTC TGC TTT CGC T
	526295-R10	ACT CAC TTG CGG TCT CCC AGT
	526295-R11	GTG CTG GAG TGG TGG TAT GTG T
	526295-R12	GCA AGC ACA CAG AGA ACA TCG G
NAR1.1	NAR1.1 mut_scr F1	AAGCGACTTCAGAGCGACCG
	NAR1.1 mut_scr F2	CCTCTTCATCCCGCCTCCGC
	NAR1.1 mut_scr F3	GGTGTGTTCCTGCACGCTTACAG
	NAR1.1 mut_scr R1	GCCGCACGGTATTGTCTGGTT
	NAR1.1 mut_scr R2	GGTCATCTACTTGGCAGCAGCA
	NAR1.1 mut_scr R3	AGTTCTTTGCCAGGTCCTGTGG
509757	509757 mut_scr F1	TTCCGCATAGACCTATTCACTGTCCG
	509757 mut_scr F2	ACTCATACCGCTGGCTGGAG
	509757 mut_scr F3	AGCACCTACACCGCTGCCA
	509757 mut_scr F4	ATCAGCCAGGGACAGGGTGT
	509757 mut_scr F5	CGTGTCCTGCCGATGAGTTTG
	509757 mut_scr R1	AGGATTGCAGACGACAGGGAAAGT
	509757 mut_scr R2	CTTCGTTAGCAGAGCCAATACCGT
	509757 mut_scr R3	AACAACCATCCGACAGTAGCCCAA
	509757 mut_scr R4	ACTACGACCTTGATTGCTCGCCAA
	509757 mut_scr R5	AGTGGCTGTCGTGCTTGGT
	509757 mut_scr R6	ATCCACGGCTCCCATTTGCG

LCI5	LCI5-F1	CGCACAGATTCACCTTCAGGCA
	LCI5-F2	ACGCTGCTCAACTGGTGTACTG
	LCI5-F3	GCAAGTCCAAGCCCGAGATCAA
	LCI5-R1	CCA ACA CCT GCT GAC AAG CCA T
	LCI5-R2	GTT AGG CAA GCT GCT TAC AGG C
	LCI5-R3	GGA AAC GGC AAG CAA ACG TGT C
CIA6	CIA6-F1	AGGTGAATCCAGGCTCTGACCA
	CIA6-F2	TGATGACGCAGCGGCTCT
	CIA6-F3	ACGGCAGTTGGGATGAGGC
	CIA6-F4	AAAGCCGTAGCCACAGCCAAAG
	CIA6-R1	AGG CAT GAG AGA GAA CCG CTG A
	CIA6-R2	TAC GGG CAA CAG GGC TGC AT
	CIA6-R3	AAA CTG ATC CCG ATG CCG ATG C
	CIA6-R4	TTG CAC CCG AAA CCT TGA GAC C
PGP2	PGP2-F1	CCTACACAGCCGTGCAAAGAGG
	PGP2-F2	TACGTGATTGGCGAGGAGGG
	PGP2-F3	CACGCACCAAGTAGCGAGAGAC
	PGP2-F4	GGCGAGTGTAAGTGCGTGTAGG
	PGP2-R1	ACA TGA TGG GCA CGC CGT AC
	PGP2-R2	CCA GAA GTG CAG CAT GGA GGT G
	PGP2-R3	GGA GCC AGG CAC GTC AAA GT
	PGP2-R4	CAG CGT ACT GCC TTT CCA GAG C
CGL28	CGL28 mut_scr F1	AGCCGCAGCAGTTACAACAACAAC
	CGL28 mut_scr F2	AGCCGCAGCAGTTACAACAACAAC
	CGL28 mut_scr F3	ACCGCTCCGTTCTCCCATTCTC
	CGL28 mut_scr R1	TGGGTAGGTTGATCCTGTCTTAGC
	CGL28 mut_scr R2	TATCCTGCGTCAAGTGCTACCCA
	CGL28 mut_scr R3	AACTGCCAACTACATTGCCCTGC
	CGL28 mut_scr R4	GGAGAGGACAGGAGGGCAGA
	CGL28 mut_scr R5	TCATTAAGCCTCTCCGCCAGC
BOR1	BOR1 mut_scr F1	CCTTTCACCTCTCAACTCTTGCGT
	BOR1 mut_scr F2	TGTGAACTATGACCCACGCAAGGTGT
	BOR1 mut_scr F3	GCTTGCCAGGGTCGTGAGAA
	BOR1 mut_scr F4	CCACGGGAGATTCTTCGTCACTTTC
	BOR1 mut_scr F5	AATGCTGACATGGCTTCGGAGCTG
	BOR1 mut_scr F6	TGTCAGACCACAGCGTGTCCA
	BOR1 mut_scr F7	CAGCACCTGCGGCTGTAGCA
	BOR1 mut_scr F8	TACCTGGAGACGGTGCCCTTT

	BOR1 mut_scr F9	ACACCACCACCACAGGCTGTTC
	BOR1 mut_scr R1	TCTATGTCAGGCTTGTGCGATGGA
	BOR1 mut_scr R2	GGTAGTGGGACGTACTGAGTTGAATGT
	BOR1 mut_scr R3	AGCAACCCACCCAGCCCT
	BOR1 mut_scr R4	GCCCACCTCACCGTCACATTA
	BOR1 mut_scr R5	CCGCTACCAAGGCAATCATGGAAT
	BOR1 mut_scr R6	TGCCATCCCAGCCTGCAC
	BOR1 mut_scr R7	GATTGAGAGCCCTGTCGTTGGTTA
	BOR1 mut_scr R8	TGTGAGCGGAGTGGAGTGGA
	BOR1 mut_scr R9	AGCACCCTCAAACACACACCTCACAT
	BOR1 mut_scr R10	AGGCAGCCAGCAGCAGGAC
	BOR1 mut_scr R11	CCATTCATTCTCACAAGCCACCCT
GPX5	GPX5 mut_scr F1	GCAGCTTCGCCTGAAAGAGAAAG
	GPX5 mut_scr F2	TCAGCCAGACCACACATACAGTGA
	GPX5 mut_scr F3	AGAGATGGAGTTGTCAGCCGTGTT
	GPX5 mut_scr R1	CAGTTCAGGAAACATTATAGGTGCGGG
	GPX5 mut_scr R2	GGAAGGAAGCAGTCGAGCATTGTT
	GPX5 mut_scr R3	TTAGGCGATTGGTTATTGGCGACC
512404	512404 mut_scr F1	GCGAGCATAGCTTTACGCCAGT
	512404 mut_scr F2	GCAGCGGTGTATCTCCTGTTCCT
	512404 mut_scr F3	GTGTGTTTACATCCCTCGCTGTGT
	512404 mut_scr F4	TGGATGCTGATCGTGTACGTCTAC
	512404 mut_scr F5	GCCCCGAACTACTTACTTGAGCCC
	512404 mut_scr F6	ACTACAGGACCGAGGACGGAGAT
	512404 mut_scr F7	GCTGTTGGCTATTGTGATGCTCGT
	512404 mut_scr F8	GGACTTCTTGGACCTGGCTACG
	512404 mut_scr F9	CGACTGTTTCCTTACGGGATTGGT
	512404 mut_scr F10	ACCTGGAGTTCGCAGTCATGCT
	512404 mut_scr R1	ACCTTTCTTATCGGGCAACTCTGC
	512404 mut_scr R2	ATCACCTCCTGCGTGTCGGAATAA
	512404 mut_scr R3	AAGCATCAGGCAGTAGGGCTAAGA
	512404 mut_scr R4	AGACCCACGTCCATCCATCAGTAT
	512404 mut_scr R5	ATCACCATCACCCAACCCACCAT
	512404 mut_scr R6	TACCTGTAGTGTGCGTGCGTCC
	512404 mut_scr R7	AGCAGAACGCAAATCAATGCCTGG
	512404 mut_scr R8	CCATCATACATCTTCGTTCACTGCCAG
	512404 mut_scr R9	AGCCTCGTCCAACCAGCG
CAH6	CAH6-F1	CCACTGCTCTCAACATACACGACC

	CAH6-F2	GTGCCTGCGGAAATTGTGTTCG
	CAH6-F3	AGGTCCGCTCGTGATTCTGGAA
	CAH6-F4	GCTGCATTTGGTCCCTAAGGCA
	CAH6-R1	ACC ATT CAC GCA TGT GGC AAG C
	CAH6-R2	ACG ATA CAC GGG CAG ATC ACG A
	CAH6-R3	CCA CCT GAA AGT GCA GCC TTC A
	CAH6-R4	GCA GGT GAG TCG GAT TGC ACA A
513120	513120 mut_scr F1	TACAAGTGGATGTCCGAGCAGGT
	513120 mut_scr F2	CTGTGCAACACCAACGTGAGT
	513120 mut_scr F3	AATGCCGTGTCGTCTGAAGTCCA
	513120 mut_scr F4	TCTTGACATCCCGTCAGGCAGTTA
	513120 mut_scr R1	CTTCCTGAGGTAATCTTTCGCCCACT
	513120 mut_scr R2	GTGTTGTCCACTTCCACTCCCAA
	513120 mut_scr R3	CCACATCCCTCCTCTCCCAAC
	513120 mut_scr R4	GTCCAAAGTAGCTTGTCAGTGCGA
	513120 mut_scr R5	CACGATGCCCGCCAGC
RMT2	RMT2-F2	ACCGTGTGTGAGCCTACGAAGG
	RMT2-F3	GGGTCGTGGTGTGGGATGG
	RMT2-F4	CGGCTCGGAGATGCTCCTAAAC
	RMT2-F5	GAAAGTGCGTGACAGGGAGTCG
	RMT2-F6	CTACACATTGGGCTCGGGCA
	RMT2-R1'	GAC CCT CGG GCT ATC GTA GAT T
	RMT2-R2'	ACC TTC TCA TCA GCC ACC TCG T
	RMT2-R3'	ATG AGC ACA GCA GAA GGG CAA C
	RMT2-R4	ATG TCC ACG CAT GGG CGA GCA G
	RMT2-R5	ACG CCA AAC GCC TCC TTC CT
	RMT2-R6	GCA CGC TGG CTC ATA GAT CCT G
NAR1.5	NAR1.5 mut_scr F1	GTCGGCTCAATGGCTCAGGTTT
	NAR1.5 mut_scr F2	TACGCTACTCAACACCGTGCCA
	NAR1.5 mut_scr F3	TCATTCCGACCGATAATGCCGC
	NAR1.5 mut_scr F4	TCACAGCGGGTAGAGACGCAT
	NAR1.5 mut_scr R1	ATTAAGCCGCCCATGTTGGTGC
	NAR1.5 mut_scr R2	ATGCGGTAACGGGTGGGTATGT
	NAR1.5 mut_scr R3	GTGTGTGTGTGTGCGTAATGGAAGG
	NAR1.5 mut_scr R4	ACCACCCATCAACTCCACATGC
513788	513788 mut_scr F1	CAAACCGCCATGTGCCCA
	513788 mut_scr F2	TTTACACGAACGCCCGCCATC
	513788 mut_scr R1	GCACTAACACACCAAGAACGCCAT

	513788 mut_scr R2	GAAGGATGGCGGGCGTTCG
513839	513389 mut_scr F1	CCTTCGGGTATCCATGTTGCTTGT
	513389 mut_scr F2	AATGCAGTGTTGCACGAAAGGGC
	513389 mut_scr F3	AAATGGCTGTGGATAGAAGCTGCC
	513389 mut_scr F4	GCTTCTTTGCTTTCACCCTGGCAT
	513389 mut_scr R1	TGCTAGGCGGGTGGAAATGAG
	513389 mut_scr R2	ATGGGAATGGGCTTGTGAGAGACA
	513389 mut_scr R3	ACGCACACAGTCCTCACAGTCAC
	513389 mut_scr R4	CCACACCCATACCGTGTCAGT
513843	513843mut_scr F1	GCAAGCGGTGTTGTGTGTCG
	513843mut_scr F2	AGCGGCAGTGGCAAGACTA
	513843mut_scr F3	CCTACCTACATTCCTTTCCGTGTGC
	513843mut_scr F4	TGGTTTGTGTTCAGTGGTGGGT
	513843mut_scr F5	AACATCCTACCACACGCACAGG
	513843mut_scr F6	AGAGCAACATCCAGGACCGC
	513843mut_scr F7	ACCGCACCTGGCTCTTGT
	513843mut_scr F8	CCCACCCTGTCTTGTCCTGAC
	513843mut_scr R1	GGAGGAGTCAGGACAGTTGAAGGA
	513843mut_scr R2	CCCAGTAGTAGAACAGCAGGATACGG
	513843mut_scr R3	ATGTCGCACCTGGCTAGTGAAG
	513843mut_scr R4	GCATCATGTCCTTGCTGCTGG
	513843mut_scr R5	TGGAAGTAGCACAGTGGAAGCCTT
	513843mut_scr R6	CCGCACACAATCACACTCACATGC
	513843mut_scr R7	AACCTGCCGCCACCACT
LCI6	LCI6 mut_scr F1	CCCTTGTGCGTCTTGGCGAA
	LCI6 mut_scr F2	CGCATTACATTGGACAACAACGCC
	LCI6 mut_scr R1	CTCCCACCAATTCCGACCGATT
	LCI6 mut_scr R2	ACAGCACAGCAACAGCACTGC
	LCI6 mut_scr R3	ATATGCCCACCATTCCTCACCTG
CAH7	CAH7-F1	CCACACGCATAGCCTTGCACAT
	CAH7-F2	ATGCACTTAGCCCATCCACGC
	CAH7-F3	CAGGTGGACAGGTGCGAGG
	CAH7-F4	CCTGTTCCCAATGTTGCACCCT
	CAH7-F5	AGCGAAATGGGCGTCTGACAAG
	CAH7-F6	AGGTGGTTCAACTGCATGGCTG
	CAH7-R1	TAT TGG CTC TGT GGC TGA GGC T
	CAH7-R2	TTT ACC AGA GCC CAG CAT TGC G
	CAH7-R3	AGT TCA AAG ATG GGA CGC CAC G

	CAH7-R4	GGG CAA GGG AGA GGG ATG AT
	CAH7-R5	TCT TGC TGG GCA TCT TGA TGG C
	CAH7-R6	TGC GGA CAT GCG GAT TTG TCA G
THB2	THB2-F1	GGCGGTTGAGAAGAAAGCGAGT
	THB2-F2	GTTATCCTGGGATTGTGCGGCT
	THB2-F3	TGAGGTGACTGCTGTTGATGCG
	THB2-R1'	TAC AAC CGC CGA GTC TAC ACC A
	THB2-R2	CAA GTG TGC TGC GAA ATC GGC T
	THB2-R3	AAC GTG CCA CAG ATG TCG TGA C
THB1	THB1-F1	ACGAACGCTGGGAAGTTGTGTC
	THB1-F2	GCCTTTCGTTGCCGTCCTAAGT
	THB1-F3	TATCTGCTTGGCTGGATGAGGC
	THB1-R1	TGG GTA GTC AGG ACG GTG GT
	THB1-R2	CGT GCG AGT TCC AGC TTC GTA
	THB1-R3'	GCG TGA AGC AGA TGT GGA AGG A
POLP (515848)	POLP mut_scr F1	AGTGGCATTCTGTGCGTGATTGG
	POLP mut_scr F2	TACAGCCCATACAGGGACGCTTA
	POLP mut_scr F3	CCGATGGCAAGTTTATCCGTGCT
	POLP mut_scr F4	AACGGTGGCAAGACATCCAGG
	POLP mut_scr F5	AAGACGGCTTCCTGTCTGACGTG
	POLP mut_scr F6	TGTCCGCCAAGAAGACCGATGC
	POLP mut_scr R1	GCTCGGTGTAGTCCTGAAGGT
	POLP mut_scr R2	AACCGAGCTTGCCTAAGCAGTCG
	POLP mut_scr R3	TGAGGGTTGCGAGTAGCAGTT
	POLP mut_scr R4	CAGTGTAGGATGCGAGCCACTCTT
	POLP mut_scr R5	ACCAATCAGCCGTCCACCAATCTT
	POLP mut_scr R6	TCGGCGGTCATGCCAATTAGC
RMT1	RMT1-F1	GTTTCGGCACCCGTAGTTACGC
	RMT1-F2	CATTCTTCCGCTCCACCTTCGC
	RMT1-F3'	TTCGACGTTGAATGGGTACGGG
	RMT1-F4	ACATCAAGGGTGAGAGGCAGAC
	RMT1-F5	CACACACGCACACACGGATTCG
	RMT1-F6	CACGGCAAGTTGGAATGAGGC
	RMT1-R1	CGC CAC GGT GCA ATG TCT GA
	RMT1-R2	AGA GCA ACC GCC ACA ACC AC
	RMT1-R3'	CCA CAC CTC GTT GCG GAA GAT
	RMT1-R4	ACC CAC CCA CGT CGC TAA TGT C
	RMT1-R5	GAT TCC CAA CAG ACG CCT CAC C

	RMT1-R6	GAG GGC TTC AAT CGA GAA CCG C
516273	516273 mut_scr F1	TTTACAGTGCGACGGTGTACCACG
	516273 mut_scr F2	TCCTGGGTCTCTTTGCCACTTGG
	516273 mut_scr F3	CGCCGAGATTGAGGACTACTTTGTGT
	516273 mut_scr R1	TGTTTGGGTGGCGGGTTTCA
	516273 mut_scr R2	TGTGGCGTGGTGTTTACTCGT
	516273 mut_scr R3	AGGGCGTGTGTGTGGGAA
Best_2 (516290)	Best_2 F1	TGAGTTTCGGCGTCGGAGGGAGTA
	Best_2 F2	TTTCCGCACCAACTCGTCCTA
	Best_2 F3	ACACCAAGACCATCCTGGCGGA
	Best_2 R1	AGTGTGTGTTTCCACGCAGTACCT
	Best_2 R2	CTCGGCTCGCTCATTACGCTCT
	Best_2 R3	TGGTGTTGGAGATGAAGGCGGTG
516308	516308 mut_scr F1	TAGAGGATTTACGTCGGGTTGGGC
	516308 mut_scr F2	GACGCAACACGCAGGTCTACG
	516308 mut_scr F3	CCCATTTGTGAGCTTGCGTTACC
	516308 mut_scr R1	TCAGTCTGGTAGCCTGGTTACAGT
	516308 mut_scr R2	CCAGGTTACACCGAAGCCACC
	516308 mut_scr R3	AGGTCAGGTTGTTGCTCATCTGCT
	516308 mut_scr R4	TGCTACCACTCAAGCCAACTCACT
516309	516309-F1	GCCGTCCCACATCGTACCTATCT
	516309-F2	CGGCTGTTCACCATTCCACAGT
	516309-F3	TGTCCTACACCCGCCACA
	516309-F4	TGGTCCTAACAGCTCTGGTGCT
	516309-F5	AGGTTACGGGCTAGAGCGTTGA
	516309-R1	AGC CAC ACA CAC CAG CAG A
	516309-R2	ACG CAT CAC TGC CTC ACA CT
	516309-R3	GCA GAG ACA GGA ACG GCA AGA A
	516309-R4	CAT AGG ACG AGT TGG TGC GGA
	516309-R5	GAG CAA GGA GCG ATC CAG TCA
516770	516770-F1	GAACTTTACGCCCGCTCAGCAA
	516770-F2	TTTGGATGCCACTCAGCAGCG
	516770-F3	TCTCCACCACGAACAAGTTGCG
	516770-F4	CAATGCGGTGGTGGTGGAGAA
	516770-R1	GCT CCA CAG CAG ATA CGA CCT T
	516770-R2	TCT ATC GCA CAC CCG AAA GCA C
	516770-R3	ACA ACG CAC GCA GAC TTA GCA G
	516770-R4	AGA ATC GCT GAG TAG CCT CCT GC

517053	517053-F1	TGTGCCAAGCCCTACTTCTGTC
	517053-F2	ACATGCCTTTCTGCGAGGTGAG
	517053-F3	GCGTGTGAACCTGCTCAAGATGA
	517053-F4	GTTTCCTGTGCGACCGTGGTAA
	517053-R1	CCC ACG CAT TGC TCC TCT ACA A
	517053-R2	ATC TCA CCT CTC CAC TAG CAC GC
	517053-R3	AAC GGT GCG GAA ACG ACG ATA G
	517053-R4	CCA GCT CCT CCT CAC TCA AAC CT
517880	517880-F1	CCAGTAGCCACTCATGTCAGACGA
	517880-F2	ATGTCACCGCAAGGCTCAACC
	517880-F3	GCAGACCTTCACCAACGCTGAT
	517880-F4	AAGAGTGGCTCGCATCCTACAC
	517880-F5	GCCTCATGGGAGGATGACGATT
	517880-F6	GGCTCTACGAGTTTACGGTGCT
	517880-F7	CGACCTGGAACGAAACACGGAA
	517880-F8	GCATACCACACCACCTGCCT
	517880-F9	CCGCTTCTGGTGGAAGGGAAT
	517880-F10	GCAAGTGGCTCTGACAGTGACA
	517880-F11	CACGCAGAAGCAGAACTTCGCA
	517880-F12	CAGCAGCAGGTCTCGCCAT
	517880-F13	GCCTATTTAGGACAGCAGGACGC
	517880-F14	TGCTGGACCTAGACGACTGAGA
	517880-R1	TTG GGA GGA GGA GAG TGA CTG A
	517880-R2	AAA TTC CTC GTC GGG CTC GGT A
	517880-R3	AAT CAG GGT CGG CGA GCA
	517880-R4	ATA CAC TCG CCC TCG TCT TGC T
	517880-R5	AAA TTC TGC GGG TGG ACC TCT G
	517880-R6	TTT GCC GTA CAG CAG CAG AGC
	517880-R7	TCC TCC TCA TCC TCG CTG GAA T
	517880-R8	CCT GGA ACC TCT GCC GCT
	517880-R9	ATT GCT CAA ACG CTG CCT GCT
	517880-R10	TCC GAC GAG CTG GGT TGG ATA A
	517880-R11	GGT CTT CGC AGT CAT CCC ATG T
	517880-R12	TAT CCT GGC ACT TGG CAA AGC G
	517880-R13	AGC CCT GGT TGG AGC GTG
	517880-R14	ATG GCA GCA GTT AGG TTG TGC G
520182	520182-F1	CTCAACACCACCTCGCCCATAA
	520182-F2	CCCGCACGCCTTTGTGTGTATT

	520182-F3	CGGCTGGTCGGAGTATGA
	520182-F4	CACTCGGGTCTTGGCAGCA
	520182-F5	AGGGTTGACGATGCTCCAGAG
	520182-F6	GCCTTTCGTCTTCTGGTAGCCTC
	520182-F7	GGGCGTATTTGTGCTCACCATGTG
	520182-F8	ACGGGTGGGTTTGGTAGTTTGC
	520182-F9	TTGCTGGCTCAGGACAGGACT
	520182-F10	TGGACCGAGTGATTGAGGCG
	520182-F11	TGGGTGTGGGCTAGGAGAAACA
	520182-F12	ATGTGTTGGCTGTGGCTGTTGG
	520182-F13	ACAGTAGGGCGATGGGAAGCAA
	520182-F14	GCGGCAGTGACGGATACTACGA
	520182-F15	CATCTACAAGCCAGCAGCAGCA
	520182-F16	TAGGCTCAATGGGAGGGCAAGT
	520182-R1	CGG CAA CTC GTT TCT CTC CGC
	520182-R2	AGA ATG GTG GGC GGC TTG AAC
	520182-R3	CCC AAC CCA TTT ATT CAC CTC GC
	520182-R4	GAC TGG AAG AAA GCG GAG GCA T
	520182-R5	AGG GAA TGG GCA CCA GAG AGA
	520182-R6	GGC TAG GCT CAG CAA CCA TGA A
	520182-R7	GCC ACC TGC GAG TTT GGT GT
	520182-R8	CAC ACA CAA CCC ACC ACT TCC T
	520182-R9	AAA CCC ACC CGT CTC CTC CAT
	520182-R10	CGG TGG TGA CTT GGT GTT GCT T
	520182-R11	GCA ACT CGC ATC TTC CCG TCT T
	520182-R12	GCG GCA TCA AGA CCA AGA GC
	520182-R13	AGG TCA TTG CTA CTG CGG CG
	520182-R14	GGG AAA GGT GCC AGG GTA ACA A
	520182-R15	ACC TCC ACT CTG ACC GCC A
	520182-R16	CCA TGT CAA AGC CTC CGC TTC C
522781	522781-F1	ACCAACTACTCGCACACGATGG
	522781-F2	TAGGTGGTTAGGGTGGTTGGGT
	522781-F3	CACACGCACAGGTACGACAAGT
	522781-F4	GTATGACTACCTGGGTCACGACAG
	522781-F5	TGACGCAGTGTGGAAGTGAGGA
	522781P-R1	TTG AGG GAG TGT GGC TTC TTT CAG
	522781P-R2	AGT ACG ACA GAG CCG ACT GTA C
	522781P-R3	TAC CCA GCA CGC CTA ATT CCC A

522781P-R4	CAC AGC CCA ACG TGC TCA TCA T
522781P-R5	CGG TGG TGT TGG TAG TGT GGT

a. Primers are listed by genes in the same order as Table 7.2

b. The Apostrophe sign means this primer is designed the second time to replace the ones that did not work for the first time.

APPENDIX VI
PERMISSION TO REPRINT

This chapter first appeared as **Ma, Y., Pollock, S.V., Xiao, Y., Cunnusamy, K., and Moroney, J.V.** (2011a). Identification of a novel gene, CIA6, required for normal pyrenoid formation in *Chlamydomonas reinhardtii*. Plant Physiol 156, 884-896. Reprinted by permission.

Dear Yunbing Ma,

Thank you for your message.

Please see permissions information at:

http://www.aspb.org/publications/permission.cfm

Let us know if you have further questions.

Regards,

Sarah Wilson

On the website:

Permission to make digital or hard copies of part or all of a work published in *Plant Physiology* or *The Plant Cell* is granted without fee for personal or classroom use, provided that copies are not made or distributed for profit or commercial advantage and that copies bear the full citation, the journal URL (www.plantphysiol.org or www.plantcell.org), and the following notice: “Copyright American Society of Plant Biologists.”

VITA

Yunbing Ma, was born in Suzhou, Jiangsu Province, China, in February, 1983. She completed a bachelor degree of Bio-engineering in 2005 at Shanghai University, Shanghai, China. Yunbing then came to the United States in July 2006 to pursue her doctoral degree at Louisiana State University in Baton Rouge. In 2008, Yunbing married to Xi Yang.

In 2012, she completed the doctoral program under the supervision of Dr. James V. Moroney. Her dissertation research focused on the characterization and generation of CCM mutants in *Chlamydomonas*. In 2012, she received the C. W. Edgerton Honor Award given by the Department of Biological Sciences, Louisiana State University. After graduating from Louisiana State University, Yunbing will pursue postdoctoral training by joining the laboratory of Dr. Matthew Whim at Louisiana State University, School of Medicine at New Orleans, where she will start to explore the field in neuropeptide Y and its function in reponse to metabolic stress.